Biochemical evaluation and GC/LC-MS based metabolite analysis of three medicinal plants: Validation of anti-atherosclerotic properties of *Boswellia serrata* and *Terminalia arjuna* and cultivar variability of metabolites in *Curcuma*

Thesis submitted to the University of Hyderabad

for the Degree of

DOCTOR OF PHILOSOPHY

By

K. Praveen Kumar
Enrolment No. 07LPPH01

Supervisor: **Dr. Sarada D. Tetali**

Department of Plant Sciences
School of Life Sciences
University of Hyderabad
Hyderabad 500 046, INDIA

Nov 2013

DEPARTMENT OF PLANT SCIENCES
SCHOOL OF LIFE SCIENCES
UNIVERSITY OF HYDERABAD
HYDERABAD-500 046
INDIA

DECLARATION

I hereby declare that the work presented in this thesis entitled "**Biochemical evaluation and GC/LC-MS based metabolite analysis of three medicinal plants: Validation of anti-atherosclerotic properties of *Boswellia serrata* and *Terminalia arjuna* and cultivar variability of metabolites in *Curcuma***", has been carried out by me under the supervision of Dr. Sarada D. Tetali in the Dept. of Plant Sciences, School of Life Sciences, University of Hyderabad and this work has not been submitted for any degree or diploma of any other University or Institute.

K. Praveen Kumar
Enrol. No. 07LPPH01

Dr. Sarada D. Tetali
(Supervisor)

DEPARTMENT OF PLANT SCIENCES
SCHOOL OF LIFE SCIENCES
UNIVERSITY OF HYDERABAD
HYDERABAD-500 046
INDIA

CERTIFICATE

This is to certify that Mr. K.PRAVEEN KUMAR has carried out the research work embodied in the present thesis entitled "**Biochemical evaluation and GC/LC-MS based metabolite analysis of three medicinal plants: Validation of anti-atherosclerotic properties of *Boswellia serrata* and *Terminalia arjuna* and cultivar variability of metabolites in *Curcuma***", for the degree of Doctor of Philosophy under my supervision in the Department of Plant Sciences, School of Life Sciences, University of Hyderabad.

Dr. Sarada D. Tetali
Supervisor
Department of Plant Sciences

Head
Department of Plant Sciences

Dean
School of Life Sciences

Acknowledgements

It gives me immense pleasure to thank all the people associated with me, while pursuing the Ph.D.

With deep sense of gratitude and respect, I thank my supervisor, Dr. Sarada D. Tetali, for her guidance in shaping this piece of work and also for the encouragement, confidence and patience shown during my research. Association with her through these years has given me an opportunity to understand and learn key research and professional skills.

I am thankful to Prof A.S. Raghavendra, for giving me an opportunity to work as SRF in DBT funded project and also for his valuable suggestions and financial support to carry out my work. I am also thankful to UGC-SAP for providing me fellowship for the first three years of my Ph.D period.

I thank my doctoral committee members Prof. A. S. Raghavendra, Dr. K. P. M. S. V. Padmasree for their valuable inputs and for allowing me to use all the facilities.

I thank Prof. Madhava Chetty, Department of Botany, S. V. University, Tirupathi for providing *Terminalia arjuna* stem bark and *Boswellia serrata* gum resin for my research work.

I am thankful to Dr. Uma Maheswari, Turmeric Research Centre, Nizamabad and Dr. Nirmal Babu, Indian Institute of Spice Research, Calicut for providing *C. longa* cultivars for DBT project work.

I am grateful to Prof. P. Prakash Babu, Dept of Biotechnology for providing rat liver and heart tissue samples; Dr. Anupama Row, Chief Medical Officer, University Medical Centre, for supporting us in ethical committee for human blood collection.

I thank to Prof. Aparna Dutta Gupta and Prof. Jagan Pongubala, Department of Animal Sciences, for providing Flow cytometry facility in the School of Life Sciences.

I am thankful to Prof. Aparna Dutta Gupta, for allowing to work in spectrofluorimetry facility, and Dr. K. Arun kumar, Former Incharge of animal cell culture facility Department of Animal Sciences for permitted me to work in the facility.

I wish to express my sincere thanks to, Prof. Ch. Venkataramana, Head, Department of Plant Sciences, R. P. Sharma, Dean, School of Life Sciences and former Heads, Prof Attipalli R. Reddy and Prof. Appa Rao Department of Plant Sciences and Prof. A.S. Raghavendra and Prof. Aparna Dutta Gupta former Dean, School of Life Sciences, for allowing me to utilize the common research facilities.

I am thankful to Prof. Ch. Venkata Ramana, Department of Plant Sciences, In charge of metabolomics facility for permitting me to work; and also for allowing me to use his lab facility rotary evaporator during my sample preparation.

I am thankful to Dr. Poonam for actively associated in the DBT-project.

I am thankful to my colleagues in the lab- Dr. K.V. Ratnam (PDF), Mr. Sudhansu, Mr. Kiran and for their cooperation during my work.

I would like to thank Dr. L. Md. Bakshu for his support in my work.

I am thankful to M. Swathi, student of Dr. K.P.M.S.V. Padmasree's lab for helping me in confocal and coagulation studies.

I wish to thank Ms. Nalini for her amicable assistance in confocal microscopy; Mrs. Leena Bashyam for helping me in RT-PCR work; Mr. B. Prasanth for his assistance in using metabolite facility.

I thank Dr. Sharmista Banerjee and her students Rajesh and Benjamin for their help in using their microplate reader for ELISA.

I am thankful to Dr. Niyaz Ahmed and his student, Sandhya for their help in using FACS machine for my experiments.

I am thankful to Mr. Ram Prasad student of Prof. Ch. Venkata Ramana, for his help in metabolite analysis, integrating HPLC spectra for my manuscript.

I am thankful to Mr. Prasad, student of Dr. Naresh Babu, Department of Biochemistry in helping me in translocation studies.

Specially, I would like to thank all my friends and seniors in Prof. A. S. Raghavendra's lab and Dr. Padmasree's lab for their help and cooperation.

I am thankful to our lab assistants Mr. Prabhakar, Venu gopal, Phul Singh and Mallikarjuna for their help and cooperation in the lab.

I thank all administrative staff of Department of Plant Sciences, School of Life Sciences and other members of University of Hyderabad, who helped me in terms of administrative work for successfully completing my PhD work. My special thanks goes to Sri Mohan Rao, Sri Sai, Sri Sudharshan, Sri Srinivas and Mrs.

Margaret, Aparna, Swathi, Mr. Lakshman, Mrs. Rohini, Mr. Murty and Mr. Krishna and others.

I Thank Mr. Rajesh for helping in smooth running of network facility in the School of Life Sciences.

My work is supported by:

DBT, UGC, UPE, ICMR and IGSTC research projects of Dr. Sarada D. Tetali and DBT research project of Prof. A. S. Raghavendra.

We are Thankful to DBT-CREB, DST-FIST, UGC-SAP and OBC grants for supporting infrastructural facilities of Department of Plant Sciences and School of Life Sciences.

I thank my parents Gothiah and Narasamma for all the love, support and for giving me everything that I ever wished for.

My brothers Prasan Kumar, Pradeep Kumar and Sister Bhavana, for their love shown during these entire tough years of study- right from my Ph.D. days- for taking upon themselves my share of responsibilities.

I thank my holy mighty loving Lord JESUS CHRIST for guiding me and my family all through and for his generous blessings.

Praveen Kumar Kokkiripati

Abbreviations

AE	: Alcoholic extract
ANOVA	: Analysis of variance
APTT	: Activated partial thromboplastin time
ASE	: Ascorbic acid equivalents
AκβBA	: 3-O-acetyl-11-keto-beta-boswellic acid
BA	: Boswellic acid
BAM	: Boswellic acid mixed-fraction
BD	: Becton, Dickinson and Company
BDMC	: Bisdemethoxycurcumin
BHT	: Butylated hydroxyl toulene
BSAE	: *Boswellia serrata* alcoholic extract
BSWE	: *Boswellia serrata* water extract
BSTFA	: N,O-bis(trimethylsilyl) trifluoroacetamide
CAM	: Cell adhesion molecule
CAS	: Chemical abstracts service
CAT	: Catalase
CU	: Curcumin
DAPI	: 4',6-diamidino-2-phenylindole
CVD	: Cardiovascular disease
DCF	: Dichlorofluorescein
DPPH	: 2,2-diphenyl-1-picrylhydrazyl
DMC	: Demethoxycurcumin
ESI	: Electrospray ionization
ELISA	: Enzyme-linked immuno assay
FAC Scan	: Fluorescence activated cell sorting scan
FITC	: Fluorescein isothiocyanate
FRAP	: Ferric reducing antioxidant power
GA	: Gallic acid
GAE	: Gallic acid equivalents
GAPDH	: Glyceraldehyde 3-phosphate dehydrogenase
GC-MS	: Gas chromatography-mass spectrometry
GPx	: Glutathione peroxidase
HAEC	: Human aortic endothelial cells
Hep	: Heparin
H_2DCFDA	: 2',7'-dichlorodihydrofluorescein diacetate
HMG-CoA	: 3-hydroxy-3-methylglutaryl-CoA reductase
HPLC	: High pressure liquid chromatography
●HO	: Hydroxyl
ICAM-1	: Intercellular adhesion molecule-1
IL-8	: Interleukin-8
IC_{50}	: Inhibitory concentration 50
KβBA	: 11-Keto-β-Boswellic acid
LC-MS	: Liquid chromatography-mass spectrometry
LDL	: Low density lipoprotein
LPS	: Lipopolysaccharide
LpL	: Lipoprotein lipase
LSR	: Laser
MCP-1	: Monocyte chemoattractant protein-1

MS/MS	: Tandem mass spectrometry
MTT	: 3-(4,5-dimethylthiazol-2-yl)-2,5-diphenyltetrezolium bromide
NADPH	: Nicotinamide adenine dinucleotide phosphate
NF-κB	: Nuclear transcription factor kappa B
NIST	: National Institute of Science and Technology
PE	: Phycoerythrin
PMBC	: Human peripheral blood monocytes
PT	: Prothrombin time
QE	: Quercetin equivalents
QTOF-MS	: Quadrupole time-of-flight mass spectrometer
ROS	: Reactive oxygen species
RT	: Retention time
SD	: Standard deviation
TAAE	: *Terminalia arjuna* alcoholic extract
TAWE	: *Terminalia arjuna* water extract
TFC	: Total flavonoid content
THP-1	: Human monocytic leukemia cell line
TMS	: Trimethylsilyl
TNF-α	: Tumor necrosis factor-alfa
TPC	: Total phenol content
UA	: Ursolic acid
UAE	: Ursolic acid equivalents
VCAM-1	: Vascular cell adhesion molecule-1
WE	: Water extract
WHO	: World health organisation

Chapter 1

INTRODUCTION

Introduction

Medicinal Plants

Medicinal plants, since from the ancient times, have been used in all cultures as a source of medicine. India is one of the seventeen megadiverse nations and considered as endemism having various species of medicinal plants at several degree of taxonomic levels. India has 45,000 plant species spread over different agro-climatic zones, and 7,000-7,500 species are used by traditional medicinal systems in India (Pradeep and Pamila 2012). WHO defined health, as a state of complete physical, mental, and social well being and not merely the absence of disease or infirmity (Hoareau and DaSilva 1999). In India, Ayurveda is followed as traditional medicine for over 5000 years, which includes diet and herbal medicine, while accentuate the body, mind and spirit in prevention and treatment of various diseases. There are different methods of healing practices as the part of tradition in the respective nations.

According to WHO, 80 % of the world population rely chiefly on plant based medicine, especially for the primary health care needs (Haq, 2004). Globally, there is a great demand for extracts, formulations, metabolite components derived from traditional and modern systems of medicine as pharmaceuticals, nutraceuticals, cosmaceuticals and as functional foods (Rajeswara Rao et al., 2012). Approximately Rs. 2,00,000 crores account in world market for plant derived drugs, where the contribution of India is less than Rs. 2000 crores, (Jawla et al., 2009). Therefore there is an urgent need to evaluate the herbal products of Indian origin in terms of their medicinal value, safety and side effects.

It has been estimated that 80 % world population depend on natural plant products which are sold as food/herbal/drug supplements. Phyto antioxidants have been of great interest from the point of view of their pharmacological activity, safety and compatibility with normal human physiology. Human body also naturally produces antioxidants that differ in their composition, physical and chemical properties; mechanism and their site of action. But, they may not be sufficient in case of overproduction of free radicals and also the effectiveness of the antioxidant system declines with age. Therefore increase in antioxidant intake can prevent age-related degenerative diseases (Sen et al., 2010). Antioxidants retard or prevent oxidation and prolong the life of the oxidizable substance (Zhu et al., 2004).

Traditional medicine and herbal formulations

It is well-known fact that traditional system of medicine has been playing an important role in meeting global health needs. Indian traditional medicine, Ayurveda means “Science of Life” a holistic medical system (Fritts et al., 2008) that emphasizes the importance of physical, psychological, philosophical, ethical and spiritual well beingness and thus of maintaining proper life style for keeping positive health. Concept of world health organization is in similar lines with concept of health as defined in Ayurveda (Ravishankar and Shukla 2007). Chinese traditional medicine has been successfully being promoted its therapies across the world and extensive scientific validation being taken up in order to integrate with modern medicine, referred as evidence based medicine. China is able to take their traditional medicine towards evidence based medicine. Ayurveda also needs extensive scientific investigation and validates herbal medicine in terms of efficacy and safety (Patwardhan et al., 2005). Scientific investigation with medicinal plants opened up for a wide range of novel phytochemicals possessing various pharmacological activities. Increasing awareness and acceptability of herbal drugs in today’s medical practice has lead 80 % of world population to depend on herbal medicine/products for healthy living (Kunle et al., 2012).

Role of inflammation in human health and disease

In response to injury or infection, inflammatory responses offer protection at the sites but can sometimes become deleterious to the host (Serhan et al., 2007). Therapeutic interventions are required to maintain a balance between suppressing an ongoing inflammatory process and maintaining normal function of essential immune responses (Evans and Robbins 2000). A wide range of therapies exist for the treatment of inflammation driven diseases such as asthma, arthritis, crohn’s disease, sclerosis, but such therapeutics have equal proportion of side effects. For example, steroids, which are in use for treating some of the afore mentioned health issues can cause osteoporosis, impair wound healing and etc. Therefore alternative approaches for treating inflammatory diseases are of great interest.

However, it has been reported that the situation, when the balance between antioxidant system and production of free radicals is impaired results in oxidative stress (Fig. 1).

The generation of free radicals in biological system was discovered 50 years ago. The significance and science of free radicals in living organisms commenced after the discovery of superoxide dismutase (Wulf Droge, 2002). Free radicals play an irreplaceable role in cell signalling processes and are part of several biochemical reactions involving hydroxylating, carboxylating or peroxidating reactions or in the reduction of ribonucleotides (Durackova, 2010). Cellular metabolism constantly generates reactive oxygen species (ROS) (e.g. of highly unstable superoxide anions, hydroxyl radicals and freely diffusible hydrogen peroxide). Biological cells are equipped with various types of ROS dissipating systems consisting of enzymes such as catalase (CAT), superoxide dismutase (SOD), glutathione peroxidase (GPx), and numerous non-enzymatic antioxidants (Miranda-Vilela et al., 2010) such as methionine sulfoxide dismutases and also the enzymes, which can reverse oxidative modifications (Avery, 2011). “The state in which oxidation exceeds the antioxidant systems in the body” (Yoshikawa and Naito 2002) is referred as oxidative stress which leads to cellular damage.

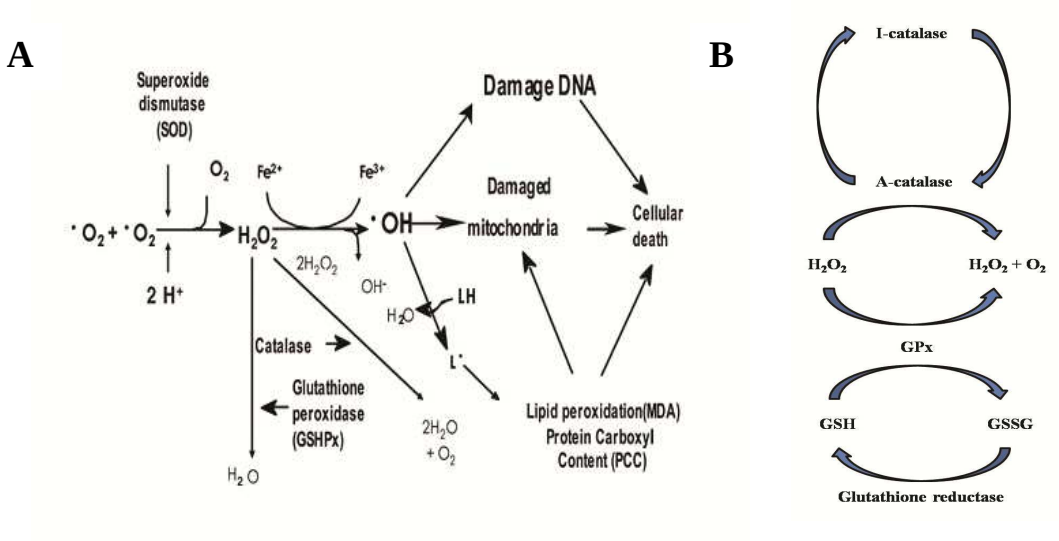

Moron and Cortazar, 2012 and Baud, 2004.

Figure. 1. (A) Mechanism of oxidative cellular damage. Reactive oxygen radicals are reduced into water with the cooperation of antioxidant enzymes. The pathways showing oxidative damage leads to cellular death. (B) Diagram represents the detoxification of H_2O_2 by catalase and glutathione peroxidase GPx. GPx appears to be the limiting for the degradation of H_2O_2. Reduced GSH is oxidized to GSSG and recycled back by glutathione reductase. Auto-inactivation of catalase (I-catalase) by H_2O_2 is prevented by GPx, which maintains catalase in active form (A-catalase).

Therefore, there has been increase in the demand, particularly, in western countries, for phytopharmaceutical products because of their antioxidant nature. Antioxidants help in treating several metabolic and infectious diseases which are promoted by oxidative stress. Oxidative stress leads to various pathological conditions, viz. AIDS, ageing, arthritis, asthma, atherosclerosis, autoimmune disease, Alzheimer's disease, amytropic lateral sclerosis, cancer, cardiovascular diseases, cataract, diabetes, gastro-duodenal pathogenesis, genetic disorders, inflammatory diseases, muscular dystrophy, neurodegenerative diseases, Parkinson's dementia, pulmonary fibrosis, retinopathy, rheumatism, skin disease porphyria and senile dementia stroke and many others (Vivek and Surendra 2006; Cooke et al., 2003).

Atherosclerosis

Atherosclerosis, a disease of large arteries, is the number one primary cause of heart disease and stroke globally, accounting for ~ 30 % of deaths and disability worldwide (Lockhart et al., 2012). It is characterised by the accumulation of lipids and fibrous elements in the vessel wall of large arteries. The vessel wall consists of three morphologically distinct layers known to be intima (thin with connective tissue matrix) the innermost layer lined by the endothelial cells on the luminal side with a sheet of elastic fibres and lamina; middle layer, media with smooth muscle cells. Adventitia, outer layered connective tissue with fibroblasts and smooth muscle cells (Lusis, 2000).

Under normal haemostatic conditions, monolayer of endothelium maintains normal blood fluidity, with no or little expression of proinflammatory factors. However risk factors including metabolic disorders and infectious diseases are associated with endothelial dysfunction accompanied by loss of antithrombotic factors with increase in vasoconstrictor and abnormal vasoreactivity. Reactive oxygen species generated at the sites of inflammation also take part in promoting inflammatory responses (Hadi et al., 2005).

Risk factors for the development of atherogenesis/atherosclerosis

A practical approach with transgenic and gene-targeted mice revealed more than hundred genes influence atherosclerosis. Risk factors include metabolic diseases, bacterial and viral infections play a pivotal role in the development of atherosclerosis. Epidemiologic studies supports that cigarette smoking to be major

health hazard as it contains free radicals and are associated with increasing oxidative stress and sets the stage for the cardiovascular dysfunction (Ambrose et al., 2004).

►High-fat diet, showed increased concentrations of inflammatory and endothelial dysfunction markers (interleukin, tumor necrosis factor-α, monocyte chemoattractant protein (MCP-1), VCAM-1 and E-selectin) in the circulating blood and endothelial cells (Shi et al., 2005). High fat diet also leads to hyperlipidemia especially increased LDL which is also an risk factors for atherogenesis (Tomkin and Owens 2012).

►Clinical, experimental and pathologic studies strongly indicated that hypertension as one of the risk factors that elevates blood pressure causing tangential tension over walls of arteries (Hollander, 1976).

►Chronic hyperglycemia and insulin resistance in diabetes mellitus patients alters functions of smooth muscle cells; platelets render the arteries susceptible to atherosclerosis (Beckman et al., 2002).

■Infections due to bacteria or viruses can lead to the development of atherosclerosis. Pathogens, either as whole organism or their structural components have potential to induce proatherogenic and prothrombotic response in the blood vessel leading to atherogenesis (Shah, 2001). Bacteria like *Chlamydia pneumonia*, *Helicobacter pylori* and viruses like human immunodeficiency virus, cytomegalovirus, Epistein-Barr virus, herpes simplex virus and measles shown to play a role in the pathogenesis of atherosclerosis (Morre et al., 2000).

Cellular and molecular mechanisms of atherogenesis

As described above, several conditions including exposure to cigarette smoke, dust and pollution, fatty diet, hyperglycemia, hyperlipidemia, infections activate leukocytes in the blood. These cells release proinflammatory cytokines up on activation, increased cytokine content in the blood plasma activate endothelial lining layer of the blood vessel wall. Activated endothelium expresses cytokines, chemokines and cell adhesion molecules leading to adhesion of monocytes and platelets to the endothelium (Davis et al., 2003). Vascular cell adhesion molecule-1 (VCAM-1) expressed on endothelial cell surface play a major role in monocyte recruitment, adherence to endothelial cell monolayer and diapedesis between intact endothelial cells and penetrate into subendothelial cell space. This type of leukocyte migration requires chemoattractant gradient, particularly monocyte chemoattractant protein-1 (MCP-1).

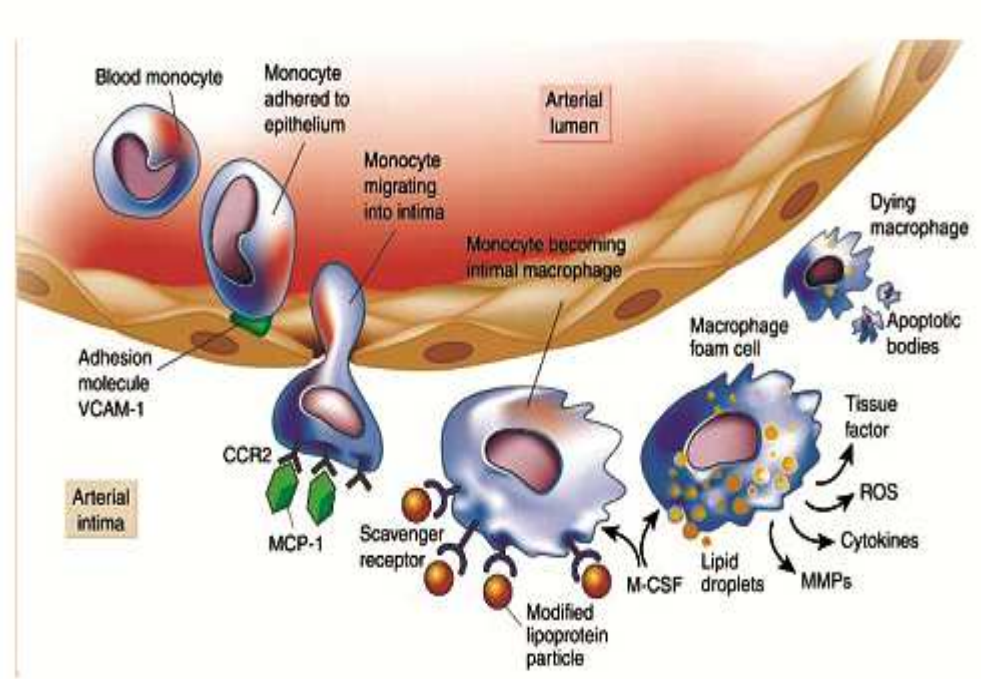

Libby, 2002

Figure. 2. This figure is a schematic representation of the steps in the inflammation and intiation of the atherosclerosis. Molecular mechanisms of the attachment of white blood cells to endothelium. Under normal circumstances, arterial endothelium resists prolonged contact with leukocytes and monocytes. When endothelial cells undergo inflammatory activation, they increase various leukocyte adhesion molecules, in this context vascular cell adhesion molecule-1 (VCAM-1) seems to have major role. Further various chemokines participate in the process of diapedeses leading to foam cell formation. Notably, these foam cells amplify local inflammatory lesions and reactive oxygen species by secreting proinflammatory cytokines finally playing a key role in thrombotic complications of atherosclerosis, hence producing atherosclerotic lesion.

Monocytes resided in the intima acquire characteristics of macrophages and express receptor that binds to lipoprotein particles, leading to foam cell formation which secrete proinflammatory cytokines (e.g., TNF-α, IL-1α and IL-6) and amplify local inflammatory responses and finally into fatty streak lesion/plaque formation in the blood vessel wall. Plaques with thin wall rupture permitting blood to contact to another macrophage and so on, as shown in Fig. 2. Thus for maintaining normal cardiac health, antioxidants, statins and antiplatelet drug agents, TNF-α lowering drugs are recommended and till date there are therapeutics developed which can

manage all the afore mentioned events. Therefore, screening and identification of medicinal plants having compounds which are antiinflammtory, antioxidant and antithrombotic is highly essential for the development of CVD therapeutics.

Rationale for selecting medicinal plants for the present study

Heart health is a major concern in developed and developing countries. Cardiovascular ailments (*Hrudroga*) have been addressed in detail, in Ayurveda. The plants, majorly used for preparing formulations for treating heart diseases and / or blood disorders in Ayurveda are *Azadirachta indica*, *Boswellia serrata*, *Cassia fistula*, *Cedrus deodara*, *Cocos nucifera*, *Curcuma species*, *Myristica fragrans*, *Picrorhiza kurrooa*, *Terminalia arjuna* and *Terminalia chebula* (Lokhande et al., 2006).

Short list of allopathic drugs derived from plants used for treating CVD

►Digitoxin and digoxin from *Digitalis purpurea:* Most effective for congestive heart failure – over dosage is highly toxic.
►Aspirin from *Salix alba*: remarkably fast and can help survival during heart attack – over dosage can cause ulcers and stomach bleeding.
►Statins from fungus, *Monascus purpurus*: lipid lowering drug, saving millions of lives, however, side effects can be fatal including permanent damage to liver, muscles and nervous system.

The origin of afore mentioned allopathic CVD drugs and Ayurvedic formulations for Hrudroga suggests that medicinal plants are the best resource for developing new therapeutics for treating complexed diseases like CVD.

The selection of the plants for the present study is primarily based on their traditional use in Ayurveda for either treating cardiovascular or blood disorders and further on scientific reports for their safety in use. Gum resin of *Boswellia serrata* and stem bark of *Terminalia arjuna* were selected for the present study and validated for their antitherogenic effects as well as for their metabolite profile. Studies with rhizomes of *Curcuma* were limited to metabolite analysis to establish cultivar variability within *Curcuma*.

Boswellia serrata's gum resin containing medical preparations are described in Ayurvedic text books like Charaka Samhita (1st and 2nd century AD) and Astangahrdaya Samhita (during 7th century AD) to treat various blood related

diseases (Ammon, 2006). Stem bark of *Terminalia arjuna* (TA) has been noted for its beneficial effects for cardiac ailments in "Atharva Veda" from which Indian system of medicine originated. Cardioprotective properties of the TA-stem bark are mentioned in the book of 'Astang Hridayam' (Dwivedi, 2007). Thirdly, rhizomes of *C. longa* and *C. aromatica* mentioned in the records of ancient systems of medicines like Ayurveda, Greek, Roman, Siddha and Unani, for treating various inflammatory conditions (Mohanty et al., 2006).

Herbal formulations of *T. arjuna* and *B. serrata* available in the market for treating CVD or other inflammatory diseases

► **Arjuna ghrita** (*T. arjuna* –stem bark)-Cardio Tonic -Dabur, Zandu, Baidyanath.

► **Arjun capsules** (*T. arjuna* –stem bark)-Ischemic Heart Disease -Himalaya Drug Co. Ltd.

►**Arjunin capsules** (*T. arjuna* –stem bark)-Coronary Vasodilator and Cardiotonic -Charak Pharma Pvt. Ltd.

►**Rheumatic-X®** -(*B. serrata*-gum resin)-Arthritis relieving Cream -Sunrise Herbals,
Varnasi.

►**Shallaki** -(*B. serrata*-gum resin)- Arthritis and Joint Pain -Himalaya Drug Company.

Boswellia serrata

Taxonomic hierarchy

Gum resin

Kingdom: Plantae
Division: Magnoliophyta
Class: Magnoliopsida
Sub Class: Rosidae
Order: Sapindales
Family: Burseraceae
Genus: *Boswellia* Roxb. ex Colebr.
Species: *B. serrata* Roxb. ex Colebr.
Binomial name: *Boswellia serrata* (Roxb.) Wight and Arn
English name: *Frankincense, Indian olibaum*

Habitat

Boswellia serrata is a medium to large sized deciduous tree, grows normally 18 m height, commonly found in India, in the regions of western Himalayas, Rajasthan, Gujarat, Maharashtra, Madhya Pradesh, Bihar, Orissa and many other countries (Alam et al., 2012).

Botanical characteristics

The bark of this plant is thin, peeling off as flakes with small drops of resin (Alam et al., 2012).

Phytochemistry of gum resin

Boswellia serrata's stem-bark secretes gum resin containing essential oil. Essential oil is enriched with monoterpenes (α-thujene), diterpenes, sesquiterpenes, diterpene alcohol and phenolic compounds. Gum portion consists of sugars like pentose and hexose sugars with some digestive enzymes (Sharma et al., 2007). Resinous part contains triterpenes (α- and β- amyrins), tetracyclic triterpenic acids (tirucall-8, 24 dien-21-oic acids) and pentacyclic triterpenic acids (boswellic acids). These boswellic acids include α-boswellic acid (α-BA) $C_{30}H_{48}O_3$, MWt 456.7; β-boswellic acid (β-BA) $C_{30}H_{48}O_3$, MWt 456.7; acetyl-β-boswellic acid (AβBA) $C_{32}H_{50}O_4$, MWt 498.74; 11-keto-β-boswellic acid (KβBA) $C_{30}H_{46}O_5$, MWt 470.69; acetyl-11-keto-β-boswellic acid (AκβBA) $C_{32}H_{48}O_5$, MWt 512.73 (Siddiqui, 2011).

Table 1. Summary of the literature on pharmacological studies with *Boswellia serrata* gum resin

Gum resin preparation /extraction	Study objective/ Model system	Results/conclusions	Reference
1) Gum resin was defatted with petroleum ether and percolated with ethanol (95 % v/v) and dried	i) Study - *Pharmacology- new NSAID's.* ii) Model-Male albino Charles Foster rats and	a) Bs-gum resin inhibited the inflammation and increased the serum glutamic-pyruvic transaminase (SGPT) and serum glutamic	Singh and Atal, 1986.

under vacuum and administered in (2 g /kg BW)	albino mice. iii) Phenylbutazone (PNB) –standard drug. iv) Carrageenan and dextran was used to induce Oedema.	oxaloacetic transaminase (SGOT) levels. b) It also showed no mortality, B.P., heart rate and responses to various autonomic agents and respiration were observed when administered intra venously up to 100 mg/kg or intraduodenally up to 500 mg/kg. c) It does not possess any analgesic or antipyretic activities. It is free from any effect on central nervous and cardiovascular systems.	
2) B. serrata gum resin dry powder labelled as BE-018.	i) Study- *therapeutic use.* ii) Model- Healthy male subjects were given 3 capsules of BSE-018 equivalent to 786 mg dry extract of BS-gum resin in fasted state or along with high fat diet.	a) Plasma samples were analysed. b) Acetyl-α-boswellic acid (AαBA) and α-BA were detectable when administered along with high-fat meal. c) First time these data reveal bioavilability of BAs after oral dosing of an extract.	Sterk et al., 2004.
3) *B. serrata* gum resin was boiled in water for 4 h, and cooled, followed by	i) Study-*Lipid profile and toxicological safety.* ii) Model- Albino rats. Macrophages	a) BS-extracts reduced serum total cholesterol and increased HDL. b) BS reduced SGPT and blood urea in the	Pandey et al., 2005.

filtering and dried into powder was used for experiments.	from rats were induced with LPS which is used as controls. iii) Rats were fed on atherogenic diet.	atherogenic diet-fed animals, thus showed strong hypocholesterolemic property.	
4) Alcoholic extract of salai guggal (AESG)	i) Study-*Cellular and humoral response*. ii) Model-Male albino Charles Foster rats; Swiss albino mice. 3) PMNL harvested from peritoneal cavity of rabbit.	a) Oral administration of AESG strongly inhibited the antibody production and cellular responses to sheep red blood cells in mice. b) AESG showed no cytotoxic effect.	Sharma et al., 1998.

Terminalia arjuna

Taxonomic hierarchy

Kingdom: Plantae
Division: Magnoliophyta
Class: Magnoliopsida
Sub Class: Rosidae
Order: Myrtales
Family: Combretaceae
Genus: *Terminalia*
Species: *T. arjuna*
Binomial name: *Terminalia arjuna* (Roxb.) Wight and Arn
English name: *Arjuna*

Stem bark

Habitat

Terminalia arjuna Wight & Arn. is a deciduous and ever-green tree, growing to 20–30 m above ground level (Dwivedi, 2007). It is distributed throughout the greater part of Indian Peninsular along rivers (Paarakh, 2010) and found in sub-Himalayan tracts of Uttar Pradesh, South Bihar, Madhya Pradesh and Deccan regions (Jain et al., 2009).

Botanical characteristics

Terminalia arjuna's stem bark is smooth, pinkish-grey from outside (Dwivedi, 2007). and shows a broad phloem comprise ceratenchyma, phloem parenchyma, phloem fibres and crystal fibres with calcium oxalate (Paarakh, 2010).

Phytochemistry of stem-bark

i) *Polyphenols*: Several polyphenolic compounds are identified from the bark of *T. arjuna* (Lin et al., 2000). Polyphenols are group of natural metabolites characterised with phenolic structural features. These exist as glycosides with sugar units or acylated sugars on different position of polyphenolic skeleton (Patnaik et al., 2007; Tsao, 2010). These compounds include bicalein, ethyl gallate, gallic acid, kaempferol, oligomeric proanthocyanidins, pelorgonidin, quercetin (Dwivedi, 2007); arjunin, arjunone, arjunolone, ellagic acid, ellagic acid derivatives and luteolin (Ahmad and Beg, 2001; Saha et al., 2012; Subramaniam et al., 2011).

Tannins: Pyrocatechols, punicallin, punicalagin, terchebulin, terflavin C, castalagin, casuariin, casuarinin (Dwivedi, 2007; Patnaik et al., 2007) are water-soluble polyphenols having sufficient hydroxyl and carboxyl groups to form strong complexes with proteins or other macromolecules (Bele et al., 2010).

ii) *Triterpenoids*: Oleanane and ursane type are pentacyclic triterpenes containing six isoprene units (Pant and Rastogi, 1979).

iia) *Oleanane derivative triterpenoids*: These are derived basically from C_{30} precursors e.g. arjunolic acid, arjunic acid, arjungenin, arjunglycosides (Subramaniam et al., 2011); arjunin, terminic acid (Dwivedi, 2007) arjunetin, termiarjunosides, olean-3β,22β-diol-12-en-28-oic acid-28β-D-glucopyranoside, terminolitin (Kaskoos et al., 2012); arjunglucoside II (Pawar and Bhutani, 2005); arjunglucosides I-III, arjunglucosides IV- V, bellericoside, crataegioside and

sericoside (Wang et al., 2010); termiarjunoside I and termiarjunoside II (Ali et al., 2006).

iib) *Ursane derivative triterpenoids*: These include 2α,3β-dihydroxyurs-12,18-dien-28-oic acid 28-O- β-D-glucopyranosyl ester, 2α,3β,23-trihydroxyurs-12,18-dien-28-oic acid 28-O-β-D-glucopyranosyl ester, quadranoside VIII, kajiichigoside F1, 2α,3β,23-trihydroxyurs-12,19-dien-28-oic acid 28-O-β-D-glucopyrano-syl ester (Wang et al., 2010a).

iii) *Phytosterol*: Sitosterol (Dwivedi, 2007).

iv) *Minerals/trace elements*: Stem bark shown to have minerals/trace elements of calcium, aluminium, magnesium, silica, zinc and copper and etc (Dwivedi, 2007).

Pharmacological studies with TA-stem bark

Pharmacological studies are being carried out extensively to investigate/validate the therapeutic properties of *T. arjuna's* stem bark (Sheng and Sun, 2011). Scientific reports demonstrating pharmacological properties including mode of action and molecular targets in related to cardiovascular system are shown in the following table.

Table 2. Summary of the literature on pharmacological studies with *T. arjuna* stem bark

Stem-bark preparation /extraction	**Study objective/ Model system**	**Results/conclusions**	**Reference**
1) Direct water, ethanolic, chloroform and petroleum ether extracts were used.	i) Study-*Cardiovascular disorders*. ii) Model-Atria of rats.	a) Ethanol extract decreased the frequency of the left atria. b) Significant positive inotropic property on rat atria *in vitro*.	Radhakrishnan et al., 1993.

2) Direct stem bark powder.	i) Study-*Cardioprotective effects*. ii) Model- Euthyroid albino rats. iii) Role of thyroid hormones.	a) High amounts of bark powder (43 mg/kg BW) should not be consumed; hepato toxicity as well as hypo thyroidism may be caused.	Parmar, 2006.
3) 50 % water-ethanolic extract.	i) Study-*Chronic heart failure*. ii) Model- Wistar albino rats were treated with isoproterenol for induction chronic heart failure. iii) Fluvastatin was drug control. iv) (500 mg/kg BW) of bark extracts given for 15 days.	a) *T. arjuna's* stem bark significantly attenuated cardiac dysfunction and myocardial injury in CHF rats possibly through maintaining endogenous antioxidant enzyme activities, inhibiting lipid peroxidation and TNF-α cytokine levels.	Parveen et al., 2011.
4) Direct stem bark powder.	Study-*Coronary heart disease*. i) Model-Wistar rats, ii) Rats induced with caffeine to cause coronary heart disease. iii) Bark powder was given 6.75 mg/kg of BW.	a) Rats fed with bark powder increased HDL; decrease in total serum cholesterol, LDL, VLDL, triglycerides, and thus protective towards CHD.	Asha and Taju, 2012.
5) Direct stem bark powder.	i) Study-*Lipid metabolism*. ii) Model-Rat. iii) Triton was induced and cholesterol diet fed	a) Stem bark powder regulated lipid metabolism in hyper lipaemic rats by decreasing lipids and	Khanna et al., 1996.

	in rats to cause hyper lipaemia.	protein levels of β-lipoproteins followed by an increase in HDL.	
6) Stem bark powder fractionated with hexane, ethyl acetate , chloro form and decoction.	i)Study-*Adult ventricular myocytes* (AVM). ii)Model- Sprague–Dawley rats. iii)AVM isolated from hearts of adult male Sprague–Dawley rats. iv) Caffeine induced for myocyte contraction.	a) *T. arjuna* aqueous extracts able to release caffeine induced myocyte contraction-suggesting TA bark is promising and relatively safe cardiotonic.	Oberoi et al., 2011.
7) Diethyl ether, ethyl acetate and ethanol fractions of *T. arjuna* stem-bark.	i) Study-*Coronary artery disease (CAD).* ii) Model-Albino wistar rats. iii) Rats induced with Poloxamer (PX)-407 to cause hyperlipidemia.	a) Ethanolic fraction showed therapeutic potential for prevention of CVD.	Subramaniam et al., 2011.
8) Ethanolic extract prepared using soxhlet method.	i) Study-Cholesterol lipoproteins, atherosclerosis and tissue lipids. ii) Model-Adult albino rabbits. iii) Rabbits fed with atherogenic and normal diet.	a) Biochemical tests for liver and renal functions and haematological parameters were conducted. No toxicity or any side effects observed in study.	Ram et al., 1997.
9) Methanolic extracts of stem bark powder.	i) Model-Human neutrophils. ii) Study-*Effects of* arjunic acid, arjungenin	a) Arjungenin exhibited moderate free radical scavenging activity.	Pawar and Bhutani, 2005.

	and their glucosides, arjunetin and arjunglucoside I on free radical scavenging action.	b) Cardioprotective action of the TA stem-bark due to the antioxidant effects of tannins.	
10) Methanol: HCl (99:1v/v) extracts were prepared using soxhlet method and aqueous extract.	i) Study-*Antioxidant effects* of *T. arjuna* and Baicalein ii) Model- Wistar rats iii) LPO, ROS scavenging activities and lipoprotein oxidation in whole human plasma was observed. iii) Female wistar rats-jejunum; liver, heart mitochondria and blood for lipid profile.	a) Baicalein recovered in native form. *T. arjuna,* reduced triglycerides, cholesterol and increased HDL; showed diuretic properties and thus showed therapeutic efficacy.	Tilak et al., 2006.
11) Ethanol extract.	i) Study-*Oxidative stress* ii) Model-Mice. iii) Activities of various antioxidant enzymes and levels of cellular metabolites in cardiac tissues were studies. iv) Oxidative stress induced by NaF. v) 50 mg/kg BW were fed for group of mice for 1 week.	a) Ethanolic extracts enhanced the cardiac intracellular antioxidant activity.	Sinha et al., 2008.
12) T. *arjuna* capsules.	i) Study-*Atherosclerosis*.	a) In cholesterol fed rabbits aorta, TA	Shaila et al., 1997.

	ii) Model- Rabbits and Human subjects. iii) Cholesterol fed rabbits and hyper lipidemic patients are used in the study.	showed regression of athero sclerotic plaque size. b) Capsules decreased cholesterol, LDL, VLDL and increased HDL, Apo AI. c) *T. arjuna* protected against the development of atherosclerosis.	
13) Direct stem bark powder.	i) Study-*Platelet aggregates and thrombogenic response on ADP induction.* ii) Model-Rabbits. iv) Rabbits treated with 250 and 500 mg/kg bark powder.	a) *T. arjuna* bark reduced the circulatory platelet aggregates and ECG abnormalities on ADP in induced rabbits. *b) T. arjuna* bark in prevention of thrombo embolic disorders in atherosclerotic subjects.	Chatterjee, 2000.
14) 90 % alcoholic extract prepared in soxhlet apparatus and dried.	i) Study-*Endogenous antioxidant status and oxidative stress induced reperfusion heart injury*. ii) Model-Wistar albino rats. iii) Isoproterenol induced for myocardial injury.	a) TAAE augmented the endogenous antioxidant compounds and prevented myocardium from ischemic reperfusion injury.	Karthikeyan et al., 2003.
15) 70 % alcohol extract	i) Study-*Hypotensive action*.	a) Presence of compounds acting	Nammi et al., 2003.

was prepared in soxhlet apparatus.	ii) Model-Dogs. iii) Dogs injected with thiopental sodium. iv) Intravenous administration of 6 mg/kg dose of extract was given to the dogs.	peripherally through adrenergic β2-receptor mechanism and/or by direct action on the cardiac muscle.	
16) Direct stem bark powder.	i) Study-*Ischemic heart disease.* ii) Model-Rats. iii) Rats- Expression in cardiac cells induced with Heat shock protein Hsp72. iv) 500 and 750 mg/kg BW, for 90 days.	a) Heart tissues were quantified of Hsp 72. b) Densitometric scanning results showed an increased expression of Hsp 72 in rats fed with TA. c) Thus *T. arjuna* provide Hsp 72 mediated cardio-protective action.	Gauthaman and Devaraj, 2003.
17) *T. arjuna* 70 % ethanol in water	i) Study-*Cardiac oxidative stress.* ii) Model- Swiss albino mice iii) Swiss albino mice are administered with CCl_4 iii) Mice fed with 50 mg/kg BW of ethanolic extracts for 7 days.	a) Histological studies were carried out on the cardiac tissues. b) *T. arjuna* treated groups restored all antioxidant activities and correlated with FRAP activity, increased GSH and decreased level of lipid peroxidation products.	Manna et al., 2007.
18) Direct stem bark powder	i) Study-*Myocardial fibrosis and oxidative stress*. ii) Model-Rats	a) Isoprenaline caused fibrosis, increased oxidative stress and cardiac hypertrophy.	Kumar et al., 2009.

	iii) Rats-induced with Isoprenaline. iv) Captopril used as the standard. v) Rats fed with 250 mg/kg BW for 28 days.	b) *T. arjuna* bark extract and captopril significantly prevented the isoprenaline - induced oxidative stress *c) T. arjuna* protected against myocardial changes stimulated by chronic β- adrenoceptor.	

Table 3. Clinical evidence for the benefits of *T. arjuna* stem bark extract in treating cardiovascular diseases

Stem-bark preparation /extraction	**Study Objective/ Model system**	**Results and conclusions**	**Reference**
19) Ethanol extract.	i) Study-*Antithrombotic properties and CAD*. ii) Model-Human subjects. iii) *In vitro* effect of TA on ADP induced platelets.	a) TA decreased platelet activation showing antithrombotic properties.	Malik et al., 2009.
20) Direct stem bark powder capsules.	i) Study-*Antioxidant and hypo cholesterolaemic effects*. ii) Model-Human subjects with coronary heart disease. iii) *T. arjuna* capsules 500 mg daily were given to the subjects.	a) Total cholesterol, triglycerides, HDL and LDL cholesterol and lipid peroxide estimated as TBARS were determined. b) *T. arjuna* tree bark powder has significant antioxidant action that is comparable to	Gupta et al., 1999.

	iv) Vit E 40 U/day is given as standard.	vitamin E. In addition to significant hypocholesterolaemic effect.	
21) Ethanolic extract (90 %) and water extract mixed at 70 ^{o}C and dried.	i) Study-*Refractory chronic congestive heart failure*. ii) Model- Human subjects with cardiomyopathy.	a) No significant clinical unwanted effect occurred during *T. arjuna* or placebo therapy. b) Patients with cardiomyopathy had undergone *T. arjuna* therapy are appeared safe and caused long lasting improvement.	Bharani et al., 1995.
22) Direct stem bark powder	i) Study-*Angina pectoris, congestive heart failure*. ii) Model-Human subjects with myocardial infarction iii) Bark stem powder of *T. arjuna*. 500 mg, 8 h was administered to the patients.	a) Prolonged administration of *T. arjuna* did not show any adverse effects on renal, hepatic, haematological parameters. b) Significant reduction in anginal frequency and improvement in left ventricular ejection fraction.	Dwivedi and Jauhari, 1997.

23) Direct stem bark powder.	i) Study-*Ischemic heart disease.* ii) Model-Human subjects with chronic stable angina having provocable ischemia. iii) 500 mg at 8 h for one week were given to patients. iv) Isosorbide mononitrate standard drug 40 mg/day used to treat ischemic heart disease.	a) The benefits of *T. arjuna* similar to that of isosorbide mononitrate. b) Limitations of this study include applicability of the results to only men with chronic stable angina but not necessarily to women as they were not studied.	Bharani et al., 2002.
24) Direct stem bark powder.	i) Study- *Endothelial dysfunction in chronic smokers.* ii) Model-Human subjects. iii) *Terminalia arjuna* therapy (500 mg q8h).	a) Baseline brachial artery reactivity studies were performed using high frequency ultrasound. b) *T. arjuna* therapy caused significant regression in endothelial abnormality in smokers.	Bharani et al., 2004.
25) Direct stem bark powder.	i) Study-*Ischemic mitral regurgitation (IMR).* ii) Model-Human subjects with (IMR) and acute myocardial infarction (AMI). iii) Stem-bark powder	a) Clinical examination with reference to risk factor and cardiovascular system carried out. b) IMR decreased; diastolic function significantly	Dwivedi et al., 2005.

	capsules (500 mg) 8 h for period of 3 months.	improved. c) Major side effect is mild gastritis.	
26) Direct stem bark powder.	i) Study-*Toxicity.* ii) Model-Patients with coronary arterial disease. iii) Dosage 1–2 g/day.	a) Fewer side effects like mild gastritis, headache and constipation.	Dwivedi, 2007

Rhizomes of *Curcuma longa* and *C. aromatica*

Turmeric *Curcuma longa* L. (Zingiberaceae) belongs to genus *Curcuma*, perennial herb with fleshy rhizomes. Andhra Pradesh stands first in large production of turmeric in India (Parthasarathy and Chempakam 2008). There are many species of *Curcuma*, the genus includes, *C. amada* Roxb, *C. augustifolia* Roxb, *C. aromatica* Salisb, *C. caesia* Roxb, *C. longa* and *C. zedoaria*, which are related to turmeric and economically useful as tribal or herbal medicine. Diarylheptanoids are the principal curcuminoids of the family (Akram et al., 2010; Ammayappan et al., 2012).

Taxonomic hierarchy

Kingdom: Plantae
Order: Zingiberales
Family: Zingiberaceae
Genus: *Curcuma*
Species: *C. longa*
C. aromatica
Botanical name: *Curcuma longa*
Curcuma aromatica
English name: Turmeric

Curcuma rhizomes

Habitat

Curcuma plant grows about 3-feet in height and possess lance shaped leaves, spiked with yellow flowers (Nagpal and Sood 2013). There are 41 species of genus *Curcuma* of which 10 are endemic and 20 are improved varieties of *C. longa* and in India (Sasikumar, 2005). India is one of the largest producers and consumer of

turmeric and it also exports to countries like Japan, Srilanka, Iran, North African countries, United States and United Kingdom (Parthasarthy et al., 2007). Within *C. longa* there are several cultivar varieties grown in different areas and these greatly differ each other from the yield of turmeric and also in its chemical composition.

Pharmacological studies with turmeric

In Indian traditional medicine, turmeric powder used for the treatment of biliary disorders, anorexia, coryza, diabetis, wounds, hepatic disorders, rheumatism, sinusitis (Chattopadhyay et al., 2004) and is reported to be anti-inflammatory, anti-fertility, anti-cancer, antioxidant, hypolipidemic and anti hepato-toxic, anti-venom, nephroprotective in nature (Yadav et al., 2013). Crude turmeric extracts reduced hepatotoxicity and oxidative stress in rats induced with liver carcinogens like *p*-dimethylaminoazobenzene and phenobarbital (Khuda-Bukhsh et al., 2008). Such medicinal properties of turmeric is majorly attributed to its chemical constituents of phenolic compounds, especially curcuminoids and terpenes. Furthermore, curcumin has been shown to have beneficial effects in neoplastic, neurological, cardiovascular and pulmonary and metabolic diseases (Aggarwal and Sung 2008). Various animal models and clinical trials demonstrated safe and non toxic nature of turmeric (Anand et al., 2007).

Phytochemistry and metabolomic studies with *Curcuma*

Phytochemical investigation of *Curcuma* species revealed the presence of various secondary metabolites including curcumin, de-methoxy-curcumin, bis-demethoxy-curcumin, zingiberene, curcumenol, curcumol, eugenol, tetra-hydrocurcumin, triethyl-curcumin, turmerin, turmerones, and turmeronols (Bizuneh Adinew, 2012), some of which are known to be biologically and medicinally important (Jiang et al., 2006). Curcumin is the most active component that gives yellow colour to turmeric, it is hydrophobic in nature and freely soluble in ethanol, alkalis, ketone, acetic acid and choloform, but insoluble in water (Gupta Sandeep et al., 2010). Aroma of turmeric comes from its volatile oil components (Singh et al., 2011).

Metabolite profile changes in the rhizomes of *C. longa* L. through the development (Xie et al., 2009). These metabolites majorly include the class of diarylheptanoids, of which mainly, curcumin, demethoxycurcumin and bisdemethoxycurcumin, occupy the major portion for attributing to turmeric's bright

yellow colour (Hiserodt et al., 1996). HPLC-MS analyses confirmed the presence of various other diarylheptanoids and their derivatives in turmeric powders (Halket et al., 2005). Methanol is shown as an appropriate solvent for maximum extraction of curcuminoids (Paramasivam et al., 2009), identitification of each curcuminoid confirmed by colour and retention times by HPLC (Revathy et al., 2011), structures of curcuminoids were described by Li et al., (2009). Presence of many different types of diarylheptanoids in the turmeric extracts is authenticated based on their MS/MS spectra and fragmentation rules (Jiang et al., 2006 a, b and Koichi Inoue et al., 2008). Electrospray ion source LC-ESI-MS-based metabolite profiling of fresh rhizomes, grown from *in vitro* micropropagation or conventional greenhouse cultivation, revealed their high variability (Ma and Gang 2006). In concordance with increase turmeric importance in spice industry and also in preparing cosmetic and pharmaceutical products, the present objective is framed, i.e., metabolite profiling of five cultivars of *C. longa* namely, Alleppey Supreme, Duggirala Red, PCT-13, Prathibha, Salem and two cultivars of *C. aromatica* cvs, Kasturi Araku and Kasturi Avidi to establish cultivar variability. Curcuminoid content in cvs. Alleppey, Salem and PCT-13 have been reported by Taylor and McDowell, (1992); Jayaprakasha et al., (2002) and Paramasivam et al., (2009). To the best of our knowledge there are no reports on the complete metabolite profiling of the selected seven cultivars of *Curcuma.*

STUDY DESIGN

Objectives of the present study

1. Phytochemical analysis of hydroalcoholic and water extracts of *B. serrata*- gum resin and *T. arjuna*-stem bark and evaluation of their antioxidant activity in human monocytic (THP-1) cells.
2. Evaluation of antiinflammatory activity of boswellic acid mixed-fraction (BAM) isolated fraction of *B. serrata* gum resin and TA-stem bark extracts on human monocytic (THP-1) and human aortic endothelial cells (HAECs).
3. Evaluation of antithrombotic property of *B. serrata*-gum resin and BAM using human platelets and coagulation factors.
4. LC-MS based metabolite profiling of cultivars of *Curcuma longa and C. aromatica* and the use of metabolite profile for constructing cultivar variability.

Significance of metabolomics

►Metabolomic study is the emerging platform involves the quantitative and qualitative analysis of specific set of metabolites present in cell, tissue or organism and well being used in discovery of lead compounds, drug discovery and quality control of medicinal plants (Shyur et al., 2013).

►Metabolite profiling has a number of applications include, fingerprinting of species, genotypes or ecotypes for taxonomic or biochemical purposes; monitoring the behaviour of specific class of metabolites upon physical/chemical/exogenous stimuli; studying the developmental processes such as symbiotic association; comparing and contrasting the metabolites between the mutant and wild type (Sumner et al., 2003).

Metabolite fingerprinting of plant secondary metabolites

Metabolite fingerprinting had been done with various genotypes of *Arabidopsis thaliana* (Scholz et al., 2004); transgenic *Lactuca sativa* L. (Garratt et al., 2005); Malaysian *Zingiber officinale* Roscoe (Mahdi et al., 2010); *Sedivitax gocce*, *Finocarbo Plus opercoli*, *Sollievo Bio tavolette*, *MiniMas opercoli* and *Ruscoven gocce* (Luisa et al., 2011); *Angelica sinensis* (Qian et al., 2013); salt stressed *Solanum lycopersicum* (Smith et al., 2003); *Panicum miliaceum* L. (Kim et al., 2013); *Withania somnifera* (Chatterjee et al., 2010); *Curcuma* species (Jung et al., 2012; Halket et al., 2005) etc.

Metabolomics technology applying to medicinal and aromatic plants is advantageous as it permits the collecting information on various metabolites that have importance in pharmacology culinary and cosmetic areas (Okada et al., 2010). Medicinal plants are natural source of pharmaceutical drugs, the composition of metabolites vary with developmental stage and change in the environment (Commisso et al., 2013). The identification of metabolites is another daunting task due to their chemical diversity. Several databases such as Mass Bank, Metlin, MS2T are available online, but still the information provided by these databases are inadequate. Accurate mass determination, particularly, fragmentation patterns obtained by MS/MS with combined effects of electrospray ionization time-of-flight mass spectrometry have been helpful for identification of phenolic compounds, terpenoids, flavonoids from the extracts.

Hyphenated techniques, liquid chromatography-mass spectrometry (LC-MS)

At the early stages of the invention of mass spectrometry, the applications of such techniques were limited to mass determination and purity of the sample (Griffiths, 2008). Mass spectrometry (MS) is now around one hundred years old, undergoing rapid development, and extended use of its application for biological specimens, particularly of low molecular weight compounds. Developing the electrospray ionization (ESI), has further taken lead to its application in research, pharmaceutical industry and clinical laboratories (Grebe and Singh 2011). The coupling of MS with LC (LC-MS) was an obvious extension during 1990s and started playing an important role in areas of clinical biochemistry (Pitt, 2009). Mass spectrometers operate by converting the molecule to ionised state, during the ionisation process the fragment ions produced are separated based on their mass to charge ratio (*m/z*). A mass spectrum is a plot of ion abundance verses m/z (Glish and Vachet 2003).

Electrospray ionization (ESI)

The ionised analytes are then transferred into high vacuum of the mass spectrometer, the energy imparted on the analyte causes the fragmentation of molecules, including the detection of positive and negative ions during the analysis. In the MS technique, ESI is the most commonly used ion source for the bio-molecules (Dwivedi et al., 2011).

Mass analyzers

After ions are formed in the source region, they are accelerated into mass analyzers by electric field. Ultimate target analytes is achieved with quadrupole time-of-flight mass spectrometer (QTOF) for single MS as well as MS/MS operation modes, with sensitivity, high resolution and high mass accuracy for both precursor and fragment ions (Lacorte and Fernandez-alba 2006).

Mobile phase

Typical solvents like water, acetonitrile, methanol, ethanol, chloroform that are used in reverse and normal phase LC are compatible with ESI. Certain buffers containing inorganic ions such as phosphate and sodium acetate should be avoided, since they cause significant suppression of ions and get contaminated with MS adducts. Buffers

such as ammonium acetate, ammonium formate or ammonium bicarbonate is generally compatible with MS (Pitt, 2009). Flow rate of the mobile phase also determines the resolution of metabolite separation.

Oxidative stress and markers

Lipid peroxidation and consequences of lipid peroxides

Lipid peroxidation is one of the most important organic expressions of oxidative stress that promote the pathogenesis of many diseases, including cardiovascular diseases, (Simopoulos, 2008). Lipids of membranes or circulation with high polyunsaturated fatty acids (PUFA) and their derivatives, sphingolipids, sterol lipids and saccharolipids (Fahy et al., 2005) are vulnerable to oxidation, yielding to lipid hydroperoxides (Dixon et al., 1998) as shown in Fig. 3.

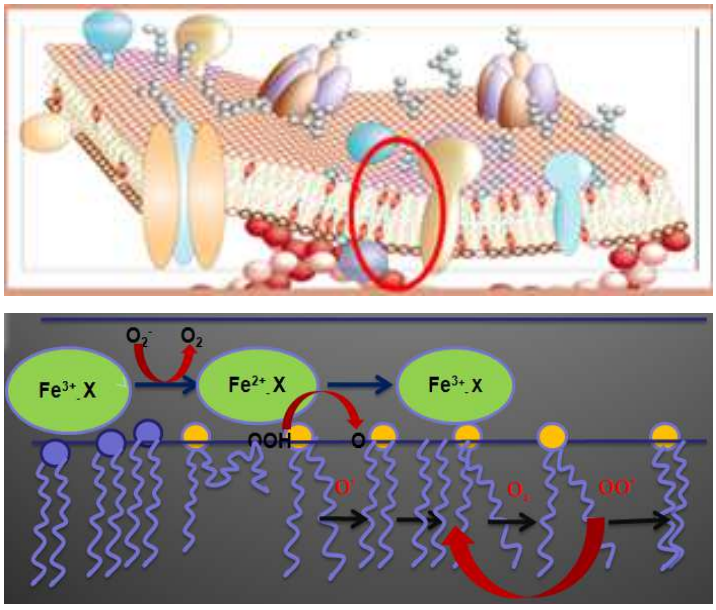

Figure. 3. A lipid bilayer of biological membrane having saturated and polyunsaturated fatty acids. Mechanism for initiation of lipid peroxidation. Ferrous iron initiate lipid peroxidation in the presence of oxidant either molecular oxygen or H_2O_2.

Thus, the lipid peroxidation occurs in plasma membrane and other organellar membranes (Pizzimenti et al., 2010). Lipid peroxides are end products of lipid peroxidation and their increased levels cause cellular damage, such peroxidation in the blood vessel causes endothelial injury and promotes atherogenesis by inducing platelet aggregation, there by triggering a cascade of events involved in the formation

of atheromatous plaque (Yagi et al., 1988). So research on oxidation of unsaturated phospholipids has gained significant importance.

Human cellular models to study the events leading to atherosclerosis

Human THP-1 monocytic cells are well accepted model system to study monocytic responses for the following reasons :

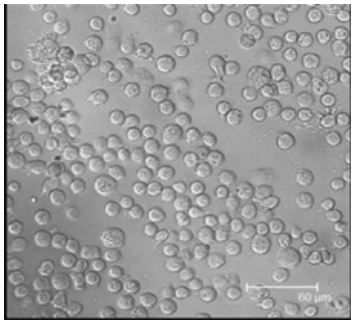

► Highly differentiated cells with phagocytic properties.
►Show less variability compared to monocytes isolated from blood and high throughput assays are feasible as these can be cultured.
►THP-1 cells serve as the best *in vitro* model system to understand monocyte and macrophage biology as it relates to human diseases and is the most commonly used model for foam cell formation. THP-1 cells reported to produce proinflammatory cytokines, chemokines similar to peripheral blood monocytes, in response to LPS stimulation and therefore are also used as model system for direct testing of compounds/metabolites for anti-inflammatory effects.

Human aortic endothelial cells (HAECs)

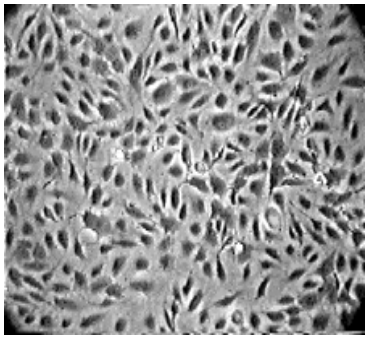

►Endothelial cells have been considered in medicine and physiology due to its important role in separating blood and vessel wall tissues and endothelial function/dysfunction are strongly associated with physiological as well as pathological processes respectively.
►They are capable to proliferate for many generations and sustain their features and seems to have homogenous morphology as a monolayer at high level of confluence.

Platelets role in atherosclerosis

In response to vascular injury platelets form mechanical plugs, followed by activation, where the platelets play major role in haemostatic process and thrombus formation. Platelet-monocyte interactions, inflammatory cytokines, chemokines, and

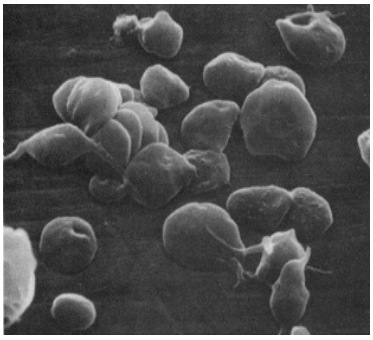

P-selectin play significant role in development of atherosclerosis (Huo and Ley 2004).

High incidence of thromboembolic complications found in rheumatism and atherosclerosis, of which chronic conditions play important role in thrombus formation (Angelov, 1975). Diverse stimuli activate platelets, mediated by binding to specific platelet receptors. Examples of stimuli include collagen, thrombin or trypsin, ADP, serotonin, epinephrine (Zucker and Nachmias, 1985) and etc. These stimuli produce changes within the platelets and finally bind to fibrinogen. This connection link between platelet via fibrinogen brings about platelet aggregation (Kamath et al., 2001). ADP is actively secreted from platelet granules and also passively released from damaged erythrocytes and endothelial cells (Woulfe et al., 2001). ADP causes number of intracellular events like calcium influx, mobilization of calcium stores, inhibition of adenyl cyclise and increase intracellular calcium (Daniel et al., 1998). Thrombin is primarily known as inducer of blood coagulation and platelet activation. Activation of platelets vary with respect to different concentrations of thrombin, lower doses induce platelet activation with small percentage of platelet apoptosis, whereas higher doses trigger platelet apoptosis (Leytin et al., 2007).

Stimulants for oxidative stress

Induction of oxidative stress by using hydrogen peroxide (H_2O_2)

H_2O_2 is an important representative ROS that arises during the aerobic respiration process. It induces a diverse set of physiological responses and also deleterious effects including DNA damage, mutagenesis, cell death and so on (Asad et al., 2004). H_2O_2 induced oxidative stress in cell systems can be used as an experimental system to test efficacy of antioxidants. Teramoto et al., (1999), investigated the effect of H_2O_2 induced ROS in human lung fibroblasts cells and reported that lower concentrations of ROS ranging from 10 µM to 100 µM, induce apoptosis, whereas higher concentrations ranging from 1 mM to 10 mM induce necrosis. Similarly another group showed that 25 and 50 µM H_2O_2, in human caucasian hepatocyte carcinoma cells (HepG2 cells), can induce DNA damage significantly (Benhusein et al., 2010). Another research group Malinouski et al., (2011) showed that

extracellularly added H_2O_2, penetrated to all the compartments of the target cell within 2 to 4 min and oxidized directly.

Detection and quantification of cellular ROS

Studies aiming at oxidative stress investigated using the fluorescent probe 2,7-dichlorofluorescin diacetate (H_2DCFDA), for the detection of H_2O_2 in cells. H_2DCFDA is a non-fluorescent lipophilic ester that easily diffuses across the plasma membrane and passes into cytosol where it gets rapidly cleaved by unspecific esterases to form DCFH, which up on further oxidation by fenton reaction gets converted to highly green fluorescent dichlorofluorescein (DCF) (Cohn et al., 2008), which can be excited at excitation 488 nm and measured at emission 525 nm.

Cellular ROS scavenging mechanisms

Catalase (CAT)

Catalase has been considered to be the major primary enzyme that scavenges intracellular H_2O_2 (Cohen and Hochstein 1963). The enzyme is localized primarily in matrix of peroxisomes in mammalian cells and is present in all tissues, particularly observed in erythrocytes, liver, kidney and adipose tissues (Kenneth, 2004) but relatively smaller amounts are found in heart tissue therefore, it is highly sensitive to oxidative injury. Alternations of catalase activity are highly observed and are associated with disease and stress conditions. CAT has one of the highest turnover rates for all enzymes: one molecule of catalase can convert approximately 6 million molecules of hydrogen peroxide to water and oxygen per minute (Rahman, 2007). The cellular catalase activity can easily be determined using whole cell homogenates by measuring absorbamce at λ 240 nm and monitoring exponential decay of millimolar amounts of H_2O_2.

Glutathione peroxidase (GPx)

Glutathione peroxidises are members of the family of antioxidant enzymes discovered by Mills in 1957, those scavenge harmful peroxides in the presence of reduced glutathione and protects the membrane and other cellular components against oxidative damage. There are four isoforms of glutathione peroxidases (GPx-1, GPx-2, GPx-3 and GPx-4) containing selenocysteine at the active site. GPx-1 can

metabolize hydrogen peroxide and a range of organic peroxides, including cholesterol and long-chain fatty acid peroxides. GPx-2 occur in cytosol, has 60 % sequence identical to GPx-1 and its mRNA can be found in liver and large intestine but not in other organs. They can reduce hydrogen peroxide or fatty acid hydroperoxides rapidly but not phospholipid hydroperoxides. GPx-3 is a glycoprotein, occurs in plasma, with an extracellular function and distinct from GPx-1 and also found in epithelial cells of kidney. GPx-4 localized in peroxisomes and different from other GPx in being monomeric form (Arthur, 2000).

Measurement of GPx activity in different disease states suggest that GPx-1 involved in cell antioxidant systems (Arthur, 2000). It also plays an active role in detoxification of oxidant damage to DNA, organic epoxides, lipid hydroperoxides and unsaturated aldehydes (Gago-Dominguez et al., 2007), finally it is found to be an indicator for oxidative status assessment (Gomez-Espina et al., 2012). Thus it is very much convinced that CAT and GPx are the two routes and equally involved for H_2O_2 breakdown/detoxification (Gaetani et al., 1989 and Baud et al., 2004).

Microbial products function as adjuvants and enhance specific immune responses in humans e.g., Lipopolysaccharide, viruses, fungal or parasitic antigens. Such stimuli cause both transcription and translation of TNF-α release into circulation while some remain in cell-associated transmembrane form (Feldman et al., 2000).

Humans are sensitive to LPS, at dose as low as 1 to 2 µg caused increase in plasma TNF-α, IL-6 peak levels within 2 h (Dinges and Schlievert 2001), and higher doses caused rapid physiological response in humans including (fever, tachycardia and hypotension). In case of mice, inflammatory responses are found to be similar to humans (Copeland et al., 2005). LPS dose response studies in THP-1 cells revealed maximum stimulation of TNF-α in the culture supernatants for 4 h incubation at an LPS concentration 50 µg/L (Singh et al., 2005).

Inflammatory markers in monocytes

Secretion of cytokines by activated monocytes plays a pivotal role in the progression of inflammatory states and also leads to secondary mediators of inflammation. Activated monocytes/macrophages produce TNF-α, IL-1β, IL-4, IL-13, IL-6, IL-12, IFN-γ and IL-10 (Osterud and Bjorklid, 2003) as shown in Fig. 4.

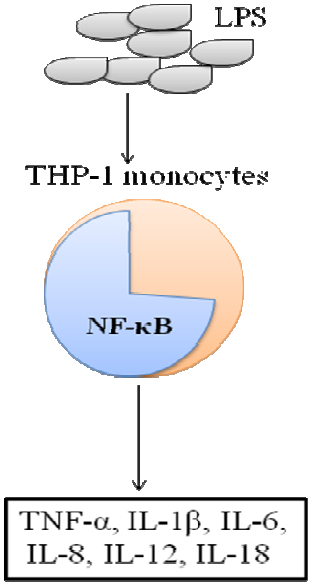

Figure. 4. LPS stimulation of monocytes produce TNF-α and other related cytokines, which further activate inflammatory cascade.

Tumor necrosis factor (TNF)-α

Cell to cell communications is the most important phenomenon in order to carry out cellular functions in the complex organisation of the body. Signals must be sent and received by precisely. Soluble polypeptide messenger proteins, called cytokines, are responsible for such signal transduction. Tumor necrosis factor-α (TNF-α) is a multifunctional cytokine produced by various cell types, including basophils, B lymphocytes, astrocytes, keratinocytes, but primarily secreted by monocytes and macrophages and plays a key role in host defense and immunosurveillance against infection and also strongly involved in chronic inflammatory diseases (Tabaka et al., 2012). It acts as a potent agonist in the activation of endothelial cells (Imaizumi et al., 2000) in response to endotoxin induced inflammation. Therefore it is named as endotoxin induced serum factor (Adams and Czuprynski 1990).

TNF-α has become a major target of numerous pharmaceutical investigations. Grattendick et al., (2008) screened three anti-TNF-α drugs, namely, Etanercept, Infliximab and Pirfenidone, based on their inhibitory effect on release of TNF-α into the medium by LPS induced THP-1cells. Compounds that control TNF-α production could have the therapeutic possibilities as they can downstream inflammatory responses, particularly of endothelial cells (Fig. 5).

Proinflammatory effect of TNF-α in the lumen of blood vessel

TNF-α directly increases endothelial permeability both *in vitro* and *in vivo* (Ishii et al., 1992) and thereby associated with atherosclerosis. It also associated with the increased risk of thromboembolic consequential complications by increase in circulatory levels of IL-6 (Ridker et al., 2000), C-reactive protein (Hirschfield and Pepys 2003), fibrinogen (Koopman et al., 1997; Sabeti et al., 2005); intercellular adhesion molecule-1 (ICAM-1) (Blankenberg et al., 2003) and many other markers.

Further the role of TNF-α in pathophysiologic effects of atherosclerosis is been precisely demonstrated using knock out mouse models of apoE-/- and apoE-/- / TNF-α -/-. Upregulation of ICAM-1, VCAM-1 and MCP-1 on endothelium of vessel wall in apoE-/- mice was much more than in apoE-/- / TNF-α -/-, which demonstrated TNF-α dependent recruitment of monocytes/macrophages at the site of lesions. Macrophages from apoE-/- mice increased scavenger receptor expression than those from apoE-/- / TNF-α -/- shows that TNF-α promotes foam cell formation and finally concluded that TNF-α has atherogenic property (Ohta et al., 2005).

Association of chemokines with atherosclerosis

Chemokines mainly are responsible for cellular trafficking, and they play pivotal role in the development of vascular diseases by being associated with vasodysregulation, vessel-wall remodelling and atherothrombotic complications (Weber, 2008). The best characterized members of chemokine family, monocyte chemoattractant protein-1 (MCP-1) and IL-8 are induced primarily by LPS and TNF-α in a number of cell types, including monocytes and endothelial cells (Yeh et al., 2001).

MCP-1 and IL-8 pause the rolling monocytes to adhere on monolayers of endothelium by expressing E-selectin, VCAM-1 and MCP-1. These markers found to be highly expressed in human atherosclerotic lesions and thus considered as key players in monocyte recruitment into arterial wall (Braunersreuther et al., 2007). This concept was further experimentally evidenced using human apo B transgenic (HuBTg) mice with MCP-1 gene knockout and fed with high fat diet. These mice showed minimal infiltration of macrophages and protection from atherosclerotic lesion without altering lipid metabolism (Gosling et al., 1999). Role of MCP-1 in atherogenesis was also assessed through autoradiography studies in rabbits fed with atherogenic diet and by injecting radiolabelled MCP-1 intravenously showing its

localization in arterial lesions (Ohtsuki et al., 2001). IL-8 also showed as mediator of angiogenesis, it was found in homogenised tissues obtained from the patients undergoing surgery for coronary atherectomy. IL-8 shown to be expressed in plaque-macrophages as well as circulating monocytes (Simonini et al., 2000).

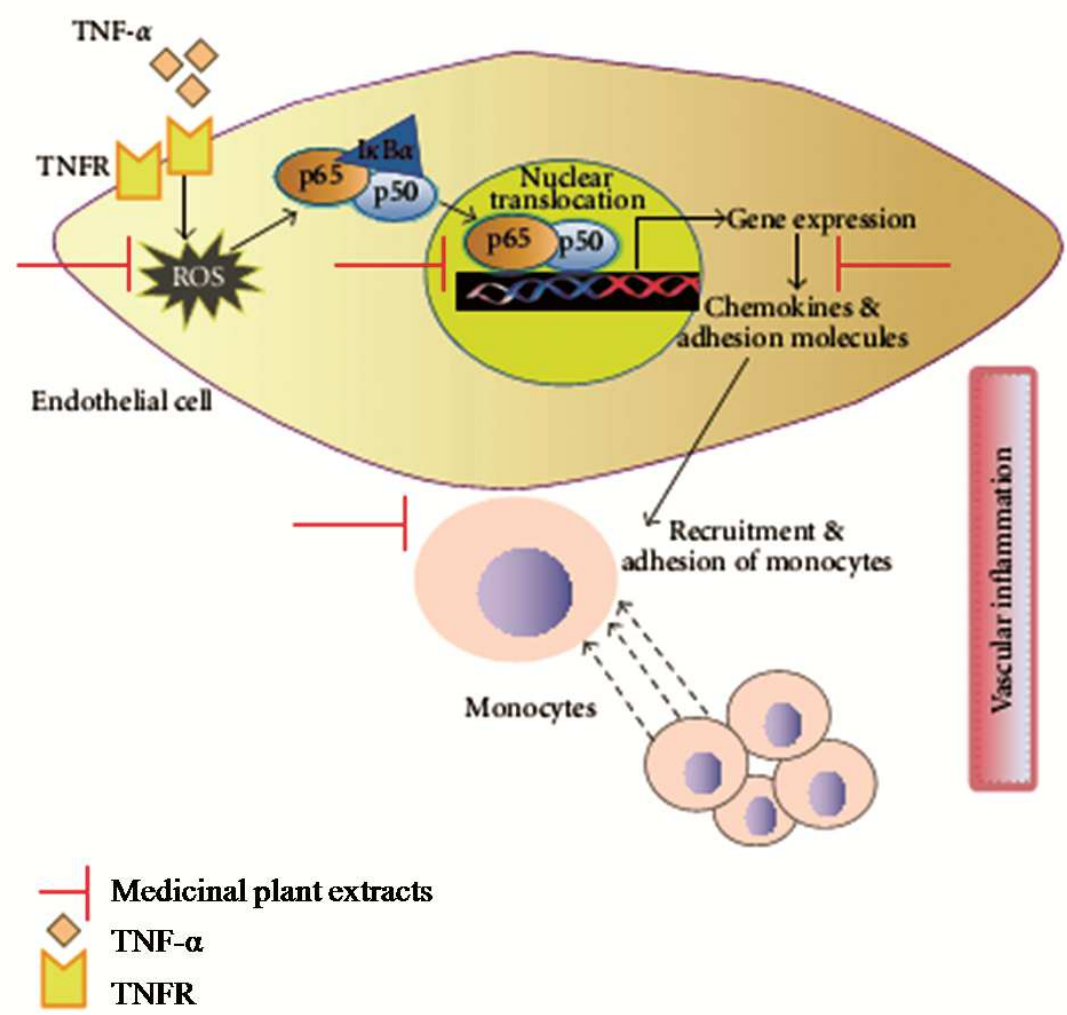

Lee et al., 2011.

Figure. 5. Schematic diagram showing signalling pathway medicinal plant extracts against TNF-α induced vascular inflammation. Medicinal plants may protect vascular inflammation through suppression of ROS production and the expression of NF-κB related adhesion molecules in endothelial cells, which in turn, prevent monocyte adhesion to endothelial cells.

Cell adhesion molecules and scientific evidences supporting their pathogenic roles

Cell adhesion molecules (CAMs) are transmembrane proteins that mediate adhesion and interactions between cells or cell and extra-cellular matrix (Ling et al., 2012).

Vascular cell adhesion molecule (VCAM)-1

VCAM-1 is one of the important markers indicating atherogenesis and it is expressed on the surface of endothelial cells, promote monocyte accumulation in arterial intima (Ley and Huo 2001). Several lines of evidence indicated association of VCAM-1 with atherosclerosis including from the investigations on apoE -/- mice fed with western type diet. Electron microscope images of apoE -/- mice aorta showed the presence of number of VCAM-1 positive cells in advanced aortic lesions and fatty streaks (Nakashima et al., 1998).

In another study, hypercholesterolemia was induced in LDLR-/- mice. LPS was used for systemic activation of endothelium. VCAM-1 and ICAM-1 expressed in hypercholesterolemia mice and in rabbits though their magnitude varied. VCAM-1 was restricted to the central region of the lesions whereas ICAM-1 expressed in non-aortic regions. E-selectin was not detected in aorta of mice and rabbits. Therefore VCAM-1 expression is considered as phenotypic marker to atherogenesis (Iiyama et al., 1999).

TNF-α, IL-1β and LPS endotoxin have the capacity to induce with regard VCAM-1 expression in human pulmonary and human umbilical vein endothelial cells, of which, TNF-α was the most potent signal for VCAM-1 expression in both cell lines (Sano et al., 1997).

Intercellular adhesion molecule (ICAM)-1

Association of ICAM-1 with atherosclerosis is showed through knockout mice studies using models apoE-/-/ICAM-1-/- and apoE-/-/ICAM-1+/+ and fed with normal diet. Heart homogenates and aorta were cross sections of second group showed the presence of ICAM-1 expression strongly on endothelium (Kitagawa et al., 2002).

E-selectin

Selectins, the family of cell adhesion molecules, act as mediators for the firm attachment of leukocytes to endothelial cells. E-selectin, L-selectin and P-selectin are closely related cell-surface molecules (Tedder et al., 1995). L-selectin expressed on surface of leukocytes, P-selectin released from storage granules of platelets, E-selectin found only on endothelial cells stimulated by inflammatory cytokines. Immunohistochemical analysis with mice models LDLR-/-, P/E-/- and LDLR-/-, P/E+/+ fed with atherogenic diet for 8, 22 and 37 weeks indicated that both P and E-selectin play important role in early and advanced stages of atherosclerotic lesion development (Dong et al., 1998).

Transcription factor NF-κB p65 and its phosphorylation

The transcription factor, NF-κB, consists of homo or hetrodimers of Rel family proteins, namely p50/NF-κB1, p52/NF-κB2, p65/RelA and c-rel. In most of the cell types, these dimers retain in the cytoplasm by a specific IκB inhibitor proteins. Upon stimulation, these inhibitor proteins (IκB) become hyperphosphorylated, ubiquitinated and subsequently degraded in the proteasomes, thereby allowing the translocation of dimers towards nucleus where they bind to specific DNA nucleotide sequences to modulate the expression of target genes (McDonald et al., 1997). Wide variety of genes and those genes encode cytokines, chemokines, cell adhesion molecules, intravascular coagulation and other factors are regulated by NF-κB and thus considered as an effective therapeutic strategy for combating various chronic inflammatory diseases (Pascale et al., 2009; Liu and Malik 2006). Immunofluorescence and immunohistochemical techniques showed that NF-κB activation is detected in atheromatous area of atherosclerotic lesion, but not in normal cells, suggesting the functional importance of this transcription factor in the development and or progression of atherosclerotic lesions (Brand et al., 1996). The most abundant and well studied complex is p65/p50 of which p65 posttranslational modification is critical for regulating NF-κB transcriptional activity, whereas p50 lack transactivation domain which can be readily detected in resting cell nuclei (Fig. 6) (Ghosh and Karin 2002).

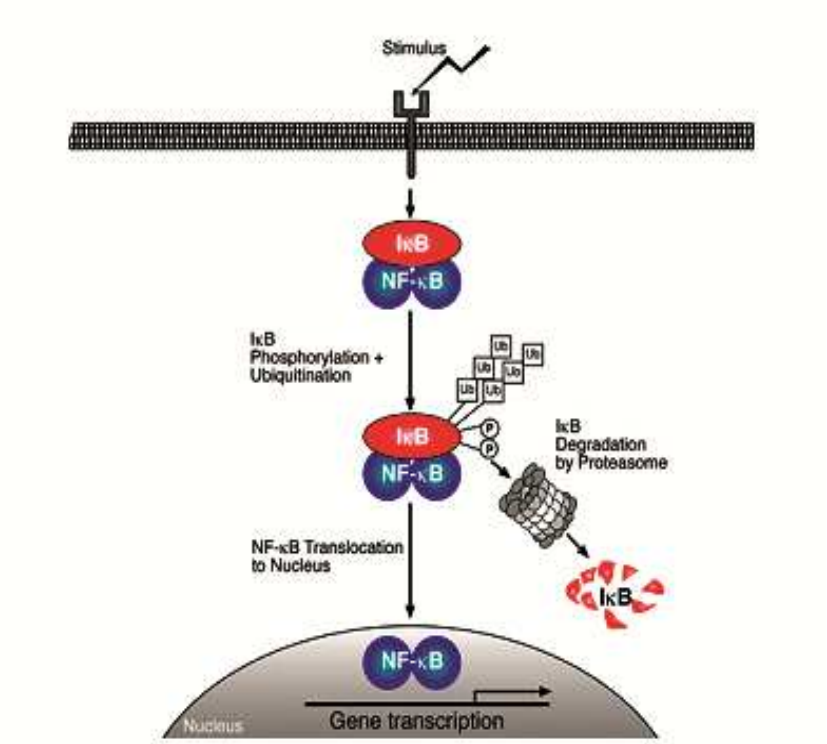

Beinke and Ley 2004

Figure. 6. Model of the NF-κB activation pathway. Various stimuli induce phosphorylation and subsequent polyubiquitination of IκBs, which are targeted for degradation and associated NF-κB dimmers are thereby released to translocate into the nucleus, where they modulate their expression of genes.

Thrombosis

Plasma coagulation time periods

Prothrombin time (PT) and activated partial prothrombin time (APTT)- clinical evidence

PT and APTT are used to assess the coagulation system of patient population. Patients with more thromboembolic events namely thrombosis or bleeding disorders are shown to have short APTT values (Korte et al., 2000). Studies with non-human primates fed with high or low fat concluded that low fat diet enhanced anticoagulant response to thrombin (Lentz et al., 2002). Single apoE-/- and double knockout mice apoE-/-, FVIII-/- were generated and fed with normal and hypercholesterolemic diet and observed for aortic lesions. ApoE-/- deficient mice contained abundant fibrinogen with adhered platelets, whereas apoE-/-, FVIII-/- mice devoid of

fibrinogen and no platelets which demonstrates the activation of intrinsic pathway in early stages of atherogenesis (Laschet et al., 2005).

Tissue factor, formerly known as thromboplastin expressed both in vascular and non-vascular cells. Under physiological conditions endothelial cells do not express tissue factor but induced upon stimulus with cytokines, histamine, thrombin and other agents (Steffel et al., 2006). Intrinsic and extrinsic pathway converges at activation of factor X to Xa. To determine thrombin's role in induction of inflammatory process, atherosclerosis established ApoE-/- mice are divided into three groups, one of them received chow diet; other with chow diet and rivaroxaban (FXa inhibitor) and third group with inhibitor only. Mice undergone diet with inhibitor did not significantly alter progression of atherosclerotic plaque whereas the group that received only rivaroxaban showed significant reduction in erosions and downregulates mRNA expression of inflammatory cytokines in aortic tissue (Zhou et al., 2011) indicating the importance of coagulation cascade associated with atherosclerosis Fig. 7.

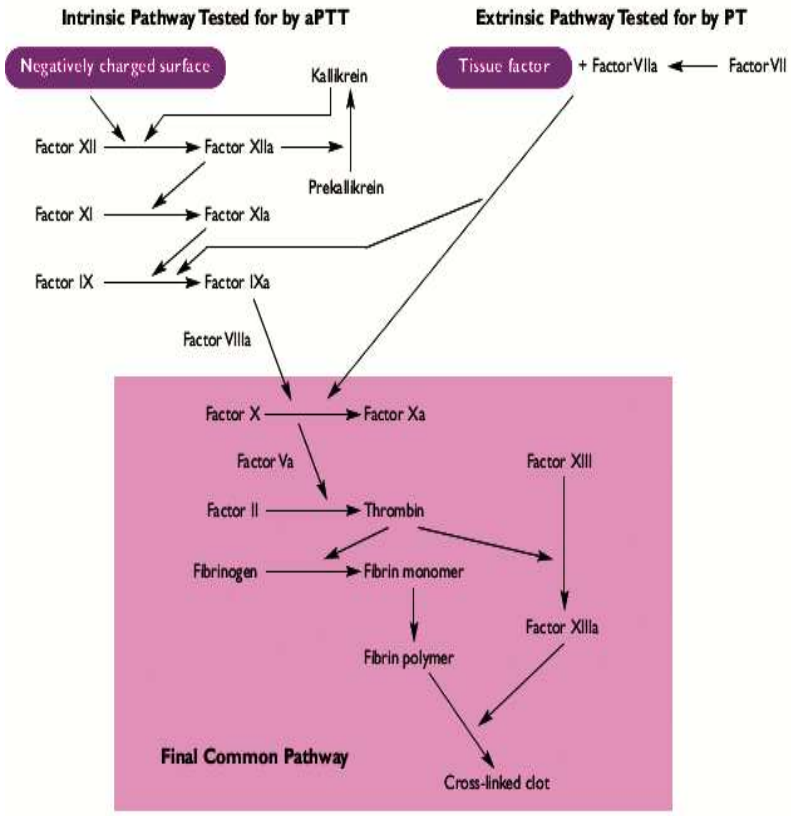

Lefkowitz. J. B. 2008

Figure. 7. A model of the classic extrinsic and intrinsic coagulation pathways.

Chapter 2

MATERIALS and METHODS

Materials

Collection of plant materials and identification

The plants materials of *Boswellia serrata*–gum resin (Fig. 2.1) voucher specimen (# 528) and *Terminalia arjuna*-stem bark (Fig. 2.2) voucher specimen (# 428) were collected from Seshachalam hills, part of the eastern ghats of Andhra Pradesh and authenticated by Dr. K. Madhava Chetty and deposited at Sri Venkateshwara University Herbarium, Tirupati, India. The stem bark was cut into pieces; sun dried and ground into fine powder, similarly dried gum was ground to fine powder with the help of mortar and pestle and stored in an air tight container.

Fresh rhizomes (Fig. 2.3) from four cultivar varieties of *Curcuma longa* (cvs. Duggirala Red, PCT-13, Prathibha, and Salem) and two of *C. aromatica* (cvs. Kasturi Araku and Kasturi Avidi) were provided by Turmeric Research Station-Kammarpally of A.P. Horticultural University. *C. longa* cv. Alleppey Supreme was provided by Indian Institute of Spice Research, Calicut (IISR) Kozhikode, Kerala.

Fig. 2.1 *B. serrata* gum resin

Fig. 2.2 *T. arjuna* stem-bark

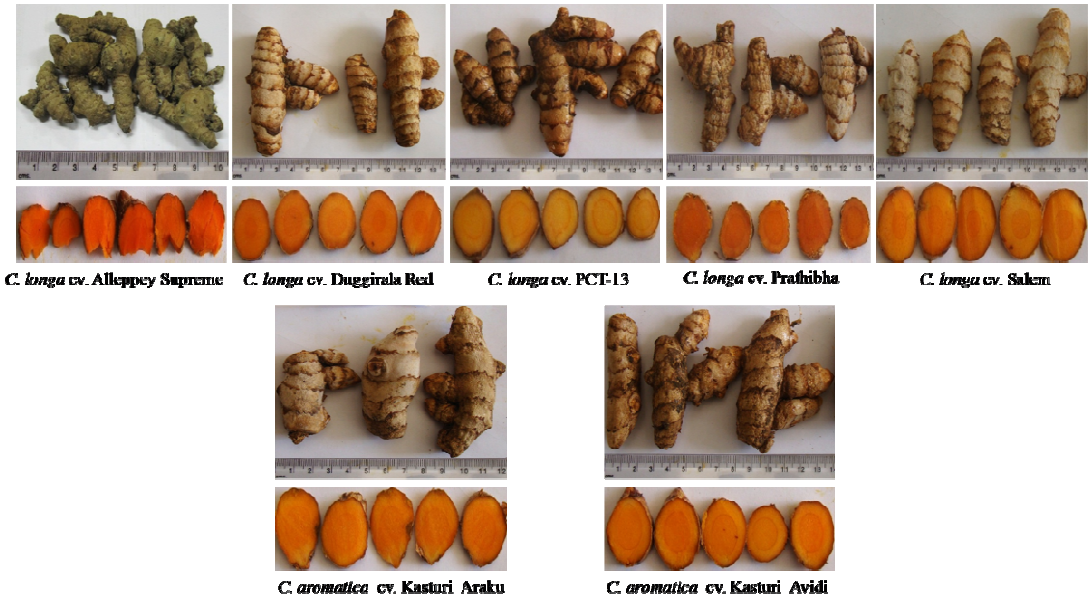

Fig. 2.3 Rhizomes and cross sections of *Curcuma* cultivars

Chemicals

Ascorbic acid, butylated hydroxytoulene (BHT), 3-(4,5-dimethylthiazol-2-yl)- 2,5-diphenyltetrezolium bromide (MTT), sodium acetate trihydrate, 2,4,6-tripyridyl-s-triazine (TPTZ) were from Hi-media, India. α-boswellic acid, β-boswellic acid, 3-O-acetyl-α-boswellic acid, 3-O-acetyl-β-boswellic acid, 3-acetyl-11-keto-β-boswellic acid, 11-keto-β-boswellic acid, curcumin, de-methoxycurcumin, bis-demethoxycurcumin were purchased from Chromadex, CA, USA. Adenosine diphosphate (ADP), 2,7-dichlorofluorescin diacetate (H_2DCFDA), 4-fluoro-4'-hydroxy benzophenone, gallic acid (GA), glutathione, human tumor necrosis factor (TNF-α), HMG-CoA reductase kit, lipoprotein lipase (LpL; bovine milk), lipopolysaccharide-*Escherichia coli* (LPS), methanol, nicotinamide adenine dinucleotide phosphate (NADPH), N,O-bis (timethylsilyl) tifloro acetamide (BSTFA), Orlistat, *p*-nitrophenyl butyrate, ursolic acid, 2-thiobarbituric acid (TBA), trimethyl chlorosilane (TCMS) and trypan blue were purchased from Sigma–Aldrich (Germany). Penicillin-streptomycin, RPMI 1640 medium, L-glutamine, fetal bovine serum (FBS), low serum growth supplement (LSGS), M200 medium, trypsin neutralizer, trypsin EDTA were purchased from Invitrogen (Germany). CD106-FITC, CD62E-PE antibodies, TNF-α ELISA kit from BD Bioscience (USA). Ferric chloride, hydrogen peroxide (H_2O_2) obtained from Merck. Heparin purchased from Samarth Life Sciences (Mumbai). Human blood clotting factors IXa, Xa, XIa, XIIa and VIIa purchased from American Diagnostic Inc., Stanford. All other reagents used were of analytical grade.

Methods

Preparation of medicinal plant extracts

Hydroalcoholic extracts (Sharma et al., 2001) were prepared by infusion of 1g dried gum resin of *B. serrata* or stem bark powder of *T. arjuna* with 20 mL of 80 % (v/v) ethanol and by heating at 40 ^{o}C with continuous stirring for 5-6 h, i.e., until the extract volume attains 1/5th of initial volume. Water extracts (Tilak et al., 2006) were prepared by soaking 1 g powder of respective plant material in 4 mL of distilled water for overnight at room temperature. Both the extracts were centrifuged at 10,000 rpm for 10 min at room temperature and the supernatant volumes were

recorded for each time of the fresh preparation and normalized to express the extract dry weight for various bioassays.

The supernatants were subjected to complete dryness under vacuum. Dry weight of the extracts was determined to calculate the yield. Concentration of the extracts in the assays was represented based on their respective dry weights. The yields obtained for *B. serrata* gum resin powder were 4.8 % (w/w) and 5.2 % (w/w) for hydroalcoholic and water extracts, respectively. Yields obtained were 15 % (w/w) and 5 % (w/w) for *T. arjuna* hydroalcoholic and water extracts, respectively.

Methanolic extracts of fresh rhizomes of all seven cultivars of *Curcuma* were prepared according to Jiang et al., (2006). Fresh turmeric rhizomes of *Curcuma longa* cvs. Alleppey Supreme, Duggirala Red, PCT-13, Prathibha, Salem and *C. aromatica* cvs. Kasturi Araku and Kasturi Avidi were ground using a mortar and pestle in presence of LN_2. The ground material was soaked in LC grade methanol (1g fresh wt/ 2 mL), sonicated for 30 min and extracts were centrifuged at 1500 rpm for 25 minutes. Finally the collected supernatant was filtered through 0.2 µm PTFE membrane filter. Filtered extracts were kept in -20 ºC until analysis.

Phytochemical analysis of plant extracts

Determination of total polyphenols

Preliminary phytochemical screening was done to quantitate total amounts of polyphenols, flavonoids and triterpenoids in the extracts. The content of the total polyphenols was determined in plant extracts by a spectrophotometric method using Folin-Ciocalteu method as described in Singleton (1999). Assay of total polyphenols by Folin-Ciocalteu reagent (FC) relies on the transfer of electrons in alkaline medium from phenolic compounds to phosphomolybdic / phosphotungstic acid reagent to form blue coloured complexes. We have used this assay to assay total phenolic compounds extracted into hydroalcoholic and water extracts of *B. serrata* gum resin and *T. arjuna* stem-bark. This assay initially was predesigned for analysis of protein containing the active tyrosine (containing phenol group) residues, and it is non-specific to phenolic compounds as it can be reduced by many non-phenolic compounds like vitamin C and other trace elements (Huang et al., 2005).

Preparation of solutions

Standard Gallic acid compound: For calibration, gallic acid of 0.5 g was dissolved in 1 mL of 80 % ethanol and diluted to 10 mL volume with water, and the stock was stored in a refrigerator and used within 2 weeks.

Sodium Carbonate Solution: Anhydrous sodium carbonate of 200 g dissolved in 800 mL of water and heated slightly for solubilisation, after cooling, added a few crystals of sodium carbonate and left it at room temperature for 24 h, then filtered using whatman paper, made up to 1 L and stored at room temperature.

Working solutions of Gallic acid with concentrations of 0, 50, 100, 150, 250, and 500 µg/mL were prepared from the stock of 500 mg/L. Aliquots of 20 µL from each of the working solutions or different aliquots of plant extracts into separate tubes, 1.58 mL of water was added to each tube, followed by adding 100 µL of FC reagent. After incubation for 30 sec to 8 min, 300 µL of sodium carbonate solution was added, and vortexed to mix. Left the solutions at 20 ^{o}C for 2 h and the absorbance of the reaction mixture read at λ 765 nm against blank. The amount of total phenol content was expressed as mg gallic acid equivalents (GAE)/g dwt of plant material. Calibration curve generated with gallic acid pure compound showed a correlation coefficient $R^2 \geq 0.99$.

Determination of total flavonoids content

Total flavonoid content was determined using aluminium chloride ($AlCl_3$) method (Sultana et al., 2007). Quercetin was used as a reference standard. Ten milligrams of quercetin was dissolved in 1 mL of DMSO and concentrations from 0.1 mg to 1.2 mg/mL were used for constructing calibration plot. 1 mL of each concentration of quercetin or 1 mL of plant extract was pipetted into 10 mL volumetric flask; 5 mL of distilled water and 0.3 mL of 5 % $NaNO_2$ were added and incubated for 5 min. After incubation, 0.6 mL of 10 % $AlCl_3$ was added and continued to incubate for another 5 min, followed by addition of 2 mL of NaOH (1M) and made the volume to 10 mL with distilled water. The solution was mixed vigorously and absorbance was measured at λ 510 nm using a Shimadzu UV-160A spectrophotometer (Kyoto, Japan). The amounts of total flavonoids were expressed in quercetin equivalents per g dwt of plant extracts. All samples were analyzed in triplicates.

Determination of total triterpenoids

The content of the total triterpenoids was determined by a spectrophotometric method as described in Jie-Ping and Chao-Hong (2006). Ursolic acid was used as the standard compound. Ursolic acid of 500 µg was dissolved in 1 mL of ethanol and the concentration ranging from 10 µg to 60 µg/mL used for constructing calibration plot. The aliquots of extracts and the respective standards were completely dried in speed vac before adding 0.3 mL of 5 % vanillin in glacial acetic acid (w/v) and 1 mL of perchloric acid. The reaction mixture was heated to 60 ^{o}C for 45 min. After cooling, 5 mL of glacial acetic acid was added, mixed well and read the samples at λ 548 nm using a Shimazdu 160 A UV–Vis Spectrophotometer.

HPLC analysis of BS-gum resin

Using one of the major boswellic acids, 3-acetyl-11-keto-β-boswellic acid (AκβBA) BSAE and BSWE has been quantitated by subjecting the extracts to HPLC analysis. Commercially available AκβBA (95 % purity) was used for constructing the calibration curve. The assay was out-sourced to Pharmatrain, Kukatpally, Hyderabad, and methodology for HPLC analyses in brief is as follows: The instrument used was Waters HPLC 2487 dual λ absorbance detector and 2695 separation module. The separation was performed on C_{18} 100 Å (250 mm × 4.6 mm, make: Waters) reverse phase analytical column. Compound was eluted using a mobile phase consisted of water (A) and acetonitrile (B), used in 35A and 65B in an isocratic mode at a flow-rate of 0.6 mL/min for 9 min. Absorption spectra and retention times were recorded at λ 210 nm with a UV detector connected to the HPLC system.

Isolation of boswellic acids from gum resin of BS-extracts

In order to isolate bioactive compounds from BS-gum resin, the gum resin was subjected to extraction protocol as described in Taneja et al., (1997). 25 g crushed granules of gum resin was extracted in 700 mL of methanol for 12 h. The extraction process was repeated twice with methanol, and the total extract was filtered and concentrated in the rotary evaporator. The red brown syrupy mass (1.5 g) obtained after concentration was treated with 3 % potassium hydroxide (KOH) with continuous stirring until syrupy mass attains pH 9-10. Afterwards the solution was vigorously stirred for 12 h to obtain uniform emulsion, which was further extracted

with three portions (25 mL each) of dichloromethane in the separating funnel. The lower layer was discarded, the upper aqueous fraction was treated with dilute hydrochloric acid solution (5 %) until the pH, 3-4 is achieved, at which boswellic acids are precipitated. The precipitate was filtered and washed several times with mineral free water and subjected to dryness in speed vac at 40-45 ^{o}C, forming a creamish yellow boswellic acid mixture (BAM). The calculated yield of BAM obtained was about 11.5 % i.e., 115 mg per gm dry weight of gum resin.

Metabolite profiling by GC-MS analysis

BS-gum resin extracts and boswellic acid mixed fraction (BAM)

An aliquot (100 µL) of the BS-gum resin extracts (BSAE and BSWE) or BAM was air dried, dissolved each of them in 100 µL of pyridine N,O-bis (trimethylsilyl) trifloro acetamide (BSTFA) and trimethyl chlorosilane (TCMS), incubated for 1 h (Villas-Boas et al., 2006) and subjected to GC-MS analysis on Agilent 7890 gas chromatograph connected to LECO mass spectrometer, equipped with 30.0 m x 320 µm HP5-MS capillary column with 0.25 µm film thickness. 1 µL of sample was injected into the GC-MS system using splitless mode. The injector temperature was 280 °C. The program of the column temperature was as follows: 80 °C (2 min), 10 °C to 270 °C for 2 min; 5 °C to 300 °C for 16 min. GC-MS data were obtained on LECO mass spectrometer using the following settings: ion source temperature, 250 °C; solvent delay, 0 min. Helium was used as carrier gas at a flow rate of 1.2 mL/min. All data were obtained by collecting the full scan mass spectra within a scan range of 40-1000 amu with an acquisition rate of 10 spectra/sec. Compounds were identified by comparing their mass spectra with those of National Institute of Standards and Technology (NIST) library.

Metabolite profiling by LC-MS

ESI-MS is an analytical technique for qualitative or quantitative measurement of metabolites of biological samples. ESI-MS coupled with HPLC has become a powerful technique in analysing both small and large molecular weight molecules of assorted polarities in a complex biological sample (Ho et al., 2003).

LC-MS analysis of ethanolic and water extracts of *T. arjuna* stem bark (TAAE and TAWE) and methanolic extracts of rhizomes of all seven cultivars of

Curcuma extracts were performed on 6520 Accurate Q-TOF (Agilent Santa Clara, CA) mass spectrometer coupled to HPLC equipped with UV–VIS detector. The column used for the separation of metabolites from the plant extracts was Zorbax Eclipse XDB- C 18, 4.6 × 50 mm, 1.8 µ. The solvent elution conditions used for *T. arjuna* extracts were as follows: (A) acetic acid (0.1 % v/v) and (B) acetonitrile; Gradient (in buffer A): (i) 20-55 % B from 0 to 15 min, (ii) 55-90 % B from 15 – 20 min (iii) isocratic 90 % B from 20 to 23 min (iv) 90-20 % B from 23-26 min (v) isocratic 20 % B from 26-35 min. Flow rate was maintained at 0.2 mL/min; Injection volume was 2 µL/sample; ESI parameters were both negative and positive ion mode; mass range was 100-1700 m/z with spray voltage 4 KV; helium gas temperature was 325 ^{o}C with flow rate of 8 L/min; nebulizer pressure was maintained at 35 psi.

The parameters set for LC-MS analysis of methanolic extracts of fresh *Curcuma* rhizomes were: mobile phase- (A) 5 mM ammonium formate in 0.1 % formic acid (v/v), and (B) 100 % (v/v) acetonitrile. Gradient used in buffer A was: 0–2 min, 5 % B; 2–57 min, 5–100 % B; 57–60 min, 100 % B; 60–65 min, 100-5 % B; Flow rate: 0.25 mL/min; temperature at 40 ^{o}C; Injection volume for each sample was 5 µL. The acquisition parameters for negative mode were: drying N_2 temperature, 350 ^{o}C, 8 L/min; nebulizer pressure was 40 psi; HV capillary 4000 V; skimmer 65.0 V (negative mode); mass range measured was 110–1700 m/z; spray voltage was 4 KV with scan rate 1.4.

Measurement of the antioxidant activity

Total antioxidant capacities of the samples were determined by phosphomolybdenum method described by Raghavan et al., (2003). The assay is based on the reduction of Mo (VI) to Mo (V) by the sample and subsequent formation of a green phosphate/Mo (V) complex at acidic pH. Various aliquots of standard solutions of ascorbic acid (2.5, 5, 10, 15, 20 and 25 µg) or plant extracts added to 1 mL of reagent (0.6 M sulphuric acid, 28 mM sodium phosphate and 4 mM ammonium molybedate). The tubes containing reaction mixture were capped and incubated in a thermal block at 95 °C for 90 min. The reaction mixture was cooled to room temperature and absorbance was measured at λ 695 nm against reagent blank. The antioxidant capacity was expressed as ascorbic acid equivalents.

Free radical scavenging assays

DPPH radical scavenging test

2, 2-diphenyl-1-picrylhydrazyl (DPPH) scavenging capacity of the plant extracts was measured as described in Nabasree and Bratati (2006). DPPH of 0.004 % (w/v dissolved in methanol) was freshly prepared and was added to different concentration of the extracts. The reaction mixture was vortexed for 10 s and allowed to stand at room temperaturre for 30 min. The discolouration of initial purple colour was measured spectrophotometerically at λ 517 nm. Gallic acid was used as standard reference compound. The capability to scavenge the DPPH radical was calculated as follows: [A $_{\lambda 517\ nm}$ of control– A $_{\lambda 517\ nm}$ of sample / A $_{\lambda 517\ nm}$ of control] x 100.

Hydrogen peroxide scavenging activity

Hydrogen peroxide scavenging assay was measured by the method of Pedraza et al., (2006). Phosphate buffer of 0.1 M (pH 7.4), 40 mM hydrogen peroxide in PBS and xylenol orange reagent containing 250 mM ammonium iron (II) sulfate, 25 mM H_2SO_4, 100 mM sorbitol and 125 mM xylenol orange were prepared and stored at 4 ^oC. Xylenol orange solution was stored in amber bottle.

Various aliquots of plant extracts were pre-incubated with 10 µL of 40 mM hydrogen peroxide for 15 min in dark and added 400 µL of xylenol orange reagent. After 30 min, the absorbance of the reaction mixture was read for the intensity of chromophore (Fe (III)-xylenol orange complex) at λ 584 nm. Gallic acid was used as a reference compound. % scavenging of hydrogen peroxide radical by plant extracts or reference compound was calculated using the formulae (A_0-A_1 / A_0 × 100). A_0 – absorbance of control (reagent with hydrogen peroxide but without plant extract), A_1 – absorbance in presence of plant extract.

Ferric chloride induced lipid peroxidation in rat liver and heart tissue homogenates

The assay is based on the extent of formation of thiobarbituric acid reactive substances (TBARS) from the peroxides formed by lipid by oxidizing agents. Polyunsaturated fatty acids with three or more double bonds are particularly more susceptible to peroxidation. Once the reaction is initiated, the process proceeds as a free radical chain reaction.

Male Wistar rats weighing 180-200 g were used. The animals were housed in wire-bottom cages and allowed to free access to standard laboratory chow and water. Animals were sacrificed by cervical dislocation and the organs were rapidly removed. Animal tissues were provided by Prof. P. Prakash Babu, Head, Dept of Biotechnology, University of Hyderabad.

Rat liver tissue homogenate

Preparation of rat tissue homogenate was done according to Ohkawa et al., (1979). Rat liver was excised after decapitation, weighed and rinsed with ice-cold 0.9 % NaCl to get rid of blood. Liver tissue homogenate was prepared in 10 % (w/v) of 0.15 M KCl using a teflon homogenizer followed by centrifugation at 800 *g* for 15 min, and clear cell-free supernatant was used for further assays.

The peroxide formation in the liver homogenate was induced and assayed according to the method of Gaurav et al., (2007). Lipid peroxidation was initiated by adding 100 µL of 10 mM ferric chloride to the reaction mixture containing rat liver homogenate and incubated for 30 min at 37 ^{o}C. Different concentrations of the plant extracts were added prior to incubation to test peroxidation inhibitory activity. The reaction was terminated by adding 2 mL of ice cold HCl (0.25 N) containing 15 % (v/v) trichloroacetic acid (TCA), 0.38 % (w/v) thiobarbituric acid (TBA) and followed by heating at 80 ^{o}C for 60 min. The samples were cooled and centrifuged at 5000 g for 15 min; absorbance of the supernatants was measured at λ 532 nm against the blank.

Rat heart tissue homogenate

Rat heart was excised after decapitation; blood was drained completely to avoid interference in the reaction and the tissue was transferred to liquid nitrogen to prevent from oxidation and stored at -80 ^{o}C until use. Tissue was homogenized in ratio of 10 % (w/v) of 0.15 M KCl flushed with nitrogen gas, and centrifuged at 1500 g for 5 min; the supernatants were collected and used for the assay.

This assay was performed according to the method reported by Meera et al., (2009). The reaction mixture containing 50 µL heart homogenate and various concentrations of plant extracts were exposed to 10 mM ferric chloride and incubated at 37 ^{o}C for 1 h. After incubation, the reaction was stopped with 500 µL of 70 % ethanol, followed by addition of 1 mL of TBA (1 % w/v) and the samples were

subjected to boiling in a water bath for 20 min. After incubation, samples were brought down to room temperature and centrifuged at 5000 g for 15 min. Acetone of 50 µL was added to the supernatant and the absorbance was measured at λ 532 nm in a spectrophotometer. Gallic acid was used as a reference compound. The effect of different extracts or test/standard compound against lipid peroxidation were calculated as follows: % Inhibition = (control-sample/control) × 100. Control is uninduced reaction mixture without plant extracts.

Coagulation studies

Collection of blood sample

Venous blood drawn from the healthy volunteers were transferred to a sterile tube containing anticoagulant acid citrate dextrose (ACD: 22 g/L trisodium citrate dehydrate, 8 g/L citric acid monohydrate and 24.5 g/L dextrose). ACD of 1.5 mL was added as anticoagulant for every 8.5 mL of blood, mixed gently by inverting the vacutainer for several times without producing froth.

Platelet aggregation activity

Platelet aggregation activity was determined according to Mary et al., (2003). Platelet rich plasma (PRP) was collected by centrifuging the blood at 200 × g for 5 min, red and white blood cells were pelleted, leaving a cloudy yellow colour supernatant containing platelets. This supernatant was transferred carefully into a sterile polypropylene tube. Platelet poor plasma (PPP) was collected by the centrifugation of the remaining blood at 1500 × g for another 5 min.

Platelet aggregation assay was done by measuring the changes in the optical density (ie, light transmittance) of the platelets that were exposed to aggregating agent (Saxena et al., 2007). PRP with or without different concentrations of plant extracts or heparin were added to microwell plate. Aggregation of the platelets was initiated by adding ADP (20 µM). Absorbance of sample was recorded at λ 600 nm using a mulitimode detection plate reader (Tecan, Germany) preset at 37 ^{o}C for time period of 12 min and O.D. values recorded at an interval of 2 min. Commerical heparin (10 U/mL) was used as a reference anticoagulant standard.

Assay of plasma clotting times

Prothrombin time (PT) and activated partial thromboplastin time (APTT) assays belong to group of diagnostic tests to assess the function of blood coagulation system. These assays were sourced to Regional Diagnostic Centre, Hyderabad.

Prothrombin time (PT)

PT was performed by adding plasma to thromboplastin protein that converts prothrombin to thrombin. The reaction mixture was incubated at 37 ^{o}C for 1-2 min.

Activated Partial Thromboplastin Time (APTT)

The time required for the plasma to clot when a reagent having optimal phospholipid with intrinsic pathway activator like silica and calcium are provided. APTT is sensitive to abnormalities in intrinsic and common coagulation factors.

To assay the effect of extracts on extrinsic and intrinsic pathways of coagulation, PT and APTT time periods of normal human plasma were compared with plasma coagulation time periods in the presence of plant extracts or test compounds. These reactions were carried out using kit UNIPLASTIN obtained from Tulip diagnostics (Goa, India) by using the instrument MC100 single channel coagulation analyzer. Samples were outsourced commercially to analyse at Regional Diagnostic Centre, Hyderabad. The protocol followed was briefly as follows: 0.9 mL of blood sample was transferred into a 0.109 M trisodium citrate (1:9, v/v) and then centrifuged at 1800 × g for 10 min to obtain plasma. 100 µL of the plasma were mixed with different concentrations of plant extracts or test compounds and the coagulation was started by addition of $CaCl_2$. 100 µL of thromboplastin was added to the incubated plasma for PT and APTT assays individually as per the kit protocol.

Clotting factors

Human clotting factors were assayed according to Robert et al., (2010). Incubations were performed in 96-well plates. The final concentration of the coagulation factors used in the present study were 0.56 U or 2.8 µg of HFIXa, 0.009 U or 70 ng of HFXa, 0.02 U or 100 ng of HFXIa and 0.09 U or 1.32 µg of HFXIIa. Different concentrations of plant extracts or test compounds added in 200 µL of buffer containing 50 mM Tris, pH 8.3 containing 5 mM calcium chloride and 0.2 mM

sodium chloride. Coagulation factors to be tested were added last to initiate the reaction. After 60 s of incubation at room temperature, 0.8 mM of chromogenic peptide substrate was added. Peptide CH_3OCO-D-CHA-Gly-Arg-pNA-AcOH was used for the assays of HFIXa, HFXa or HFXIa and peptide H-D-CHT-Gly-Arg-pNA-2AcOH for HFXIIa. The absorbance of the reaction at λ 405 nm was recorded for 5 min. Heparin was used as positive drug control.

Assay of factor VIIa was performed using a commercial ELISA kit. The monoclonal antibody specific to FVIIa was pre-coated onto 96 well microplate which is recognised by anti-rabbit horseradish peroxidase (HRP) labelled secondary antibody. 3,3',5,5'-tetramethylbenzidine (TMB) was used as a substrate solution. The colour development was stopped by addition of 1 N H_2SO_4 and the intensity of the colour was measured at λ 450 nm using a microplate reader.

Lipid metabolizing enzyme

HMG-CoA Reductase Assay

The conversion of HMG-CoA and NADPH to mevalonate and NADP respectively in the presence of the enzyme HMG-CoA reductase is an important step in the lipid metabolism.

The commercial kit used in the present study provided with assay buffer, NADPH, HMG-CoA substrate, enzyme HMG-CoA reductase (HMGR) and standard inhibitor solution, Pravastatin (0.5 µM). The reaction was carried out at 37 ^oC using Infinity M200 microplate reader (Tecan, Germany) with kinetic program. Absorbance of the reaction was read for every 20 sec up to 10 min at λ 340 nm. Assay was carried out according to manufacturer's instructions. To the 181 µL of assay buffer, substrate HMG-CoA, plant extract or test inhibitor compound was added followed by NADPH, the cofactor. In the assay, decrease in absorbance at λ 340 nm represents the rate of oxidation of NADPH to NADP in the presence of the substrate HMG-CoA and the rate of decrease in absorbance is directly proportional to the activity of HMGR enzyme.

Lipoprotein lipase (LpL) assay

Commercially available lipoprotein lipase (bovine milk) was used to test the effect of plant extracts or standard compound on their inhibitory activity on the enzyme. *p*-

nitrophenyl butyrate (PNPB) was used as a substrate. Scheme of the reaction: PNPB + H_2O → *p*-nitrophenol + butyric Acid.

The enzyme assay was performed using microplate reader set at 37 ^oC, with kinetic program reading absorbance at λ 400 nm for 5 min at an interval of 1 min. Different concentrations of the plant extracts were added to lipoprotein lipase enzyme solution in bufferA containing 100 mM sodium phosphate buffer, 150 mM sodium chloride and 0.5 % (v/v) triton x-100, pH 7.2 at 37 ^oC, mixed well and added PNPB. Substrate Blank contained buffer and enzyme. LpL enzyme activity was assayed as per manufacturer's instruction, which monitors the release of *p*-nitrophenol (increase in absorbance against substrate blank) at $\Delta A_{\lambda 400\ nm}$/minute. Orlistat was used as the standard inhibitor.

Cell culture

THP-1 human monocytes were purchased from National Centre for Cell Science (NCCS Pune, India) and cultured in endotoxin-free RPMI 1640 medium containing 10 mM HEPES, 1 mM sodium pyruvate, 4.5 g/L glucose, 1.5 g/L sodium bicarbonate supplemented with 2 mM l-glutamine, 1xPenStrep (penicillin (100 U/mL) and streptomycin (100 U/mL)) and 10 % fetal bovine serum. Cells were maintained in 5 % CO_2 and 95 % air at 37 ^oC during growth and treatments.

HAECs were purchased from Invitrogen (USA), and grown to confluence in Medium 200, supplemented with 10 % (v/v) heat-inactivated fetal bovine serum, low serum growth medium (LSGS), penicillin (100 U/mL) and streptomycin (100 U/mL). An acute inflammatory stimulus was produced by coincubating with human recombinant TNF-α. Prior to TNF-α treatment, cells were incubated with plant extracts or test/reference compound for 16-18 h.

Cell viability

Cell viability assay was performed using 3-(4,5-dimethylthiazol-2-yl)-2,5-diphenyltetrezolium bromide (MTT) assay according to manufacturer's protocol. Cells were seeded in 24-well plate (2×10^5 cells/well) and pre-treated with or without extracts or standard compounds. After respective time periods of incubation, cells were washed twice with medium in order to remove trace amounts of extracts or standard compounds. Similarly, wells with media without cells were processed. 100 µL of MTT (5 mg/mL) was added to the each well with or without cells and

incubated for 3 h. Cell suspension was solubilised with 100 µL of solution of 4 % HCl 1 N in isopropanol. Absorbance of the dye was measured at λ 570 nm with background subtraction at λ 690 nm. Media without cells with respective concentrations of extracts or standard compounds were taken as respective blanks.

To exclude the possibility of loss of cells while washing or seeding issues, cell viability at different concentrations of extracts was tested by trypan blue exclusion method. The dye exclusion test was used to determine the number of viable cells present in a cell suspension. It is based on the principle that live cells possess intact cell membranes that exclude certain dyes, such as trypan blue whereas dead cells do not. In this test, a cell suspension of 20 µL was mixed with 10 µL of (0.004 %) dye and then examined under microscope. All viable cells will have the clear cytoplasm whereas nonviable/dead cells will appear in blue colour (Strober, 2001).

Cell based assays

Measurement of intracellular ROS in THP-1 cells

Intracellular ROS in the cells were measured by using cell permeable fluorescent dye 2', 7',-dichlorofluorescein-diacetate (H_2DCFDA) (also known as dichlorofluorescein diacetate) according to Evgeniy et al., (2010). It is non-polar in nature and can diffuse across cell membranes, upon cleavage of acetate groups by cytosolic intracellular esterases, it undergoes oxidation with oxidizing species (e.g. hydrogen peroxide) and converts the nonfluorescent H_2DCFDA to the highly fluorescent 2',7'-dichlorofluorescein (DCF) (Bass et al., 1983 and Carter et al., 1994).

THP-1 cells (5×10^5 cell per well) were pre-incubated with or without different concentrations of plant extracts or test/reference compound for overnight at 37 ^oC in a humidified incubator containing 5 % CO_2. After preincubation, 5 µM H_2DCFDA was added in dark and further incubated for 30 min at 37 ^oC. Then the cells were washed twice with growth medium RPMI (FBS free) to wash out excess dye in the medium. After washing, the cells were exposed to 10 µM H_2O_2 for 5 min to induce intracellular ROS. Images were obtained by subjecting the cells to confocal laser-scanning electron microscope (Leica DMR). The quantification of fluorescence intensities of cell samples was done by spectrofluorimetric analysis using excitation and emission wavelengths at λ 488 and λ 525 nm respectively.

Assay of ROS scavenging potential in THP-1 cells

ROS scavenging assays were done in THP-1 cell lysates according to the method of Prasenjit et al., (2007). After pretreatment with plant extracts, cells were washed with RPMI media to wash out plant extracts in the medium. This is to ensure that hydrogen peroxide added to the medium is not scavenged extracellularly by the plant extracts. After two washes, cells were exposed to 10 µM H_2O_2 for 5 min and then sonicated on ice for 3 min, followed by centrifugation at 10,000 rpm for 2 min at 4 ^oC. Supernatants were collected and subjected to catalase, glutathione peroxidise or ferric ion reducing antioxidant power (FRAP) assay.

Enzyme assays

Catalase assay

Catalase (CAT) converts hydrogen peroxide to water and oxygen. Its activity is located largely in peroxisomes and is known to be specific scavenger of H_2O_2 (Baud et al., 2004). Intracellular CAT was assayed by adding 7.5 mM of H_2O_2 to the 200 µL of cell lysates and the consumption of H_2O_2 or decrease in absorbance was measured at λ 240 nm was monitored at 37 ^oC using a multimode microplate reader for about 5 min and absorbance was recorded at an interval of 10 s. CAT activity was expressed in fold changes which reduced 1 µmol of H_2O_2 per min at 25 ^oC.

Glutathione peroxidise assay

Glutathione peroxidise (GPx) is one of the main enzyme involved in H_2O_2 detoxification. GPx activity was measured indirectly by a coupled reaction with glutathione reductase. Oxidized glutathione produced on reduction of hydroperoxide by GPx was recycled to its reduced form by the oxidation of NADPH to NADP which was accompanied by a decrease in absorbance (Baud et al., 2004). GPx assay was done with cell lysates of 1 mL reaction mixture by mixing with 550 µL of 0.1 M KH_2PO_4 buffer containing 1 mM EDTA (pH 7.5), 50 µL of 2 mM NaN_3, 100 µL of GR (2.4 U/mL) and 100 µL of 10 mM GSH. After 10 min of incubation at 37 ^oC, 100 µL of 1.5 mM NADPH dissolved in water was added to the above mixture. The reaction was initiated by adding 100 µL of pre-warmed (37 ^oC) 1.5 mM H_2O_2 and the decrease in absorbance at λ 340 nm was monitored for 5 min in microplate reader.

Ferric ion reducing antioxidant power assay (FRAP)

FRAP method was used for assessing the effect of plant extracts or test/reference compound on cellular antioxidant power in combating oxidative stress. FRAP reagent is an oxidant, at low pH, Fe^{III}-TPTZ complex is reduced to ferrous form (Fe^{II}), and results in the formation of intense blue colour, has the absorption maximum at λ 593 nm (Benzie and Strain, 1996; Haung et al., 2005).

The FRAP assay was done according to the method of Prasenjit et al., (2007). 1.5 mL of freshly prepared pre-warmed FRAP reagent (300 mM acetate buffer, pH 3.6, 10 mM TPTZ in 40 mM HCl and 20 mM $FeCl_3 \cdot 6H_2O$ in the ratio of 10:1:1) was added to 200 µL of THP-1 cell lysates and incubated at 37 ^oC for 10 min. Blue colored Fe^{II} -tripyridyltriazine compound is formed from the colourless oxidized Fe^{III} by the action of electron donating antioxidants and the absorbance of the sample was read at λ 593 nm against reagent blank (1.5 mL FRAP reagent + 50 µL distilled water) in a microplate reader. The change of absorbance ($\Delta A = A_{10\ min} - A_{0\ min}$) is calculated and related to ΔA of Fe (II) standard solution. ΔA is linearly proportional to the concentration of antioxidant. One FRAP unit is arbitrarily defined as the reduction of 1 mol of Fe (III) to Fe (II).

Lipopolysaccharide (LPS) induced tumor necrosis factor alfa (TNF-α) production by THP-1 monocytic cells-ELISA

THP-1 cells were pretreated with or without plant extracts or test/reference compound, for 16 h in 5 % CO_2 at 37 ^oC. After exposure to LPS (0.5 µg/mL) for 3 h, the cells were centrifuged at 10,000 rpm for 5 min at 4 ^oC, and the supernatants were stored at -80 ^oC, until assayed. Supernatants were subjected to TNF-α assay according to BD OptEIA ^{TM} Set Human TNF-α kit method (BD Biosciences).

The BD OptEIA™ test is a solid phase sandwich ELISA (Enzyme-Linked Immunosorbent Assay). Kit contains human recombinant TNF-α standard; anti-human monoclonal coating antibody; biotinylated anti-human TNF-α monoclonal detection antibody; streptavidin-horseradish peroxidise enzyme; substrate solutions, 3,3',5,5'-tetramethylbenzidine (TMB) reagent and hydrogen peroxide. It utilizes a monoclonal antibody specific for TNF-α coated on a 96-well plate. Standards or samples of supernatants were added to the wells, TNF-α present in the samples binds to the immobilized antibody. The wells were washed and a streptavidin-horseradish

peroxidase conjugate mixed with a biotinylated anti-human TNF-α antibody was added, producing an antibody-antigen-antibody "sandwich". The wells were again washed and TMB substrate solution was added, which produces a blue colour in direct proportion to the amount of TNF-α present in the initial sample. The 50 µL of stop solution (1 M H_3PO_4) changes the colour from blue to yellow and the microwell absorbances are read at λ 450 nm.

Reagents *Coating buffer* (0.1 M sodium carbonate): 7.13 g $NaHCO_3$, 1.59 g Na_2CO_3 mixed well in 800 mL water, adjusted pH to 9.5 with 10 N NaOH and made up the final volume to 1 L. Freshly prepared and used within 7 days of preparation, stored at 2-8 ^oC.

Assay diluent: PBS with 10 % FBS (heat inactivated) pH 7.0.

Wash buffer: PBS with 0.05 % Tween-20. Freshly prepared and used within 3 days of preparation, stored at 2-8 ^oC.

Stop solution: 1 M H_3PO_4.

Standard preparation (Stock): Lyophilized standard TNF-α was reconstituted in 1 mL of deionized water that yielded a stock of 100 ng/mL (varies along with Lot number), allowed it to equilibrate for at least 15 min, then vortexed and stored at -80 ^oC and used within the period of six months.

Standard preparation (working): 500 pg/mL TNF-α was prepared on the day of ELISA experiment.

►Labelled eight 1.7 mL microfuge tubes as 1000, 500, 250, 125, 62.5, 31.3, 15.6 and 7.8 pg/mL and added 600 µL assay diluents to first tube and 300 µL to the remaining tubes.

► Pipetted 6 µL of working standard (500 pg/mL) from the stock into first tube containing 600 µL assay diluent (concentration 1000 pg/mL) and perform serial dilution by transferring 300 µL from tube 1 to last tube (containing volume 600 µL), and blank contained only assay diluent.

Transcript analysis

RNA isolation in THP-1 cells

THP-1 cells were seeded into T 25 cm^2 vent flask each containing 5 mL of cells and allowed them to grow till they reach the cell density 5×10^5/ flask. The flasks were pretreated with or without plant extracts or test/reference compound for 16 h in 5 %

CO_2 at 37 ^oC. After pre-treatment, cells were induced with LPS (0.5 µg/mL) for 3 h and centrifuged at 10,000 rpm, 5 min at 4 ^oC, supernatants were discarded. To the cell pellets, 250 µL media and 750 µL of Trizol reagent were added as per manufacturer's instructions and incubated at room temperature for 5 min.

5) After incubation, 150 µL chloroform was added, the tubes were capped and vortexed vigorously and incubated at 15-30 ^oC for 2-3 min, followed by centrifugation at 12,000 × g for 15 min at 2-8 ^oC. Upper colourless aqueous phase was transferred into fresh tubes, 500 µL of isopropanol was added and incubated at room temperature for 10 min followed by centrifugation at not more than 12,000 × g for 10 min at 2-8 ^oC, supernatant was discarded and RNA pellet was washed with 1mL of 75 % ethanol and pelleted down by centrifuging at not more than 7500 × g for 5 min at 2-8 ^oC or 12,000 × g for 10 min at 2-8 ^oC. RNA pellet was dried in air/vaccum dry for 5-10 min and dissolved in 50 µL DEPC water followed by incubation at 55-60 ^oC for 10 min. RNA concentration was checked using nanodrop at $A_{260/280}$ and stored at -80 ^oC until further use.

RNA isolation in HAEC

HAEC at 4th passage were seeded in T 25 cm^2 vent flask and grown to 75-80 % confluence (2 × 10^5 cell/mL) in M 200 medium, cells were pretreated with or without plant extracts or test/reference compound and incubated for 16 h in 5 % CO_2 at 37 ^oC. After pre-treatments, the cells were exposed to TNF-α (10 ng/mL) for the period of 4 h, after incubation, media were removed and small aliquot of Trizol reagent (1 mL for 10 cm^2 area) was added, and incubated for 5 min at 15-30 ^oC. Remaining steps are same as THP-1 cells, but the volumes of chloroform and isopropanol varies according to volume of reagent and cell number.

cDNA synthesis

iScript^{TM} cDNA synthesis kit from BioRad Laboratories (USA) was used for cDNA synthesis using total RNA isolated from the cultured THP-1 cells or HAEC's. The reaction mixture of 20 µL contained 5x iScript reaction mix 4 µL; iScript reverse transcriptase 1 µL; Nuclease-free water in µL (varies for every treatment) and RNA template of 1 µg. PCR machine was set up for about 30 cycles as per manufacturer's protocol and incubated the complete reaction mixture in cycling reactions: Denaturation step at 25 ^oC for 5 min followed by annealing at 42 ^oC for 30 min and

extension at 85 ^{o}C for 5 min. After the synthesis cDNA samples were stored at -20 ^{o}C.

Real-time quantitative PCR

Real-time-PCR was performed using PCR cycles ("cycle threshold" C_T) done to achieve a given level of fluorescence. C_T was fixed in the exponential phase of the PCR. During the initial PCR cycles, the fluorescence signal emitted by SYBR-Green bound to cDNA was usually too weak. Indeed, a difference could not be defined until after about 15 PCR cycles. During the exponential phase of the PCR the fluorescence is doubled at each cycle. After 35 cycles, the intensity of fluorescent signal usually began to plateau, indicating that the PCR had reached a saturation status. As a C_T is proportional to the logarithm of initial amount of target in a sample, the relative concentration of one target with respect to another is reflected in the difference in cycle number (ΔC_T) necessary to achieve the same level of fluorescence (Ponchel et al., 2003).

E-selectin	Forward	5´-GCTCTGCAGCTCGGACAT-3´
	Reverse	5´-GAAAGTCCAGCTACCAAGGGAAT-3´
ICAM-1	Forward	5´-CAGAAGAAGTGGCCCTCCATAG-3´
	Reverse	5´-GGGCCTTTGTGTTTTGATGCTA-3´
VCAM-1	Forward	5´-GGTGGGACACAAATAAGGGTTTTGG-3´
	Reverse	5´-CTTGCAATTCTTTTACAGCCTGCC-3´
IL-8	Forward	5´-GTGTAAACATGACTTCCAAGCTGG-3´
	Reverse	5´-GCACCTTCACACAGAGCTGC-3´
MCP-1	Forward	5´-GCCAAGGAGATCTGTGCTGAC-3´
	Reverse	5´-CATGGAATCCTGAACCCACTTC-3´
GAPDH	Forward	5´-CACCAACTGCTTAGCACCCC-3´
	Reverse	5´-TGGTCATGAGTCCTTCCACG-3´

The real time quantitative PCR was performed in triplicates. Reaction mixture (10 µL). 5 µL contained of 1x SYBR® green mixed with 0.5 µL each of forward and reverse primer, 2 µL of water and 2 µL of cDNA (1: 10). Negative controls were no template and no reverse transcriptase. The specificity of the SYBR green fluorescence was tested by plotting fluorescence as a function of temperature

to generate the melting curve of the amplicon. The transcript levels of marker genes were normalized with GAPDH mRNA.

Fluorescence activated cell sorting (FACS)

Flow-cytometry is a method used for cell specific counting. It is also used for studying the expression of cell surface proteins. The sample flow in a single file with a stream of liquid and the light scattering at different angles can distinguish differences in the size and internal complexity, whereas light emitted from fluorescently labelled antibodies can identify a specific subset of cells from the mixed samples (Brown and Wittwer, 2000).

Requirements: Staining buffer: PBS without mg^{++} or Ca^{++} containing 1 % heat inactivated FBS; 0.09 % sodium azide.
Antibodies: CD106—FITC (VCAM-1) and CD62E--PE (E-selectin).

Measurement of cell surface adhesion molecules (VCAM-1 and E-selectin) by flow cytometry

HAECs at 4^{th} passage were grown to confluence in medium 200 and pretreated with and without plant extracts or test/reference compound and incubated for 16 h in 5 % CO_2 at 37 ^{o}C. After treatment with TNF-α (10 ng/mL) for 4 h, cells were washed PBS. After trypsinization, cell suspension was transferred to 2 mL microfuge tube as described in Mullick et al., (2007). Cells were pelleted and washed with 1.2 mL of staining buffer and resuspended in 150 µL of staining buffer; 5-10 µL of surface staining antibodies CD106—FITC (VCAM-1) and CD62E--PE (E-selectin) were added to the tubes. After incubation for 30 min at 4 ^{o}C in the dark, 1.2 mL of staining buffer was added and cells are pelleted down to discard the supernatant. To the cell pellet, 150 µL of cytofix/cytoperm was added and incubated for 20 min at 4 ^{o}C. The cells were pelleted down to remove the fixation solution and resuspend the cells in 500 µL staining buffer for flow cytometry. Expression of VCAM-1 and E-selectin on HAECs was assayed with a BD LSR Fortessa^{TM} FACScan. For each sample, 5000 to 10,000 events were collected, with triplicate samples and data analysis was done with FACS Diva software. Positive and negative controls for each fluorophore were performed to determine optimal levels of PMV gain and sensitivity and set correct parameters for compensation.

Nuclear translocation of NF-κB in THP-1 and HAECs

Reagents: Tris buffer saline (TBS): 20 mM Tris HCl and 150 mM NaCl at pH 7.5.
Tris buffer saline and Tween-20 (TBST): Add 0.05 % Tween 20 in 100 mL TBS.
4 % Paraformaldehyde (PFA).

Procedure

The assay was slightly modified according to the method of Zhou et al., (2004). THP-1 cells or HAECs pretreated with or without plant extracts or test/reference compound and incubated for 16 h in 5 % CO_2 at 37 ^{o}C. After pre-treatment with extracts, cells were exposed to LPS (0.5 µg/mL) for 3 h in THP-1 cells or TNF-α (10 ng/mL) for 4 h in HAECs. After incubation, cells were washed in serum free medium, followed by fixation of cells with 4 % paraformaldehyde for 20 min. After washing thrice with TBS, cells were permeabilized in ice cold acetone: methanol (1:3) for 20 min and washed with TBS (as mentioned above), followed by staining with transcription factor p65 (NF-κB p65 sub unit 1: 200 in 3 % BSA; incubated for 2 h at 37 ^{o}C) and cells were washed with TBS, TBST and TBS. After removing the unbound antibody, cells were stained with Alexa Fluor 594 goat-anti rabbit secondary antibody (1: 200) and incubated in dark for 1 h, followed by washing as above. Nuclei of the cells were visualized by staining with nuclear stain, 4',6-diamidino-2-phenylindole (DAPI) and then images were taken using confocal laser scanning electron microscope (Zeiss).

Statistical analysis

All the data were subjected to one way analysis of variance (ANOVA) test using Statistical Package for the Life Sciences (SPLS version 11). The values were expressed as mean ± standard deviation (S.D.). Variance at p <0.001 was considered to be highly significant.

Chapter 3

RESULTS and DISCUSSION

Objective 1: Phytochemical analysis of *B. serrata*- gum resin and *T. arjuna*-stem bark extracts and evaluation of their antioxidant activity in human monocytic (THP-1) cells

Results

Phytochemical analysis

Hydroalcoholic extracts yielded 4.8 % (w/w) and water extracts of *B. serrata* yielded 5.2 % (w/w) based on extract dry weight obtained from initial material of dried gum resin taken for extraction procedure. The phytochemical screening of gum resin showed positive reaction for polyphenols, flavonoids and triterpenoids are extraplotted using the standards gallic acid, quercetin and ursolic acid respectively (Fig. 3.1). BSAE contained total phenolic content of 26.8 ± 0.1 GAE mg/g dwt; 1.6 ± 0.05 QE mg/g dwt and 450.3 ± 3.1 UAE mg/g dwt. Whereas BSWE contained 68 ± 2.1 GAE mg/g dwt; 5.4 ± 0.5 QE mg/g dwt and 231.1 ± 2.3 UAE mg/g dwt (Table 3.1). In summary hydroalcoholic extracts had higher total amounts of triterpenoids whereas water extracts had phenolics and flavonoids (Table 3.1).

In case of *Terminalia arjuna*, yields of hydroalcoholic extracts 15 % (w/w) and water extracts were 5 % (w/w) respectively. The phytochemical screening showed positive reaction for polyphenols and flavonoids. TAAE contained 894.6 ± 8.2 GAE mg/g dwt and 17.7 ± 0.1 QE mg/g dwt. Whereas TAWE contained 158.2 ± 4.8 GAE mg/g dwt and 27.4 ± 3.3 QE mg/g dwt. In summary hydroalcoholic extracts had higher amounts of TPC and flavonoids than water extracts, Table 3.2.

Table 3.1. Total polyphenol, flavonoids and triterpenoids content in the extracts of *B. serrata* gum resin

Type of MPE	Total Phenolics GAE mg/g dwt	Total Flavonoids QE mg/g dwt	Total Triterpenoids UAE mg/g dwt
BSAE	26.8 ± 0.1	1.6 ± 0.05	450.3 ± 3.1
BSWE	68 ± 2.1	5.4 ± 0.5	231.1 ± 2.3

Table 3.2. Total polyphenol, flavonoids and triterpenoids content in the extracts of *T. arjuna* stem bark

Type of MPE	Total Phenolics GAE mg/g dwt	Total Flavonoids QE mg/g dwt
TAAE	894.6 ± 8.2	17.7 ± 0.1

TAWE	158.2 ± 4.8	27.4 ± 3.3

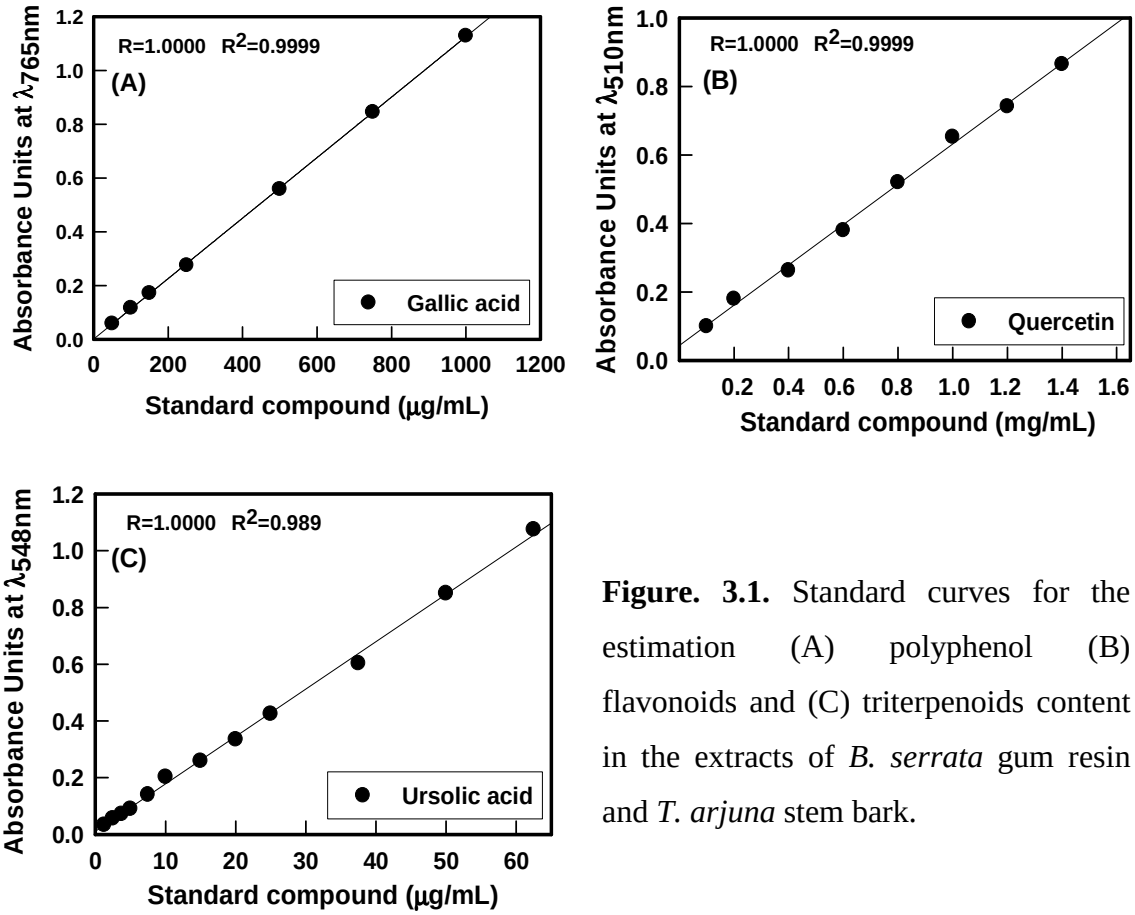

Figure. 3.1. Standard curves for the estimation (A) polyphenol (B) flavonoids and (C) triterpenoids content in the extracts of *B. serrata* gum resin and *T. arjuna* stem bark.

Quantititation of AκβBA

HPLC analyses with BSAE and BSWE showed peaks corresponding to standard AκβBA of 4.784 min (Fig. 3.2. B) with retention times (min) of 4.623 and 4.616 respectively (Fig. 3.2. C). Calculations with corresponding peak areas determined that AκβBA content in BSAE of 9 % (w/w) and BSWE of 7.8 % (w/w) of their extracts' on dwt basis. To test the linearity of the compound, the standard solutions of AκβBA in the range between 10 µg/mL to 120 µg/mL were used. 20 µL each of these standard solutions were injected for HPLC assay, which correspond to 200–2400 ng (Fig. 3.2. A). Least amount of detection (LOD) and quantification (LOQ) under the experimental conditions were 2.69 ± 0.17 µg/mL and 9.08 ± 0.58 µg/mL respectively. Each sample was measured in triplicate (Fig. 3.2. B).

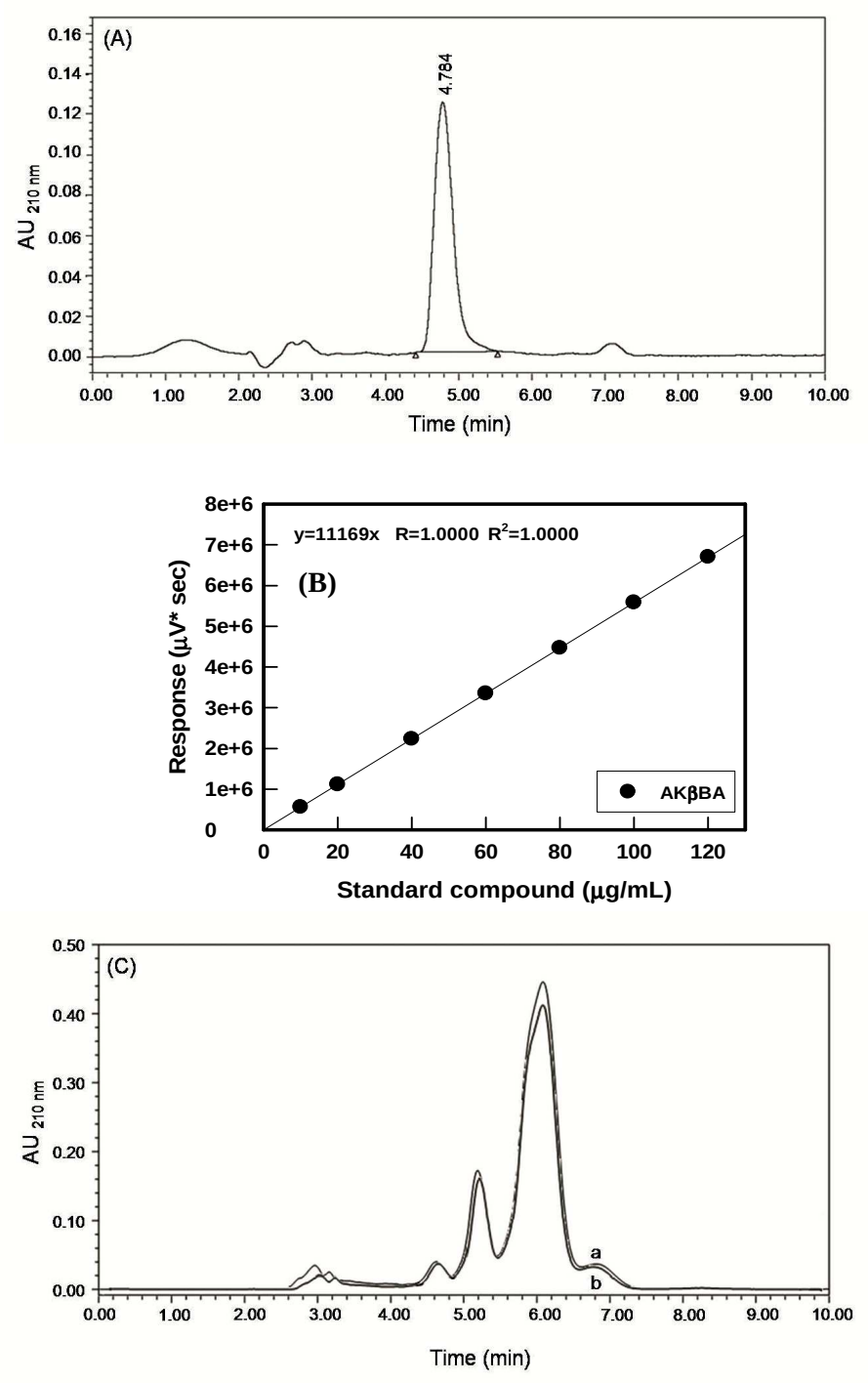

Figure. 3.2. HPLC analysis for quantification of AκβBA in plant extracts. (A) An example chromatogram of standard compound AκβBA showing a peak with the retention time period of 4.784 min. (B) Regression plot with varied concentrations of AκβBA ranging from 20 to 120 µg/mL. (C) Example chromatograms of BSAE (a) and BSWE (b), with marked peak, corresponding to standard AκβBA with retention times of 4.623 min and 4.616 min respectively. Peak areas were used to determine the AκβBA content in the extracts.

GC-MS analysis of BS-gum resin

Hydroalcoholic and water extracts from gum resin of *B. serrata* and its alkali-acid fractionated boswellic acid mixed-fraction (BAM) were analysed by GC-MS in order to profile their constituents. The compounds were identified based on their retention time and mass fragmentation spectra and were compared with the published data; matching was also done against NIST library. For such analysis, the optimal result was achieved by derivatizing the sample using N,O-bis(trimethylsilyl) trifluoroacetamide (BSTFA) (Mathe et al., 2004). BSTFA used can be referred as trimethylsilyl (TMS) donor for the silylation to various functional groups especially of carboxylic acids, N-nitrosoamino acids, β-ketoesters and many other polar compounds. Nevertheless, some dehydration products were observed in the gas chromatograms due to the high temperatures in the injection of the sample. Injection parameters and GC operation conditions were adjusted to be able to obtain best separation for triterpenes and other components like other types of terpenes and their various derivatives and fatty acids. GC-spectra of BSAE and BSWE are shown in Figs. 3.3 and 3.4 and compound identified were listed in Tables 3.4 and 3.5.

Table 3.3. shows the compounds identified from hydroalcoholic extracts of BS-gum resin. The analysis revealed that, BSAE contained 31 compounds which are largely of aromatic compounds like verbenyl ethyl ether; *cis*-2-hexen-1-ol; *trans*-3-acetoxy-1,8-cineole; α-calacorene and 11-hexadecyn-1-ol. These compounds predominantly belong to derivatives of monoterpenes (e.g. myrtenol 2.1 %; limonene diepoxide 2.5 %; α-pinene 0.47 %; *trans*-3-acetoxy-1,8-cineole 4.27 %, sesquiterpenes (e.g. α-calacorene 0.06 %; 5-azulenemethanol, 1,2,3,4,5,6,7,8-octahydro-α,α,3,8-tetramethyl- 0.15 %; caryophyllene oxide 5.26 % and pentacyclic triterpenes (e.g. α-amyrin 0.8 %; 3-O-acetyl-β-boswellic acid 6.68 %; ursa-9(11),12-dien-3-one 0.4 %; 9,11-dehydro-β-boswellic acid 1.93 %; 3-O-acetyl-11-keto-β-boswellic acid 6.3 %; 3-O-acetyl-α-boswellic acid 2.4 %; lanost-9(11)-en-12-one 1.13 %. Metabolites identified from GC-MS analysis of BSWE are listed in Table 3.4. Majority of compounds identified are derivatives of sesquiterpenes (e.g. caryophyllene oxide 0.1 %; *trans*-farnesol 0.03 %; α-farnesene 0.16 %, pentacyclic triterpenes e.g. olean-12-ene 1.4 %; urs-12-ene 1.4 %; 3-O-α-methoxycycloartenol 0.45 %; β-amyrin acetate 1.65 %; lupeol 0.05 %; 3-O-acetyl-11-keto-β-boswellic acid 4.09 % and alcohol e.g. 1-heptatricotanol 0.054 %. As shown in Tables 3.3 and

3.4 both the extracts are enriched with oleanane and ursane group of pentacyclic triterpenoids with 30 carbon atoms. 3-O-acetyl-11-keto-β-boswellic acid (AκβBA) was commonly found in both BSAE and BSWE, other tritepenoids varied in terms of functional groups and their positions. Sesquiterpenes- of caryophyllene oxide, alcohol-1-heptatriacotanol and fatty acid-palmitic acid were also found to be common between the BSAE and BSWE.

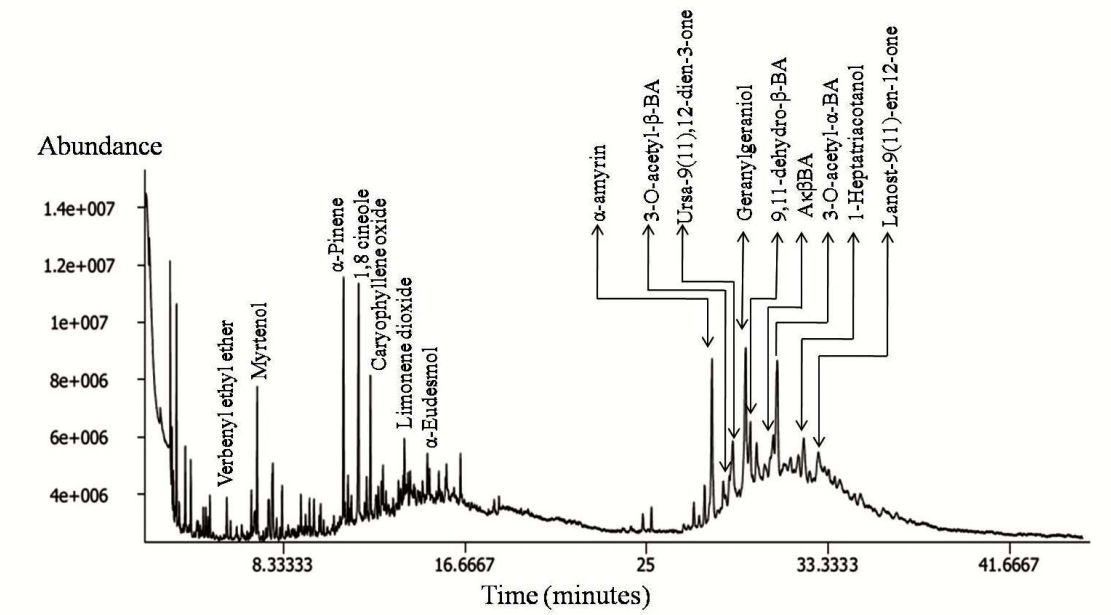

Figure. 3.3. GC/MS analysis of hydroalcoholic extracts of *Boswellia serrata* gum resin (BASE).

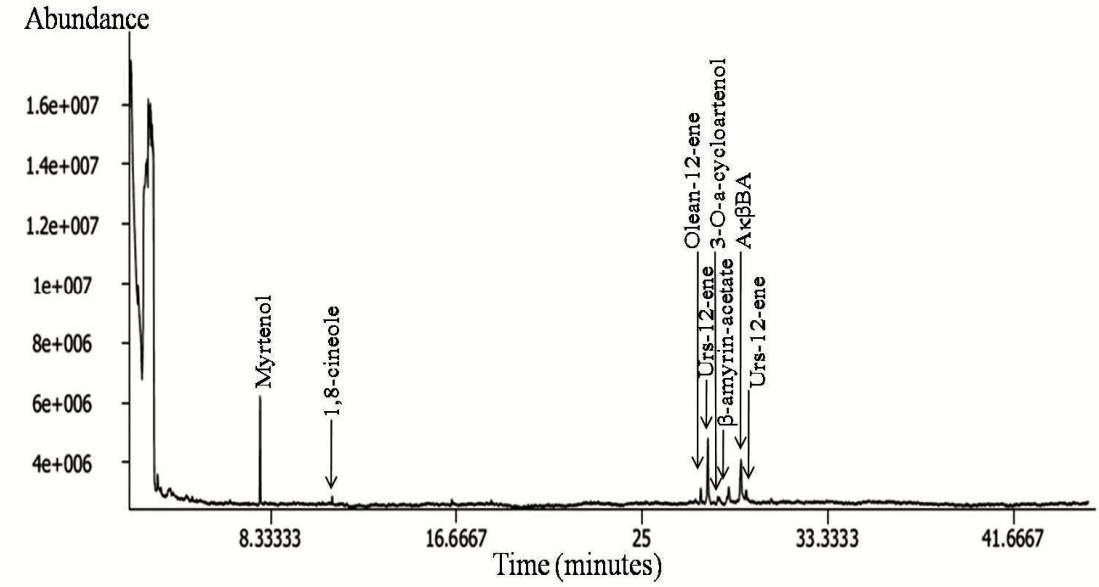

Figure. 3.4. GC/MS analysis of water extract of *Boswellia serrata* gum resin (BSWE).

Table 3.3. Represents the metabolites identified from the derivatised hydroalcoholic extracts of *B. serrata* gum resin by GC-MS analysis.

RT min	Name of compound	Formula	Mass	Area	Area %	Compound type	Reference
3.36	Butanoic acid, 3-methyl-	$C_8H_{18}O_2$	102.1076	4772830	0.2	Carboxylic acid	NIST CAS 503-74-2
6.42	Verbenyl ethyl ether	$C_{12}H_{20}O$	180.2866	11761861	0.3	Oxygenated monoterpene	NIST CAS 80581-06-2
7.0	4-pentene-2-ol, 2-methyl	$C_6H_{12}O$	100.0888	17149014	0.40	Aromatic hydrocarbon	NIST CAS 624-97-5
7.04	4, 4-dimethyl-3-[(trimethyl silyl) oxy] dihydro-2(3H)-furanone	$C_9H_{18}O_3$	202.1025	17538255	0.40	Furanones	NIST CAS 56051-80-0
7.13	(-)-Myrtenol	$C_{10}H_{16}O$	152.1596	90080790	2.1	Monoterpenoid alcohol	NIST CAS 19894-97-4
9.1	Camphenone, 6-	$C_{10}H_{14}O$	150.1045	27104370	0.63	Monocyclic terpene	NIST CAS 55659-42-2
9.5	Myrtenoic acid	$C_{13}H_{22}O_2$	210.1620	24561068	0.57	Cyclic terpene alcohol	NIST CAS 0-00-0
9.7	*cis*-2-hexen-1-ol	$C_6H_{12}O$	100.1283	33375647	0.77	Alkenol	NIST CAS 928-94-9
10	α-pinene	$C_{10}H_{16}$	224.1540	90080790	0.47	Monoterpene	NIST CAS 80-56-8

Continued……

11.1	*trans*-3-acetoxy-1,8-cineole	$C_{12}H_{20}O_3$	212.1412	183101545	4.27	Oxygenated monoterpene	Kubota et al., 1998
11.2	α-calacorene	$C_{15}H_{20}$	200.1565	2868596	0.06	Sesquiterpene	NIST CAS 21391-99-1
11.7	Caryophyllene oxide	$C_{15}H_{24}O$	220.1827	225504057	5.26	Sesquiterpene	NIST CAS 1139-30-6
12.1	Bicyclo[5.3.0]decan-2-one, 9-methylene-10-	$C_{14}H_{24}O$	208.1827	25749050	0.6	Bicyclo alkane	NIST CAS 0-00-0
12.5	α-limonene diepoxide	$C_{10}H_{16}O_2$	168.1150	7964555	2.5	Cyclic terpene	NIST CAS 96-08-2
12.7	5-azulene methanol, 1,2,3,4,5,6,7,8-octahydro-α,α,3,8-tetramethyl-	$C_{15}H_{26}O$	222.19	6730482	0.15	Sesquiterpene	NIST CAS 13822-35-0
12.8	9,12-octadeca diynoic acid	$C_{21}H_{36}O_2$	320.2715	20449632	0.47	Fatty acid	NIST CAS 0-00-0
12.9	11-hexadecyn-1-ol	$C_{16}H_{30}O$	238.2297	31993915	12.9	Alcohol	NIST CAS 65686-49-9
13.3	Limonene dioxide	$C_{10}H_{16}O_2$	168.1150	25542558	0.7	Diterpene	NIST CAS 96-08-2
14.0	Azelaic acid, bis	$C_{15}H_{32}O_4$	276.2300	24491282	0.57	Dicarboxylic acid	NIST CAS 17906-08-0
14.9	α-eudesmol	$C_{18}H_{34}O$	266.2609	43926202	1.02	Terpene alcohol	NIST CAS 0-00-0

Continued……

16.4	Palmitic acid	$C_{16}H_{32}O_2$	256.2798	35696799	0.83	Fatty acid	NIST CAS 57-10-3
18.2	Stearic acid	$C_{18}H_{36}O_2$	356.3111	796723574	18.2	Fatty acid	NIST CAS 57-11-4
27.6	α-amyrin	$C_{33}H_{58}O$	470.4457	30243926	0.8	Triterpene	NIST CAS 1721-67-1
28.0	3-O-acetyl-β-boswellic acid	$C_{32}H_{50}O_4$	498.3709	286577932	6.68	Triterpene	Mathe et al., 2004
28.5	Ursa-9(11),12-dien-3-one	$C_{30}H_{46}O$	422.3549	14056143	0.4	Triterpene	NIST CAS 72093-24-4
29.5	Geranylgeraniol	$C_{20}H_{34}O$	290.2610	362130178	8.4	Polyprenyl alcohol	NIST CAS 24034-73-9
30.0	9,11-dehydro-β-boswellic acid	$C_{30}H_{46}O_3$	454.3446	83079370	1.93	Triterpene	Mathe et al., 2004
30.2	3-O-acetyl-11-keto-β-boswellic acid	$C_{32}H_{48}O_5$	512.3501	272849533	6.3	Triterpene	Mathe et al., 2004
30.9	3-O-acetyl-α-boswellic acid	$C_{32}H_{50}O_4$	498.3709	101120929	2.4	Triterpene	Mathe et al., 2004
32.2	1-heptatriacotanol	$C_{37}H_{76}O$	536.5896	58827278	1.37	Aliphatic hydrocarbon	NIST CAS 105794-58-9
32.8	Lanost-9(11)-en-12-one	$C_{30}H_{50}O$	426.3862	48037227	1.13	Triterpene	Mathe et al., 2004

MS fragmentation of some of the compounds are represented in Figs. 3.5 and 3.6.

Verbenyl ethyl ether (Fig. 3.5. A) an oxygenated monoterpene having molecular weight 180.2866 and molecular formula $C_{12}H_{20}O$ yielded the most intense ion m/z 91.

Camphenone, 6- (Fig. 3.5. B) is a monocyclic terpene having molecular weight 150.1045 and molecular formula $C_{10}H_{14}O$ yielded the mass fragmentation leading to the formation of an intense peak of m/z 108.

α-pinene, a monoterpene (Fig. 3.5. C) having molecular weight 224.1540 and molecular formula $C_{10}H_{16}$ yielded the most intense ion peaks for m/z 91 and 135.

Trans-3-acetoxy-1,8-cineole (Fig. 3.5. D) oxygenated monoterpene yielded the major peak ion of m/z 161, 126 and 81.

(-)-Myrtenol spectra and fragmentation (Fig. 3.5. E) with molecular weight 152.1596 and molecular formula $C_{10}H_{16}O$ yielded the low mass region in spectra of m/z 45 with relatively low intensity and main ions of m/z 144 and 73.

α-calacorene (Fig. 3.5. F) a sesquiterpene with molecular weight 200.1565 and molecular formula $C_{15}H_{20}$ yielded the minor peak m/z 51, 115 and 200 and major peak spectrum yielded m/z 157.

Caryophyllene oxide (Fig. 3.5. G) has the molecular weight 220.1827; molecular formula $C_{15}H_{24}O$ and molecular peak ion m/z 79.

α-limonene diepoxide (Fig. 3.5. H) with molecular weight 168.1150; molecular formula $C_{10}H_{16}O_2$ yielded the mass fragmented peaks of m/z 162 and 81.

11-hexadecyn-1-ol (Fig. 3.5. I) has the molecular weight 238.2297; molecular formula $C_{16}H_{30}O$ yielded fragmented peak ions of m/z 194, 137 and 96.

α-eudesmol (Fig. 3.5. J) terpene alcohol with molecular weight 266.2609; molecular formula $C_{18}H_{34}O$ yielded mass fragmentation pattern with m/z 189, 131 and 73.

α-amyrin (Fig. 3.5. K), a triterpene compound, chemically known as 3β-hydroxy-urs-12-en-3-ol with molecular weight 470.4457; molecular formula $C_{33}H_{58}O$ yielded the MS ion peaks of m/z 498, and a high intense ion m/z 218. These amyrins do occur in many plants, but among resin-producing plants the Burseraceae family can be regarded as the only possible source for this type of amyrin (Norbert Vavra, 1993).

3-O-acetyl-β-boswellic (3-O-AβBA) acid and **3-O-acetyl-α-boswellic (3-O-AαBA) acid** (Figs. 3.5. L and P): The spectrum of pentacyclic triterpene isoforms having molecular weight 498.3709 and molecular formula $C_{32}H_{50}O_4$ yielded the fragmentation ions in loss of methyl and acetyl groups and finally exhibited the base peak of m/z 203 which vary in the intensities of α and β forms, and the other m/z 394, 279, 218, 190 and the effect of mass spectra is clearly visible by the presence of peaks of m/z 73 represents ($(CH_3)_3Si^+$).

Ursa-9(11),12-dien-3-one (Fig. 3.5. M) with molecular weight 498.3709 and molecular formula $C_{32}H_{50}O_4$ yielded the mass fragmentation pattern with m/z 367, 312, 255, 133 and 91 and matched to the GC-MS mass spectrum of Mathe et al., (2009).

Geranylgeraniol, a diterpene alcohol, (Fig. 3.5. N) with molecular weight 290.2610 and molecular formula $C_{20}H_{30}O$ exhibited the fragmentation pattern with m/z 218 and high intense m/z 81.

9,11-dehydro-β-boswellic acid (Fig. 3.5. O) molecular weight 454.3446 and molecular formula $C_{20}H_{34}O$ yielded the mass spectral fragmentation of m/z 218 which varies in the intensities with the other boswellic acids and also shows the m/z 278, 148, 95 and 73.

3-O-acetyl-11-keto-β-boswellic acid (AκβBA) shown in Fig. 3.5. Q, has no derivatives of boswellic acids, with molecular weight 512.3501, molecular formula $C_{32}H_{48}O_5$ and yielded fragment ions signals of m/z 382, 273, 175, 135, 95 and 73. Lanost-9(11)-en-12-one (Fig. 3.5. R) has molecular weight 426.3862 and molecular formula $C_{30}H_{50}O$ exhibited the mass fragmentation pattern of m/z 386, 313, 273, 218, 135 and 95.

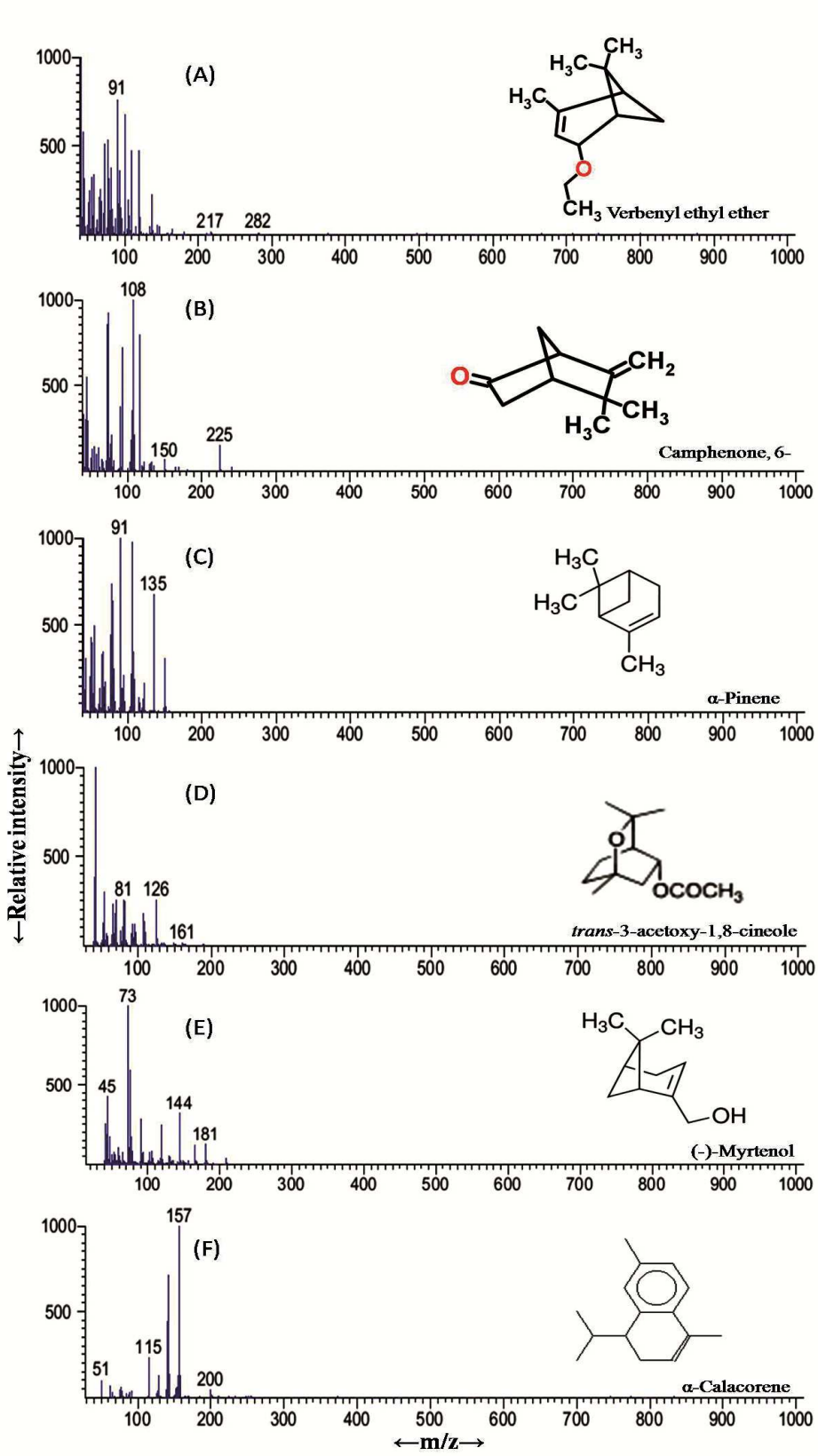
(A)
91
217
282
Verbenyl ethyl ether
(B)
108
150
225
Camphenone, 6-
(C)
91
135
α-Pinene
(D)
81
126
161
trans-3-acetoxy-1,8-cineole
(E)
73
45
144
181
(-)-Myrtenol
(F)
157
115
51
200
α-Calacorene
←Relative intensity→
←m/z→

Continued……

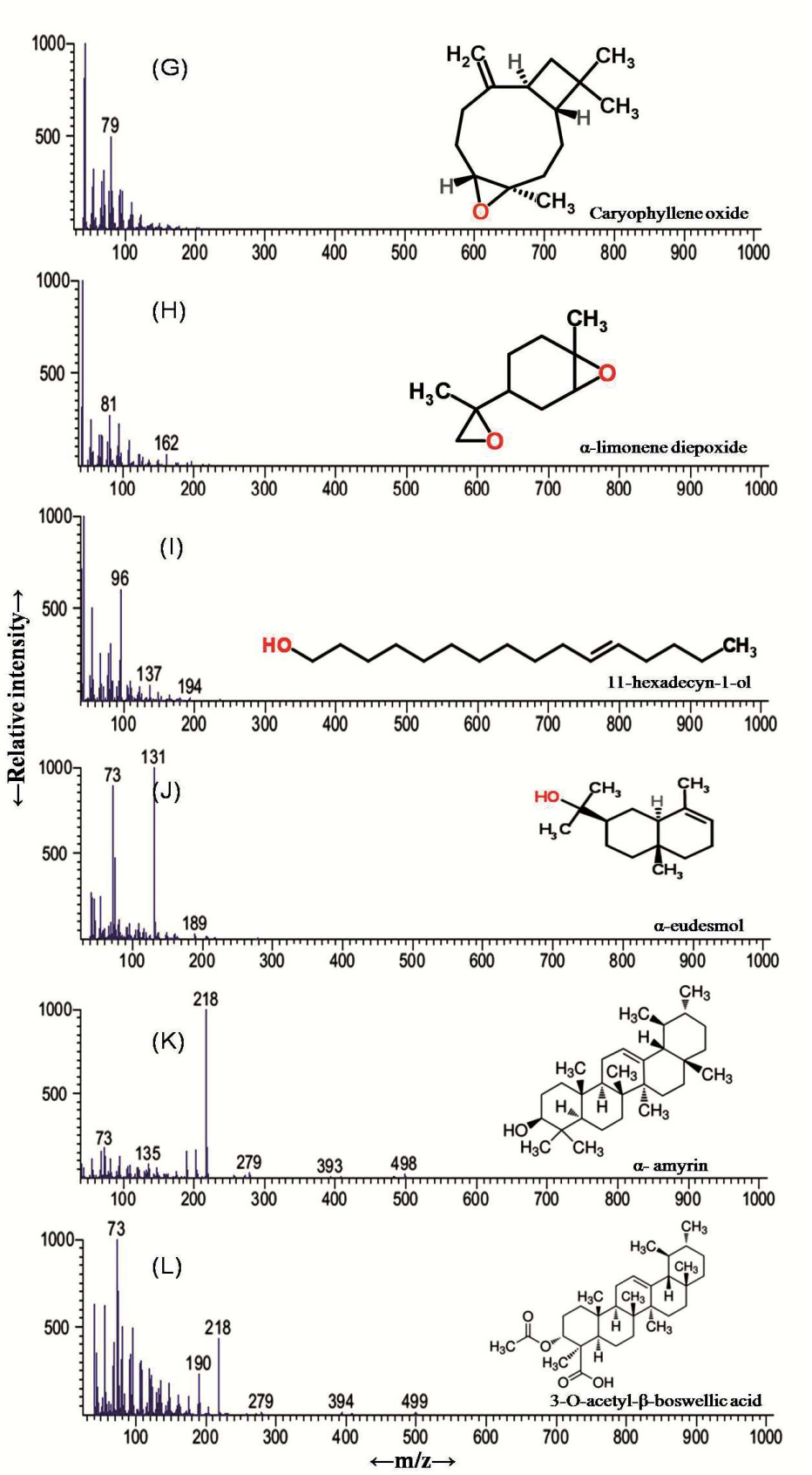
(G)
79
Caryophyllene oxide
(H)
81
162
α-limonene diepoxide
(I)
96
137
194
11-hexadecyn-1-ol
(J)
73
131
189
α-eudesmol
(K)
218
73
135
279
393
498
α- amyrin
(L)
73
218
190
279
394
499
3-O-acetyl-β-boswellic acid
←Relative intensity→
←m/z→

Continued……

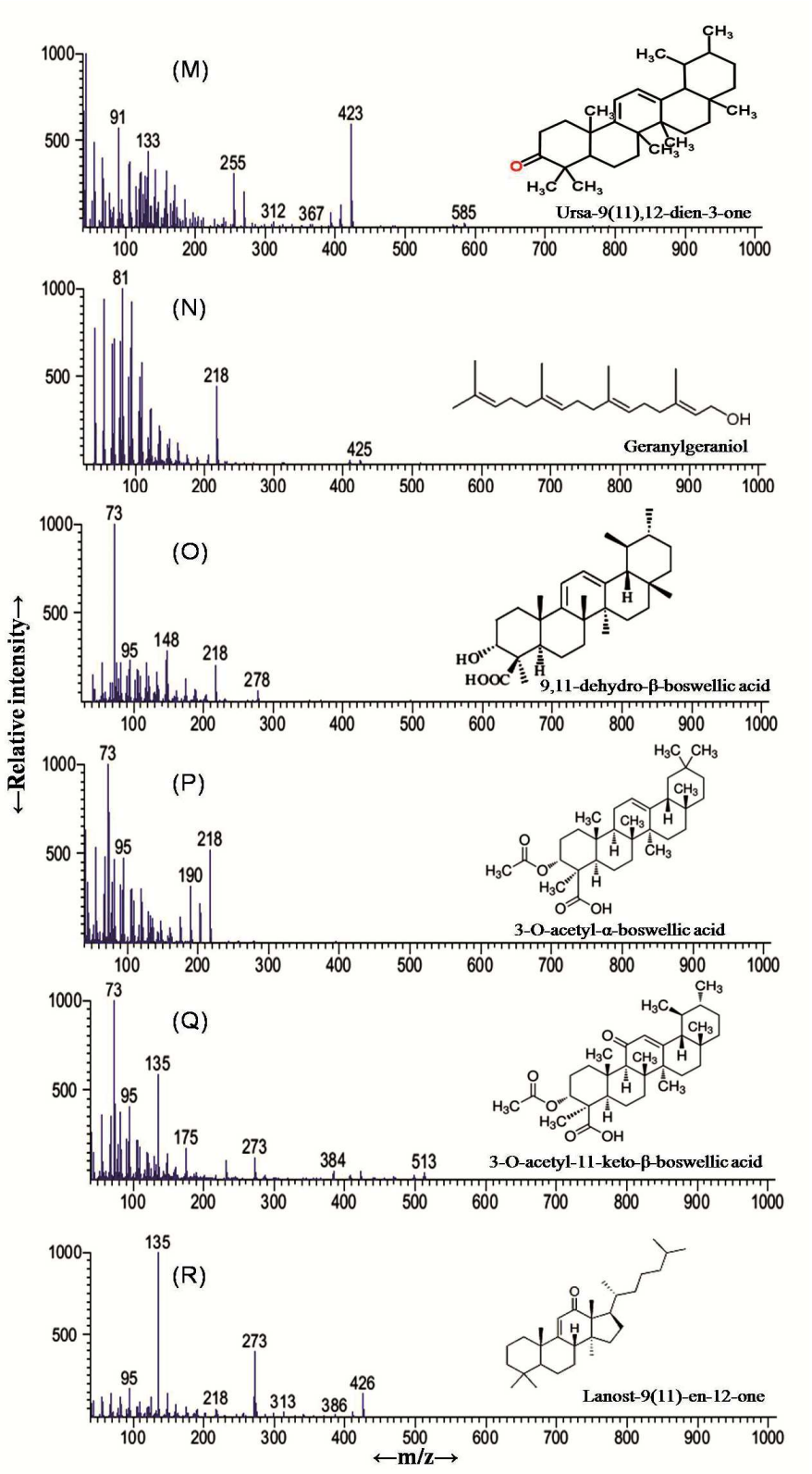

Figure. 3.5. Mass fragmentation spectra of the metabolites identified from the hydroalcoholic extracts of BS-gum resin (BSAE).

Table 3.4. Represents the metabolites identified from the derivatised water extracts of *B. serrata* gum resin by GC-MS analysis.

RT min	Name of compound	Formula	Mass	Area	Area %	Compound type	Reference
11.0	1,8-cineole	$C_{10}H_{18}O$	154.2492	3884184	0.26	Terpenoid oxide aromatic	NIST CAS 470-82-6
11.7	Caryophyllene oxide	$C_{15}H_{24}O$	220.1827	1511167	0.1	Sesquiterpene	NIST CAS 1139-30-6
12.0	*trans*-farnesol	$C_{15}H_{26}O$	222.3378	451238	0.03	Sesquiterpene alcohol	NIST CAS 106-28-5
16.4	Palmitic acid	$C_{16}H_{32}O_2$	256.2798	2253648	0.15	Fatty acid	NIST CAS 57-10-3
27.6	Olean-12-ene	$C_{30}H_{50}$	410.3902	15411400	1.4	Triterpene	Mathe et al., 2004
27.8	α-farnesene	$C_{15}H_{24}$	204.1811	2382622	0.16	Sesquiterpene	NIST CAS 502-61-4
28.3	3-O-acetyl-6-methoxycycloartenol	$C_{33}H_{54}O_3$	498.4072	6765415	0.45	Triterpene	NIST CAS 0-00-0
28.4	1-heptatriacotanol	$C_{37}H_{76}O$	536.5896	8091212	0.54	Alcohol	NIST CAS 105794-58-9
28.8	12-oleanen-3-yl acetate	$C_{32}H_{52}O_2$	468.7567	24252969	1.65	Triterpene	Mathe et al., 2004
29.2	Lupeol	$C_{30}H_{50}O$	426.7174	539736	0.05	Triterpene	NIST CAS 545-47-1
29.4	3-O-acetyl-11-keto-β-boswellic acid	$C_{32}H_{48}O_5$	512.7256	60487152	4.09	Triterpene	NIST CAS 67416-61-9
29.6	Urs-12-ene	$C_{30}H_{50}$	410.3952	4185099	0.28	Triterpene	NIST CAS 464-97-1
30.7	α-Linolenic acid	$C_{18}H_{30}O_2$	278.4296	967947	0.07	Fatty acid	NIST CAS 463-40-1

The fragmentation pattern of the metabolites in BSWE matched against NIST library and shown in Fig. 3.6.

Olean-12-ene and **urs-12-ene** are triterpenoids (Figs. 3.6. A and B) yielded identical fragmentation spectra. Olean-12-ene was eluted before urs-12-ene. Olean-12-ene and

urs-12-ene have same molecular weight 410.3902 and molecular formula $C_{30}H_{50}$ but differ in their similarity by having their molecular ion of m/z 394 for urs-12-ene and m/z 218 for olean-12-ene. The fragment m/z 190 gives the more specific information for the identification of olean-12-ene, absence of this fragment in urs-12-ene indicated the missing of methylene unit (CH_2) (Haven and Rullkotter 1989).

12-oleanen-3-yl acetate,3-α (Fig. 3.6. C), a triterpene, molecular weight 468.7567, molecular formula $C_{30}H_{50}O$, also commonly known as β-amyrin acetate and known to occur as a precursor of boswellic acid, characterised by intense m/z 218 fragment attesting to oleanane structure (Lavrieux et al., 2011).

Lupeol (Fig. 3.6. D) $C_{30}H_{50}O$, comparison of MS fragmentation pattern with published spectra (Kumar et al., 2013) and NIST library data base by displaying abundant fragments at m/z values at 427, 218, 207, 189, etc. It was shown to have antioxidant status in heavy metal, cadmium exposed mice (Nagaraj et al., 2000).

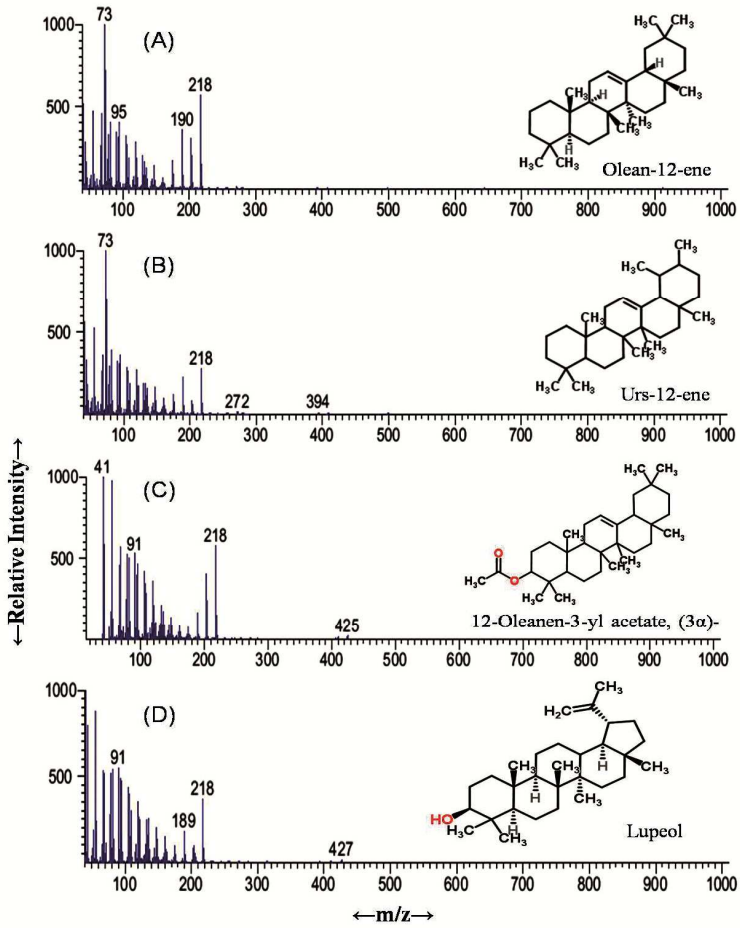

Figure. 3.6. Mass fragmentation spectra of the metabolites identified from the aqueous extract of BS-gum resin (BSWE).

Boswellic acid mixed-fraction (BAM)

We isolated boswellic acid from the BS-gum resin and estimated total polyphenolics and triterpenoids in the boswellic acid mixed-fraction (BAM). It contained total polyphenols of 0.4670 ± 0.11 GAE mg/g dwt and triterpenoids of 0.926 ± 0.21 UAE mg/g dwt. 50 g of gum resin yielded 0.68 g (w/w) and BAM, which was solubilised in ethanol for further pharmacological assays.

GC-MS analysis of BAM

BAM fraction was subjected to derivatization in order to detect non-volatile compounds by GC-MS. GC-MS analysis revealed the presences of thirty seven compounds in it. Confirmation of the compounds was done based on the retention time and their MS fragmentation spectra. The detection of α- and β-boswellic acids and their 3-O-acetyl derivatives is only possible by derivatization. The β-configuration always gave longer retention time than α-configuration (Mathe et al., 2004). The total ion chromatogram (TIC) of boswellic acid fraction shown in the Fig. 3.7.

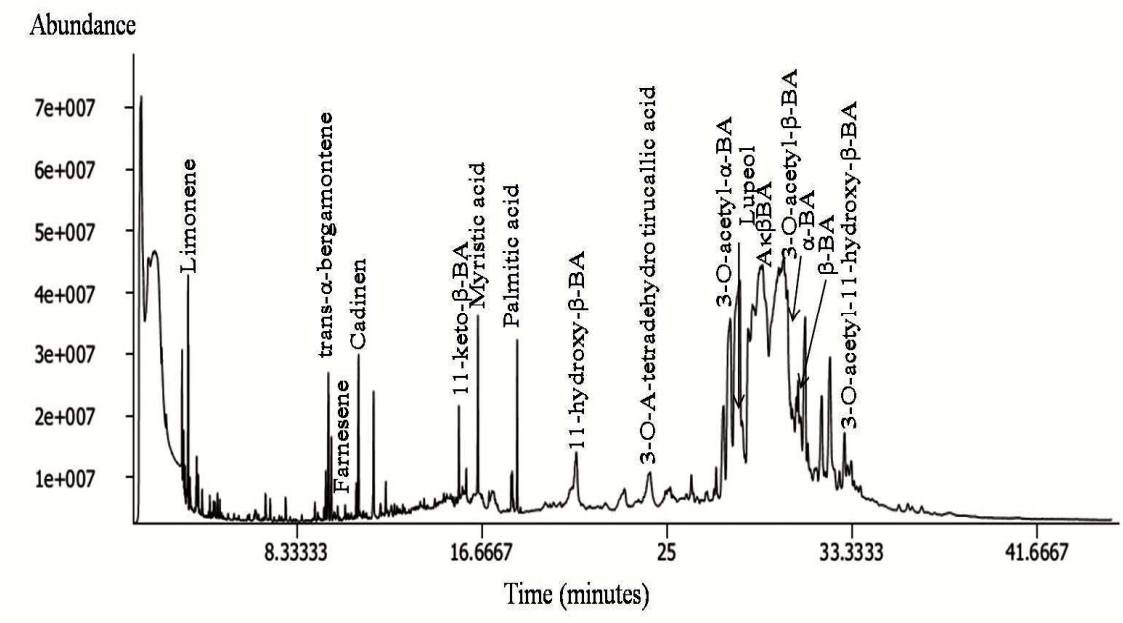

Figure. 3.7. GC/MS analysis of boswellic acid mixed-fraction (BAM) of *Boswellia serrata* gum resin.

Table 3.5. It represents the complete list of metabolites identified from the TIC chromatogram of the GC/MS analysis of boswellic acid mixed-fraction (BAM) of *Boswellia serrata* gum resin.

Rt $_{min}$	**Compound**	**Formula**	**MW**	**Area**	**Area %**	**Compound Type**	**Reference**
4.37	Limonene	$C_{10}H_{16}$	136.2340	17440604	0.42	Monoterpene	NIST CAS 138-86-3
5.5	Myrcenol	$C_{10}H_{18}O$	154.1393	19213127	0.15	Monoterpenoid	NIST CAS 543-39-5
9.15	α-linolenic acid	$C_{18}H_{30}O_2$	278.4321	62098368	0.48	Fatty acid	NIST CAS 463-40-1
9.27	α-bourbonene	$C_{15}H_{24}$	204.1411	29604107	0.12	Sesquiterpene	NIST CAS 5208-59-3
9.64	*trans*-α-bergamontene	$C_{15}H_{24}$	204.1835	138553123	1.14	Sesquiterpene	NIST CAS 13474-59-4
9.75	Caryophyllene	$C_{15}H_{24}$	204.3511	527515126	3.08	Sesquiterpene	NIST CAS 87-44-5
9.88	α-pyronene	$C_{10}H_{16}$	136.1223	139076203	0.5	Monoterpene	NIST CAS 514-94-3
10.0	epi-α-santalene	$C_{15}H_{24}$	204.3511	20197572	0.1	Sesquiterpene	NIST CAS 512-61-8
10.5	α-farnesene	$C_{15}H_{24}$	204.1843	44912234	2.32	Sesquiterpene	NIST CAS 502-61-4
11	α-cadinene	$C_{15}H_{24}$	204.1833	600226783	1.0	Sesquiterpene	NIST CAS 24406-05-1
12	*cis*-z-a-bisabolene epoxide	$C_{15}H_{24}O$	220.1805	21127267	0.75	Sesquiterpene	NIST CAS 00-0-0
13	Caryophyllene oxide	$C_{15}H_{24}O$	220.3535	18843219	0.03	Sesquiterpene	NIST CAS 1139-30-6
15.5	*cis*-farnesol	$C_{15}H_{26}O$	222.1921	47309839	2.0	Sesquiterpene alcohol	NIST CAS 106-28-5
15.7	11-keto-β-boswellic acid	$C_{33}H_{54}O_2$	470.6801	511297892	4.0	Triterpene	NIST CAS 17019-92-0
16.4	Myristic acid	$C_{14}H_{28}O_2$	228.3709	43892528	1.74	Fatty acid	NIST CAS 544-63-8

Continued……

18.0	Oleic acid	$C_{18}H_{34}O_2$	282.4614	120914076	0.9	Fatty acid	NIST CAS 112-80-1
18.2	Palmitic acid	$C_{16}H_{32}O_2$	256.4241	437354415	1.42	Fatty acid	NIST CAS 57-10-3
20.8	Myricyl alcohol	$C_{30}H_{62}O$	438.8112	82847136	0.14	Fatty alcohol	NIST CAS 593-50-0
21.1	11-hydroxy-β-boswellic acid	$C_{30}H_{48}O_4$	472.2131	73660981	0.21	Triterpene	Mathe et al., 2004
24.7	3-O-acetyl-8,9,24,25-tetradehydro-tirucallic acid	$C_{30}H_{50}O_4$	474.1021	5512126	0.09	Tirucallic acids	Ali sha et al., 2009
28.2	3-O-acetyl-α-boswellic acid	$C_{32}H_{50}O_4$	498.7408	1182472084	7.3	Triterpene	Mathe et al., 2004
28.84	Lupeol	$C_{30}H_{50}O$	426.7274	235261354	1.84	Triterpene	NIST CAS 545-47-1
29	3-O-acetyl-11-keto-β-boswellic acid	$C_{32}H_{48}O_5$	512.7205	954535427	7.57	Triterpene	Belsner et al., 2003
30.1	3-O-acetyl-β-boswellic acid	$C_{32}H_{50}O_4$	498.7408	1772527376	3.49	Triterpene	Mathe et al., 2004
30.2	3-oxo-8,9, 24,25-tetra dehydro-tirucallic acid	$C_{33}H_{50}O_5$	454.1343	658439814	1.49	Tirucallic acids	Mathe et al., 2004
30.3	Cholesta-7,9(11)-dien-3-ol, 4,4-dimethyl-, (3α,5α)-	$C_{29}H_{48}O$	412.3221	566918499	1.05	Steroid	NIST CAS 53368-67-5
30.37	9,11-dehydro-β-boswellic acid	$C_{30}H_{46}O_3$	454.3183	173607072	1.38	Tirucallic acids	Belsner et al., 2003
30.38	Cholest-4-en-26-al, 3- oxo-, cyclic 26-	$C_{29}H_{46}O_3$	442.6737	747543257	1.35	Steroid	NIST CAS 00-0-0
30.45	α-boswellic acid	$C_{30}H_{48}O_3$	456.7209	2284539107	9.89	Triterpene	Mathe et al., 2004 NIST CAS

Continued……

							47-66-9
30.5	3-O-acetyl-9,11-dehydro-β-boswellic acid	$C_{32}H_{48}O_4$	496.4211	13089571	2.6	Triterpene	Belsner et al., 2003
30.6	11-hydroxy-α-boswellic acid	$C_{30}H_{48}O_4$	472.2121	81190815	1.0	Triterpene	Mathe et al., 2004
30.8	β-boswellic acid	$C_{30}H_{48}O_3$	456.7202	97829975	6.04	Triterpene	Mathe et al., 2004 NIST CAS 631-69-6
31.25	Olean-12-ene, 3-methoxy-(3α)-	$C_{31}H_{52}O$	440.7439	105300290	1.18	Tirucallic acids	NIST CAS 00-0-0
31.42	3-O-acetoxy-11-methoxy-β-boswellic acid	$C_{33}H_{52}O_5$	528.3261	394510096	1.1	Tirucallic acids	Mathe et al., 2004
31.74	9,11-dehydro-α-boswellic acid	$C_{30}H_{46}O_3$	454.5531	34375146	0.5	Tirucallic acids	Mathe et al., 2004
33.0	3-O-acetyl-11-hydroxy-β-boswellic acid	$C_{32}H_{50}O_5$	514.6351	325762664	2.55	Tirucallic acids	Mathe et al., 2004

11-Keto-β-boswellic acid (KβBA) (Fig. 3.8. A): Mass spectrum of KβBA yielded to have no boswellic acid derivatives. KβBA produced fragment ions shows m/z 513 indicates the loss of trimethylsilyl group, followed by the fragmentation pattern m/z 470, 423, 346, 288, 232, 175, 135, 105 and 83.

3-O-acetyl-α-boswellic acid (3-O-AαBA) and **3-O-acetyl-β-boswellic acid** (3-O-AβBA) (Figs. 3.8. B and D): Same fragmentation pattern as KβBA was observed in the case of derivatives of 3-O-AαBA and 3-O-AβBA. The spectra of both acids exhibited the fragmentation ions without methyl and acetyl groups and showing the base peak of m/z 203 (Fig. 3.8. B). The spectrum was observed to be 50 % more abundant in 3-O-AαBA. The effect of TMS-derivatisation on the mass spectra of these triterpenes is clearly visible by the presence of peaks at m/z 73 representing

[$(CH_3)_3Si$+]; m/z 147 represents loss of CH_3 from TMS and TMSOH; m/z 292 for carboxyl groups.

AκβBA (Fig. 3.8. C): Mass spectrum of AκβBA yielded to have the mass signal of m/z 497 with the loss of TMSOOCH, followed by fragmentation of ions m/z 427, 352, 278, 218, 148, 103, 73 and 55. AκβBA has no boswellic acid derivatives like 11-κβBA (Fig. 3.8. A) and fragment ions shown to have slight variation between these two boswellic acids (Figs. 3.8. C and A).

α-boswellic acid (α-BA) and **β-boswellic acid** (β-BA) (Figs. 3.8. E and F): Silylated derivatives of α-BA and β-BA identified according to their molecular weight 456.7209, molecular formula $C_{30}H_{48}O_3$ and their mass spectra in which the molecular ion peak was m/z 600, the fragment ion signals represents m/z 585 indicating the loss of methyl group, m/z 495 represents the loss of silylated with methyl group for both α-BA and β-BA further fragmentation leads to intensive signals with m/z 218 fragment. According to Mathe et al., (2004) the mass spectrum of α-BA is different than the β-BA by showing the m/z 218 fragment was more abundant in α-BA than β-BA, the higher intensity in the signal may be due to the more stable ion it formed from α-BA.

Furthermore fatty acids, sesquiterpenes and tirucallic acids have also been detected in BAM and confirmed by comparing of their mass spectra with those from NIST database (Table 3.5).

LC-Q-TOFMS-based metabolite profiling of TA-stem bark

TA-stem bark reported to have several compounds of phenolics, flavonoids, terpenes and so many other (Dwivedi, 2007). In the present study alcohol and water extracts of *T. arjuna*-stem bark (TAAE and TAWE) subjected to LC-Q-TOFMS for the reasons most importantly to (1) authenticate plant samples (2) to distinguish the metabolite profile of TAAE and TAWE. Data was acquired in both negative and positive ion modes. Ionization of the compounds in the negative mode gave higher sensitivity and better detection compared to positive ion mode. Therefore, the mass spectra and fragmentation patterns obtained in the negative mode are discussed in detail. Negative ion mode detected a total of 13 metabolites from TAAE (Table 3.6) and 9 from TAWE (Table 3.7). Both TAAE and TAWE contained some of the

compounds in common, like kaempferol, epigallocatechin, ellagic acid pentose, ellagic glycoside, terminolic acid and arjunic acid.

TAAE exclusively contained glycopyranosides (e.g. 26-O-β-D-glucopyranosyl-furostan-5,25(27)-diene-1β,3β,22β,26-etrahydroxy-1-O-α-L-arabino pyranoside; 16α-hydroxy protobassic acid 3-O-β.-D-glucopyranoside), steroid glycoside (e.g. (1β,3β,8ξ,9ξ,14ξ,16ξ,17ξ,22ξ)-3-hydroxy spirost-5-en-1-yl 2-O-(6-deoxy hexo pyranosyl) pento pyranoside) and few other compounds whereas TAWE contained gallic acid, catechin and a derivative of ellagic acid i.e. 3'-O-methyl-4-O-(β-D-xylopyranosyl) ellagic acid (Tables 3.6 and 3.7). MS-MS spectra of the compounds detected in TAAE and/or TAWE are shown in (Figs. 3.9 and 3.10).

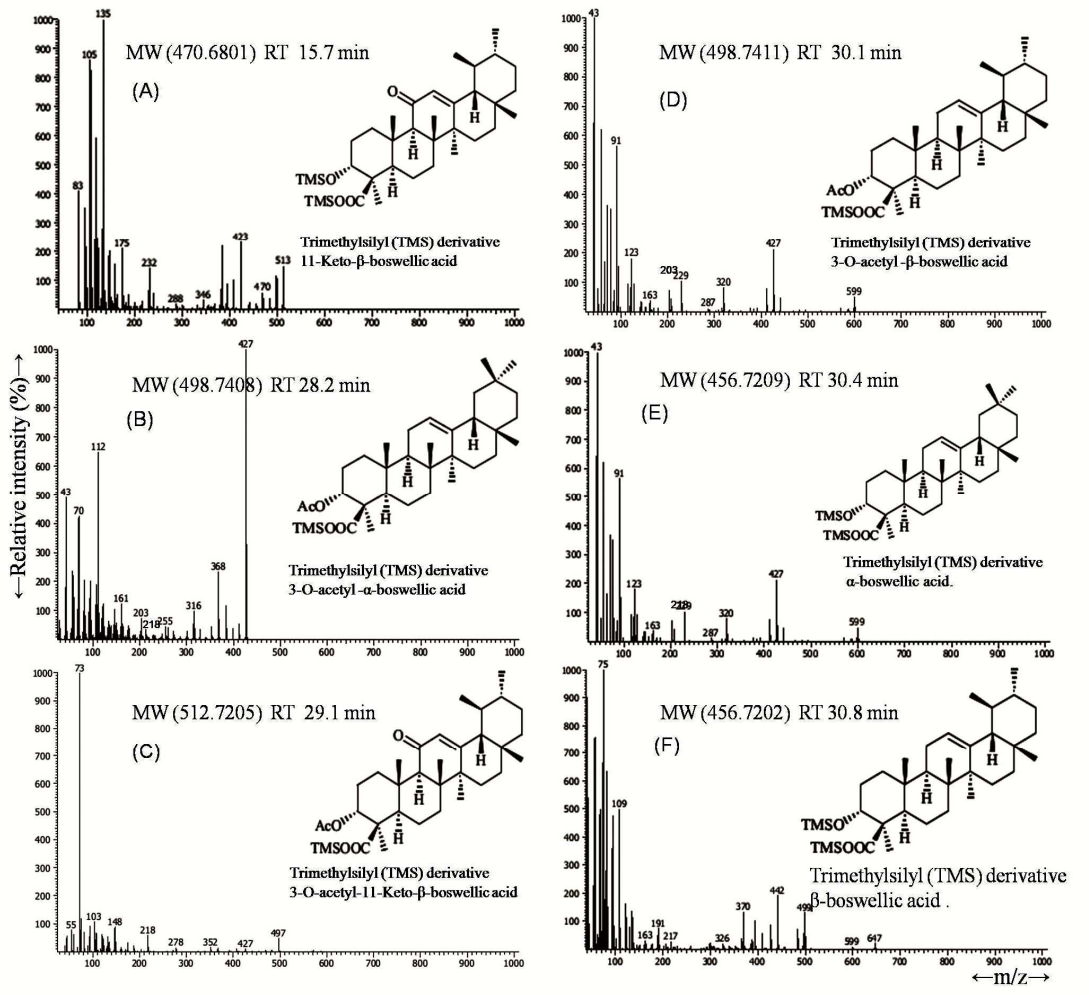

Figure. 3.8. Representative mass fragmentation spectra of the metabolites identified from the BAM. (A)11-keto-β-boswellic acid (B) 3-O-acetyl-α-boswellic acid (C) 3-O-acetyl-11-keto-β-boswellic acid (D) 3-O-acetyl-β-boswellic acid (E) α-boswellic acid (F) β-boswellic acid.

Table 3.6. Q-TOF profile negative ion mode of TAAE used in LC-MS/MS analysis.

RT min	Compound name	Mol formula	Exact mass	Abund	Compound type	Reference
2.53	Kaempferol-3-glucoside-6-*p*-coumaroyl	$C_{30}H_{26}O_{13}$	594.13	32004	Flavonoid	Mass Bank. Leibniz institute for Plant Biochemistry, Halle, Germany
3.15	(-)-Epigallocatechin	$C_{15}H_{14}O_7$	306.08	51648	Flavan-3-ol	Mass Bank. Leibniz institute for Plant Biochemistry, Halle, Germany
3.8	(-)-Epicatechin	$C_{15}H_{14}O_6$	290.07	47088	Flavonoid	Mass Bank. Leibniz institute for Plant Biochemistry, Halle, Germany
4.0	Ellagic acid pentose	$C_{19}H_{14}O_{12}$	434.04	30076	Tannin	RIKEN MSn spectral data base for phytochemicals
5.4	3'-O-methyl-4-O-(β-D xylo pyranosyl) ellagic acid	$C_{20}H_{16}O_{12}$	448.06	112577	Flavonols	Beate et al., 2010.
8.2	26-O-β-D-glucopyranosyl-furostan-5,25(27)-diene-1β,3β,22β,26-etrahydroxy-1-O-α-L-arabino pyranoside	$C_{38}H_{60}O_{14}$	740.39	9965	Glycopyranosides	ChemSpider, Royal Society of chemistry, London.
12.0	16α-hydroxy protobassic acid, 3-O-β.-D-glucopyranoside	$C_{38}H_{60}O_{13}$	726.41	116681	Glycopyranosides	ChemSpider, Royal Society of chemistry, London.
14.5	(1β,3β,8ξ,9ξ,14ξ,16ξ,17ξ,22ξ)-3-hydroxy spirost-5-en-1-yl 2-	$C_{38}H_{60}O_{12}$	708.40	58860	Steroid glycoside	ChemSpider, Royal Society of chemistry,

Continued……

	O-(6-deoxy hexo pyranosyl) pento pyranoside					London
15.0	(4aR,5R,6aR,6aS,6bR,8R,8aR,9R,10R,11S,12aS,14bS)-5,8,11-tri hydroxy-9-(hydroxymethyl)-2, 2, 6a, 6a, 6b, 9, 12a, 14b-octamethyl	$C_{38}H_{62}O_{12}$	710.41	719438	Steroid glycoside	National centre for Biotechnology information (NCBI) – PubChem Compound
18.4	Arjungenin	$C_{30}H_{48}O_6$	504.33	141813	Triterpenoid	Jain et al., 2009.
23.8	Arjunolic acid	$C_{30}H_{48}O_5$	488.34	52287	Triterpenoid	Yang et al., 2011.
24.1	Arjunic acid	$C_{30}H_{48}O_5$	488.34	128461	Triterpenoid	Yang et al., 2011.
25.7	3-(3,5-di-tert-butyl-4-hydroxy phenyl) propanoic acid, 3-(3,5-di-tert-butyl-4-hydroxy phenyl) propionic acid	$C_{17}H_{26}O_3$	278.17	202275	Steroid glycoside	National centre for Biotechnology information (NCBI) –Pub Chem Compound.

The fragmentation pattern of the metabolites detected by LC-MS/MS analysis in TAAE and TAWE are shown in Figs. 3.9 and 3.10 respectively.

Kaempferol-3-glucoside-6-*p*-coumaroyl, $C_{30}H_{26}O_{13}$ (Figs. 3.9. A and 3.10. A): It yielded the peak at RT 2.53 min from TAAE and RT 2.46 min in TAWE. Identification of the compound confirmed by $[M-H]^-$ with m/z 594.1370. The mass fragmentation pattern $[M]^-$ of the compound were m/z 424, 408, 306, 290, 180, 178, 166, 162 and 126. This compound was confirmed by the hit from the data bases (Plant Science Centre, RIKEN, Accession number PS092512, CAS number 20316-62-5; Mass bank record PR101023).

(-)-Epigallo catechin, $C_{15}H_{14}O_7$ (Figs. 3.9. B and 3.10. B): It was eluted at RT 3.15 min in TAAE and RT 2.52 min from TAWE. Identification of the compound was confirmed by their the MS-fragmentation spectra exhibiting the ions $[M-H]^-$ with m/z 305.0727 and secondary fragmentation ions at m/z 217, 167, 165, 123, 121, 111

and 109 with 1 % intensity and m/z 137, 139 having 2 % and m/z 125 exhibited 100 % intensity respectively. The detailed information of (-)-epigallocatechin compared with Metlin MID 3550 data base, which has previously been characterised by Mizooku et al., 2003.

(-)-Epicatechin, $C_{15}H_{14}O_6$ (Fig. 3.9. C): It belongs to flavanols with defined C-ring fragments, of peaks at RT 3.8 min from TAAE, identification confirmed by $[M-H]^-$, m/z 289.0790. The mass fragmentation pattern $[M]^-$ with m/z 289, 271 and 231 with intensity of 75 % , 5 % and 4 % respectively from Metlin MID 3420 data base. Along with these fragments, fragments with m/z 283, 255 and 112 were also formed in the cleavage and are identified from Mass bank record PR020001.

Ellagic acid pentose, $C_{19}H_{14}O_{12}$ (Fig. 3.9. D): It is a derivative of ellagic acid $[M-H]^-$, m/z 433.0485, yielded the peak at RT 4.0 min from TAAE and RT 4.7 min from TAWE. The mass fragmentation pattern generated were $[M-H]^-$ with m/z 300, 301 and 303. The product ion m/z 303 with higher intensity suggests the presence of ellagic acid core in the component, which has previously been characterised by Quave et al., (2012). This compound was confirmed by the hit from the data bases (Plant Science Centre, RIKEN, Accession number PM011331 and Publication PUBMED ID 18774147 CAS number N/A).

3'-O-methyl-4-O-(β-D xylopyranosyl) ellagic acid, $C_{20}H_{16}O_{12}$ (Fig. 3.9. E): It is a glycosylated derivative of ellagic acid. It's peaks are comparable with reported mass fragmentation data of polyphenols from *Terminalia chebula* Retz. (Sarabhai et al., 2013; Beate et al., 2010). Identification of the compound confirmed by $[M-H]^-$, peak obtained of m/z 447.05 at RT 5.4 min in both TAAE and TAWE with fragmentation of m/z 302; 300 and 299.

26-O-β-D-glucopyranosyl-furostan-5,25(27)-diene-1β,3β,22β,26-etrahydroxy-1-O-α-L-arabinopyranoside, $C_{38}H_{60}O_{14}$ (Fig. 3.9. F): It yielded the peak at RT 8.2 min in TAAE. The identification of the compound confirmed by its mass spectrum exhibiting the ions $[M-H]^-$ of m/z 739.3911, mass fragmentation pattern $[M-H]^-$ of the compound were m/z 456, 457, 472, 500, 518, 519 and are comparable with Chemspider CB81468612.

16α-hydroxy protobassic acid, 3-O-β.-D-gluco pyranoside, $C_{38}H_{60}O_{13}$ (Fig. 3.9. G): It yielded the peak at RT 12.0 min from TAAE. Identification of the compound confirmed by the mass spectrum exhibiting the ions $[M-H]^-$ with m/z 726.4101 and

of mass fragmentation pattern $[M-H]^-$ with m/z 503, 501, 484, 458 and 440. It is a triterpenoid saponin and has previously been characterised by Sahu (1996).

(1β,3β,8ξ,9ξ,14ξ,16ξ,17ξ,22ξ)-3-hydroxy spirost-5-en-1-yl 2-O-(6-deoxy hexo pyranosyl) pentopyranoside, $C_{38}H_{60}O_{12}$ (Fig. 3.9. H): It yielded the peak at RT 14.5 min from TAAE. Identification of the compound is confirmed by the mass spectrum exhibiting the ions $[M-H]^-$ with m/z 707.4021 and mass fragmentation pattern $[M-H]^-$ of m/z 487 and 486 compared with Chemspider CB25027828.

(4aR,5R,6aR,6aS,6bR,8R,8aR,9R,10R,11S,12aS,14bS)-5,8,11-trihydroxy-9-(hydroxy methyl)-2, 2, 6a, 6a, 6b, 9, 12a, 14b-octamethyl, $C_{38}H_{62}O_{12}$ (Fig. 3.9. I): It yielded the peak at RT 15.0 min from TAAE. Identification of the compound confirmed by the mass spectrum exhibiting the ions $[M-H]^-$ with m/z 709.4112. Mass fragmentation pattern $[M-H]^-$ was of m/z 489 and 488 as reported in glycoside data base (ID GSD1002155; PubChem 464978).

Arjungenin, $C_{30}H_{48}O_6$ (Fig. 3.10. G): It yielded the peak at RT 18.4 min from TAAE and RT 18.5 min from TAWE. The identification of the compound was confirmed by the mass spectrum exhibiting the ions $[M-H]^-$ of m/z 503.3385. MS fragmentation pattern $[M-H]^-$ were m/z 485, 457, 453, 442, 441, 393 and 379. It belongs to oleanolic acid group with chemical name 2α, 3β, 19α, 23-tetrahydroxy-olean-12-en-28-oic acid and has been previously reported by Chen-Chen et al., (2012).

Arjunolic acid, $C_{30}H_{48}O_5$ (Fig. 3.9. J): It is a oleane derivative and it was eluted at RT 23.8 min from TAAE. Identification of the compound was confirmed by the mass spectrum exhibiting the ions $[M-H]^-$ with m/z 487.3499. MS fragmentation pattern $[M-H]^-$ of the compound were m/z 395, 294, 284, 256, 144, 117 and 113.

Arjunic acid, $C_{30}H_{48}O_5$ (Figs. 3.9. K and 3.10. H): It eluted with RT at 24.1 min from TAAE and TAWE. Identification of the compound was confirmed by the mass spectrum exhibiting the ions $[M-H]^-$ with m/z 487.3469 and MS fragmentation pattern $[M-H]^-$ of the compound were of m/z 427, 426, 424, 408 and 394.

3-(3,5-di-tert-butyl-4-hydroxyphenyl) propanoic acid, $C_{17}H_{26}O_3$ (Fig. 3.9. L): It yielded the peak at RT 25.7 min from TAAE. Identification of the compound was confirmed by the mass spectrum exhibiting the ions $[M-H]^-$ with m/z 277.1713. MS fragmentation pattern $[M-H]^-$ were of m/z 234, 232, 206, 205, 176 and 120 reported in Chemspider CB79743 and PUBCHEM ID 88389.

Gallic acid, $C_7H_6O_5$ (Fig. 3.10. C): It yielded the peak at RT 3.0 min from TAWE. The identification of the compound was confirmed by the mass spectrum exhibiting the ions $[M-H]^-$ of m/z 169.0142. It's MS fragmentation pattern $[M-H]^-$ with m/z 112, 109, 107 and 97 have been identified through Metlin MID 3295; Mass bank KO000889; Plant Science Centre, RIKEN, Accession number PM012529, Publication PUBMED ID 17044128 CAS number 149-91-7 and also as previously been characterised by Beate et al., (2010).

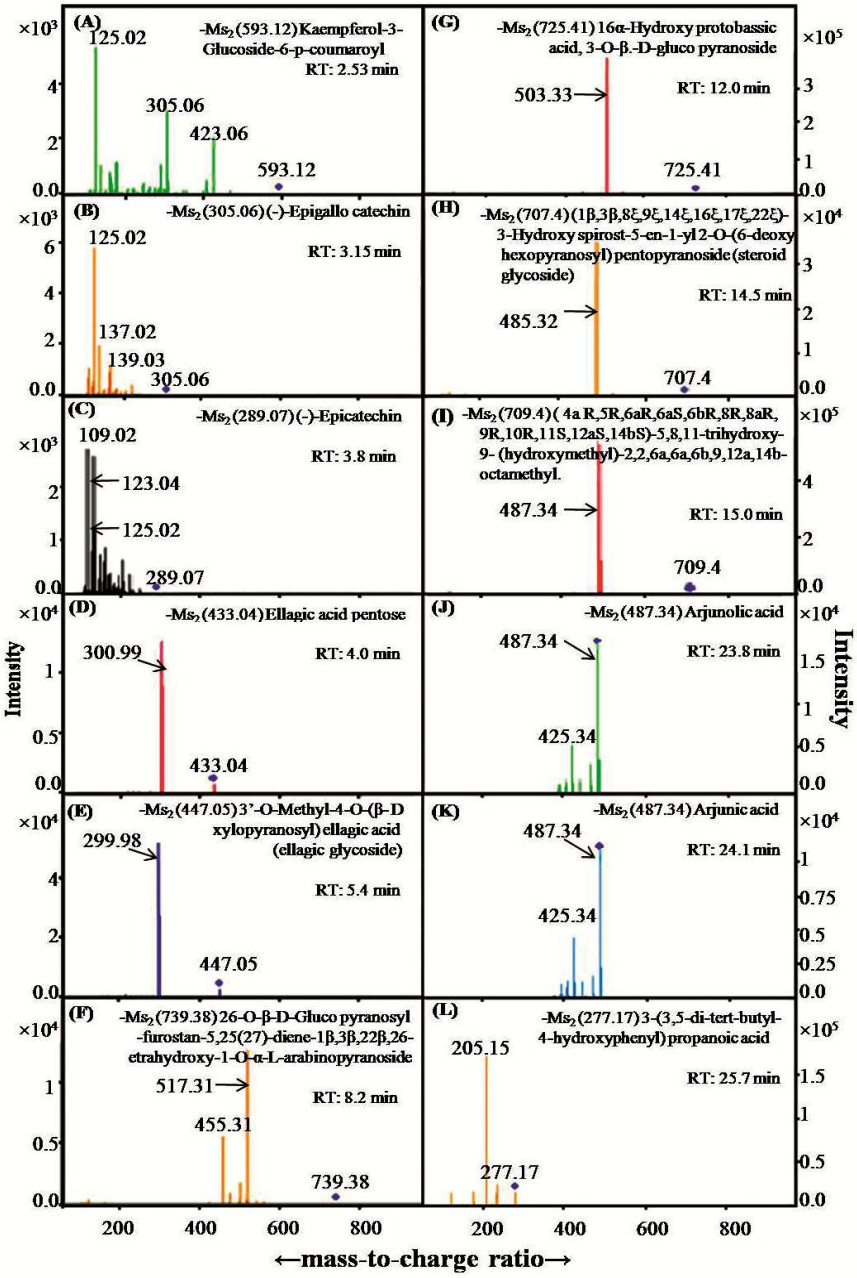

Figure. 3.9. Negative ion (−) ESI/MS/MS of alcoholic extracts (TAAE) of TA-stem bark. Product ion labels correspond to MS fragments.

Table 3.7. Q-TOF profile negative ion mode of TAWE used in LC-MS/MS analysis

RT min	Compound name	Mol formula	Exact mass (calc.)	Abund	Compound type	Reference
2.46	Kaempferol-3-glucoside-6-*p*-coumaroyl	$C_{30}H_{26}O_{13}$	594.13	38776	Flavonoid	Mass Bank. Leibniz institute for Plant Biochemistry, Halle, Germany
2.52	(-)-Epigallo catechin	$C_{15}H_{14}O_7$	306.08	34517	Flavan-3-ol	Mass Bank. Leibniz institute for Plant Biochemistry, Halle, Germany
3.0	Gallic acid	$C_7H_6O_5$	170.01	152036	Phenolic acid	Beate et al., 2010.
3.8	Catechin	$C_{15}H_{14}O_6$	290.06	72187	Flavonoid	Mass Bank. Leibniz institute for Plant Biochemistry, Halle, Germany
4.7	Ellagic acid pentose	$C_{19}H_{14}O_{12}$	434.03	15588	Tannin	RIKEN MSn spectral data base for phytochemicals
5.4	3'-O-methyl-4-O-(β-D xylo pyrano syl) ellagic acid	$C_{20}H_{16}O_{12}$	448.05	148922	Ellagic glycoside	Beate et al., 2010.
7.7	3,3'-di-O-methyl-4-O-(β-D-xylo pyranosyl) ellagic acid	$C_{21}H_{18}O_{12}$	462.07	14507	Flavonols	Beate et al.,2010.
18.5	Terminolic acid / Arjungenin	$C_{30}H_{48}O_6$	504.33	118374	Triterpenoid	Jain et al., 2009.
24.1	Arjunic acid	$C_{30}H_{48}O_5$	488.34	23076	Triterpenoid	Yang et al., 2011.

Catechin, $C_{15}H_{14}O_6$ (Fig. 3.10. D) yielded the peak at RT 3.8 min in TAWE. Identification of the compound was confirmed by $[M-H]^-$, m/z 290.0790. The mass fragmentation pattern [M]- with m/z 222, 204, 188, 162, 152, 150, 138, 136, 126, 124 and the detailed information of each peak in the compound is similar to Metlin MID 3419 and Mass bank record PB002429.

3,3'-di-O-methyl-4-O-(β-D-xylo pyranosyl) ellagic acid, $C_{21}H_{18}O_{12}$ (Fig. 3.10. F) yielded the peak at RT 7.7 min from TAWE. The identification of the compound was confirmed by the mass spectrum exhibiting the ions $[M-H]^-$ of m/z 461.07. The compound gave the MS fragmentation pattern $[M-H]^-$ with m/z 328, 317, 316, 315, 313, 301, 300 and has previously been characterised by Beate et al., (2010).

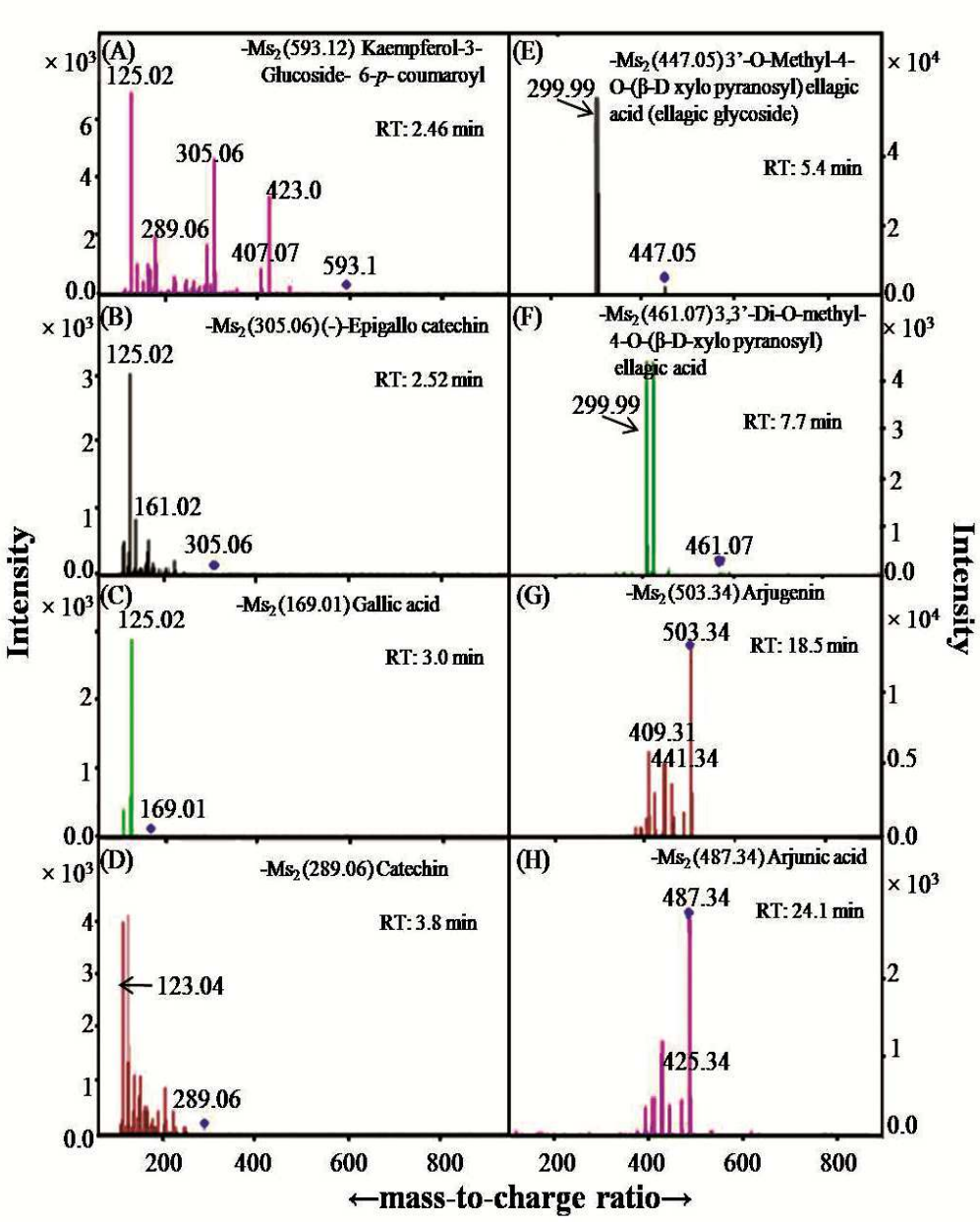

Figure. 3.10. Negative ion (−) ESI/MS/MS of water extracts (TAWE) of TA-stem bark. Product ion labels correspond to MS fragments.

Total antioxidant activity

Total antioxidant capacity of the hydroalcoholic and water extracts of BS-gum resin showed to be 121.1 ± 3.1 mg ASE/g dwt and BSWE with 72 ± 2.7 mg ASE/g dwt. While, TAAE showed high antioxidant activity (207.1 ± 2.7 mg ASE/g dwt) than TAWE (80.3 ± 0.5 mg ASE/g dwt) in Table 3.8.

Table 3.8. Total antioxidant activity in the extracts of *B. serrata* gum resin and *T. arjuna* stem bark.

Type of MPE	Aqueous extract mg ASE /g dwt	Hydro alcoholic extract mg ASE /g dwt
B. serrata gum resin	72 ± 2.7	121.1 ± 3.1
T. arjuna stem bark	80.3 ± 0.5	207.1 ± 2.7

Free radical scavenging assays

2,2-diphenyl-1-picrylhydrazyl (DPPH) assay

Both BSAE and BSWE scavenged DPPH radical significantly in a dose dependent manner (Fig. 3.11). Among them, BSAE showed much higher activity compared to BSWE in their capacity of scavenging the radical. BSAE scavenged 92 % of DPPH radical with the IC_{50} being 1.65 mg dwt/mL, where as BSWE scavenged only 40 % of the radical at 10 mg dwt/mL (Fig. 3.11. A).

TAAE and TAWE scavenged DPPH radical up to 90 % in a dose dependent manner. IC_{50} values of TAAE and TAWE were 6.4 µg dwt/mL and 5 µg dwt/mL respectively (Fig. 3.11. C).

Reference compounds, ascorbic acid and gallic acid showed their inhibition towards DPPH radical in concentration dependent way. The IC_{50} value of ascorbic acid IC_{50} value found in 3 µg/mL and gallic acid was found to be 1 µg/mL (Fig. 3.11. E).

Hydrogen peroxide (H_2O_2) radical scavenging assays

We tested *in vitro* H_2O_2 scavenging capacity of plant extracts and standard compounds. BSAE and BSWE showed biphasic mode in terms of H_2O_2 scavenging activity. BSAE showed maximal scavenging of 60 % with IC_{50} 3.2 mg dwt/mL and BSWE showed maximal scavenging capacity of 53 % with IC_{50} of 3.8 mg dwt/mL (Fig. 3.11. B).

In case of *T. arjuna*, both types of extracts showed significant H_2O_2 scavenging activity. TAAE showed maximal scavenging of 58 % with IC_{50} 0.35 mg

dwt/mL and TAWE showed maximal scavenging capacity of only 38 % where IC_{50} could not be determined (Fig. 3.11. D).

Reference compounds, ascorbate and gallic acid showed their H_2O_2 scavenging property in a concentration dependent manner. Ascorbic acid showed its maximum scavenging potential 50 % and IC_{50} at 100 µg/mL. Whereas gallic acid exhibited maximum percentage of inhibition of 89 % inhibition at 100 µg/mL with an IC_{50} value of 10 µg/mL (Fig. 3.11. F).

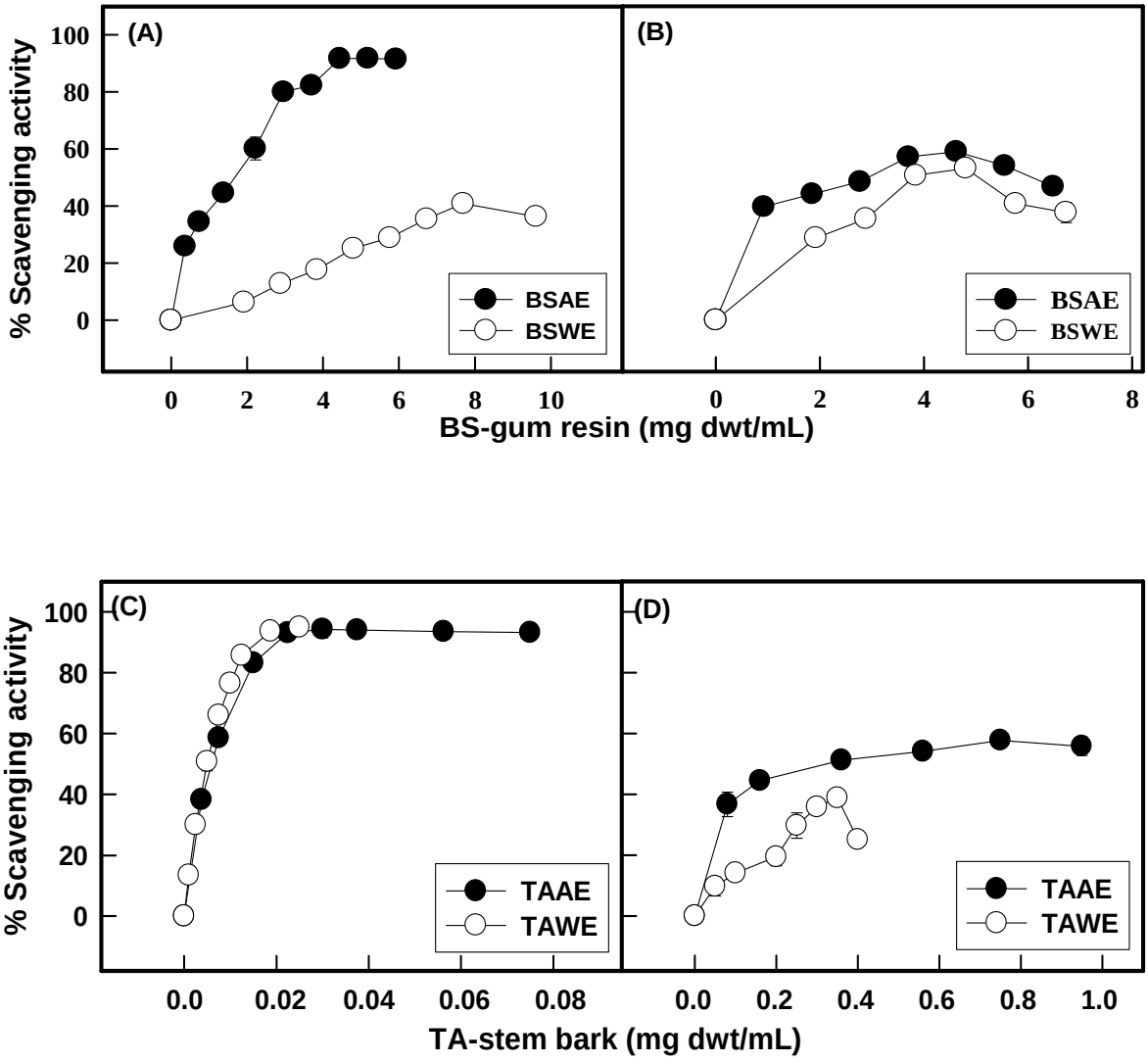

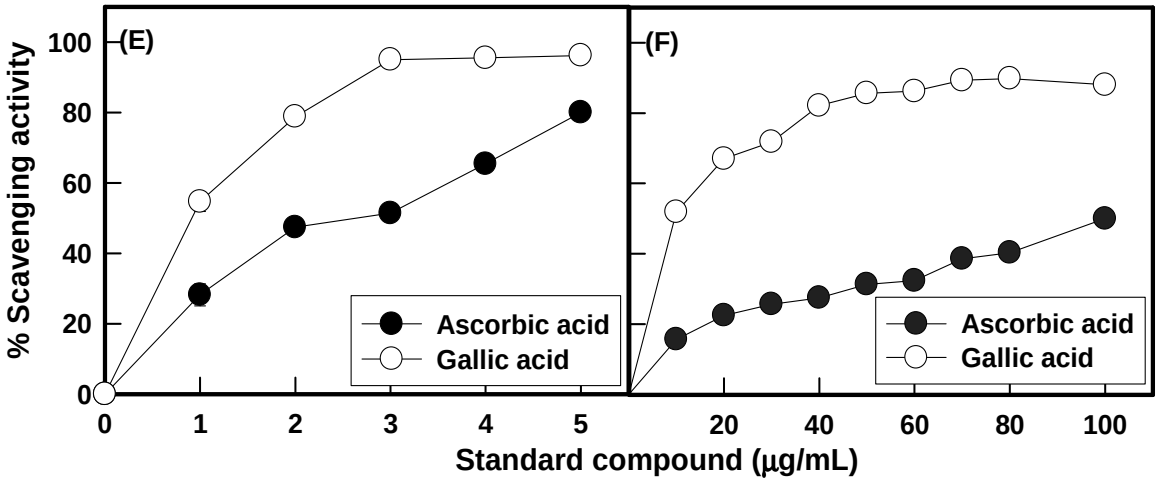

Figure. 3.11. Free radical scavenging activity of the extracts of BS- gum resin, TA-stem bark and standards compounds ascorbic acid and gallic acid. (A, C and E) DPPH and (B, D and F) Hydrogen peroxide activity. Data presented are mean ± S.D., *n*=6. S.D not seen where S.D. values are within the symbol of data point. All values are statistically different ($p < 0.001$).

Effect of BS-gum resin and TA-stem bark extracts on ferric chloride induced lipid peroxidation in rat liver and heart tissue homogenates

Liver tissue homogenates

BSWE inhibited $FeCl_3$ induced peroxidation in liver homogenates by 90 % at 3.8 mg dwt/mL with an IC_{50} value of 34 µg dwt/mL. Whereas BSAE showed maximum inhibition of only 40 % at 18 mg dwt/mL shown in Fig. 3.12. A. Boswellic acid mixed-fraction (BAM) at 100 µg dwt/mL and AκβBA (100 µg dwt/mL) inhibited $FeCl_3$ induced peroxidation in liver homogenates by only 40 %, whereas α-BA (100 µg dwt/mL) inhibited about 80 % (Fig. 3.12. B).

The presence of TAAE (0.01 mg dwt/mL) or TAWE (0.04 mg dwt/mL) inhibited the liver lipid peroxidation by 90 % (Fig. 3.12. C). The IC_{50} values for such inhibition of TAAE and TAWE were 10 and 3 µg dwt/mL respectively.

Ascorbate, BHT and gallic acid was used as positive controls (Fig. 3.12. D) and exhibited maximum inhibition of 80 % lipid peroxidation but ascorbate and gallic acid having the IC_{50} values of 38 µg/mL and 1.29 µg/mL respectively.

Heart tissue lipid peroxidation

Both BSAE and BSWE inhibited maximum of 50 % lipid peroxidation. IC_{50} of these extracts were 129 µg dwt/mL and 88 µg dwt/mL respectively (Fig. 3.13. A). The extracts showed lower efficacy in inhibiting peroxidation in heart tissue homogenates compared to liver tissue homogenates.

TAAE and TAWE exhibited a maximum inhibitory effect of 89 % at varied concentration 0.2 mg dwt/mL and 0.1 mg dwt/mL and IC_{50} values of these extracts were 30 and 10 µg dwt/mL respectively (Fig. 3.13. B).

Reference compounds, ascorbate and gallic acid exhibited only 55 % and 80 % with IC_{50} values of 153 µg/mL and 10 µg/mL respectively (Fig. 3.12. C).

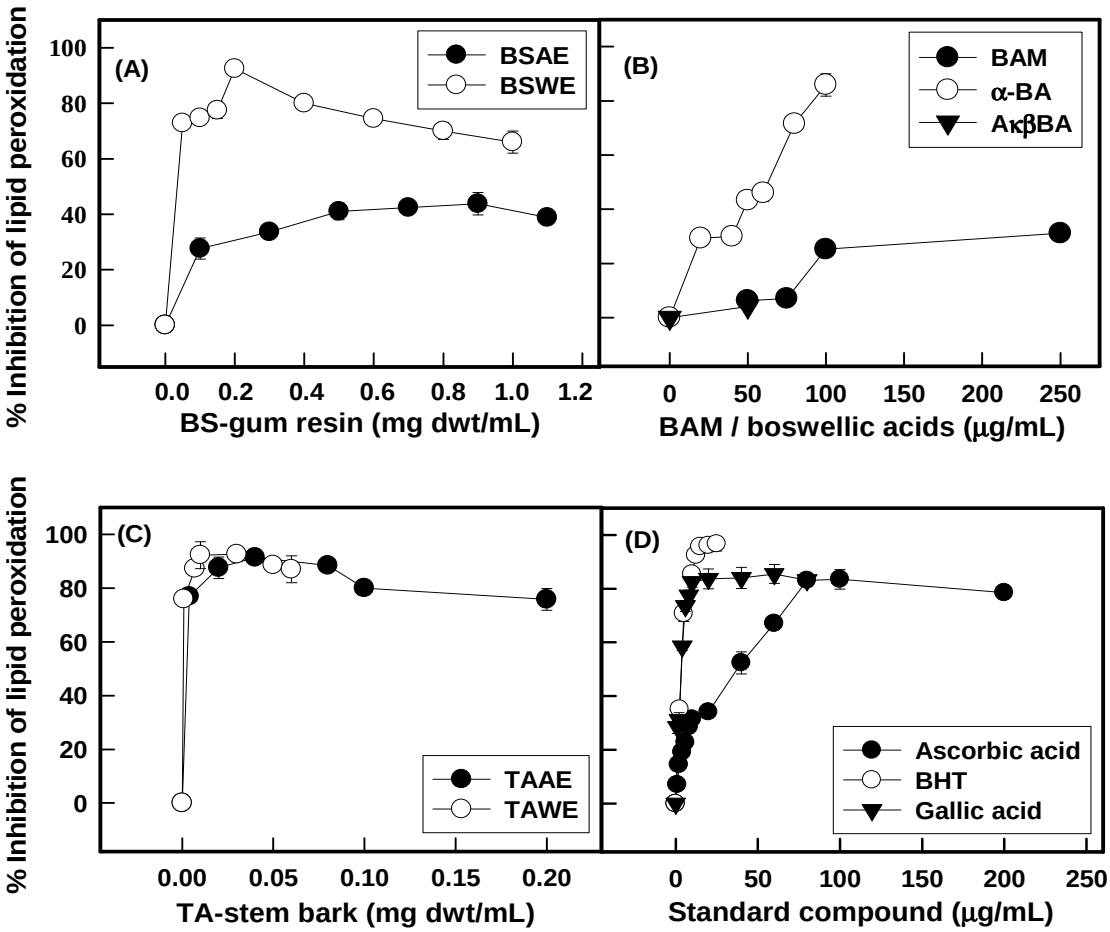

Figure. 3.12. Inhibitory effect of plant extracts or standard compounds on ferric chloride induced lipid peroxidation in rat liver tissue homogenate (A) BS- gum resin (B) BAM, α-BA and AκβBA (C) extracts of TA-stem bark (D) Standard compounds. Data presented are mean ± S.D., *n*=6. S.D not seen where S.D. values are within the symbol of data point. All values are statistically significant $^{\#}p < 0.001$ vs. Control.

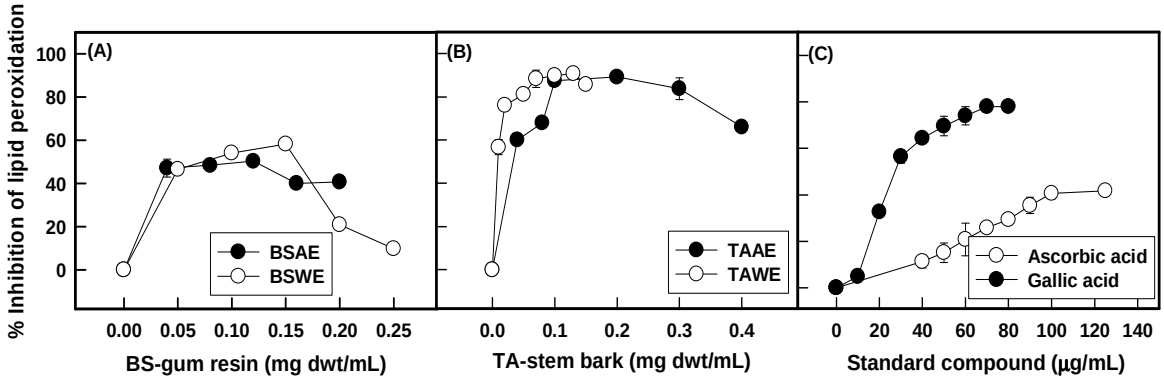

Figure. 3.13. Inhibitory effect of plant extracts or standard compounds on ferric chloride induced lipid peroxidation in rat heart tissue homogenate (A) BS- gum resin (B) extracts of TA-stem bark (C) standard compounds. Data presented are mean ± S.D., n=6. S.D not seen where S.D. values are within the symbol of data point. All values are statistically significant $^{\#}p < 0.001$ vs. Control.

Effect of medicinal plant extracts on cell viability

THP-1 cells

Significant cell death was not found due to treatments with BSAE up to 40 µg dwt/mL and 400 µg dwt/mL of BSWE (Figs. 3.14. A and B). There was no cytotoxicity was observed with boswellic acid mixed-fractions (BAM) up to 100 µg/mL (Fig. 3.14. C) and 10 µg/mL (20 µM) ofα-BA or AκβBA (Figs. 3.14. D and E). In case of TA-stem bark extracts, there was no cytotoxicity shown up to 150 µg dwt/mL of TAAE and 500 µg dwt/mL of TAWE (Figs. 3.14. F and G). In case of standard compounds, there was no cell death found after treatments with ascorbate up to 50 µg/mL, BHT up to 10 µg/mL and GA up to 150µg/mL (Figs. 3.14. H, I and J).

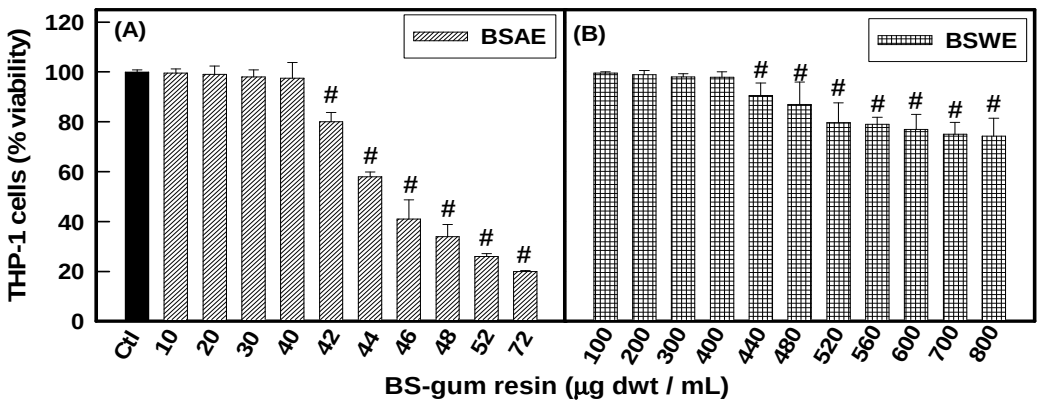

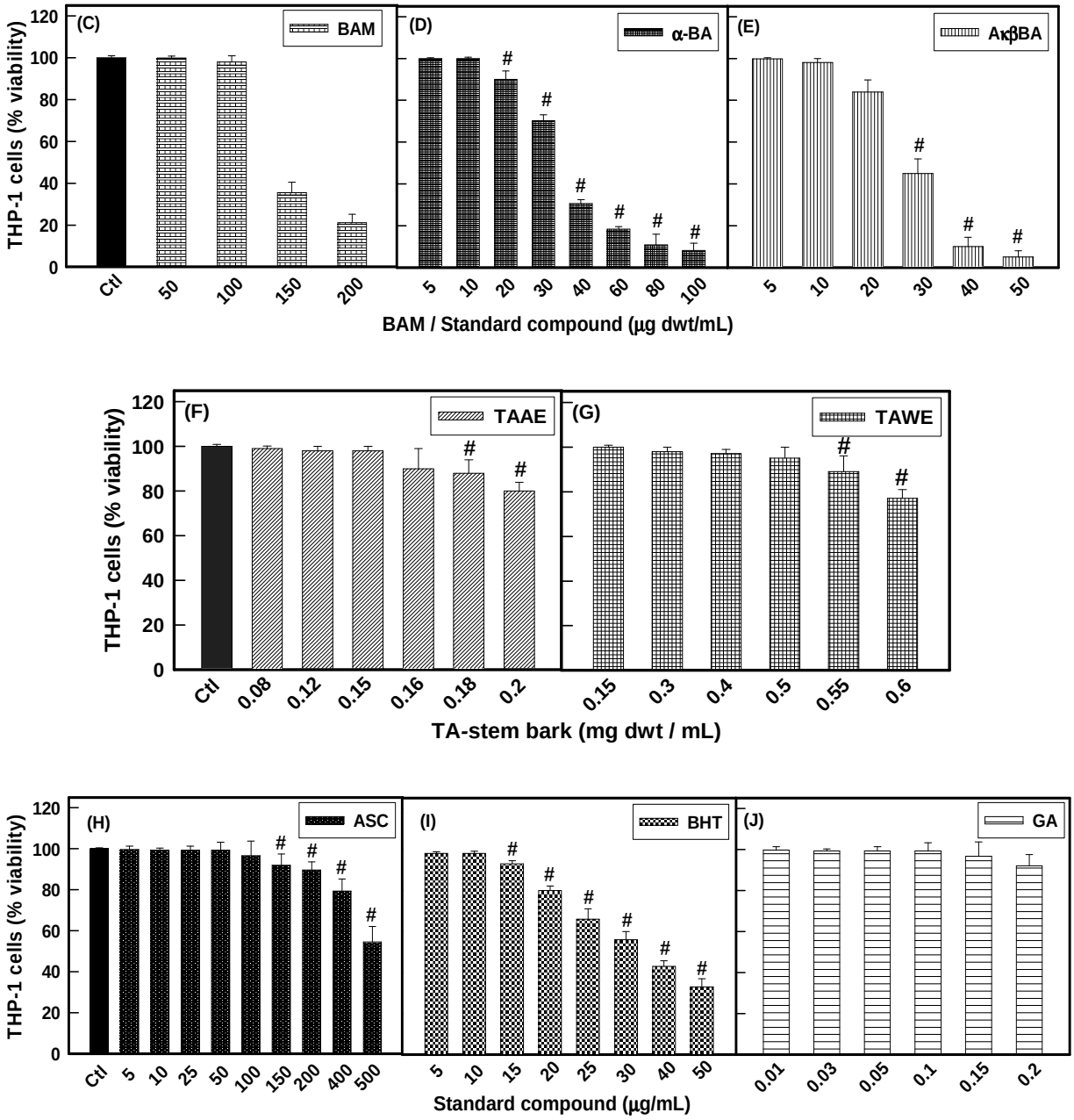

Figure. 3.14. Cell viability in THP-1 cells was checked by MTT assay after treatment with (A) BSAE (B) BSWE (C) BAM (D) α-BA (E) AκβBA (F) TAAE (G) TAWE (H) Ascorbate (I) BHT and (J) GA, at 37 ^{o}C and 5 % CO_2. Media without cells but with respective concentrations of standard compounds or plant extracts were used as appropriate blanks. Data presented are mean $\pm$ S.D., n=6.

Measurement of ROS scavenging potential of the extracts

H_2O_2 is one of the main reactive oxygen species (ROS), it can rapidly cross the cell membranes and generates different types of ROS which are highly damaging to the

cells. Excess ROS generated due to imbalance with cellular scavenging system can lead to oxidative stress mediated pathophysiology. Therefore antioxidants are considered as potential therapeutic agents. In the present work, we evaluated the potential of BS-gum resin extracts and TA-stem bark extracts in scavenging excess ROS generated due to treatment with H_2O_2 in THP-1 cells- using a cell permeable ROS sensitive fluorescent marker H_2DCFDA. Furthermore, isolated boswellic acid mixture from BS-gum resin and pure boswellic acid of α-BA and AκβBA and standard compounds ASC, BHT and GA were evaluated. H_2DCFDA dyed THP-1 cells treated with 10 µM H_2O_2 for 10 min showed much brighter fluorescence compared to cells not treated with H_2O_2 (Fig. 3.15. A, B). The cells were washed twice with dye free medium prior to exposing them to H_2O_2, to ensure not only the removal of excess fluorescent dye, but also removal of plant extracts from the medium, otherwise there is a possibility of extracts scavenging H_2O_2 extracellularly in the medium. THP-1 cells treated with 10 µM H_2O_2 for 10 min showed about 5 fold greater fluorescence compared to cells not treated with H_2O_2 (Figs. 3.17. A and B).

Pretreatment of cells with BSAE (30–40 µg dwt/mL) or BSWE (300–400 µg dwt/mL) markedly attenuated H_2O_2-dependent fluorescence increase. IC_{50} of BSAE (0.01 mg dwt/mL) was much lower than IC_{50} of BSWE (0.05 mg dwt/mL), which reflects that alcoholic extract was highly potential in scavenging intra cellular ROS (Fig. 3.17. A).

Isolated boswellic acid mixed-fraction from BS-gum resin (BAM) at 50 and 100 µg dwt/mL markedly attenuated H_2O_2-dependent fluorescence increase in the cells. Pure commercially available α-BA, AκβBA (Figs. 3.15. I, J and K, L panels) at 10 µg dwt/mL (20 µM), scavenged intracellular ROS, but AκβBA is more potential than α-BA and BAM (Fig. 3.17. A). Positive drug controls ascorbic acid (20 µg/mL), BHT and GA at 10 µg/mL completely scavenged intracellular ROS (Fig. 3.17. B).

Pretreatment of cells with TAAE (Figs. 3.16. A and B) or TAWE (Figs. 3.16. C and D) markedly attenuated the H_2O_2-dependent ROS production as shown in Fig. 3.17. B. Thus, our results demonstrated that both TAAE and TAWE possess significant intracellular ROS scavenging activity, similar to standard compounds (ASC, BHT and GA).

Scavenging mechanism of cellular ROS

To elucidate the mechanism offered by plant extracts/reference compounds in scavenging intracellular ROS, ROS scavenging enzymes and cellular redox potential were assayed. Effect of BSAE/BSWE and BAM were tested on cellular catalase enzyme activity and total reducing power assays. The amount of plant extracts for these assays were selected based on their ROS scavenging activity as shown above. On exposure of cells to H_2O_2 for a short period, catalase activity was increased by 40 % (Fig. 3.18. A) and its total reducing power of the cells was rapidly declined by 70 % in the THP-1 cells. Catalase activity (Fig. 3.18. A) increased by two fold in the THP-1 cells treated with BSWE at 300 µg dwt/mL, with a statistical significance of $p < 0.001$ and exhibiting its cellular reducing power by 70 % (Fig. 3.18. B), where as in BSAE treated cells, the enzyme activity was increased by only 40 % but maintained cellular reducing power by 80 %. Treatment with standard compound, ascorbate 20 µg/mL increased catalase activity by two folds and found similar to BSWE and its reducing power in cells showed by 60 %, but BHT showed minimal inhibition at 10 µg/mL by 50 % and has showed maximum potential of reducing power in THP-1 cells by 100 % (Fig. 3.19. A).

Upon pretreatment with boswellic acids, BAM (50 and 100 µg dwt/mL) caused to increase CAT by 4-fold, both α-BA (10 µg dwt/mL or 20 µM) and AκβBA (10 µg dwt/mL or 20 µM) induced about 3 fold respectively but they had no effect on maintaining the total reducing power in the cells (Figs. 3.18. A and B).

Pretreatment with TAAE (114 µg dwt/mL) caused an increase in CAT by 10-fold and GPx by 7-fold, compared to control (vehicle) cells and also sustained reducing power to be kept at 60 %. Similarly, TAWE (375 µg dwt/mL) induced 8- and 6-fold increase in CAT and GPx activities, respectively and sustained reducing power at 70 %. In contrast to TAAE and TAWE, GA (10 µg/mL) stimulated activity of CAT and GPx activity by only 2 and 4.5-fold, respectively but did not help much in sustaining redox potential whereas BHT (10 µg/mL) completely restored cellular reducing power. The changes induced in CAT and GPx activities were all significant (Figs. 3.19. A, B and C). These results suggest that the BS, BAM and TA-extracts help the cells combating with oxidative stress and mechanism may vary depending on their metabolite profile.

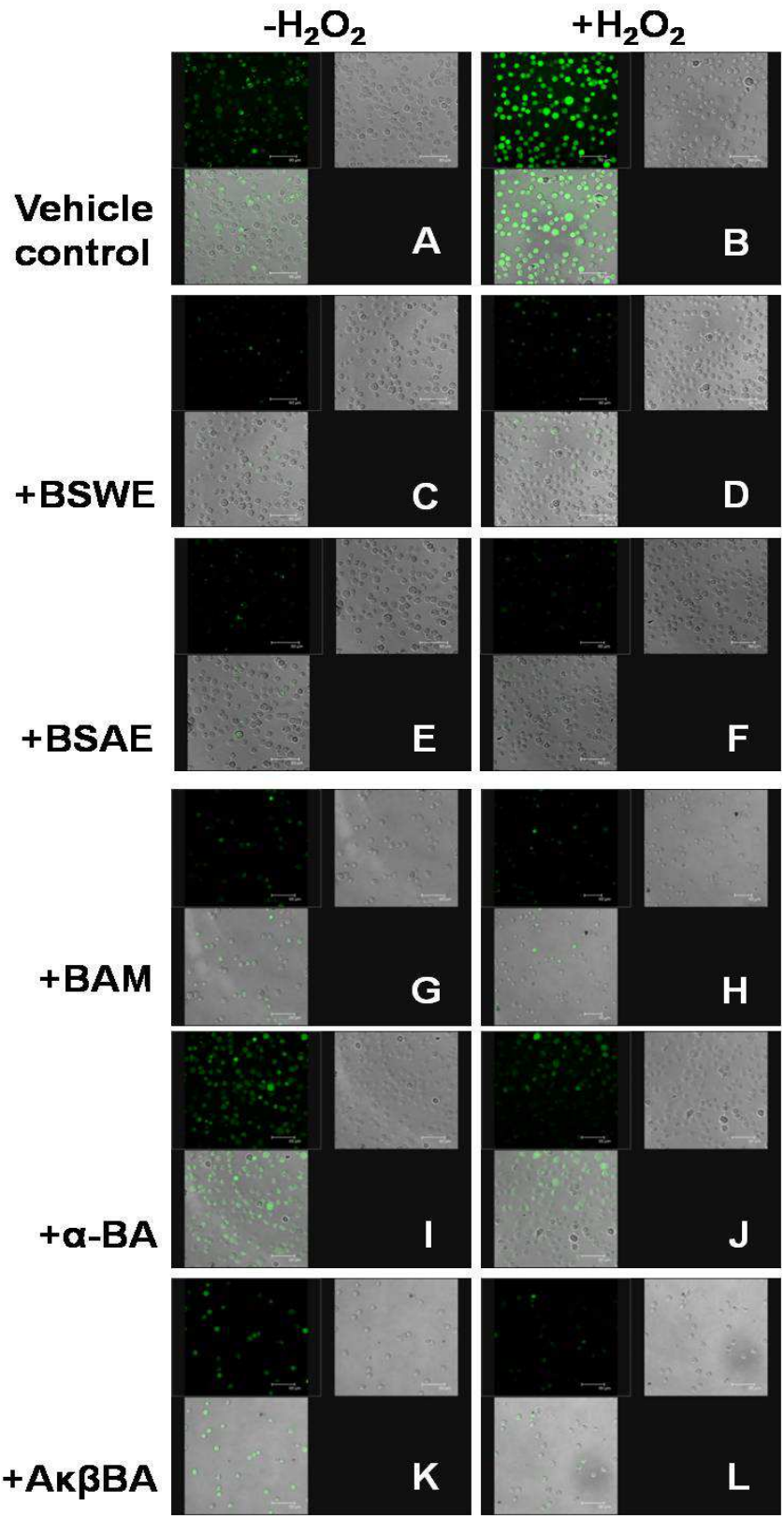

Figure. 3.15. Effect of BS-gum resin extracts, BAM, α-BA and AκβBA on H_2O_2 induced ROS generation in THP-1 cells. Cells were observed in fluorescence microscopy.

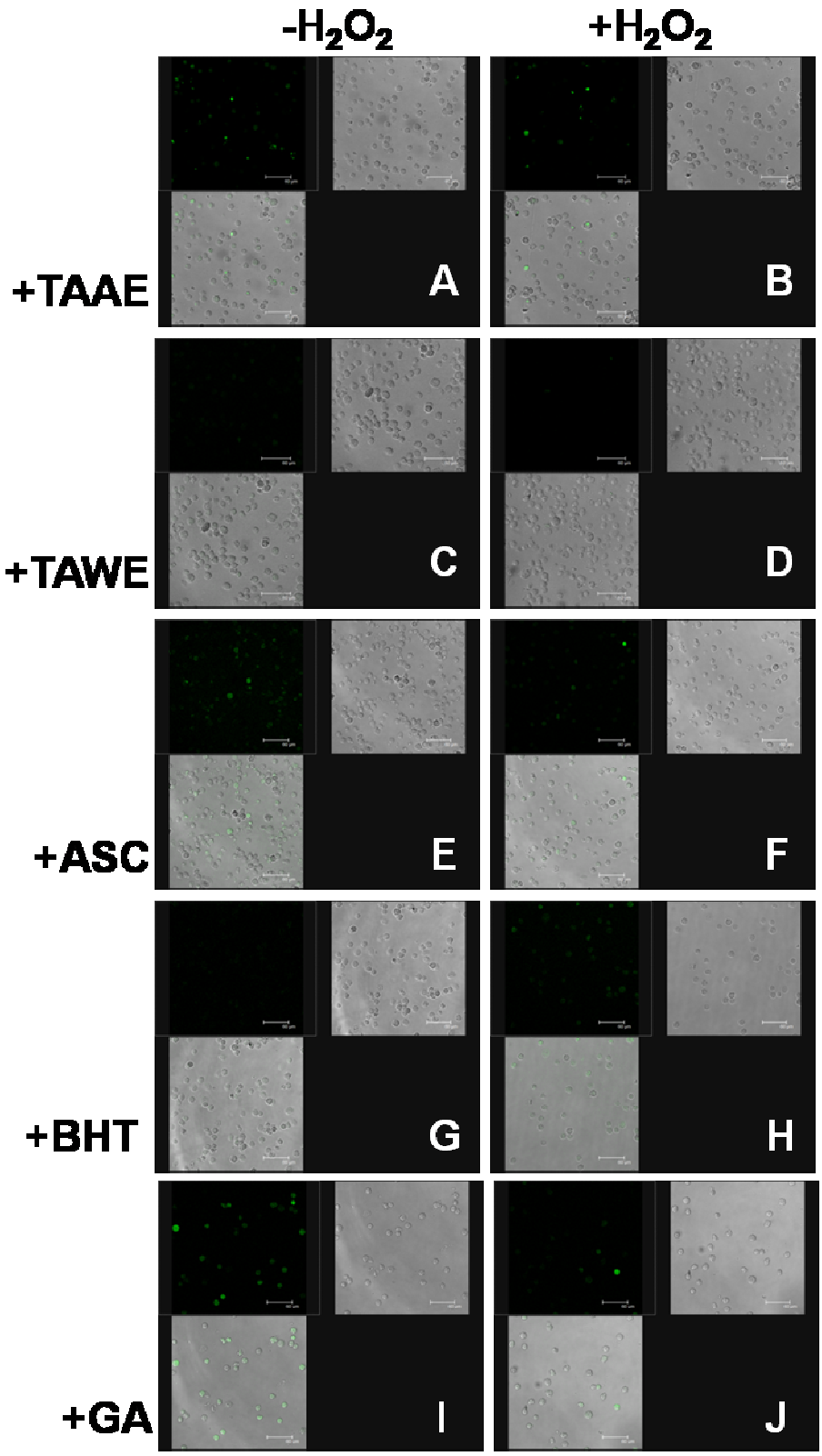

Figure. 3.16. Effect of TA-stem bark extracts and standards ASC, BHT and GA on H_2O_2 induced ROS generation in THP-1 cells. Cells were observed in fluorescence microscopy.

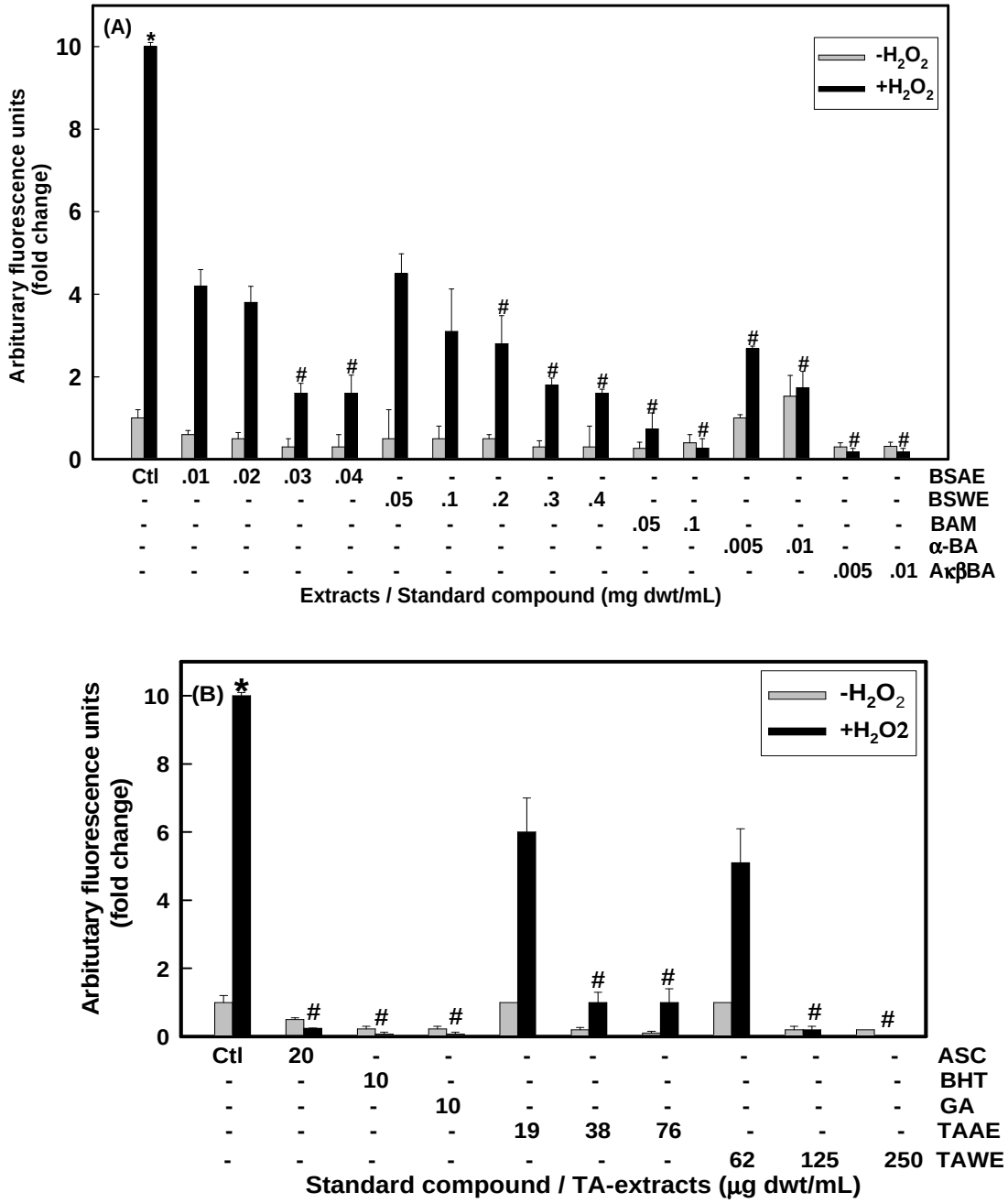

Figure. 3.17. Effect of plant extracts on H_2O_2 induced ROS generation in THP-1 cells represented in fluorescence intensity of H_2DCFDA taken by the cells treated as above was measured by spectrofluorimetry at 525 nm. (A) BS-gum resin extracts, BAM, α-BA and AκβBA (B) TA-stem bark extracts, standard compounds ASC, BHT and GA. One-way ANOVA test was performed between the experimental groups represent mean ± S.D. (n=4), *indicates statistical significance of $p < 0.001$ within the control groups ie. cells + H_2O_2 *vs* cells – H_2O_2, $^{\#}$ indicates statistical significance of $p < 0.001$ for groups of cells treated with H_2O_2 in presence of extracts *vs* in absence of extracts.

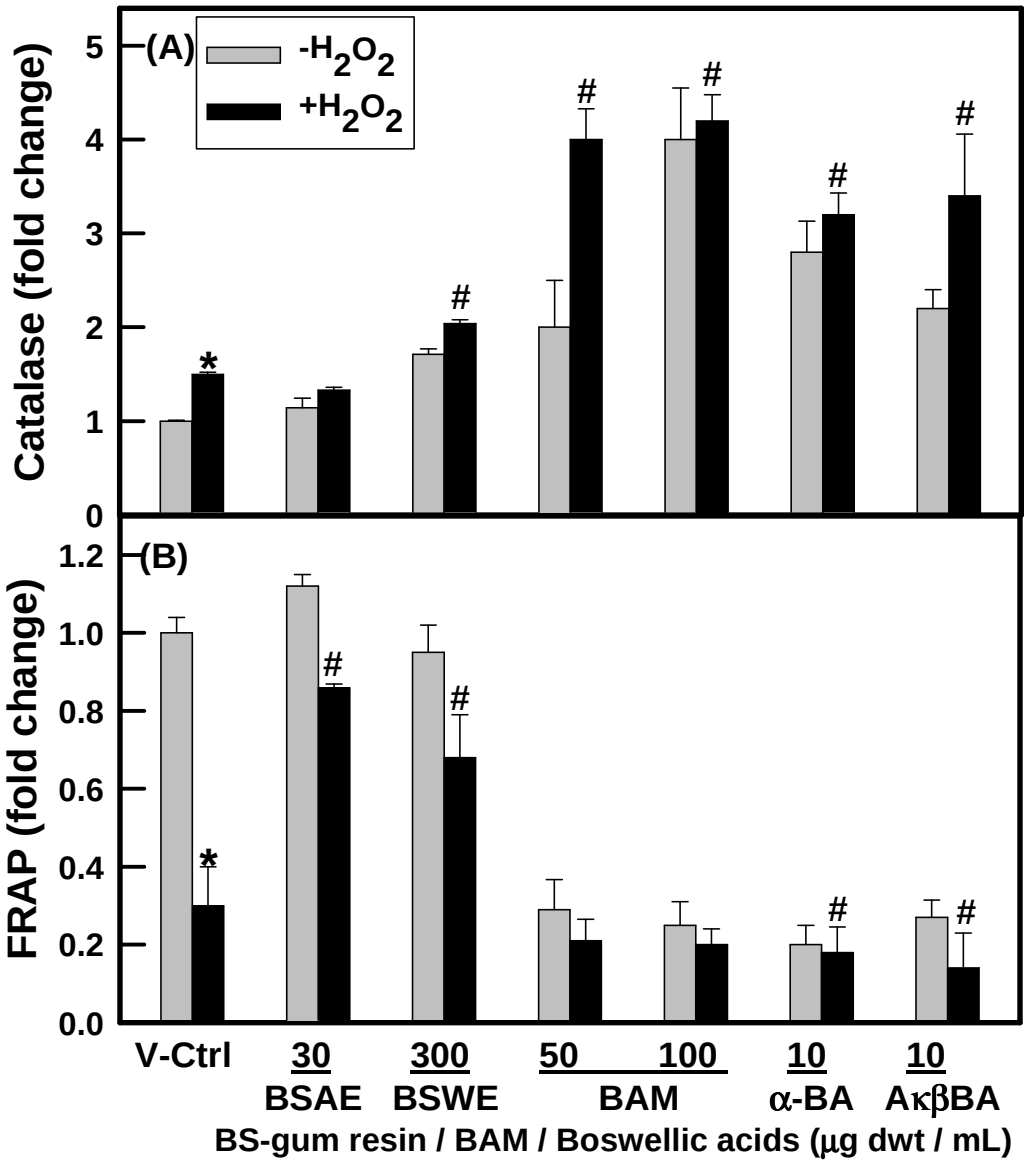

Figure. 3.18. (A) Effect of BS-extracts, boswellic acid mixed-fraction (BAM), α-BA and AκβBA on catalase enzyme activity in THP-1 cells exposed to H_2O_2. (B) FRAP assay performed with cells pretreated with BS-extracts, BAM, α-BA, AκβBA and induced with H_2O_2. Data represented mean ± S.D., n=4; *statistical significance of $p < 0.001$ within the control group i.e. cells $+H_2O_2$ *vs* cells $–H_2O_2$, $^{\#}$statistical significance of $p < 0.001$ for group of cells treated with H_2O_2 in the presence or absence of BS-extracts, BAM, α-BA and AκβBA.

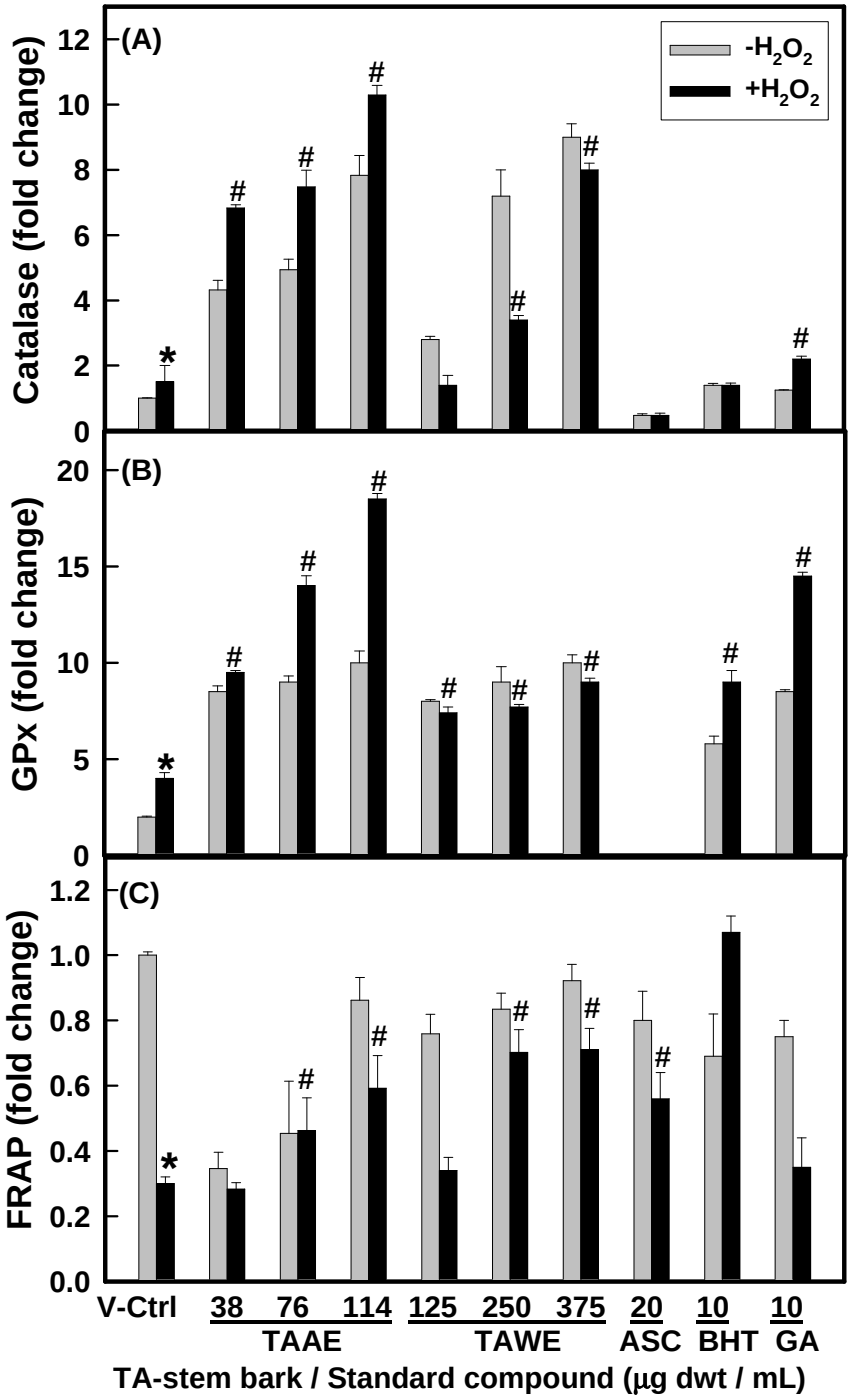

Figure. 3.19. (A) Effect of TA-extracts and positive controls ASC, BHT and GA on catalase enzyme activity (B) GPx (C) levels of FRAP in either normal or H_2O_2 exposed THP-1 cells. Data shown mean ± S.D., n=4; *statistical significance of $p < 0.001$ compared between treated and untreated with the controls, #statistical significance of $p < 0.001$ between the control groups.

Enzyme assays by Kit method

Effect of TAAE and TAWE on HMGR and LpL enzymes

The addition of TAWE inhibited HMG-CoA reductase enzyme by about 90 % at 125 µg dwt/mL and TAAE inhibited by 80 % at 75 µg dwt/mL. Pravastatin, at 0.5 µM, control drug inhibited by about 55 %, of the enzyme activity. In case of lipoprotein lipase TAAE and TAWE did not show inhibition and the drug control, Orlistat (4 mM), caused about 30 % inhibition over control (Fig. 3.20).

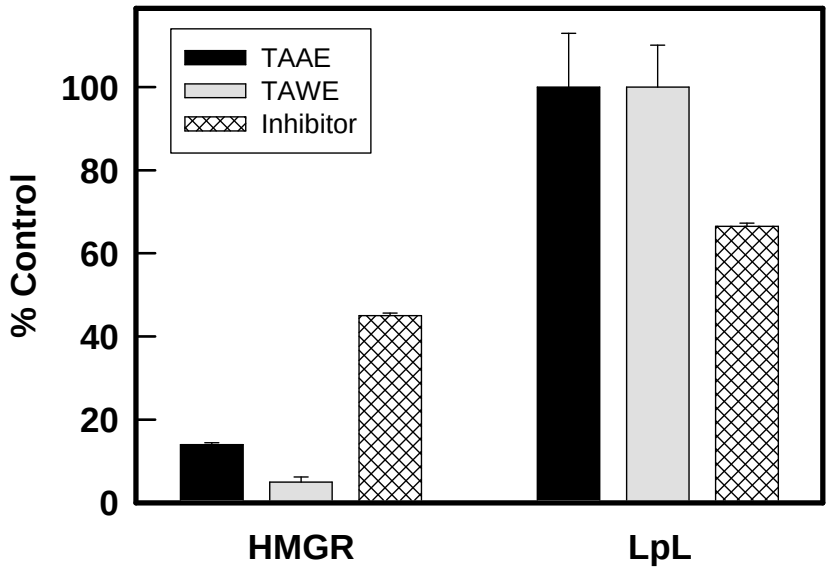

Figure. 3.20. Effect of TAAE and TAWE on activities of HMG-CoA reductase and lipoprotein lipase enzyme. Data presented are mean ± S.D., *n*=3. S.D not seen where S.D. values are within the symbol of data point.

Discussion

There has been increased global interest in traditional herbal medicine (a) Medicinal plant extracts are the natural resources for antioxidants (b) Many of the metabolic diseases include cardiovascular diseases are triggered by oxidative stress. Polyphenols are probably the most investigated molecules as the potential antioxidants in the medicinal plant extracts. Among the polyphenols, flavonoids comprise the most studied group of polyphenols and their content is an important index for estimation of medicinal quality (Zhang et al., 2012). Terpenes, particularly triterpenoids are also extensively investigated on their medicinal property, however, their antioxidant property is not well addressed. Mammals had evolved with complex endogenous antioxidant system in order to dissipate ROS generated constantly in a cell. In spite of this, oxidative stress develops occasionally in the cell due to excessive ROS production and leads to oxidative damage which is involved in several inflammatory diseases (Rahman, 2007) like cardiovascular diseases. It is well established that CVD is promoted by complex interactions between the oxidative stress, inflammation and thrombosis. Oxidative stress induced by ROS in the vasculature play a key role in the pathogenesis of atherosclerosis. Excess ROS generation in the monocytes induced their cytokine production and thereby leads to inflammation. Oxidative stress causes damage to macromolecules like lipids, proteins and DNA. Lipid peroxidation, particularly of polyunsaturated lipids, is one of the major biomarker for increased oxidative stress. Inhibiting lipid peroxidation by antioxidants is promising approach to combat oxidative stress (Prokai et al., 2013). Based on the importance of these phytochemicals, *B. serrata* extracts, alkali-acid fraction (BAM) and *T. arjuna* extracts were subjected compositional analysis and estimation of total polyphenols, flavonoids, triterpenoids.

Antioxidant activity of *Boswellia serrata's* gum resin

B. serrata gum resin is well known to be enriched with bioactive triterpenes and its reports on its antioxidant activity is controversial. Ammon et al., (1993) reported that *B. serrata* does not possess any antioxidant effect, whereas other reports showed its antioxidant activity on oil substrates and anti-mutagenic activity with *Salmonella typhimurium* (Assimopoulou et al., 2005; Magesh et al., 2008). In the present study

we have compared antioxidant activity of hydroalcoholic and water extracts of BS-gum resin.

B. serrata hydroalcoholic extracts had higher amounts of total triterpenoids and water extracts had higher amounts of TPC and flavonoids (Table 3.1), with reference to antioxidant activity, both BSAE and WE scavenged DPPH and hydrogen peroxide radical dose dependently, however BSAE showed high potent capacity in scavenging both the radicals compared to BSWE (Figs. 3.11. A and B). Both triterpenoids and phenolic components of BS-gum resin contribute to its antioxidant activity.

In case of inhibiting liver lipid peroxidation, water extract was more effective than hydroalcoholic extracts. Both BSAE and BSWE showed equal response in inhibiting heart tissue lipid peroxidation (Figs. 3.12. A and B). Thus our results suggest that extracts were also capable of scavenging ROS in human monocytic (THP-1) cells (Fig. 3.17. A). Since activated monocytes promote inflammatory cascade of events (Ross, 1999) leading to atherosclerosis. The cellular ROS scavenging activity offered by BSAE and BSWE may help in attenuating the above outlined cascade of events. BSAE did not show significant effects on catalase whereas BSWE significantly increased cellular catalase activity in THP-1 cells (Fig. 3.18. A). BSAE and BSWE helped THP-1 cells in sustaining their cellular reducing power to great extent, even on exposure to H_2O_2 (Fig. 3.18. B). Therefore, we think that BSAE and BSWE scavenge excess ROS generated by oxidative stress by modulating either cellular reducing power or catalase enzyme activity. The reasons for higher potential of BSAE (IC_{50} 0.01 mg dwt/mL), that of BSWE (IC_{50} 0.05 mg dwt/mL) in terms of ROS scavenging, cannot be explained based on the analyzed phytomarker, AκβBA. BSAE and BSWE contained AκβBA of 9 % (w/w) and 7.8 % (w/w) respectively. Since BS gum resin is enriched with α and β types of boswellic acids. α-BA, AκβBA and isolated boswellic acid mixed-fraction were investigated extensively for the antioxidant activity.

It is difficult to explain the antioxidant potential between BASE and BSWE; therefore we quantitated BS extracts by HPLC using standard 3-O-acetyl-11-keto-β-boswellic acid (AκβBA), since it is one of the most important active principle within the multicomponent mixture of the resin (Sharma et al., 2004; Sengupta et al., 2008). HPLC analyses showed that AκβBA content is high in BSAE than BSWE of their

extracts dwt (Fig. 3.2. C). We further checked the class of compounds present in BSAE and BSWE, without losing information of original ingredients using trimethylsilyation followed by GC-MS analysis (Tables 3.3 and 3.4; Figs. 3.3 and 3.4).

GC-MS analysis of *B. serrata* and BAM

GCMS of BSAE and BSWE showed the presence of aromatic hydrocarbon, terpenes, triterpenoid, alkenols, polyprenylalcohol and fatty acids (Figs. 3.5 and 3.6). The main inference from this analysis includes the presence of olean-12-ene or urs-12-ene derivatives and lupane familes in both the hydroalcoholic and water extracts and in accordance with the literature and that the presence of these compounds are characteristic of resins of *B. serrata* species and may be frequently found in some higher plants due by oxidation of alcohols or by enzymatic degradation of ketones (Mathe et al., 2004). BAM showed the presence of terpenes, triterpenes and tirucallic acid (Fig. 3.8). Boswellic acids are the pharmacologically active ingredients in the gum resin of *B. serrata* (Belsner et al., 2003).

Attenuation of H_2O_2 induced ROS by BSAE/BSWE and BAM in THP-1 cells

α-BA showed very high anti lipid peroxidation activity than BAM and AκβBA. Whereas in case of intracellular ROS scavenging activity BAM and AκβBA showed much inhibitory activity than α-BA. All three promoted catalase activity and had not much effect on cellular reducing potential (Figs. 3.18. A and B). Phytochemical analysis of BAM shows for the presence of several boswellic acids. The inability of BAM in sustaining cellular redox potential under oxidative stress could be due to qualitative and quantitative differences in phytochemical composition from BSAE and BSWE.

Phytochemical analysis and Antioxidant activity of stem-bark of *T. arjuna*

Phytochemical analysis of *T. arjuna* showed that the amount of polyphenols and flavonoids in hydroalcoholic extracts are much higher than water extracts. LC-MS analysis (Figs. 3.9 and 3.10) showed the presence of (-)-epigallo catechin; ellagic acid pentose; catechin; kaempferol-3-glucoside-6-*p*-coumaroyl; terminolic acid and arjunic acid in both TAAE and TAWE (Tables. 3.6 and 3.7). Gallic acid and ellagic

acid derivatives i.e. 3'-O-methyl-4-O-(β-D-xylopyranosyl) were found only in TAWE but not in TAAE, whereas arjungenin, arjunolic acid, glycopyranosides, steroid glycoside were only detected TAAE. Several of the compounds identified in TAAE and TAWE, e.g. arjunic acid; ellagic acid and its derivative, ellagic acid pentose; (-)-epigallo catechin (O-di-hydroxyl groups) are reported to show antioxidant and a free radical scavenging activities (Fang-Yun Sun et al., 2008; Ozkaya et al., 2010; Hu and Kitts 2001). Since clinical and animal studies reported TA-stem bark efficacy in treating various types of cardiovascular diseases (Dwivedi, 2007). TAAE and TAWE were tested for their free radical scavenging activity, both types of extracts scavenged DPPH radical by 95 %, however, not very effective in scavenging H_2O_2 radical. Antioxidant action of *T. arjuna* was further monitored by anti lipid peroxidation activity using liver or heart tissue homogenates and the intracellular activities in THP-1 cells of FRAP, catalase and gluthathione peroxidase which constitute one of the major antioxidant defense system by scavenging ROS.

The plant extracts, both TAAE and TAWE inhibited up to 90 % of ferric chloride induced lipid peroxidation in rat liver and heart tissue homogenates (Fig. 3.12. C). Furthermore, the extracts showed remarked ROS scavenging activity in THP-1 cells. In H_2O_2 treated monocytes, cellular reducing power dropped substantially compared to control cells and ROS scavenging enzymes GPx and catalase activities increased only by a small percentage and such small increase is not sufficient to scavenge intracellular ROS generated due to oxidative stress. In case of TAAE/TAWE pretreated cells, activities of CAT and GPx were enhanced by several folds and cellular redox potential also sustained significantly (Fig. 3.19). Such antioxidant activity of the extracts can be attributed to the presence of phenolic and terpenes present in TAAE and TAWE. Variability in their activities (TAAE vs TAWE) could also be due to the difference in their metabolite profile particularly in enhancing CAT and GPx activities and sustaining cellular redox potential. Response of standard compound GA was in contrast to TAWE although GA is detected in TAWE. This variability could be due to the presence of other metabolites in TAWE.

Effect of *T. arjuna* stem bark on HMG-CoA reductase and LpL enzyme

Hypercholesterolemia is also an independent risk factor for CVD. HMG–CoA reductase is a key enzyme in sterol biosynthesis and often targeted for developing

cholesterol lowering drugs. Animal studies indicated the protective effect of TA-stem bark during high fat-mediated aortic architectural changes and atherosclerotic lesion formation (Subramaniam et al., 2011), and also against other chronic heart disorders (Gauthaman et al., 2005; Karthikeyan et al., 2003; Arya and Gupta, 2011; Parveen et al., 2011; Asha and Taju, 2012). In addition, animal studies suggested TA-stem bark's effect in reducing hyperglycemia and hyperlipidemia (Shaila et al., 1998; Ragavan and Krishnakumari, 2005; Subramaniam et al., 2011). However, the exact mechanism at cellular and molecular level by which TA-stem bark extract offers the atheroprotection in humans is not clear. In the present study, extracts significantly inhibited HMGR, however had no effect on lipoprotein lipase activity (Fig. 3.20). Recent research implicates that inhibition of LpL activity is desirable and identified as potential therapeutic target, since lipolysis products generated of very low density and are shown to be proinflammatory in nature (Higgins and Rutledge, 2009; Tetali et al., 2010; Mead and Ramji, 2002). Thus the present study suggests that TA-stem bark shows hypolipidaemic activity by inhibiting HMG reductase.

Chapter 4

RESULTS and DISCUSSION

Objective 2: Evaluation of antiinflammatory activity of Boswellic acid mixed-fraction (BAM) and TA-stem bark extracts in human monocytic (THP-1) and aortic endothelial cells (HAECs)

Results

LPS induced inflammation in THP-1 monocytic cells

LPS is a bacterial endotoxin that is reported to induce inflammation in human monocytes. Therefore, we used LPS as an inflammatory agent to test anti-inflammatory activity of the selected medicinal plant extracts. In the present study, we tested the expression of inflammatory genes MCP-1 and IL-8 by real time QPCR and TNF-α secretion by ELISA after the exposure of cells to LPS for 3 h.

Antiinflammatory effect of isolated boswellic acid mixture (BAM) from BS-gum resin and TA-stem bark extracts in LPS induced THP-1 cells

Secretion of TNF-α by THP-1 cells

Secreted TNF-α by THP-1 cells (5×10^5 cells/mL) was quantitated by performing ELISA. Supernatants of control cells had negligible amounts (20.0 ± 0.5 pg/mL), whereas substantial increase in TNF-α release was observed in LPS induced cells i.e., 824 ± 50 pg/mL and accounts to 20-fold induction (Fig. 4.1. B). Cells pretreated with BS-gum resin extracts secreted significantly less amount of TNF-α compared to LPS induced cells. BSWE suppressed TNF-α release in a dose dependent manner and at 400 µg dwt/mL the secreted amount reduced to 210 ± 33 pg/mL. BSAE at 16 and 35 µg dwt/mL inhibited about 50 % of LPS induced secretion to 450 ± 37 pg/mL (Fig. 4.1. B). BAM and pure boswellic acids (α-BA and AκβBA) were also able to attenuate TNF-α release. Among them, AκβBA (10 µg/mL or 20 µM) showed highest inhibition i.e. by 80 % (175 ± 32 pg/mL) as shown in Fig. 4.1. C. Based on these results, the concentration of BAM (100 µg/mL), α-BA and AκβBA (10 µg/mL or 20 µM) were selected for rest of the THP-1 cell based assays.

TA-stem bark extracts showed strong inhibition on LPS induced TNF-α secretion. Pretreatment with TAAE (120 µg dwt/mL) reduced the LPS induction by 95 % (39 pg/mL) and TAWE (250 µg dwt/mL) by 75 % (220 pg/mL) suggesting that TAAE was more potent than TAWE, in inhibiting the activation of THP-1 cells (Fig. 4.1. D). Ascorbate (20 µg/mL), gallic acid (10 µg/mL) and BHT (5 µg/mL) showed significant effect on secretion of TNF-α. Concentrations of TAAE and TAWE of 120 µg dwt/mL and 250 µg dwt/mL respectively used for rest of the THP-1 cell based assays.

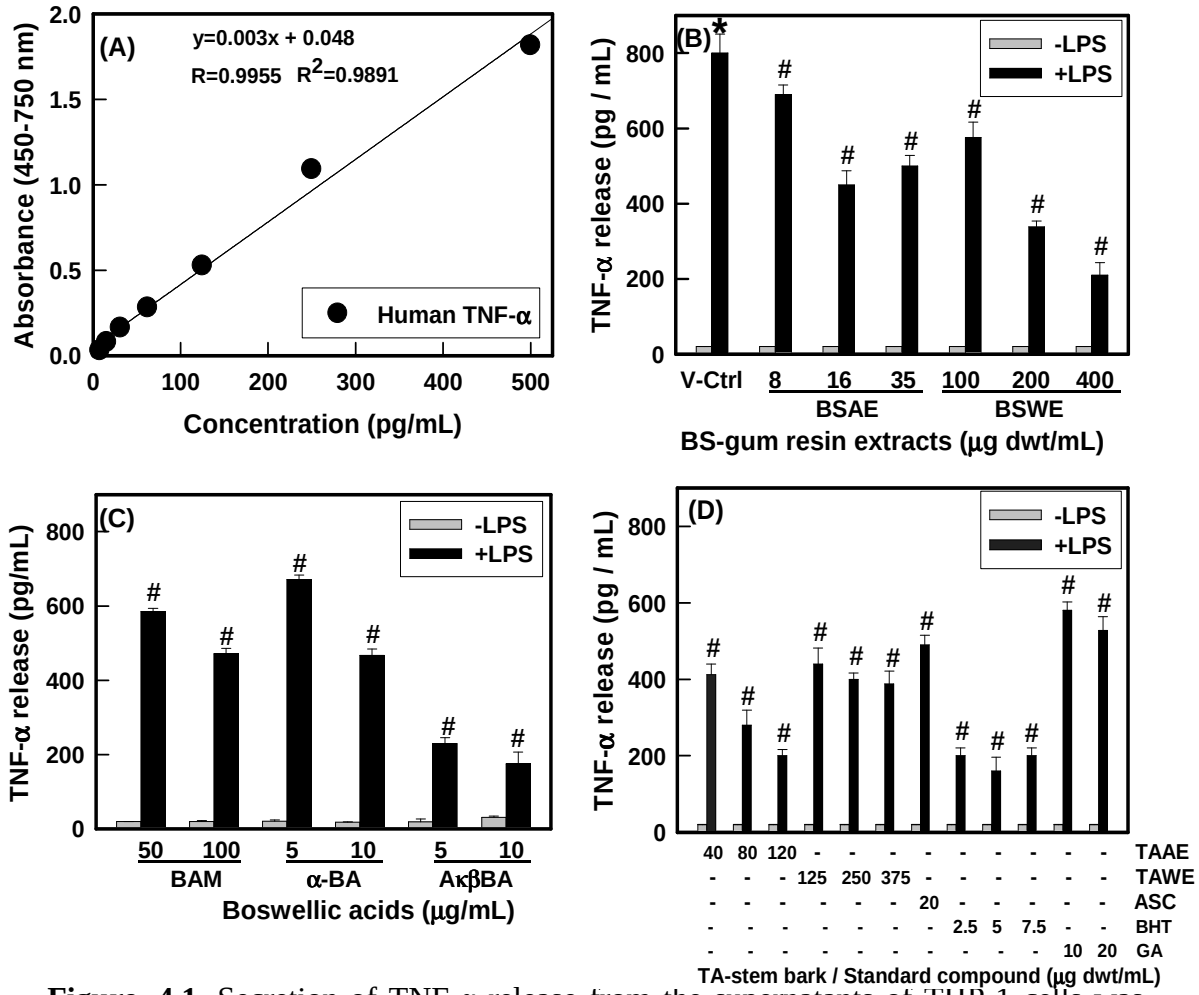

Figure. 4.1. Secretion of TNF-α release from the supernatants of THP-1 cells was measured by ELISA. (A) TNF-α standard. The effect of (B) *B. serrata* gum resin extracts (C) Boswellic acid mixed-fraction (BAM), α-BA and AκβBA (D) *T. arjuna* stem bark extracts, ASC, BHT, GA mediated attenuation of LPS-induced TNF-α secretion. THP-1 cells were pretreated with extracts for 16 h and were then further treated with LPS for 3 h. Results are expressed as mean ± S.D. of three independent experiments (#$p < 0.001$), *$p < 0.001$ between the control groups.

Gene expression of MCP-1

LPS stimulated MCP-1 gene expression in THP-1 cells increased by 22-fold compared to uninduced cells (Fig. 4.2. A). Pretreatment of the cells with BAM (100 µg/mL) did not show much effect, however, α-BA (10 µg/mL or 20 µM) and AκβBA (10 µg/mL or 20 µM) showed significant effect in attenuation of LPS induced MCP-1 expression (Fig. 4.2. A). α-BA down regulated MCP-1 expression up to 13 ± 2.0 fold change and AκβBA to 17 ± 1.7 fold change. In case of TA-stem bark extracts,

TAAE (120 µg dwt/mL) restricted the MCP-1 expression to 7.4 ± 0.7 fold whereas TAWE (250 µg dwt/mL) did not show much response (Fig. 4.2. C). GA (10 µg/mL) marginally restricted MCP-1 i.e., to 19 ± 0.5 fold (Fig. 4.2. C).

Gene expression of IL-8

LPS induced IL-8 gene expression in human THP-1 cells by 500-fold compared to uninduced control cells (Fig. 4.2. B). Pretreatment of the cells with BAM (100 µg/mL) restricted its expression to 368 ± 10 folds whereas α-BA and AκβBA did not show significant effect (Fig. 4.2. B). In case of TA-stem bark extracts, TAAE (120 µg dwt/mL) decreased IL-8 expression to 106 ± 8 fold and TAWE (250 µg dwt/mL) to 337 ± 12 fold (Fig. 4.2. D). Pretreatment with GA (10 µg /mL) did not show much

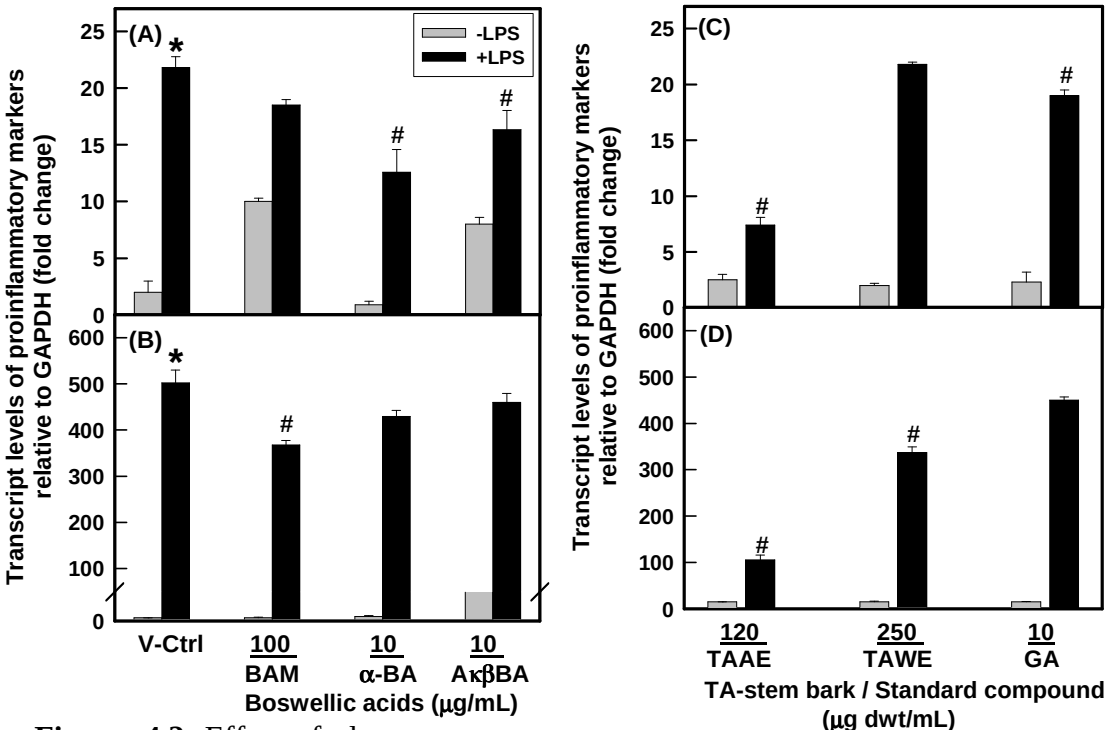

Figure. 4.2. Effect of plant extracts or standard compounds on gene expression of LPS induced MCP-1 (A and C) and IL-8 (B and D) transcripts in THP-1 cells. Data shown mean value of 3 independent experiments. $^{\#}p < 0.001$ and $^{*}p < 0.001$ between the control groups.

Effect of extracts in attenuating the translocation of NF-κB p65 into the nuclei of LPS stimulated THP-1 cells

To investigate further on anti-inflammatory mechanism, the effect of BAM, pure BAs of α-BA, AκβBA (Fig. 4.3) and *T. arjuna* stem bark extracts (Fig. 4.4) on

inhibition of NF-κB translocation into nucleus of the activated monocytes was investigated. We monitored the effect of extracts on LPS induced phosphorylation of NF-κB subunit p65, which modulates the transcription activation of NF-κB. Its activation involves cytoplasmic dissociation of the inhibitor protein IκB and facilitates translocation of the active NF-κB complex into the nucleus. THP-1 cells probed with commercially available p65 antibodies and stained using secondary antibody conjugated with Alexa Fluor 594 and nuclei of the cells were stained with DAPI. In the THP-1 cells induced with LPS (0.5 µg/mL), p65 was mostly localized in the nuclei (Figs. 4.3. D, E and F), which is not the case in uninduced cells (Figs. 4.3. A, B and C). Such LPS induced nuclear localization of p65 was significantly inhibited in the THP-1 cells, which are pretreated with the extracts (Figs. 4.3. G to O; 4.4. A to I) although the effect varied among them. Thus the study suggests that the anti-inflammatory effect of BAM, αBA, AκβBA and also TA-stem bark extracts in THP-1 cell is NF-κB mediated response.

Effect of plant extracts / standard compound on cell viability of human aortic endothelial cells (HAECs)

HAEC cells

In case of adherent HAECs, 90 % cells survived up to the concentration 40 µg/mL of BAM and 5 µg/mL (or 10 µM) of α-boswellic acid and 6 µg/mL (or 12 µM) of AκβBA (Figs. 4.5. A to C). Whereas in case of TA-stem bark extracts, about 90 % of cells were alive up to the concentration of TAAE of 20 µg dwt/mL and TAWE of 25 µg dwt/mL and standard compound, gallic acid up till 25 µg /mL (Figs. 4.5. D and E).

Effect of the plant extracts on TNF-α induced inflammatory markers in HAECs

In unstimulated HAECs, the mRNA transcripts of VCAM-1, ICAM-1, E-selectin, MCP-1 and IL-8 were very low (Figs. 4.6. A to E). Up on stimulation with TNF-α (10 ng/mL) for 4 h, the gene transcripts of these inflammatory markers significantly upregulated as shown following by VCAM-1 by ~ 2 ± 0.2 fold, E-selectin by 86 ± 2.0 fold, MCP-1 by 210 ± 10 fold, IL-8 by 95 ± 4 fold and ICAM-1 by 347 ± 15 fold compared to unstimulated control cells (Figs. 4.6. A to E).

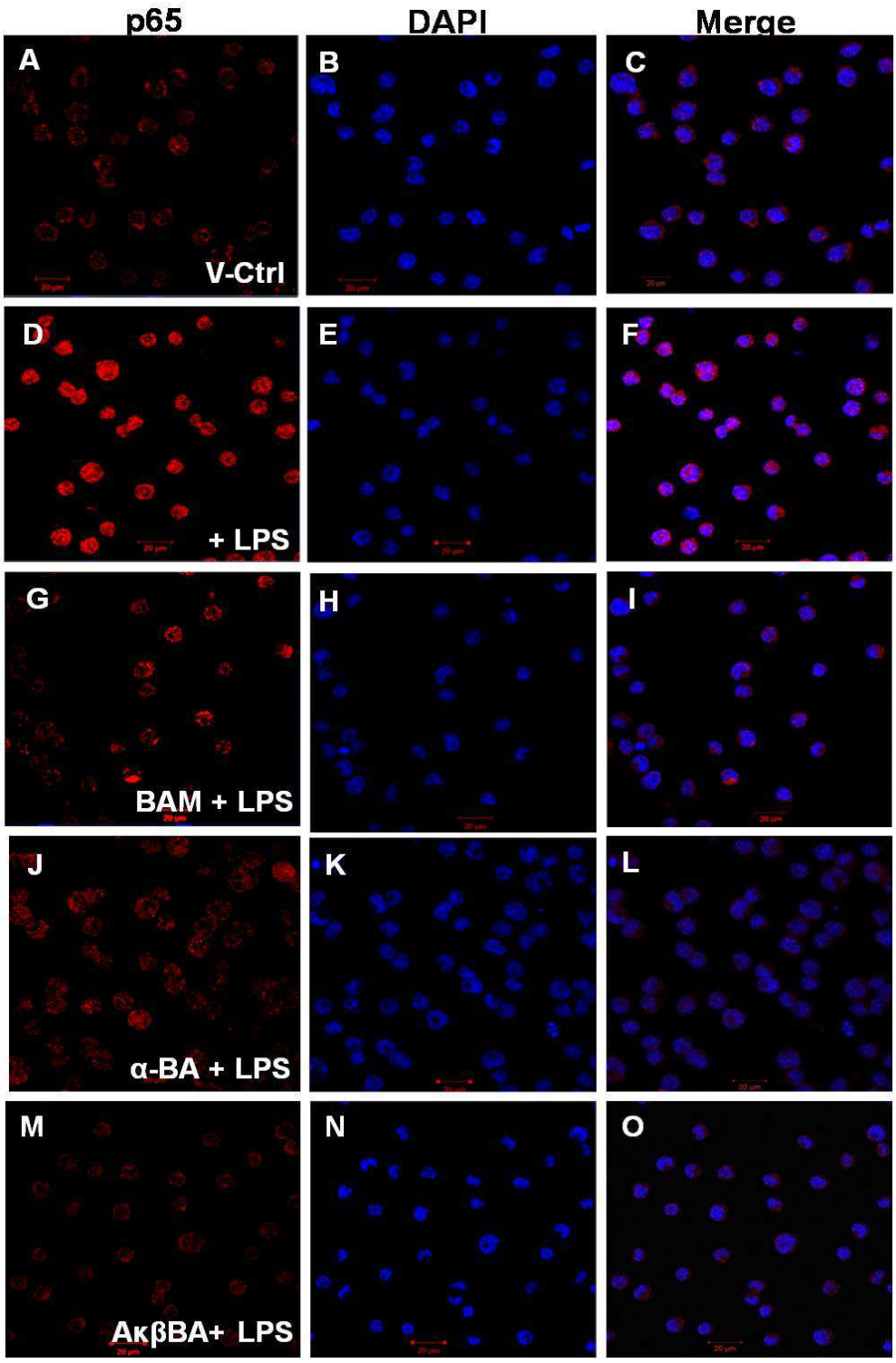

Figure. 4.3. Images showing the effect of BAM, α-BA, AκβBA on inhibition of the translocation of p65 subunit of NF-κB from cytoplasm to nucleus in LPS induced THP-1 cells. Images A, D, G, J, M and B, E, H, K, N were taken using Ex 590 nm and Em 617 nm and Ex 345 nm and Em 455 nm respectively. C, F, I, L, O are merged images.

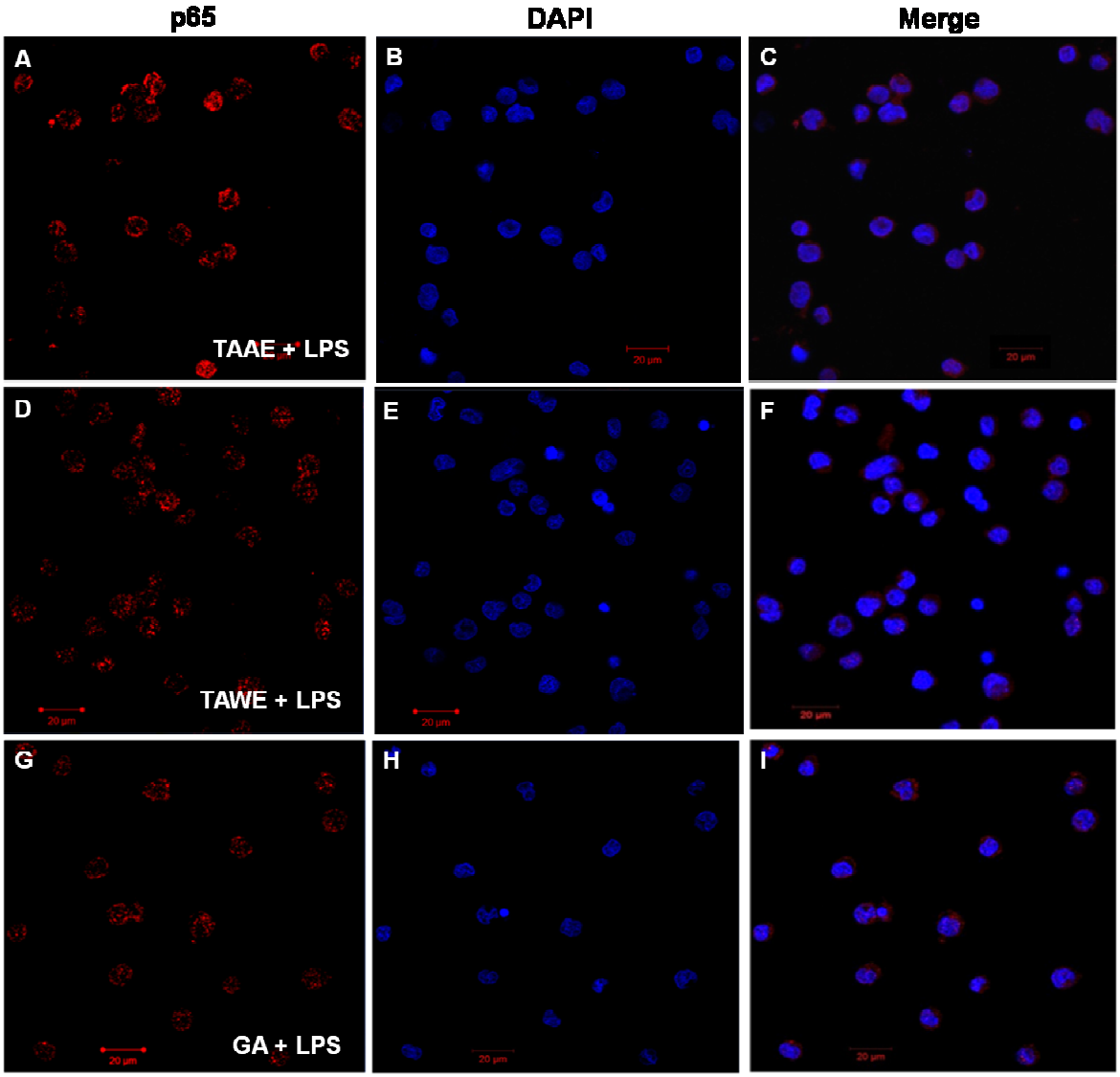

Figure. 4.4. Images showing the effect of *T. arjuna* extracts or gallic acid on inhibition of the translocation of p65 subunit of NF-κB from cytoplasm to nucleus in LPS induced THP-1 cells. Images A, D, G, and B, E, H were taken using Ex 590 nm and Em 617 nm and Ex 345 nm and Em 455 nm respectively. C, F, I are merged images.

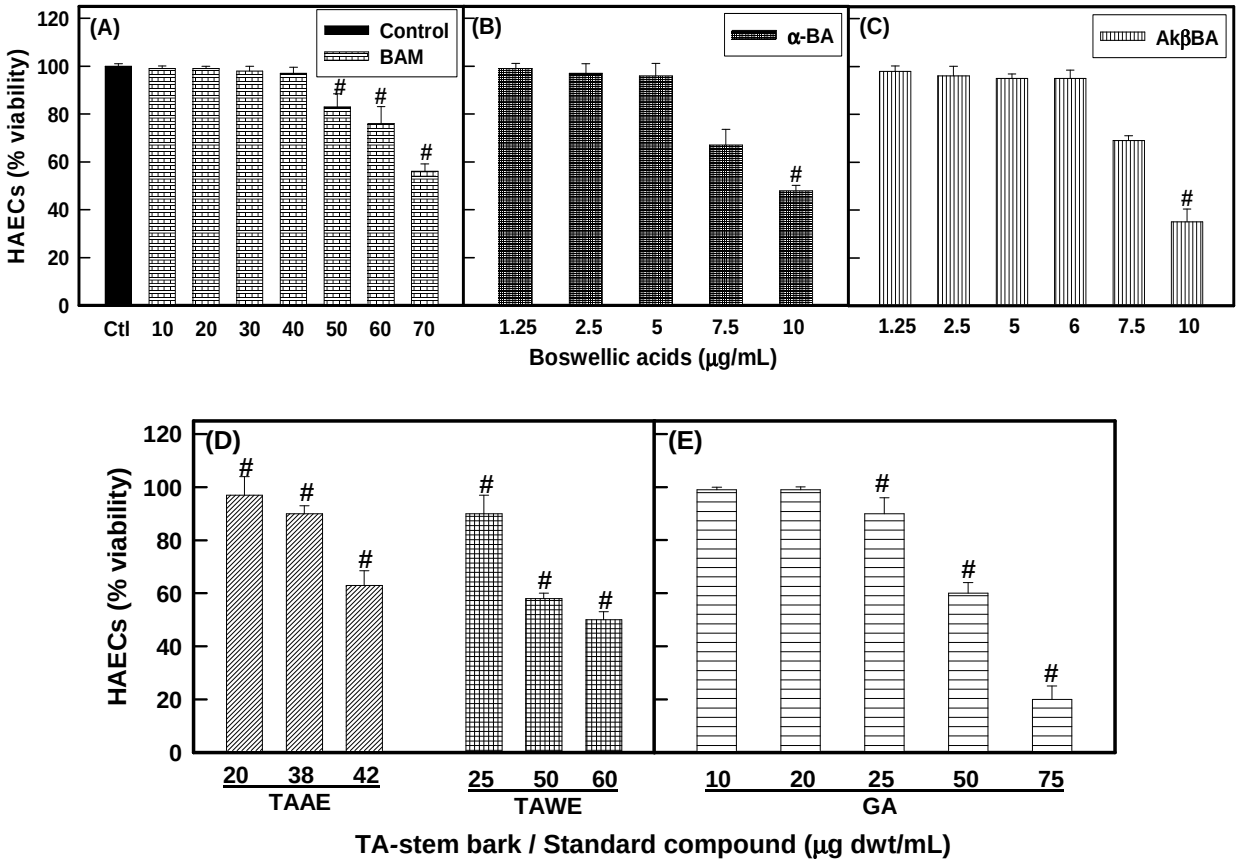

Figure. 4.5. Cell viability for HAECs was checked by MTT assay after treatment with (A) BAM (B) α-BA (C) AκβBA (D) TAAE and TAWE and (E) gallic acid for 24 h. Media without cells but with respective concentrations of standard compounds or plant extracts were used as appropriate blanks. Data presented are mean ± S.D., n = 6.

Pretreatment of HAECs with BAM (40 µg dwt/mL), α-BA (5 µg/mL or 10 µM) or AκβBA (6 µg/mL or 12 µM) significantly suppressed TNF-α induced expression of VCAM-1 (0.32 ± 0.1; 0.75 ± 0.2; 0.28 ± 0.07), E-selectin (26 ± 2.3; 52.17 ± 8; 60 ± 12), MCP-1 (2.29 ± 1.1; 1.0 ± 1; 3.28 ± 1.0), IL-8 (40 ± 3; 40 ± 9.2; 40 ± 8) and ICAM-1 (44 ± 20; 177.54 ± 18; 177.24 ± 10). These results in overall suggest that BAM showed better response compared to pure boswellic acids α-BA and AκβBA (Figs. 4.6. A to E), which may be due to other components of BAM.

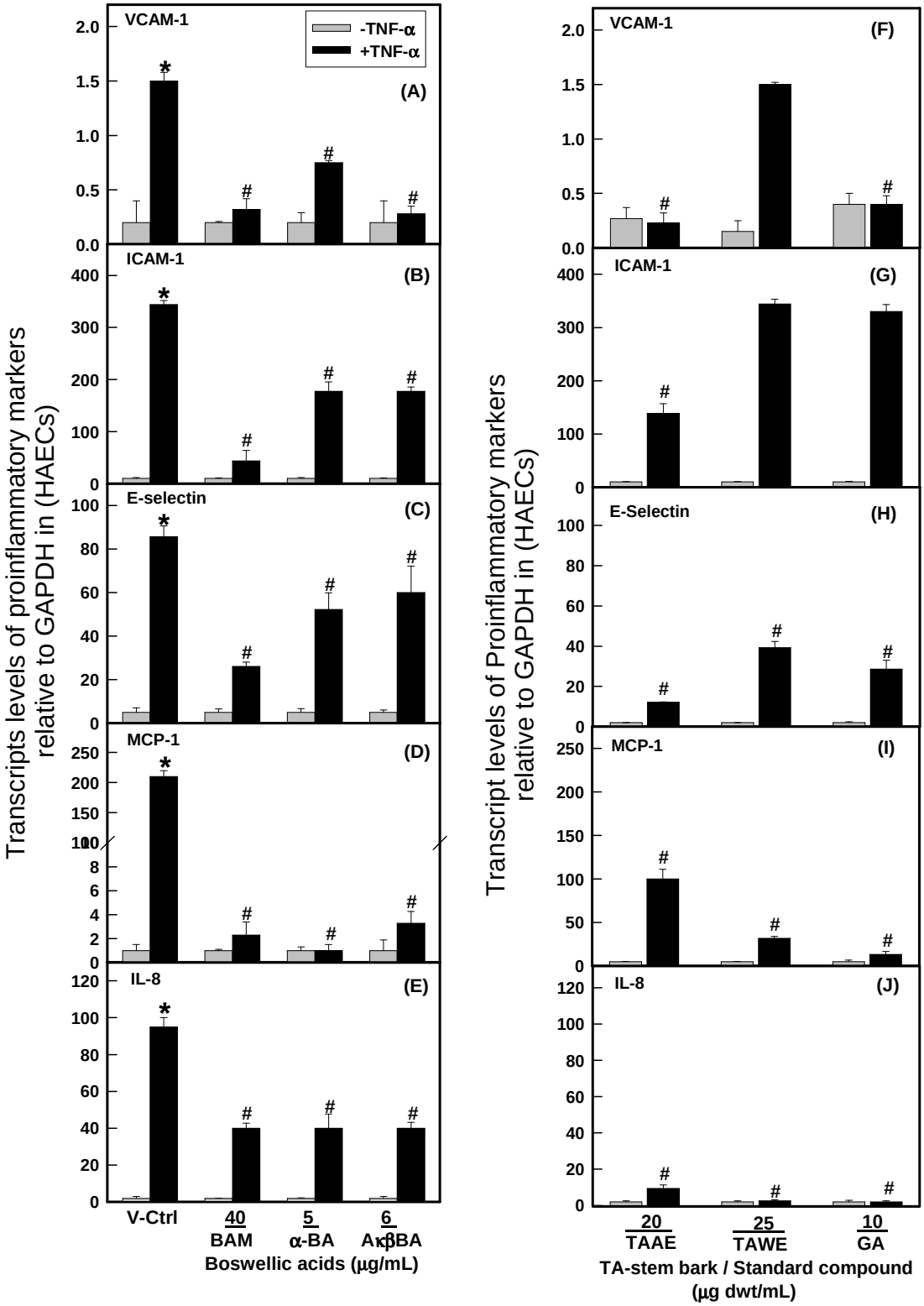

Figure. 4.6. BAM, α-BA, AκβBA (A to E) and *T. arjuna* extracts TAAE, TAWE and GA (F to J) decreases mRNA expression of (A) VCAM-1 (B) ICAM-1 (C) E-selectin (D) MCP-1 (E) IL-8 in TNF-α-induced HAECs. Data shown mean value of 3 independent experiments $^{\#}p < 0.001$ and $^{*}p < 0.001$ between the control groups.

HAECs stimulated with TNF-α in the presence of *T. arjuna* extracts also had significantly lower levels of inflammatory markers. TAAE (20 µg dwt/mL) significantly reduced the levels of mRNA expression of VCAM-1, E-selectin and IL-8 to 0.23 ± 0.1, 12.22 ± 0.5 and 9.4 ± 2.0 folds and showed moderate effect on ICAM-1 and MCP-1 (139 ± 16 and 100 ± 11 respectively) markers as compared to TNF-α treated HAECs. The pretreatment with TAWE (25 µg dwt/mL) also caused significant decrease in IL-8, MCP-1 and E-selectin (3 ± 0.5; 32.0 ± 2.2; 39.33 ± 3 folds, respectively), but had no effect on VCAM-1 and ICAM-1 (Figs. 4.6. F to J). Pretreatment with GA (10 µg dwt/mL) attenuated the gene expression of VCAM-1, E-selectin, MCP-1 and IL-8 (0.5 ± 0.1; 29 ± 5; 13.25 ± 4 and 2.0 ± 0.5 folds, respectively), but ineffective over the ICAM-1 induction (Figs. 4.6. F to J).

Flow-cytometry analyses of VCAM-1 and E-selectin

To investigate whether the extracts affected the surface protein markers of VCAM-1(CD106-FITC) and E-selectin (CD62E-PE) in TNF-α induced HAECs, the cells were immunostained with respective antibodies and subjected to FACScan (BD LSR Fortessa ^{TM}) flow-cytometry. In control cells, less than 1 % of the population expressed VCAM-1 or E-selectin. In TNF-α treated cells, 41 % ± 10 and 82 % ± 5 population of cells stained positive for VCAM-1 and E-selectin respectively (Figs. 4.7. A and B). Cells coincubated with BAM (40 µg dwt/mL), α-BA (5 µg/mL or 10 µM) or AκβBA (6 µg/mL or 12 µM) had significantly decreased VCAM-1 positive cells. In case of E-selectin expression, treatment with BAM inhibited positive population to 41 % ± 3 and AκβBA to 55 % ± 6, whereas α-BA did not inhibit the expression elicited by TNF-α (Figs. 4.7. C).

Further, pretreatment with *T. arjuna* stem bark extracts, TAAE / TAWE or gallic acid significantly attenuated the VCAM-1 positive cells down to 0.3 % ± 2.1, 7 % ± 5 and 25 % ± 4 respectively. In case of E-selectin, TAAE reduced the stained HAECs to 48 % ± 1, and TAWE or GA to 66 % ± 3 and 61 % ± 8 respectively, by comparison with TNF-α treatment alone (Fig. 4.7. D).

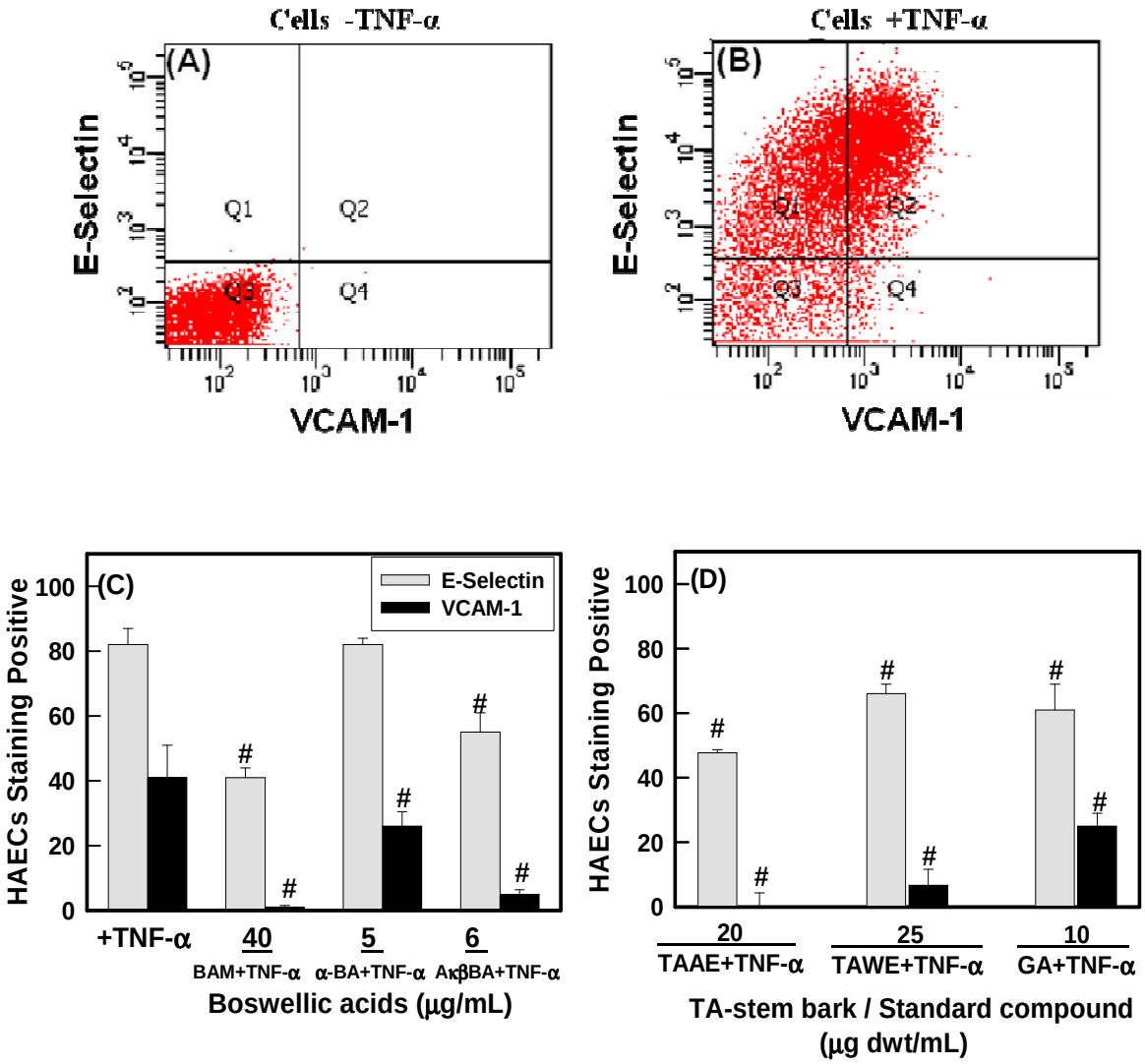

Figure. 4.7. (A) Figure represents FACS histograms of HAECs untreated (B) treated with TNF-α. (C) BAM; α-BA; AκβBA (D) TAAE/TAWE attenuated TNF-α induced protein expression of VCAM-1 and E-selectin. HAECs were stimulated with TNF-α (10 ng/mL) for 4 h and cells were analyzed by flow cytometry for surface expression of VCAM-1 and E-selectin using flow-cytometry. Cells analyzed for antibody staining. HAECs exposed to only TNF-α. (C) Cells coincubated with TNF-α and BAM (40 µg/mL); α-BA (5 µg/mL or 10 µM); AκβBA (6 µg/mL or 12 µM); (D) TAAE (20 µg dwt/mL); TAWE (25 µg dwt/mL) and gallic acid (10 µg/mL). A reduction in both VCAM-1 and E-selectin expression was seen in cells with boswellic acids and TAAE/WE coincubation $^{\#}p < 0.05$.

Effect of extracts in attenuating the phosphorylation of NF-κB p65 in TNF-α stimulated HAECs

Also in HAECs, like in THP-1 monocytic cells, the gene expressions of several proinflammatory markers including cytokines and chemokines, is regulated by NF-κB transcription factor. As shown in Figs. 4.8. A to C, control cells had p65 in the cytoplasm and predominantly located in the nuclei of TNF-α stimulated cells (Figs. 4.8. D to F). To elucidate the mechanism of anti-inflammatory activity of selected medicinal plant extracts in HAECs, their effect on TNF-α induced translocation of p65 subunit of NF-κB was studied using confocal microscopy. Cells were probed with antibody of NF-κB subunit p65 and stained using secondary antibody conjugated to Alexa Fluor 594. Nuclei were stained with DAPI. HAECs induced with TNF-α showed strong localization of NF-κB p65 into the nuclei, whereas uninduced cells showed cytoplasmic distribution (Figs. 4.8. A to F). Pretreatments with the BAM (40 µg/mL), α-BA (5 µg/mL or 10 µM), AκβBA (6 µg/mL or 12 µM) shown in Figs. 4.8. G to O or *T. arjuna* extracts or gallic acid shown in (Figs. 4.8. P to X) significantly inhibited the translocation of NF-κB p65 from cytoplasm to nucleus. TAAE (20 µg dwt/mL) and gallic acid (10 µg dwt/mL) showed highest response among above treatments. These results suggest that the plant extracts offer transcriptional factor NF-κB mediated anti-inflammatory activity in activated HAECs.

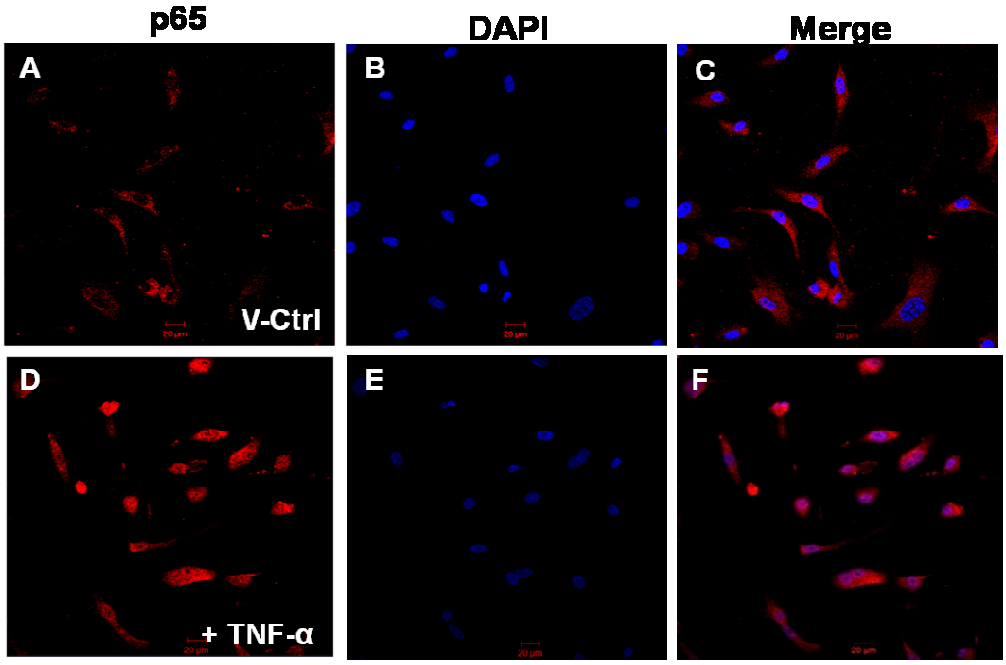

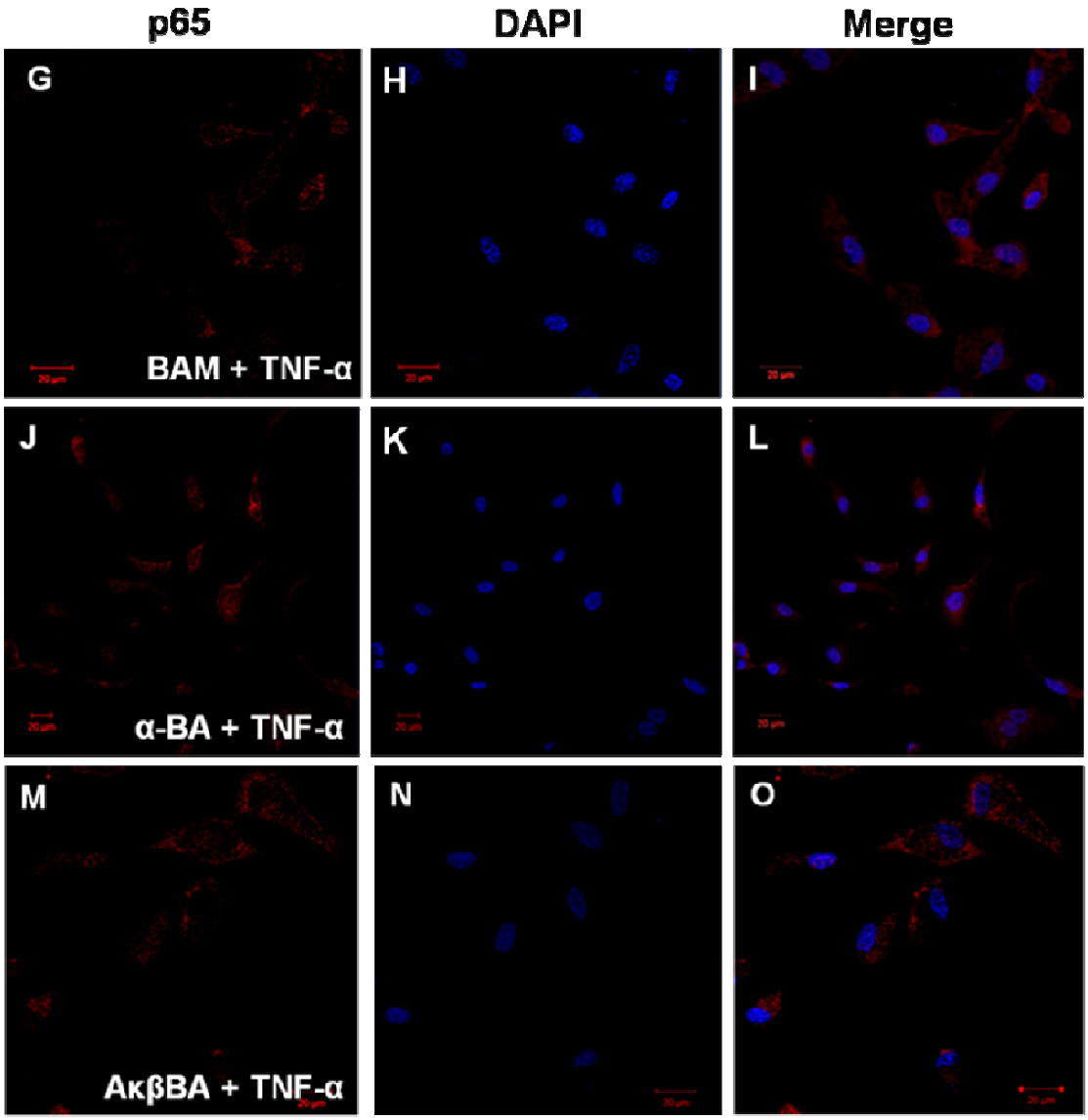
p65
DAPI
Merge
G
H
I
BAM + TNF-α
J
K
L
α-BA + TNF-α
M
N
O
AκβBA + TNF-α

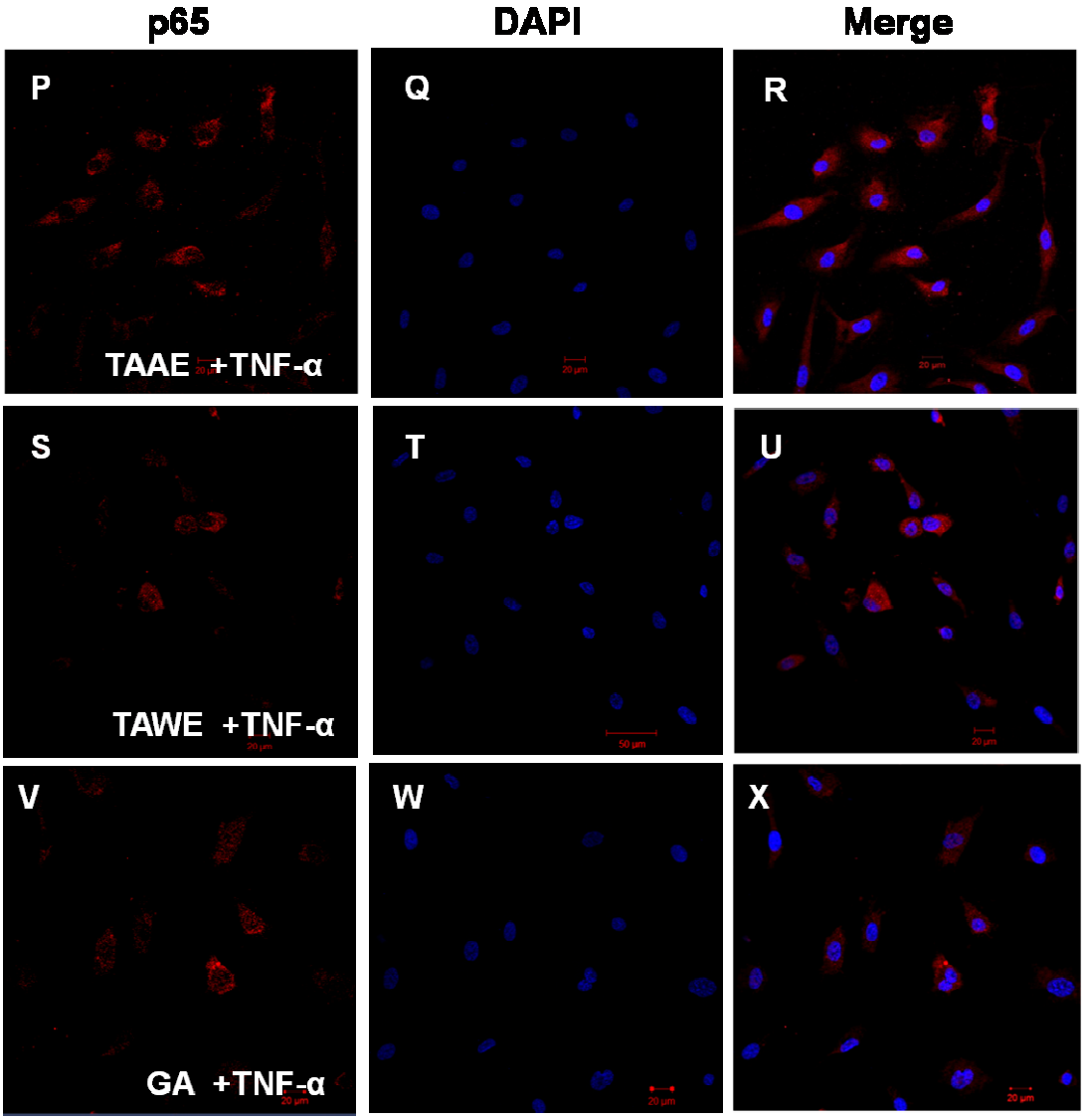

Figure. 4.8. Images showing the effect of BAM, αBA, AκβBA, *T. arjuna* stem bark extracts or gallic acid on inhibition of the translocation of p65 subunit of NF-κB from cytoplasm to nucleus in TNF-α induced HAEC cells. Images A, D, G, J, M, P, S, V and panels B, E, H, K, N, Q, T, W were taken using Ex 590 nm and Em 617 nm and Ex 345 nm and Em 455 nm respectively. Panels C, F, I, L, O, R, U, X are merged images.

Discussion

Atherosclerosis is referred as chronic inflammatory blood vessel wall disease (Ross, 1999; Libby, 2002). Several conditions including oxidative stress, hypercholesterolemia, hyperglycemia and postpandial lipolysis induce activation of monocytes and platelets in the peripheral blood, and also endothelial dysfunction and vascular permeability (Esper et al., 2006). Traditionally, TA-stem bark has been used as a cardiotonic in Ayurvedic medicine. Clinical and animal studies suggested the efficacy of TA-stem bark in treating various types of cardiovascular diseases (Dwivedi, 2007), but its mechanism of action was not clear. To the best of our knowledge, this is the first report that provides the cellular and molecular basis of cardio-protective activity of TA-stem bark extracts. Drugs targeting inflammatory mechanism are of good choice for treating several inflammatory disease including cardiovascular diseases (Bailey and Butler 1973). Therefore, herbal extracts with anti-inflammatory property are good resources for compounds with such pharmacological activity (Chen et al., 2003). In the present study we showed boswellic acids isolated from BS-gum resin and stem bark of *T. arjuna* were investigated for their effect on secretion of proinflammatory gene expression induced by, LPS in THP-1 monocytic cells and TNF-α in HAECs.

Antiinflammatory effect of BAM and TA-stem bark in THP-1 cells and HAECs

LPS, is potent bacterial endotoxin, which causes functional changes in monocytes like chemotaxis and maturation of monocyte to macrophages (Baqui et al., 1998). LPS induced THP-1 cells secrete much more higher amounts of proinflammatory cytokines particularly TNF-α compared to uninduced cells. Our results demonstrated that pretreatment of cells with boswellic acids or TA-stem bark extracts significantly attenuated LPS induced secretion of TNF-α. At mRNA transcript level, α-BA showed more effect than BAM and AκβBA in down regulating MCP-1 while IL-8 expression by BAM. In case of stem-bark extracts of *T. arjuna*, TAAE attenuated both MCP-1 and IL-8 mRNA expression levels, whereas TAWE showed effect only on IL-8. Such variation in response could be due to the difference in their metabolite profile. Regulation of several proinflammatory genes is an ideal strategy to control inflammatory diseases, the transcription of these inflammatory genes in mammalian

cells are under control of transcription factor NF-κB, Mitogen-activated protein kinases (MAPK), c-Jun NH(2)-terminal kinase (JNK), Protein kinase A (PKA) and etc (Hoareau et al., 2010). Several naturally occurring NF-κB inhibitors such as quercetin, resveratrol significantly inhibited TNF-α release by monocytic cells (Nair et al., 2006). NF-κB activation and thereby translocation into nucleus of THP-1 cells and HAECs was inhibited by boswellic acid, TAAE and TAWE. Rolling/adhesion and migration of monocytes into vasculature are essentially mediated by cell adhesion molecules (VCAM-1, ICAM-1) and selectins (E-selectin). MCP-1 mediated rolling of leukocytes (including monocytes) with the help of selectins expressed during inflammation. VCAM-1 is expressed in activated endothelial cells, macrophages, lymphoid dendritic cells and stromal fibroblasts and ICAM-1 in hematopoietic and nonhematopoietic cells including fibroblasts, vascular endothelial and epithelial cells (Couffinhal et al., 1994). Attenuation of leukocyte trafficking is one of the strategies in developing anti-inflammatory therapeutics (Wiese et al., 2009). Boswellic acid mixtures isolated from BS-gum resin (BAM) and AκβBA suppressed VCAM-1 and MCP-1 effectively in TNF-α induced HAECs. Inhibition of VCAM-1 is essential for inhibiting firm adhesion of monocytes (Alon et al., 1995; Gerszten et al., 1998). Adherence monocyte triggers intracellular signals such as ROS generation and NF-κB activation, which play crucial role in pathogenesis of atherosclerosis (Chen et al., 2002). MCP-1 expression was also inhibited by BAM, α-BA and AκβBA. Furthermore, BAM inhibited the expression of mRNA transcript levels of ICAM-1 and E-selectin more effectively than α-BA or AκβBA suggesting that other components of BAM may be responsible for its activity.

Flow-cytometric study using specific monoclonal antibodies against VCAM-1 (CD106-FITC) and E-selectin (CD62E-PE) revealed the effect of extracts or test compounds at protein level. BAM and AκβBA significantly decreased VCAM-1 and E-selectin protein markers whereas α-BA showed significant effect on only VCAM-1 but not E-selectin. Extracts of *T. arjuna* also suppressed the TNF-α stimulated expression of inflammatory markers. TAAE down regulated the levels of mRNA expression in VCAM-1, E-selectin and IL-8 more effectively than ICAM-1 and MCP-1, whereas TAWE inhibited ICAM-1, MCP-1 and IL-8, but not on VCAM-1 and ICAM-1. VCAM-1 protein expression was completely attenuated by TAAE, TAWE and E-selectin was only inhibited to some extent by both the extracts.

Chapter 5

RESULTS and DISCUSSION

Objective 3: Evaluation of antithrombotic property of *B. serrata*-gum resin and BAM using human blood platelet and coagulation factors

Results

In vitro ADP-induced platelet aggregation of BSAE/WE and BAM

Platelets in platelet rich plasma (PRP) are sensitive to aggregation by low doses of ADP (10 µM) at 37 ^{o}C. ADP at 20 µM was able to cause maximal platelet aggregation which is indicated by a marked decrease in absorbance at λ 600 nm within the first 2 min of incubation and stabilized up to 12 min period of time. In the present study, heparin was used as a positive drug control, which inhibited ADP induced platelet aggregation. Untreated platelets and ADP induced aggregation were carried out in the beginning of the each test in order to confirm the physiological status of the platelets. BSAE and BSWE (1-3 mg dwt/mL) were added to PRP, a concentration-dependent inhibition of ADP induced platelet aggregation was seen (Fig. 5.1). The analysis of these results shows that the inhibitory activity of both the extracts reached to maximum at 3 mg dwt/mL. Natural antithrombotic components those inhibit platelet aggregation are of potent interest in primary prevention of cardiovascular disease. BSAE, BSWE and the possible active metabolites of the extracts were tested for their inhibitory activity of boswellic acid mixed fraction (BAM), α-BA and AκβBA on ADP induced platelet aggregation. The results indicated that all these test samples decreased the ADP induced platelet aggregation. Effect of BAM at varied concentrations (50-500 µg dwt/mL) was tested on ADP induced platelet aggregation. In the assay, BAM showed dose dependent activity up to 250 µg dwt/mL. Antiplatelet aggregatory activity of BAM at 250 µg dwt/mL was comparable to the activity of heparin at 10 U/mL (Fig. 5.2).

Coincubations of ADP induced PRP with α-BA (200 µM - 800 µM) showed dose dependent antiplatelet aggregatory activity and showed maximum inhibition at the concentration of 600 µM (Fig. 5.3). In case of AκβBA (40 µM - 200 µM), maximum effect was observed at 200 µM concentration (Fig. 5.4). Thus these results suggest that α-BA and AκβBA, possess significant antiplatelet aggregatory activity although concentration required varied among them. Furthermore, super saturation concentration of BA's show either plateau or decline response.

Effect of *B. serrata* gum resin and its boswellic acid fraction on plasma coagulation (*in vitro*) time periods

Anticoagulant activity of isolated boswellic acid mixture (BAM) from BS-gum resin and commercially available six boswellic acids (α-BA, β-BA, 3-O-AαBA, 3-O-AβBA, KβBA and AκβBA) were assessed in order to further explore their antithrombotic activity. Intrinsic (APTT) and extrinsic (PT) coagulation time periods are specific and sensitive indicators for haemostasis of human plasma. PT and APTT time periods of control plasma are 13.2 s and 34 s respectively. Both BSAE and BSWE showed very strong activity in prolongation of these clotting times. The concentration dependent effects of BSAE and BSWE on PT and APTT clotting times of human plasma are shown in Fig. 5.5.

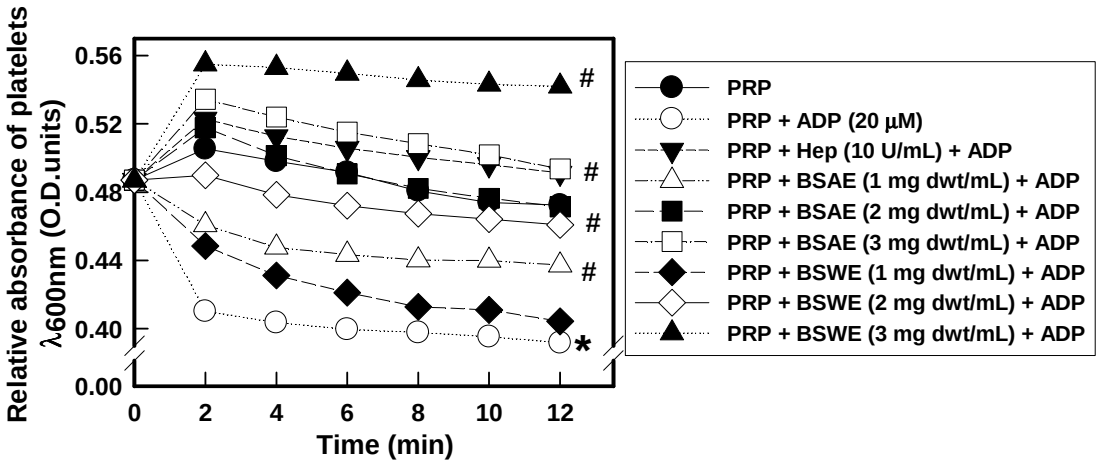

Figure. 5.1. Effect of BS-extracts on ADP induced aggregation of human platelets. PRP; PRP + ADP (20 µM); PRP + Hep (10 U/mL) + ADP; PRP + BSAE (1 mg dwt/mL) + ADP; PRP + BSAE (2 mg dwt/mL) + ADP; PRP + BSAE (3 mg dwt/mL) + ADP; PRP + BSWE (1 mg dwt/mL) + ADP; PRP + BSWE (2 mg dwt/mL) + ADP; PRP + BSWE (3 mg dwt/mL) + ADP. Data presented are mean ± S.D., n = 3. S.D. not seen where S.D. values are within the symbol of data point. $^{\#}p < 0.001$ between platelets treated with BS extracts and ADP vs treated with ADP alone, $^{*}p < 0.001$ indicates comparison between PRP + ADP vs PRP alone.

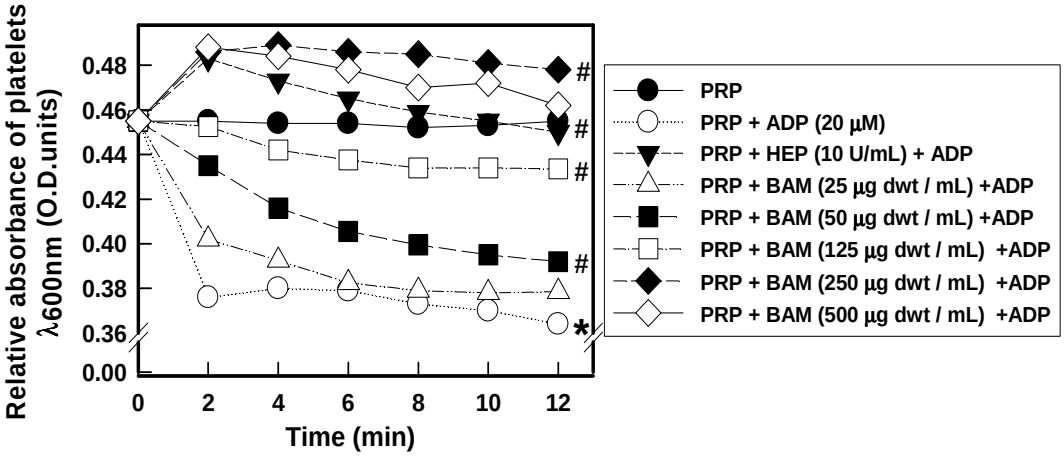

Figure. 5.2. Effect of boswellic acid mixed-fraction (BAM) isolated from BS-gum resin on ADP induced aggregation of human platelets. BAM (25 µg dwt/mL up to 500 µg dwt/mL) were tested on ADP induced platelets. Heparin used as a positive drug control. Data presented are mean ± S.D. n=3. $^{\#}p < 0.001$ between platelets treated with BAM and ADP vs treated with ADP alone. $*p < 0.001$ indicates comparision between PRP + ADP vs PRP alone.

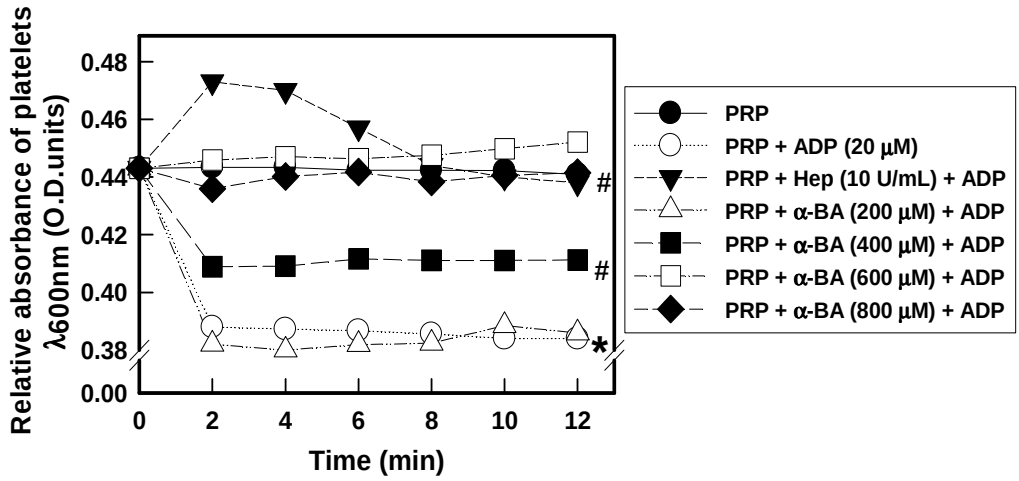

Figure. 5.3. Effect of α-boswellic acid (α-BA) at different concentrations (200 µM up to 800 µM) on ADP induced aggregation of human platelets. Figure indicates that α-BA showed its maximum effect at 600 µM (~ 300 µg dwt/mL) in attenuating the ADP induced platelet aggregation. Data presented are mean ± S.D., n=3. $^{\#}p < 0.001$ between platelets treated with α-BA and ADP vs treated with ADP alone, $*p < 0.001$ indicates comparison between PRP + ADP vs PRP alone.

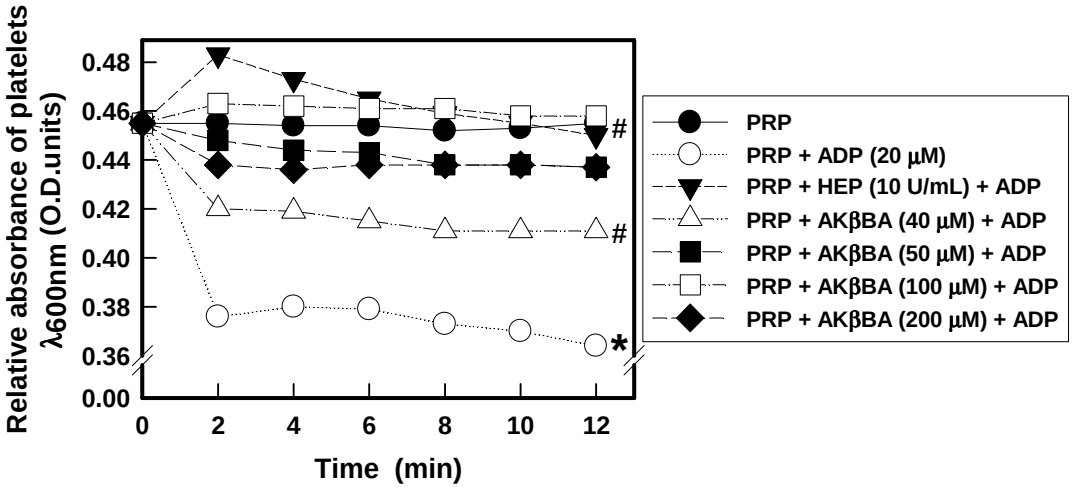

Figure. 5.4. Effect of 3-O-acetyl-11-keto-β-boswellic acid (AκβBA) (40 µM up to 200 µM) on ADP induced aggregation of human platelets. AκβBA showed its maximum effect at 100 µM (~ 50 µg dwt/mL). Data presented are mean ± S.D., n=3. $^{\#}p < 0.001$ between platelets treated with AκβBA and ADP vs treated with ADP alone, $^{*}p < 0.001$ indicates comparison between PRP + ADP vs PRP alone.

BSAE and BSWE at 60 µg dwt/mL prolonged APTT time period by 2.6 folds and PT time period by 4 folds, which demonstrated the strong anticoagulant property of BS-gum resin as shown in Fig. 5.5.

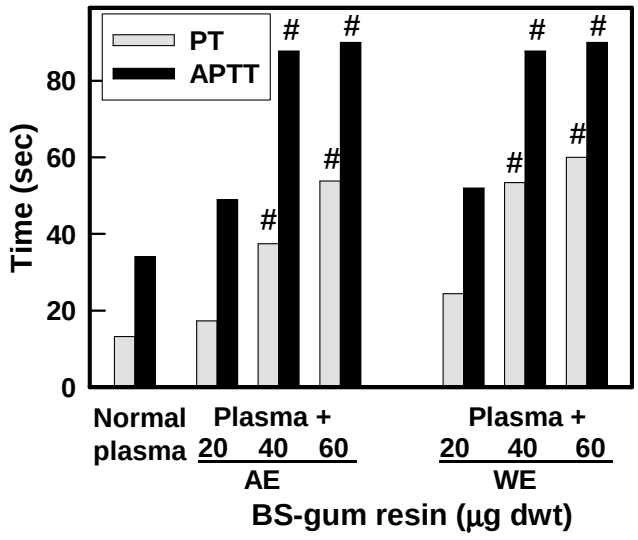

Figure. 5.5. Effects of BS-gum resin on clotting PT and APTT time periods. Data presented are mean ± S.D., n = 3. S.D not seen where S.D. values are within the symbol of data point. Statistically significant values are indicated by # with $p < 0.001$.

The effect of BAM and various boswellic acids found in BAM were tested on APTT and PT of human plasma, the results are shown in Fig. 5.6. BAM at 75 µg dwt/mL caused the increase in PT time period to 60 s and APTT clotting time period to 90 s (Fig. 5.6). Pure boswellic acids namely α-BA, β-BA, 3-O-AαBA, 3-O-AβBA, KβBA and AκβBA at 100 µM were tested for their effect on APTT and PT clotting times using human plasma. All of the BA's except β-BA and KβBA extended APTT time period from 34 s to > 90 s. β-BA and KβBA extended APTT to 80 s and 83 s respectively. All six boswellic acids also showed remarked (~ 5 fold increase) effect on extending the PT time periods. α-BA, β-BA, 3-O-AαBA, 3-O-AβBA, KβBA and AκβBA extended PT time to 50 s, 65 s, 60 s, 60 s, 77 s and 65 s respectively. Heparin (10 U/mL) significantly prolonged clotting time of APTT and PT times to 78 s and 66 s respectively (Fig. 5.6).

Coagulation factors assays

In order to know the specific target sites of inhibition in the blood coagulation cascade pathway, the effect of BSAE and BSWE on human clotting factors Xa and XIa was tested. BSAE inhibited both FXa and FXIa significantly ($p < 0.001$). BSAE at 6 and 8 µg dwt/mL inhibited 70 % of FXa (Fig. 5.7. A) and 55 % of FXIa (Fig. 5.7. B). BSWE showed poor inhibition on FXa and about 25 % inhibition on FXIa (Figs. 5.7. A and B). During the course of identifying specific active metabolites responsible for antithrombotic effect of BS-gum resin, isolated boswellic acid mixture and all six pure boswellic acids were tested for their effect on human coagulation factors, namely, FIXa, FXIIa, VIIa along with FXa and FXIa. FIXa, FXIa and XIIa are involved in intrinsic pathway, VIIa belongs to extrinsic and FXa to common pathway of human blood coagulation cascade.

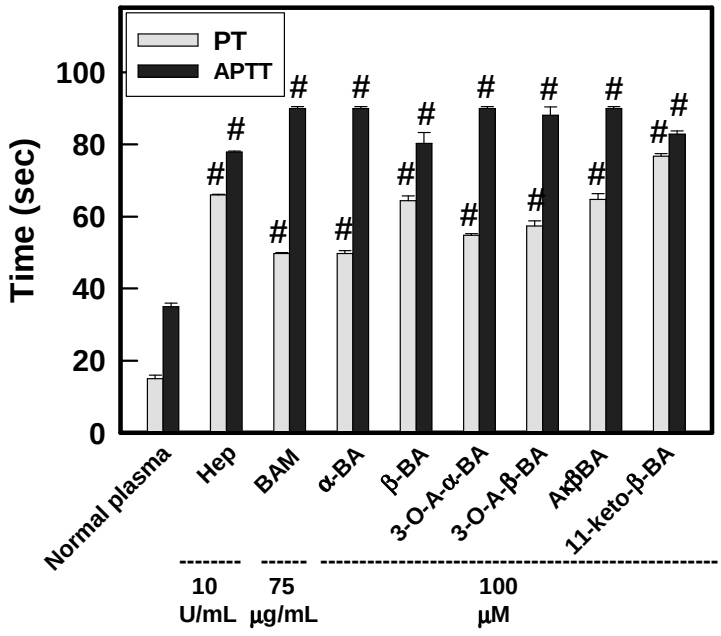

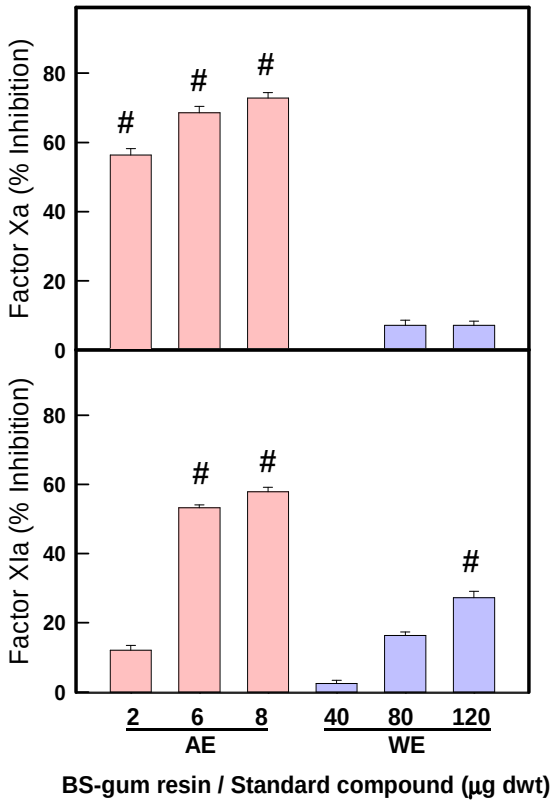

Figure. 5.6. Effects of BAM and six pure boswellic acid standards on clotting time periods of PT and APTT. Heparin was used as drug control. Data presented are mean ± S.D., n = 3. S.D not seen where S.D. values are within the symbol of data point. Statistically significant values are indicated by # with $p < 0.001$.

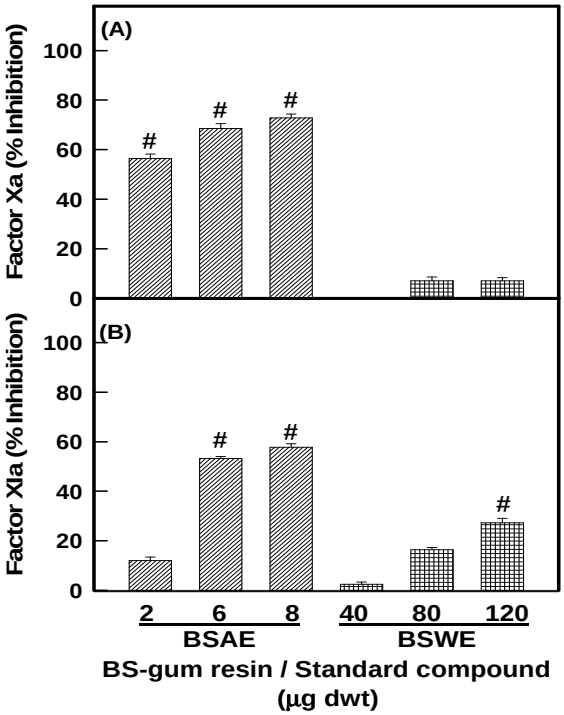

Figure. 5.7. % Inhibitory effect of BS-extracts on (A) factor Xa and (B) factor XIa. Clotting assays were conducted by monitoring decrease in the absorbance of chromogenic substrate using microplate reader. Values in the bar graphs represent mean ± S.D. (n = 4), $^{\#}p < 0.001$ highly significant compared with control.

Factor VIIa assay: FVIIa is part of extrinsic pathway and inhibition of FVIIa affect PT clotting time period. BAM (75 µg dwt/mL) showed 75 % ± 8 (Fig. 5.8. A) and boswellic acids α-BA, β-BA, 3-O-AαBA, 3-O-AβBA, AκβBA and KβBA at 100 µM showed 78 % ± 2; 78 % ± 2; 82 % ± 1.2; 80 % ± 12; 89 % ± 5 and 87 % ± 2 inhibition respectively (Fig. 5.8. A). No significant further increase in inhibition was

observed when the concentrations of boswellic acids increased to 150 µM. Heparin (10 U/mL) shown to decrease FVIIa activity by 72 % ± 3.1.

Factor IXa assay: FIXa is part of the intrinsic pathway and inhibition of FIXa affect APTT clotting time period. BAM (75 µg dwt/mL), or 100 µM boswellic acids (α-BA, β-BA, 3-O-AαBA, 3-O-AβBA, KβBA and AκβBA and heparin (10 U/mL) exhibited almost no inhibition on FIXa activity. The % inhibitions by these test compounds were 8 % ± 1; 2 % ± 1; 2 % ± 0.7; 1.3 % ± 0.24; 13 % ± 3; 5 % ± 3; 2 % ± 1 and 3 % ± 1 respectively (Fig. 5.8. B).

Factor Xa assay: FXa is part of the common pathway and inhibition of FXa affect both APTT and PT clotting time periods. The effect of BAM and six boswellic acids (α-BA, β-BA, 3-O-AαBA, 3-O-AβBA, AκβBA and KβBA) on factor Xa was assessed using chromogenic substrate assay. BAM at (75 µg dwt/mL) inhibited FXa by 76.58 % ± 5.8 (Fig. 5.8. C). α-BA, β-BA and 3-O-AαBA (100 µM) exhibited their maximum inhibition of FXa by 66 % ± 8; 53 % ± 2.7 and 68 % ± 3.4 respectively. While, 3-O-AβBA, AκβBA and KβBA showed maximum inhibition at 100 µM by 77 % ± 8.5; 63 % ± 7.6 and 77 % ± 1.1 respectively (Fig. 5.8. C) and the effects slightly declined thereafter at 150 µM (data not shown). The effect of all these boswellic acids at 100 µM on FXa are in agreement with their prolongation effect on APTT and PT time periods. Heparin (10 U/mL) caused 80 % ± 5 of FXa (Fig. 5.8. C).

Factor XIa assay: FXIa is part of intrinsic pathway and inhibition of FXIa affect APTT clotting time period. BAM (75 µg dwt/mL) and boswellic acids (α-BA, β-BA, 3-O-AαBA, AκβBA and KβBA) at 100 µM showed negligible effect on FXIa activity by 12 % ± 0; 0.5 % ± 0; 3 % ± 1; 5 % ± 0.8; 1 % ± 0.2 % and 1 % ± 0 (Fig. 5.8. D). Heparin (10 U/mL) also showed almost no effect.

Factor XIIa assay: FXIIa is part of intrinsic pathway and inhibition of FXIIa affect APTT clotting time period. BAM and pure standard boswellic acids inhibited up to 90 % of FXIIa activity. BAM at 75 µg dwt/mL showed 88 % ± 4.2. All the six boswellic acids were tested at 100 µM for their effect on FXIIa (Fig. 5.8. E). α-BA, β-BA, 3-O-AαBA, 3-O-AβBA, AκβBA and KβBA at 100 µM showed 72 % ± 3; 96 % ± 3.2; 91 % ± 0.5; 75 % ± 3; 96 % ± 5 and 90 % ± 3.2 respectively (Fig. 5.8. E). We further checked at higher concentration (150 µM) for the linearity of inhibition, but we observed slight decline thereafter (data not shown). Heparin (10 U/mL) exhibited moderate affect on the rate of factor XIIa inhibition by only 16 % ± 3 (Fig.

5.8. E). Effect of BAM and boswellic acids on APTT associated with inhibition of FXIIa activity and prolonged both APTT and PT time periods can also be mediated through FXIIa inhibition (Fig. 5.6).

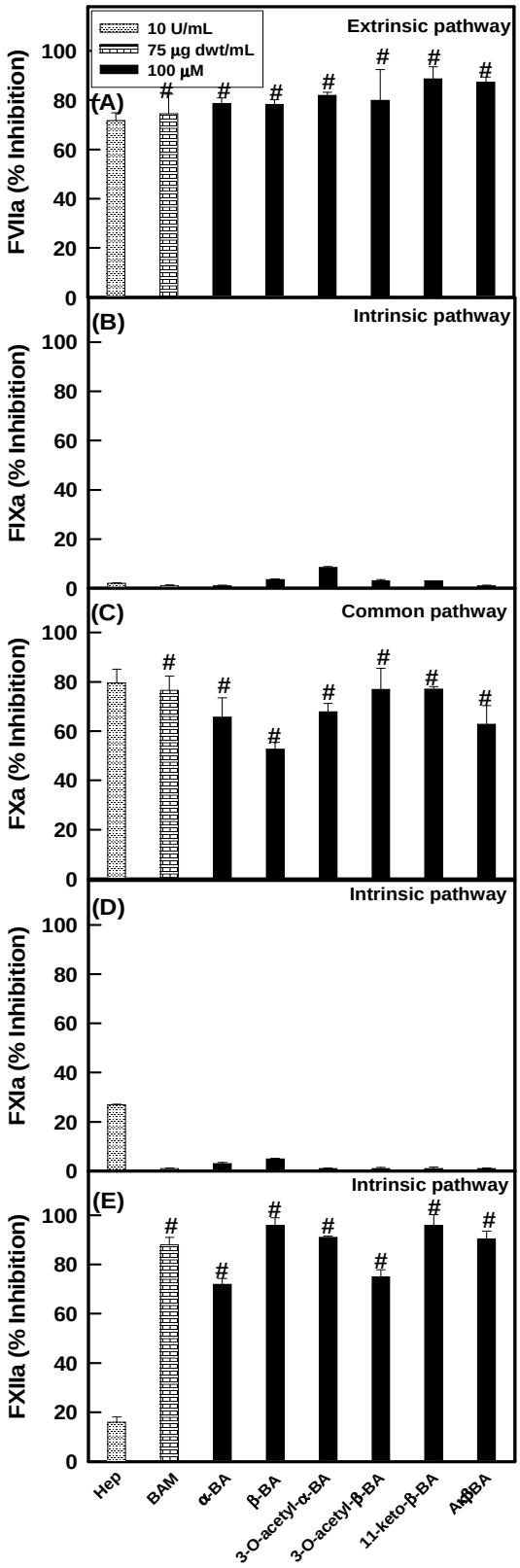

Figure. 5.8. % Inhibitory effects of boswellic acid standards / BAM / Heparin on blood coagulation factors of intrinsic, extrinsic and common pathway of coagulation cascade were monitored. Data presented are mean ± S.D., n = 3. S.D not seen where S.D. values are within the symbol of data point. Statistically significant values are indicated by # with $p < 0.001$.

Discussion

Platelets play an important role in hemostasis and thrombosis in response to atherosclerotic plaque or endothelial stimulus, promoting clot formation in the vessel and thus contributes to cardiovascular disease and stroke (Ruggeri and Mendolicchio 2007; Jennings, 2009; Ross, 1999; Boos and Lip 2006). At the same time, insufficient platelet function causes bleeding. Thus evaluating platelet function is important for estimating the risk of bleeding or thrombosis in numerous conditions (Eriksson and Whiss 2005). Natural antithrombotic compounds influence platelet aggregation is potent interest for primary prevention of cardiovascular disease. *Boswellia serrata's* gum resin is used in Indian Ayurvedic and folk medicine to treat blood disorders as well as to curtail inflammatory diseases like rheumatoid arthritis and to promote cardiac health (Clarisse et al., 2008; Moussaieff and Mechoulam 2009). In the present study, we have tested the anti-platelet effects of the hydroalcoholic and water extracts of BS-gum resin and also isolated boswellic acid mixture (BAM) from the gum resin. Commercially available pure boswellic acids tested independently to identify the active compounds from the BS-gum resin. ADP is an inducer of platelet aggregation (Cattaneo and Gachet, 2001) and contributes to the formation of occlusive platelet rich thrombi (Jennings, 2009). Epinephrine and collagen are also considered as aggregating agents and weak agonist (Zhou and Schmaier 2005) however, ADP was used for the present study (Mrowiec et al., 1995). Our results showed that BSAE, BSWE, BAM and also pure boswellic acids showed dose dependent effect on inhibiting ADP induced platelets aggregation. BSAE and BSWE at 3 mg dwt/mL markedly inhibited platelet aggregation, the effect was comparable to positive drug control, heparin at 20 µg/mL. Isolated boswellic acid mixture from BS-gum resin (BAM) at 250 µg dwt/mL and pure boswellic acids, α-BA (300 µg dwt/mL or 600 µM) and AκβBA (30 µg dwt/mL or 50 µM) were also very effective in inhibiting platelet aggregation. Among all boswellic acids, pharmacological actions of AκβBA is been extensively investigated (Tausch et al., 2009). AκβBA was reported to decrease platelet-activating factor stimulated intracellular Ca^{2+} (Poeckel et al., 2006) and also its inhibitory effect on COX-1, which is a platelet type 12-lipoxygenase. The activity of AκβBA was attributed to acetyl group on C4 ring and 11-keto functional groups

(Park et al., 2011) and it was shown to be more potent than β-BA (Poeckel et al., 2006a).

In the study of thrombosis, clotting time and factors of coagulation pathway provide information on the status of the coagulation cascade. Since, the extracts of BS-gum resin and isolated boswellic acids showed significant antiplatelet aggregatory effect, their effect on clotting time periods and clotting factors were investigated in detail. The anticoagulant effect of the BS-gum resin and boswellic acids were examined using APTT and PT assays. BS-gum resin extracts prolonged PT and APTT clotting times in concentration dependent manner. The extracts prolonged APTT time by 2.6 folds and PT time periods by 4-folds. The clotting time periods were also similarly prolonged by BAM and pure boswellic acids (α-BA, β-BA 3-O-AαBA, 3-O-AβBA AκβBA and KβBA). Among all BA's, lowest effect was shown by α-BA on PT and β-BA on APTT. However, the overall effect of BA's were comparable to heparin, the positive drug control (10 U/mL) prolonged APTT by 2.29 folds. Thus our results suggest that BA's are potential anticoagulant and BS-gum resin is a potential natural source of such compounds.

The prolongation of APTT by boswellic acids suggests their effect on both intrinsic and extrinsic coagulation pathways. To elucidate the mechanism responsible for the effect of BS-gum resin's extracts and / or boswellic acids, their inhibitory effect on factors of coagulation cascade were assayed. BSAE and BSWE with the intrinsic factor XIa and common factor Xa. BSAE significantly inhibited FXa and FXIa by 70 % and 55 % respectively at 6 and 8 µg dwt/mL. Whereas BSWE did not show inhibitory effect on FXa, but showed 25 % inhibition on FXIa (Fig. 5.7. B).

Inhibitors of FXa are of interest in treating thrombotic disorders (Shibeko et al., 2010). FXa is a protease, acts at the convergence of the intrinsic and extrinsic pathways of blood coagulation cascade, and is responsible for the activation of final components of coagulation pathway to form clots (Shibeko et al., 2010). Commercially available and widely used anticoagulants, such as heparin and warfarin have certain side effects related to infection and / or reactivity with other medications. Other FXa inhibitors namely, rivaroxaban, apixaban, endoxaban showed fruitful results on replacement with warfarin (Yeh et al., 2012). Therefore, there is a great need for identifying FXa inhibitors with minimal side effects. In the present study, all six tested boswellic acids (α-BA, β-BA and 3-O-AαBA, 3-O-AβBA, KβBA and AκβBA), at about the concentration of 100 µM, showed

significant inhibition of FXa and the results are comparable to heparin. These results suggest that BA's inhibit FXa that occupies critical position in coagulation cascade and control thrombin generation.

FXIIa triggers intrinsic pathway of coagulation, its inhibition may be useful in chronic conditions or in short term therapies associated with the risk of thrombosis during surgery (Kleinschnitz et al., 2006). It is as important factors for the fibrin formation (*in vitro*) without the influence of hemostasis (Renne et al., 2012). FXIIa activity was found to be inhibited by BAM and BA's at 100 µM, in the range of 75 % to 90 %. These results are in agreement with their prolongation effect on APTT which indicates intrinsic pathway of the coagulation cascade. Among all the six tested BA's, α-BA showed lowest effect on FXIIa, however, its effect was not compromised in enhancing APTT. Such conflicting data can be explained due to its effect on FXa or FVIIa. We have not tested BA's effect on FVIIIa. Heparin (10 U/mL) showed only 18 % inhibition on FXIIa and these results are in agreement with data published by Pixley et al., (1985) and they concluded that it may be due to protein as well as peptide substrates. Isolated boswellic acid mixed-fraction (BAM) and all tested six pure boswellic acids did not have significant effect on factor XIa and IXa. These two factors are also the components of intrinsic pathway. FXIa is involved in the formation of thrombin and protects against fibrinolysis which is a high level risk factor for deep venous thrombosis (Meijers et al., 2000). Thus FXIa plays a major role in amplification of coagulation cascade (Buchanan et al., 2008) and is essential for normal hemostasis (Naito and Fujikawa 1991). FIXa plays a key role in thrombus formation, higher levels are associated with thrombotic risk factors, its selective inhibition benefits in evaluating prophylaxis and treatment of thrombosis (Lowe, 2001). However, tested concentrations of BA's did not inhibit FIXa.

FVIIa is responsible for the blood clot formation and is a component of extrinsic pathway of coagulation (Broze et al., 1985). Our results showed that BAM and boswellic acids (100 µM) showed up to 80 % inhibition on activity of FVIIa. Their inhibitory effect is comparable to heparin at 10 U/mL. The results obtained in this assay supported the effect of BA's in prolongation of PT clotting times.

In the summary the data suggests that BA's play a significant role in inhibiting the clotting time periods of both PT and APTT by inhibiting specifically the coagulation factors namely, FVIIa, FXa and FXIIa.

Chapter 6

RESULTS and DISCUSSION

Objective 4: LC-MS Metabolite analysis of cultivars of *Curcuma longa and C. aromatica* and the use of metabolite profile for constructing cultivar variability

Results

In the present study, methanolic extracts of fresh-frozen turmeric rhizomes of five cultivars of *C. longa* (cvs. Alleppey Supreme, Duggirala Red, PCT-13, Prathibha, Salem) and two cultivars of *C. aromatica* (cvs. Kasturi Araku, Kasturi Avidi) were subjected to LC-ESI-MS/MS analysis. Electronspray ionization (ESI) is one of the major ionization tools coupled with hyphenated technique like LC/MS shown to be powerful in metabolite profiling and metabolomics research. HPLC-DAD (λ 425 nm) chromatograms of all seven cultivars showing three curcuminoids bisdemethoxycurcumin, demethoxycurcumin and curcumin are shown in Fig. 6.1. A to G. Figs. 6.2 and 6.3 show total ion current (TIC) chromatogram of all seven cultivars taken in negative ion and positive ion mode respectively. Metabolites identified from each of the TIC are shown in Tables. 6.1 to 6.14. Majority of the compounds extracted into methanol were diarylheptanoids.

Fresh rhizome methanolic extracts of *C. longa* cv. Alleppey Supreme showed the presence of total number of 80 compounds, out of which, 37 are known and 43 are unknown. Of these, known compounds, 31 were detected in (-) ESI-LC-MS (Table 6.1) and 17 in (+) ESI-LC-MS mode (Table 6.8). Eleven of the 37 known compounds were commonly detected in both the ion modes. Out of the 31 compounds detected in (-) ESI-LC-MS, 20 of them belong to the class of diarylheptanoids, 3 are from coumarins, 4 from flavonoids, 3 belong to bisabolane type of sesquiterpenes and one belongs to fatty acid and another one was aromatic compound. In case of positive ion mode, out of 17 known metabolites, 11 were diarylheptanoids which were commonly detected in both positive and negative ion modes. Of the four bisabolane type triterpenoids, only one i.e., curlone was commonly detected in both the ion modes. Among the unidentified 43 metabolites, area/abundance was generated for only 10 compounds (data not shown).

In *C. longa* cv. Duggirala Red, a total of 110 compounds were detected. Out of which, known compounds of 23 detected in (-) ESI-LC-MS (Table 6.2) and 11 in (+) ESI-LC-MS mode (Table 6.9), where 11 of the compounds were commonly detected in both positive and negative modes. Out of the 23 known metabolites detected from the negative ion mode, 19 belong to diarylheptanoids, two of them are flavonoid class of compounds, one of coumarin type and other one belongs to aromatic

compound. In case of positive ion mode, out of 11 known compounds, 8 of them were diarylheptanoids those were commonly detected in both the modes of ionization, other three are bisabolane type of sesquiterpene compounds. Out of 84 unidentified compounds, area/abundance was generated for only 34 metabolites (data not shown).

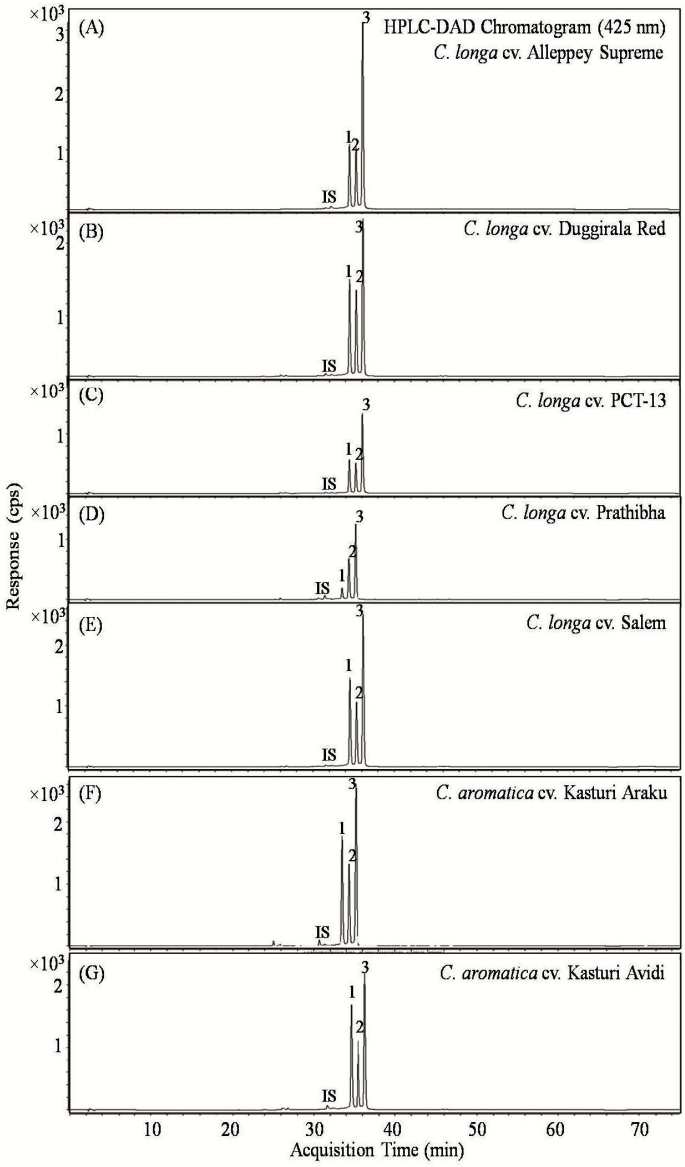

Figure. 6.1. HPLC-DAD chromatograms obtained at λ 425 nm of methanolic extracts of fresh rhizome of five cvs of *C. longa* (A) ALP (B) DRD (C) PCT (D) PRA (E) SAL and *C. aromatica* in (F) KAR (G) KAV. Peaks labelled in the chromatogram (1) bisdemethoxycurcumin (BDMC), (2) demethoxycurcumin (DMC), (3) curcumin (CU), IS: Internal standard compound 4-fluoro-4'-hydroxylbenzophenone.

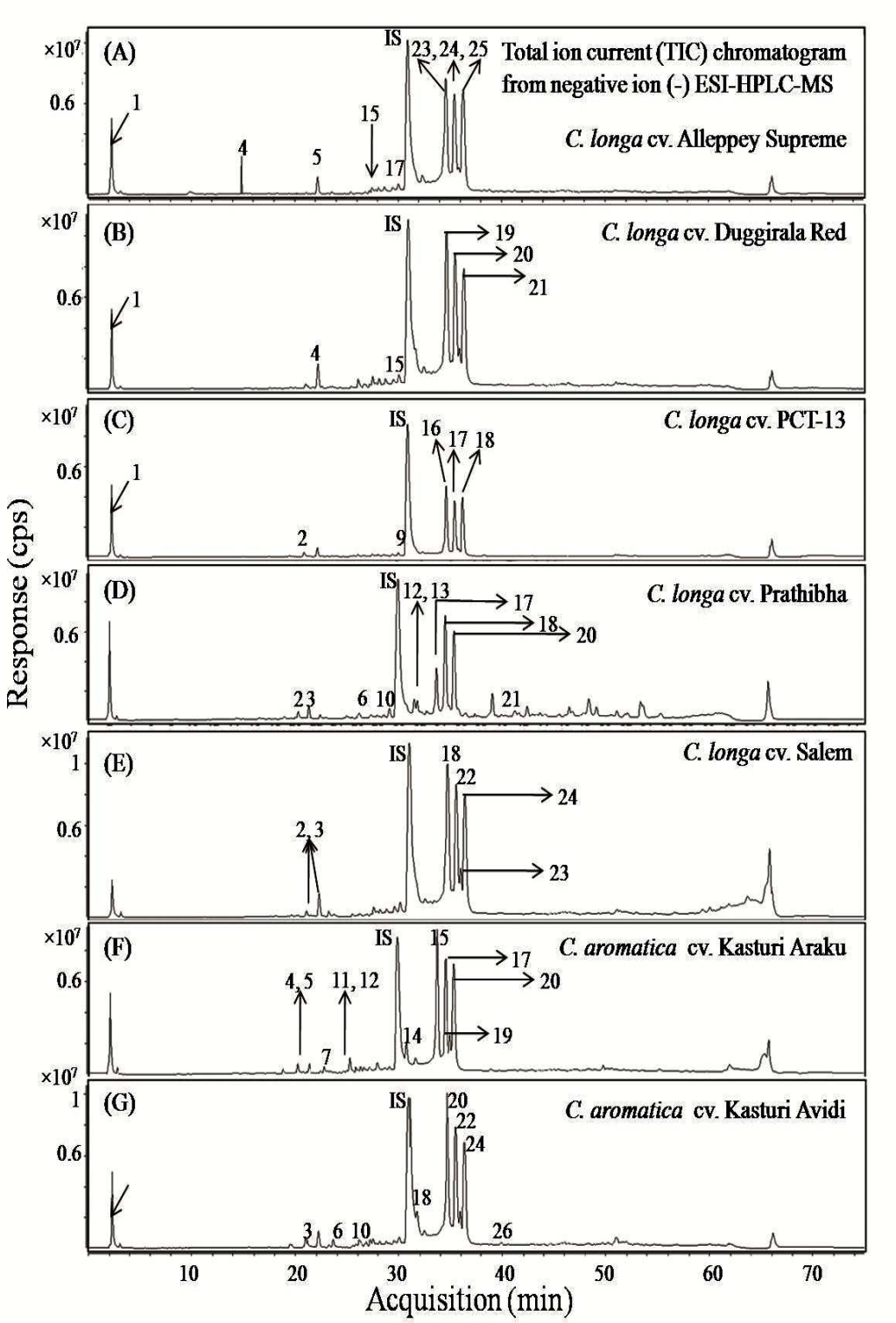

Figure. 6.2. Representative TIC chromatograms from negative ion (-) ESI-HPLC of *C. longa* cvs. (A) Alleppey Supreme, (B) Duggirala Red, (C) PCT-13, (D) Prathibha, (E) Salem and *C. aromatica* cvs (F) Kasturi Araku and (G) Kasturi Avidi. Names and details of the compounds to corresponding peak numbers are given in Tables 6.1 to 6.7.

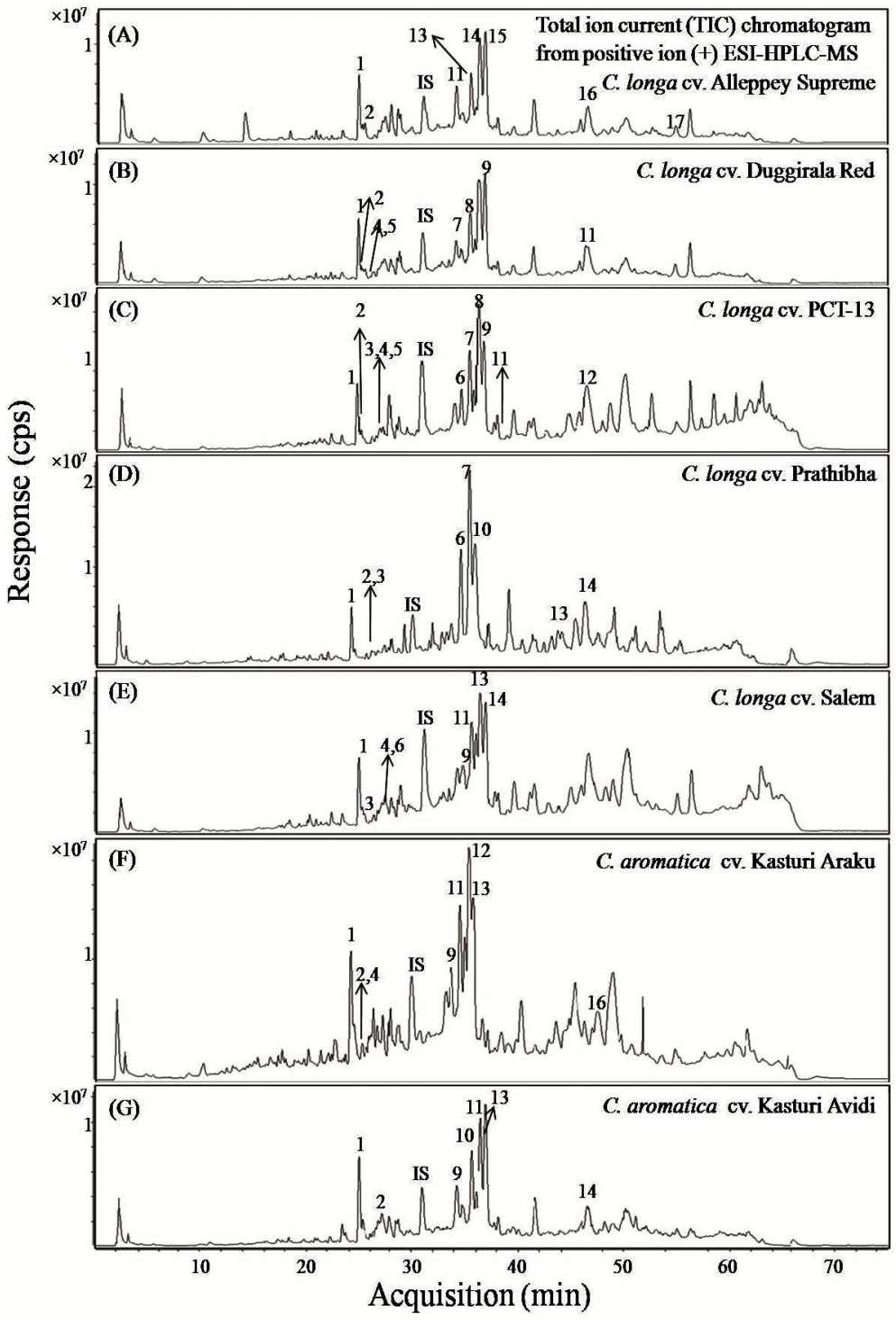

Figure. 6.3. Representative TIC chromatograms from positive ion (+) ESI-HPLC of *C. longa* cvs. (A) Alleppey Supreme, (B) Duggirala Red, (C) PCT-13, (D) Prathibha, (E) Salem and *C. aromatica* cvs. (F) Kasturi Araku and (G) Kasturi Avidi. Names and details of the compounds to corresponding peak numbers are given in Tables 6.8 to 6.14.

Table 6.1. List of compounds identified from TIC (-) ESI-LC-MS/MS of the methanolic extracts of *C. longa* cv. Alleppey Supreme. S.No. of the compounds are incompliance with peak numbers given in Fig. 6.2. A.

S.No.	RT (min)	Compound	Formula	Mass	Abund	Compound type	Mass fragment ions	Ref
1	2.2	5,7,8-trihydr oxy-2′,5′-dimeth oxy-3′,4′-methylene dioxy isoflavanone	$C_{18}H_{18}O_9$	378.1	51978	Flavonoid	101;102;113;119;161;163;	Ogundare A. O. and Olajuyigbe A.O. 2012
2	2.49	1,7-diphenyl-1,6-heptadiene-3,5-dione	$C_{19}H_{16}O_2$	276.0	9697	Diarylheptanoid	115	Sundaryono et al., 2003
3	10.76	Kaempferol-3-rhamnoside	$C_{21}H_{20}O_{10}$	432.1	5367	Flavonoid	125;142;146;150;176;184;190;293;304;308;311;316;343;345	Ruslay et al., 2007
4	12.77	Kaempferol 3,7-O-dimethyl ether	$C_{17}H_{14}O_6$	314.0	25537	Flavonoid	108;123;152;153;167	Milenanikolova, 2006
5	22.16	4-(*p*-hydroxy phenyl)-3-buten-2-one	$C_{10}H_{10}O_2$	162.0	18641	Aromatic	117;118	NIST CAS 3160-35-8
6	23.11	5-hydroxy-7-(4-hydroxyphenyl)-l-phenyl-(1E)-l-heptene	$C_{20}H_{24}O_4$	328.1	6169	Diarylheptanoid	107;119;133;134;135;136;159;161;162;177;178	Suksamrarn et al., 1994
7	23.52	1,5-bis (4-hydr oxy-3-methoxy phenyl)-1,4-pentadien-3-one	$C_{19}H_{18}O_5$	326.1	3535	Diarylheptanoid	117;118;119;120;135;145;146;159;161;187	Nugroho et al., 2009
8	25.4	Tetrahydroxybisd emethoxy curcumin	$C_{19}H_{20}O_4$	312.1	4773	Diarylheptanoid	117;118;119;120;146;161	Jiang et al., 2006
9	25.8	1-(4-hydroxy-3-methoxyphenyl)-7-(4-hydroxy-3,5-dimethoxy pheny)-4,6-heptadiene-3-one	$C_{22}H_{24}O_6$	384.1	6408	Diarylheptanoid	133;134;147;148;150;151;158;165;175;176;186;187;188;189;203;204;232	Jiang et al., 2006
10	25.9	Tetrahydrodemeth oxycurcumin	$C_{20}H_{22}O_5$	342.1	7734	Diarylheptanoid	101;113;119;120;134;146;161;162;176	Jiang et al., 2006
11	26.1	1-(4-hydroxy phenyl)-7-(4-hydroxy-3-meth oxy phenyl) 1,4,6-heptatrien-3-one	$C_{20}H_{18}O_4$	322.1	76458	Diarylheptanoid	143;155;171;183;199;211;227;231;247;275	Ma and Gang , 2006
12	26.5	Tetrahydroxy curcumin	$C_{21}H_{24}O_6$	372.1	81260	Diarylheptanoid	133;134;135;148;149;175	Jiang et al., 2006
13	26.8	1,7-bis(4-hydr oxy -3 methoxy phenyl) -1,4,6-heptatrien-3-one	$C_{21}H_{20}O_5$	352.1	97353	Diarylheptanoid	101;102;113;136;143;148;164;195;207;223;224;235;245;251;261;262;263;279	Jiang et al., 2006
14	26.84	1-(4-hydroxy-3-methoxy phenyl)-7-(4-hydroxy-3,5-	$C_{22}H_{22}O_6$	382.1	58571	Diarylheptanoid	149;159;173;197;209;211;221;233;237;239	Jiang et al., 2006

		dimethoxy phenyl)-1,4,6-heptatrien-3-one					;249;261;267;277;289;293;295;305;309	
15	27.4	1,7-bis(4-hydr oxy phenyl)-1-heptene-,35-dione	$C_{19}H_{18}O_4$	310.1	8495	Diarylheptanoid	117;118;119;145;146;161;175;176	Jiang et al., 2006
16	29.47	Tetradecanoic acid/myristic acid	$C_{14}H_{28}O_2$	228.0	2381	Fatty acid	128;130;143;155;158;182;183;184;210	NIST CAS 544-63-8
17	30.0	1,7-bis-(4-hydr oxyphenyl)-1,4,6-hepta trien-3-one	$C_{19}H_{16}O_3$	292.1	7240	Diarylheptanoid	115;117;119;120;143;145	Li et al., 2011
IS	30.8	4-fluoro-4'-hydroxybenzo phenone	$C_{13}H_9FO_2$	216.0	2299505	Carbonyl compound	120;121;133;159;161;169;185	Hiserodt et al., 1996
18	31.6	1,6-heptadiene-3,5-dione, 1-(3,4-dihydroxy phenyl)-7-(4-hydroxy phenyl)-	$C_{19}H_{16}O_5$	324.1	5753	Diarylheptanoid	134;135;136;143	Jiang et al., 2006
19	32.3	1-(3,4-dihydr oxy phenyl)-7-(4-hydroxy-3-meth oxy phenyl)hepta-1,6-diene-3,5-dione	$C_{20}H_{18}O_6$	354.1	16375	Diarylheptanoid	195;205;206;207;208;209;222;223;234;235;249;250;251;252;263;27;295;307;323	Jiang et al., 2006
20	34.36	Coumaran	C_8H_8O	120.0	6563	Coumarin	116;117;118;119	Chromadex
21	34.4	3-acetyl coumarin	$C_{11}H_8O_3$	188.0	6483	Coumarin	115;116;117;118;141;143	NIST CAS 3949-36-8
22	34.57	Dihydroxy-4-methylcoumarin,5,7-	$C_{10}H_8O$	144.0	92188	Coumarin	113;115;116;117;118;141	Chromadex
23	34.77	Bisdemthoxy curcumin	$C_{19}H_{16}O_4$	308.1	1675644	Diarylheptanoid	117;118;119;120;143;145	Jiang et al. 2006
24	34.95	Demethoxy curcumin	$C_{20}H_{18}O_5$	338.1	1302410	Diarylheptanoid	117;118;119;120;132;133;134;135;145;146;159;160;161;175;201	Jiang et al., 2006
25	35.0	Curcumin	$C_{21}H_{20}O_6$	368.1	1503497	Diarylheptanoid	132;133;134;135;149;158;160;161;175;176	Jiang et al., 2006
26	35.3	Tumerone	$C_{15}H_{22}O$	218.0	6120	Bisabolane sesquiterpene	101;103;117;129;130;131;132;133;134;145;157;146;157;158;173;201	Xian-Guo He, 2000
27	35.8	Dihydro curcumin	$C_{21}H_{22}O_6$	370.1	5151	Diarylheptanoid	132;133;134;135;148;160;161;176;191	Jiang et al., 2006
28	35.99	7-(3,4-dihydr oxy phenyl~5-hydr oxy-l-phenyl -(lE)-lheptene	$C_{19}H_{22}O_3$	298.1	18085	Diarylheptanoid	119;183;184	Suksamrarn et al., 1994
29	36.2	Curlone	$C_{15}H_{22}O$	218.0	19540	Bisabolane sesquiterpene	101;103;117;129;130;131;132;133;134;145;157;146;157;158;173	Xian-Guo He, 2000
30	42.2	Luteolin-7-O-glucoside	$C_{21}H_{20}O_{11}$	448.2	5324	Flavonoid	110;185;279;280	Mass bank ACCESSION: TY000145;

								Rahmatullah et al., 2012
31	43.2	1-heptene-3,5-dione, 1,7-bis(4-hydroxy-3-methoxyphenyl)-	$C_{20}H_{20}O_5$	340.1	5078	Diarylheptanoid	109;143;153;155;171;181;183;187;199;211;219;227;231;233;247;249;251;259;275	Jiang et al., 2006

Table 6.2. List of compounds identified from TIC (-) ESI-LC-MS/MS of the methanolic extracts of *C. longa* cv. Duggirala Red. S.No. of the compounds are incompliance with peak numbers given in Fig. 6.2. B.

S.No.	RT (min)	Compound	Formula	Mass	Abund	Compound type	Mass fragment ions	Ref
1	2.2	5,7,8-trihydr oxy-2′,5′-di methoxy-3′,4′-methylene dioxy isoflavanone	$C_{18}H_{18}O_9$	378.0	14603	Diarylheptanoid	101;113;119;131;149	Ogundare A. O. and Olajuyigbe A.O. 2012
2	10.76	Kaempferol-3-rhamnoside	$C_{21}H_{20}O_{10}$	432.1	5367	Flavonoid	125;142;146;150;176;184;190;293;304;308;311;316;343;345	Ruslay et al., 2007
3	20.98	1-hepten-3-one,5-hydroxy-1,7-bis(3,4-dihydroxy phenyl)-	$C_{19}H_{20}O_6$	344.1	2154	Diarylheptanoid	107;134;135;136;159;161;162;177;178	Jiang et al., 2006
4	22.2	4-(*p*-hydroxy phenyl)-3-buten-2-one	$C_{10}H_{10}O_2$	162.0	26843	Aromatic	117;118	NIST CAS 3160-35-8
5	23.2	5-hydroxy-7-(4-hydroxyphenyl)-l-phenyl-(1E)-l-heptene	$C_{20}H_{24}O_4$	328.1	24437	Diarylheptanoid	112;117;119;131;135;145;159;161;177;178	Jiang et al., 2006
6	23.5	1,5-bis (4-hydr oxy-3-methoxy phenyl)-1,4-pentadien-3-one	$C_{19}H_{20}O_5$	326.1	24437	Diarylheptanoid	107;117;118;119;120;133;134;135;159;161;162;177;178	Nugroho et al., 2009
7	25.4	Tetrahydroxybisdemethoxycurcumin	$C_{19}H_{20}O_4$	312.1	10678	Diarylheptanoid	117;118;119;120;146;161	Jiang et al., 2006
8	25.9	1-(4-hydroxy-3-methoxyphenyl)-7-(4-hydroxy-3,5-dimethoxy pheny)-4,6-heptadiene-3-one	$C_{22}H_{24}O_6$	384.1	2385	Diarylheptanoid	120;131;147;148;158;159;161;162;175;176;177;186;187;188;203;204;205;219;231	Jiang et al., 2006
9	25.97	Tetrahydrodemethoxycurcumin	$C_{20}H_{22}O_5$	342.1	5546	Diarylheptanoid	101;102;113;114;119	Jiang et al., 2006
10	26.1	1-(4-hydroxy phenyl)-7-(4-hydroxy-3-methoxyphenyl)1,4,6-heptatrien-3-one	$C_{20}H_{18}O_4$	322.0	4782	Diarylheptanoid	112;143;155;171;183;199;227;231;257;277	Jiang et al., 2006
11	26.3	1,4,6-heptatrien-3-one, 1,7-bis(4-hydroxy-3-	$C_{21}H_{20}O_5$	352.0	2528	Diarylheptanoid	101;115;119;133;136;142;143;148;164;207	Jiang et al., 2006

		methoxyphenyl)-					;223;224;235;245;251;261	
12	26.6	1-hydroxy-1-(3,4-dihydroxy phenyl)-7-(4-hydroxy-3-methoxyphenyl)-6-hepten-3,5-dione	$C_{20}H_{20}O_7$	372.1	1986	Diarylheptanoid	134;148;149;175;176;177;191	Jiang et al., 2006
13	26.8	1-(4-hydroxy-3-methoxy phenyl)-7-(4-hydroxy-3,5-dimethoxy phenyl) -1,4,6-heptatrien-3-one	$C_{22}H_{22}O_6$	382.1	2251	Diarylheptanoid	159;239;249;262;267;277;289;293;295;305	Jiang et al., 2006
14	27.8	1-heptene-3,5-dione, 1,7-bis(4-hydroxyphenyl)-	$C_{19}H_{18}O_4$	310.1	35801	Diarylheptanoid	117;119;120;143;145	Jiang et al., 2006
15	30.1	1,7-bis-(4-hydr oxyphenyl)-1,4,6-hepta trien-3-one	$C_{19}H_{16}O_3$	292.1	72404	Diarylheptanoid	115;117;119;120;143;145	Li et al., 2011
IS	30.8	4-fluoro-4'- hydr oxybenzo phenone	$C_{13}H_9FO_2$	216.0	2167273	Carbonyl compound	120;121;133;159;161;169	Hiserodt et al., 1996
16	31.6	1,6-heptadiene-3,5-dione, 1-(3,4-dihydroxy phenyl)-7-(4-hydroxy phenyl)-	$C_{19}H_{16}O_5$	324.1	10673	Diarylheptanoid	117;133;135;143;147;161;171;189	Jiang et al., 2006
17	32.4	1-(3,4-dihydr oxy phenyl)-7-(4-hydr oxy-3-meth oxy phenyl)hepta-1,6-diene-3,5-dione	$C_{20}H_{18}O_6$	354.1	3580	Diarylheptanoid	134;135;136;158	Jiang et al., 2006
18	34.5	Coumaran	C_8H_8O	120.0	98347	Coumarin	116;117;118	Chromadex
19	34.6	Bisdemthoxy curcumin	$C_{19}H_{16}O_4$	308.1	2135571	Diarylheptanoid	117;119;120	Jiang et al., 2006
20	34.95	Demethoxy curcumin	$C_{20}H_{18}O_5$	338.1	2099661	Diarylheptanoid	117;118;119;120;132;133;134;135;145;146;159;160;161;175;201	Jiang et al. 2006
21	36.2	Curcumin	$C_{21}H_{20}O_6$	368.1	1986244	Diarylheptanoid	132;133;134;158;160;161;175;176	Jiang et al., 2006
22	36.25	Dihydro curcumin	$C_{12}H_{22}O_6$	370.1	467158	Diarylheptanoid	101;106;109;112;113;119;132;133;147;165;166;171;191;263;279	Jiang et al., 2006
23	43.3	1-heptene-3,5-dione, 1,7-bis(4-hydroxy-3-methoxyphenyl)-	$C_{20}H_{20}O_5$	340.2	4928	Diarylheptanoid	143;155;171;181;183;187;199;211	Park and Kim, 2002

In *C. longa* cv. PCT-13, a total of 91 compounds were detected, from which 25 are known and 66 are unknown. Of the known compounds, 20 of them were detected in (-) ESI-LC-MS (Table 6.3) and 12 in (+) ESI-LC-MS (Table 6.10) of which seven were commonly detected in both the ion modes. Out of the 20 known compounds

detected from the negative ion mode, 15 were diarylheptanoids, four of them are coumarin type and one of phenolic acid. In case of positive ion mode, out of 12 known compounds, 7 of them are diarylheptanoids, those were detected in both the ion modes, remaining 5 belong to terpenoid group. Out of 66 unknown metabolites, area/abundance was generated only for only 37 metabolites (data not shown).

Table 6.3. List of compounds identified from TIC (-) ESI-LC-MS/MS of the methanolic extracts of *C. longa* cv. PCT-13. S.No. of the compounds are incompliance with peak numbers given in Fig. 6.2. C.

S.No.	RT (min)	Compound	Formula	Mass	Abund	Compound type	Mass fragment ions	Ref
1	2.2	1,7-bis(3,4,5-tri methoxyphenyl)-l,6-heptadiene-3,5-dione	$C_{25}H_{28}O_8$	456.1	28481	Diarylheptanoid	112	Anand et al., 2007
2	20.6	1-hepten-3-one ,5-hydroxy-1,7-bis (3,4-dihydr oxy phenyl)-	$C_{19}H_{20}O_6$	344.1	5086	Diarylheptanoid	107;121;133;134;135;159;161;162;177;178	Sati et al., 2011
3	23.5	1,5-bis (4-hydr oxy-3-methoxy phenyl)-1,4-pentadien-3-one	$C_{19}H_{18}O_5$	326.1	30486	Diarylheptanoid	117;118;119;120;135;145;146;159;161;187	Jiang et al., 2006
4	25.4	Tetrahydroxybisd emethoxy curcumin	$C_{19}H_{20}O_4$	312.1	6553	Diarylheptanoid	117;118;119;120;146;161	Jiang et al., 2006
5	26.0	1,5-bis(3,4-methylenedi oxy-phenyl) -1,4-pentadien-3-one	$C_{19}H_{14}O_5$	322.0	9161	Diarylheptanoid	115;119;121;133;143;235;237;247;263;275	Jiang et al., 2006
6	26.2	1,7-bis(4-hydr oxy-3 methoxy phenyl) -1,4,6-heptatrien-3-one	$C_{21}H_{20}O_5$	352.0	8654	Diarylheptanoid	115;143;207;223;235;251;261;263;279;291	Jiang et al., 2006
7	27.7	1,7-bis(4-hydr oxy phenyl)-1-heptene -,35-dione	$C_{19}H_{18}O_4$	310.1	22730	Diarylheptanoid	117;118;119;145;146;161	Jiang et al., 2006
8	29.9	1,7-bis-(4-hydr oxyphenyl)-1,4,6-hepta trien-3-one	$C_{19}H_{16}O_3$	292.1	7240	Diarylheptanoid	115;117;119;120;143;145	Li et al., 2011
IS	30.8	4-fluoro-4'- hydr oxybenzo phenone	$C_{13}H_9FO_2$	216.0	2090004	Carbonyl compound	120;121;133;159;161;169	Hiserodt et al., 1996
9	31.6	1,6-heptadiene-3,5-dione, 1-(3,4-dihydroxy phenyl)-7-(4-hydroxyphenyl)-	$C_{19}H_{16}O_5$	324.0	1062	Diarylheptanoid	119;134;135;136;143	Jiang et al., 2006
10	32.4	1-(3,4-dihydr oxy phenyl)-7-(4-hydroxy-3-methoxy phenyl)hepta-1,6-diene-3,5-dione	$C_{20}H_{18}O_6$	354.1	20689	Diarylheptanoid	134;135;136;158	Jiang et al., 2006
11	34.4	Methyl-7-	$C_{11}H_{10}O_3$	190.0	67927	Coumarin	115;116;117;1	Chromadex

		methoxy coumarin,4-					19;120	
12	34.5	Dihydroxy-4-,5,7 methyl coumarin	$C_{10}H_8O$	144.0	40413	Coumarin	112;114;115;116;117;118	Chromadex
13	34.6	Coumaran	C_8H_8O	120.0	318300	Coumarin	116;117;118;119	Chromadex
14	34.65	3-acetyl coumarin,	$C_{11}H_8O_3$	188.0	289624	Coumarin	114;115;116;117;118;141;143	NIST CAS 3949-36-8
15	34.85	Bisdemthoxy curcumin	$C_{19}H_{16}O_4$	308.1	2254674	Diarylheptanoid	117;119;143;145	Jiang et al., 2006
16	35.3	Demethoxy curcumin	$C_{20}H_{18}O_5$	338.1	2099661	Diarylheptanoid	117;118;119;120;132;133;134;135;145;146;159;160;161;175;201	Jiang et al. 2006
17	35.8	Curcumin	$C_{21}H_{20}O_6$	368.1	1948573	Diarylheptanoid	132;134;135;149;158;160;161;175	Jiang et al., 2006
18	36.0	Dihydro curcumin	$C_{21}H_{22}O_6$	370.1	1046	Diarylheptanoid	134;135;149;158;160	Jiang et al., 2006
19	36.2	Hydrocinnamic acid	$C_9H_{10}O_2$	150.0	3812	Phenolic acids	103;105;133	Ma and Gang, 2006
20	43.8	1-heptene-3,5-dione, 1,7-bis(4-hydroxy-3-methoxyphenyl)-	$C_{20}H_{20}O_5$	340.2	3696	Diarylheptanoid	101;113;137;163;167;179	Park and Kim, 2002

C. longa cv. Prathibha yielded a total of 62 metabolites, of which 30 are known and 32 are unknown. Out of 29 known metabolites, 22 were identified in (-) ESI-LC-MS (Table 6.4) and 14 in (+) ESI-LC-MS mode (Table 6.11) of which seven metabolites stand in common between the two modes. Out of the 23 known compounds in the negative ion mode, 20 were diarylheptanoids and one each from the class of coumarin, flavonoid and phenolic acid. Whereas in positive ion mode, out of 14 known compounds, 10 of the metabolites belong to diarylheptanoids, of which 7 were commonly detected in two ion modes and other 3 are cultivar specific diarylheptanoids and eluted only in positive mode of ionization. Remaining 4 belong to bisabolane type of compounds. Out of 32 unknown metabolites, area/abundance was generated for only 20 metabolites (data not shown).

Table 6.4. List of compounds identified from TIC (-) ESI-LC-MS/MS of the methanolic extracts of *C. longa* cv. Prathibha. S.No. of the compounds are incompliance with peak numbers given in Fig. 6.2. D.

S.No.	RT (min)	Compound	Formula	Mass	Abund	Compound type	Mass fragment ions	Ref
1	2.3	Tetrahydrodemethoxycurcumin	$C_{20}H_{22}O_5$	342.1	1574	Diarylheptanoid	101;113;119	Jiang et al., 2006
2	20.8	1-(4-hydroxy phenyl)-7-(4-hydroxy-3-met hoxy phenyl)1,4,6-heptatrien-3-one	$C_{20}H_{18}O_4$	322.0	3781	Diarylheptanoid	143;155;171;183;199;211;227;231;249;275	Jiang et al., 2006
3	21.2	1-hepten-3-one, 5-hydroxy-1,7-bis(3,4-di hydr oxy phenyl)-	$C_{19}H_{20}O_6$	344.1	1660	Diarylheptanoid	107;121;134;135;136;159;161;162;177;178	Sati et al., 2011
4	23.1	5-hydroxy-7-(4-hydroxyphenyl)-l-phenyl-(1E)-l-heptene	$C_{20}H_{24}O_4$	328.1	1988	Diarylheptanoid	134;135;136;177;178	Suksamrarn et al. 1994
5	25.2	4-hepten-3-one, 5-hydroxy-1,7-bis(4-hydroxy phenyl)-	$C_{19}H_{20}O_4$	312.1	1418	Diarylheptanoid	118;119;120;146;161	Jiang et al., 2006
6	26.1	1,4,6-heptatrien-3-one, 1,7-bis(4-hydroxy-3-methoxyphenyl)-	$C_{21}H_{20}O_5$	352.0	1187	Diarylheptanoid	119;143;207;223;235;251;261;263;279;291	Jiang et al., 2006
7	26.6	1-(4-hydroxy-3-methoxy phenyl)-7-(4-hydroxy-3,5-dimethoxy phenyl)-1,4,6-heptatrien-3-one	$C_{22}H_{22}O_6$	382.1	10734	Diarylheptanoid	159;239;249;261;265;267;277;289;293.	Jiang et al., 2006
8	26.8	5,7-dihydroxy-2-(4-hydroxy phenyl)chroman-4-one	$C_{15}H_{12}O_5$	272.0	12833	Phenolic acids	107;119;120	Chromadex
9	28.2	1-heptene-3,5-dione, 1,7-bis(4-hydroxyphenyl)-	$C_{19}H_{18}O_4$	310.1	17465	Diarylheptanoid	117;133;135;145;159;161;173;187;201	Jiang et al., 2006
10	28.7	1-heptene-3,5-dione, 1,7-bis(4-hydroxy-3-methoxyphenyl)-	$C_{20}H_{20}O_5$	340.0	43412	Diarylheptanoid	117;19;134;135;145;159;160	Park and Kim, 2002
11	30.4	1,7-bis-(4-hydroxyphenyl)-1,4, 6-heptatrien-3-one	$C_{19}H_{16}O_3$	292.1	18203	Diarylheptanoid	115;117;118;119;120;143;145	Li et al., 2011
IS	30.5	4-fluoro-4'- hydroxybenzo phenone	$C_{13}H_9FO_2$	216.0	1429244	Carbonyl compound	120;121;133;159;161;169;185;187	Hiserodt et al., 1996
12	31.49	1,6-heptadiene-3,5-dione, 1-(3,4-dihydroxy phenyl)-7-(4-hydroxy phenyl)-	$C_{19}H_{16}O_5$	324.0	13066	Diarylheptanoid	119;134;135;136;143	Jiang et al., 2006
13	31.9	1-(3,4-dihydroxy phenyl)-7-(4-hydroxy-3-methoxy phenyl)hepta-1,6-diene-3,5-dione	$C_{20}H_{18}O_6$	354.1	38899	Diarylheptanoid	119;143;150;151	Jiang et al., 2006

14	32.0	1-(4-hydroxy-3-methoxyphenyl)-7-(4-hydroxy-3,5-dimethoxy pheny)-4,6-heptadiene-3-one	$C_{22}H_{24}O_6$	384.1	194388	Diarylheptanoid	150;151;158;165	Jiang et al., 2006
15	33.2	Kaempferol-3-O-rutinoside-7-O-glucoside	$C_{33}H_{40}O_{20}$	756.2	3752	Flavonoid	135;161;175;176;191;193;439;579	Gall et al., 2003
16	34.41	3-acetyl coumarin	$C_{11}H_8O_3$	188.0	3974	Coumarin	115;116;117;118	NIST CAS 3949-36-8
17	34.48	Bisdemthoxy curcumin	$C_{19}H_{16}O_4$	308.1	35774	Diarylheptanoid	117;119;120;143	Jiang et al., 2006
18	34.7	Demethoxy curcumin	$C_{20}H_{18}O_5$	338.1	125020	Diarylheptanoid	117;119; 132;134;143;145;160;161; 175	Jiang et al., 2006
19	35.82	1,7-bis(3,4,5-trimethoxyphenyl) -l,6-hepta diene-3,5-dione	$C_{25}H_{28}O_8$	456.3	4972	Diarylheptanoid	280;281;298;299	Anand et al., 2007
20	35.9	Curcumin	$C_{21}H_{20}O_6$	368.1	56390	Diarylheptanoid	119;132;133;134;135;149;158;160	Jiang et al., 2006
21	40.75	1,5-bis (4-hydr oxy-3-methoxy phenyl)-1,4-pentadien-3-one	$C_{19}H_{18}O_5$	326.1	3870	Diarylheptanoid	119;183;184	Jiang et al., 2006
22	54.4	1,7-bis(3,4-dimeth oxy phenyl)-4,4-dimethyl-1,6-heptadiene-3,5-dione	$C_{25}H_{28}O_6$	447.2	9854	Diarylheptanoid	286;298;316;317	Liang et al., 2009

In *C. longa* cv. Salem, a total of 95 metabolites were detected, of which 32 are known and 63 are unknown. Out of 32 known metabolites, 28 of them were identified in (-) ESI-LC-MS (Table 6.5) and 14 in (+) ESI-LC-MS mode (Table 6.12), 10 of the compounds detected commonly in both modes of ionization. Out of 28 known metabolites in the negative ion mode, 20 of them belong to diarylheptanoid class of compound, three of each from the class of coumarin and fatty acid group of compounds and one from flavonoid class. In case of positive ion mode, out of 14 compounds detected, 12 belong to diarylheptanoids, of which 10 are commonly detected in two modes and the remaining two are cultivar specific and eluted only in positive mode of ionization, and these compounds belongs to bisabolane type of sesquiterpene. Out of 63 unknown compounds, area/abundance was generated for only 33 metabolites (data not shown).

Table 6.5. List of compounds identified from TIC (-) ESI-LC-MS/MS of the methanolic extracts of *C. longa* cv. Salem. S.No. of the compounds are incompliance with peak numbers given in Fig. 6.2. E.

S.No.	RT (min)	Compound	Formula	Mass	Abund	Compound type	Mass fragment ions	Ref
1	2.4	1,7-diphenyl-1,6-heptadiene-3,5-dione	$C_{19}H_{16}O_2$	276.0	1172	Diarylheptanoid	115	Sundaryono et al., 2003
2	21.0	1-hepten-3-one ,5-hydroxy-1,7-bis(3,4-dihy droxyphenyl)-	$C_{19}H_{20}O_6$	344.1	8072	Diarylheptanoid	107;121;134 ;135;159;16 1;162;177;1 78	Sati et al., 2011
3	21.9	4-(*p*-hydroxy phenyl)-3-buten-2-one	$C_{10}H_{10}O_2$	162.0	8994	Aromatic	117;118	NIST CAS 3160-35-8
4	23.2	5-hydroxy-7-(4-hydroxyphenyl) -l-phenyl-(1E)-l-heptene	$C_{20}H_{24}O_4$	328.1	11215	Diarylheptanoid	107;133;134 ;135;136;15 9;161;162;1 77;178	Suksamrarn et al., 1994
5	23.64	1,5-bis (4-hydr oxy-3-methoxy phenyl)-1,4-pentadien-3-one	$C_{19}H_{18}O_5$	326.1	2910	Diarylheptanoid	117;118;119 ;120;135;14 3;145;146;1 59;161;187	Nugroho et al., 2009
6	25.5	Tetrahydroxybi sdemethoxy curcumin	$C_{19}H_{20}O_4$	312.1	3037	Diarylheptanoid	117;118;119 ;146;161	Jiang et al., 2006
7	25.9	1-(4-hydroxy-3-methoxyphenyl)-7-(4-hydroxy-3,5-dimethoxy pheny)-4,6-heptadiene-3-one	$C_{22}H_{24}O_6$	384.1	1350	Diarylheptanoid	120;147;148 ;158;159;16 0;161;162;1 75;176'177; 186;188;189 ;203;204;20 5;219;232	Jiang et al., 2006
8	26.1	Tetrahydrodem ethoxycurcumi n	$C_{20}H_{22}O_5$	342.1	2213	Diarylheptanoid	117;118;119 ;120;134;14 96;148;149; 161;162;175 ;176;177	Jiang et al., 2006
9	26.2	1-(4-hydrox yphenyl)-7-(4-hydroxy-3-meth oxyphenyl)1,4, 6-heptatrien-3-one	$C_{20}H_{18}O_4$	322.0	24574	Diarylheptanoid	115;117;119 ;121;132;13 3;134;143;1 45;174;235; 237;247;263 ;274;275;29 2	Jiang et al., 2006
10	26.7	Tetrahydroxy curcumin	$C_{21}H_{24}O_6$	372.1	4463	Diarylheptanoid	134;148;149 ;175;176;17 7	Jiang et al., 2006
11	26.74	1,7-bis(4-hydr oxy-3 methoxy phenyl) -1,4,6-heptatrien-3-one	$C_{21}H_{20}O_5$	352.1	2246	Diarylheptanoid	119;143;148 ;164;193;19 5;205;207;2 17;223;224; 233;235;245 ;251;261;26 3;279;291;3 07	Jiang et al., 2006
12	26.9	1-(4-hydroxy-	$C_{22}H_{22}O_6$	382.1	3675	Diarylheptanoid	193;195;197	Jiang et al.,

		3-methoxy phenyl)-7-(4-hydroxy-3,5-dimethoxy phenyl)-1,4,6-heptatrien-3-one					;211;223;233;237;239;249;261;265;267;277;289;293;305;309;323	2006
13	27.8	1,7-bis(4-hydroxyphenyl)-1-heptene-,35-dione	$C_{19}H_{18}O_4$	310.1	4682	Diarylheptanoid	117;118;119;145;146;161	Jiang et al., 2006
14	30.74	1,7-bis-(4-hydroxyphenyl)-1,4,6-heptatrien-3-one	$C_{19}H_{16}O_3$	292.1	40301	Diarylheptanoid	115;117;119;120;130;143;145	Li et al., 2011
IS	30.82	4-fluoro-4'-hydr oxybenzophenone	$C_{13}H_9FO_2$	216.0	2380820	Carbonyl compound	120;121;133;159;161;169;185;187	Hiserodt et al., 1996
15	31.7	1,6-heptadiene-3,5-dione, 1-(3,4-dihydroxyphenyl)-7-(4-hydroxyphenyl)-	$C_{19}H_{16}O_5$	324.1	279335	Diarylheptanoid	119;134;135;143	Jiang et al., 2006
16	32.7	1-(3,4-dihydroxyphenyl)-7-(4-hydroxy-3-methoxyphenyl)hepta-1,6-diene-3,5-dione	$C_{20}H_{18}O_6$	354.1	504288	Diarylheptanoid	134;135;158	Jiang et al., 2006
17	33.5	Kaempferol-3-O-rutinoside-7-O-glucoside	$C_{33}H_{40}O_{20}$	756.0	778726	Flavonoid	134;135;149;161;175;176;177;179;180;191;193;387;424;439;563;579;580;755	Gall et al., 2003
18	34.2	Bisdemthoxy curcumin	$C_{19}H_{16}O_4$	308.1	1523101	Diarylheptanoid	117;118;119;120;143;145	Jiang et al., 2006
19	34.7	Dihydroxy-4-,5,7- methyl coumarin	$C_{10}H_8O$	144.0	145005	Coumarin	113;114;115;116;117;118;141	Chromadex
20	34.77	Coumaran	C_8H_8O	120.0	117485	Coumarin	116;117;118;119	Chromadex
21	34.9	3-acetyl coumarin	$C_{11}H_8O_3$	188.0	96079	Coumarin	114;115;116;117;118;141;145	NIST CAS 3949-36-8
22	35.35	Demethoxy curcumin	$C_{20}H_{18}O_5$	338.1	1374564	Diarylheptanoid	117;119;120;132;134;143;145;158;160	Jiang et al., 2006
23	35.98	Dihydro curcumin	$C_{21}H_{22}O_6$	370.1	95402	Diarylheptanoid	134;135;149	Jiang et al., 2006
24	36.2	Curcumin	$C_{21}H_{20}O_6$	368.1	1339840	Diarylheptanoid	132;134;135;149;158;160;161;175	Jiang et al., 2006
25	43.3	1-heptene-3,5-dione, 1,7-bis(4-hydroxy-3-methoxyphenyl)-	$C_{20}H_{20}O_5$	340.1	15686	Diarylheptanoid	109;159;181;183;191;199;211;223;227;233;235;247;249;251;253;259;26	Park and Kim, 2002

							3;275;279	
26	59.5	Palmitic acid	$C_{16}H_{32}O_2$	256.2	16809	Fatty acid	120;166	Jiang et al., 1989
27	60.2	Oleic acid	$C_{18}H_{34}O_2$	282.1	15974	Fatty acid	168;257	Ma and Gang, 2006
28	63.8	Stearic acid	$C_{18}H_{36}O_2$	284.1	76620	Fatty acid	197;199;200	Ma and Gang, 2006

In *C. aromatica* cv. Kasturi Araku, 90 metabolites were detected, from which 27 are known and 63 yet to be identified. Out of known metabolites, 21 were identified in (-) ESI-LC-MS (Table 6.6) and 16 in (+) ESI-LC-MS (Table 6.13) mode with commonly identified 10 metabolites in both the modes of ionization. Out of the 21 known metabolites detected from the negative ion mode, 19 were identified to be diarylheptanoids, two from coumarin and one from fatty acid class of compounds. Whereas in case of positive ion mode, out of 16 known metabolites, 12 are diarylheptanoids, of which 10 are common between both the modes of ionization. Out of 63 unknown metabolites, area/abundance was generated for only 43 metabolites (data not shown).

Table 6.6. List of compounds identified from TIC (-) ESI-LC-MS/MS of the methanolic extracts of *C. aromatica* cv. Kasturi Araku. S.No. of the compounds are incompliance with peak numbers given in Fig. 6.2. F.

S.No.	RT (min)	Compound	Formula	Mass	Abund	Compound type	Mass fragment ions	Ref
1	11.1	1,2,3,4-tetra phenylbutane-2,3-diol	$C_{28}H_{26}O_2$	394.1	3926	Aliphatic diol	112;129;133;180;207;243;247;263;339	Pubchem Compound ID: 344369
2	16.7	1,7-bis(3,4,5-tri methoxyphenyl)-l,6-heptadiene-3,5-dione	$C_{25}H_{28}O_8$	456.1	2489	Diarylheptanoid	112;254;297	Anand et al., 2007
3	16.8	Hydroferulic acid	$C_{10}H_{12}O_4$	196.1	13992	Phenolic acid	109;121;122	Ma and Gang, 2006.
4	20.6	1-hepten-3-one,5-hydroxy-1,7-bis(3,4-dihydroxy phenyl)-	$C_{19}H_{20}O_6$	344.1	57005	Diarylheptanoid	107;121;134;135;159;161;162;177;178	Jiang et al., 2006
5	21.2	1-(4-hydroxy phenyl)-7-(4-hydroxy-3-meth oxyphenyl)1,4,6-heptatrien-3-one	$C_{20}H_{18}O_4$	322.0	48992	Diarylheptanoid	181;183;231;233;245;247;249;251;257;275	Jiang et al., 2006
6	22.37	5-hydroxy-7-(4-hydroxyphenyl)-l-phenyl-(1E)-l-heptene	$C_{20}H_{24}O_4$	328.1	5645	Diarylheptanoid	107;133;134;135;137;159;161;162;177;178	Suksamrarn et al., 1994
7	22.74	1,5-bis (4-hydr oxy-3-methoxy	$C_{19}H_{18}O_5$	326.2	14933	Diarylheptanoid	104;112;121;135;137;151;17	Nugroho et al., 2009

		phenyl)-1,4-pentadien-3-one					3;185;201;274	
8	22.8	1,7-bis(4-hydroxy phenyl)-3,5-heptanediol	$C_{19}H_{24}O_4$	316.1	8120	Diarylheptanoid	105;106;107;119;121;147;148	Ma and Gang 2006
9	24.6	Tetrahydroxybisdemethoxycurcumin	$C_{19}H_{20}O_4$	312.1	4537	Diarylheptanoid	117;118;119;120;121;146;161	Jiang et al., 2006
10	25.1	1-(4-hydroxy-3-methoxyphenyl)-7-(4-hydroxy-3,5-dimethoxypheny)-4,6-heptadiene-3-one	$C_{22}H_{24}O_6$	384.1	4498	Diarylheptanoid	159;162;175;176;186;187;188;203;204;232	Jiang et al., 2006
11	25.18	Tetrahydrodemethoxycurcumin	$C_{20}H_{22}O_5$	342.1	78838	Diarylheptanoid	117;118;119;120;134;1496;148;149;161;162;175;176;177	Jiang et al., 2006
12	25.7	1,7-bis(4-hydroxy-3 methoxy phenyl) -1,4,6-heptatrien-3-one	$C_{21}H_{20}O_5$	352.0	36253	Diarylheptanoid	119;207;223;233;235;251;261;263;279;291	Jiang et al., 2006
13	25.8	1-hydroxy-1-(4-hydroxy-phenyl)-7-(4-hydroxy-3-methoxyphenyl)-6-Hepten-3,5-dione	$C_{20}H_{20}O_7$	372.1	6172	Diarylheptanoid	134;148;149;175;176;177	Jiang et al., 2006
IS	30.82	4-fluoro-4'- hydroxybenzophenone	$C_{13}H_9FO_2$	216.0	2068465	Carbonyl compound	120;121;133;159;161;169;185;187	Hiserodt et al., 1996
14	31.5	1-(3,4-dihydroxyphenyl)-7-(4-hydroxy-3-methoxy phenyl)hepta-1,6-diene-3,5-dione	$C_{20}H_{18}O_6$	354.1	95085	Diarylheptanoid	134;135;136;158	Jiang et al., 2006
15	33.6	Bisdemthoxy curcumin	$C_{19}H_{16}O_4$	308.1	1143027	Diarylheptanoid	117;119;120;143;145	Jiang et al., 2006
16	33.7	Coumaran	C_8H_8O	120.0	78245	Coumarin	108;116;117;118;119	Chromadex
17	34.9	Demethoxy curcumin	$C_{20}H_{18}O_5$	338.1	478250	Diarylheptanoid	117;119;120;132;134;143;145;158;160	Jiang et al., 2006
18	35.1	Hydrocinnamic acid	$C_9H_{10}O_2$	150.0	41594	Phenolic acid	105;106;132	Ma and Gang, 2006.
19	35.4	Dihydro curcumin	$C_{21}H_{22}O_6$	370.1	597824	Diarylheptanoid	101;106;165;364	Jiang et al., 2006
20	35.8	Curcumin	$C_{21}H_{20}O_6$	368.1	335879	Diarylheptanoid	119;132;133;134;135;149;158;160;161;175	Jiang et al., 2006
21	43.4	1-heptene-3,5-dione, 1,7-bis(4-hydroxy-3-methoxyphenyl)-	$C_{20}H_{20}O_5$	340.1	37175	Diarylheptanoid	109;153;183;225;231;233;247;251;253;275	Park and Kim, 2002

In case of *C. aromatica* cv. Kasturi Avidi, a total of 91 metabolites were detected, of which 31 of them are known and 60 of them are unknown. Out of 31 known metabolites, 28 identified in (-) ESI-LC-MS (Table 6.7) and 14 in (+) ESI-LC-MS (Table 6.14) mode ionisation. Out of the 28 known metabolites in the negative ion

mode, 23 were identified to be diarylheptanoids and one each from the class of coumarin, fatty acid, flavonoid, aromatic and diterpenoid. The diterpenoid identified in this mode of analysis is found to cultivar specific. Whereas in case of positive ion mode, out of 14 known metabolites, 11 are diarylheptanoids, which are commonly detected in both the ion modes and the remaining three are bisabolane type of sesquiterpene compounds. Out of 60 unknown metabolites, area/abundance was generated for only 36 metabolites (data not shown).

Table 6.7. List of compounds identified from TIC (-) ESI-LC-MS/MS of the methanolic extracts of *C. aromatica* cv. Kasturi Avidi. S.No. of the compounds are incompliance with peak numbers given in Fig. 6.2. G.

S.No.	RT (min)	Compound	Formula	Mass	Abund	Compound type	Mass fragment ions	Ref
1	2.2	5,7,8-trihydroxy-2′,5′-dimethoxy-3′,4′-methylene dioxyiso flavanone	$C_{18}H_{18}O_9$	378.0	6399	Flavonoid	101;11;113;119;131;149	Ogundare A. O. and Olajuyigbe A.O. 2012
2	17.7	1,7-bis(3,4,5-trimeth oxyphenyl)-l,6-heptadiene-3,5-dione	$C_{25}H_{28}O_8$	456.1	4402	Diarylheptanoid	112;254	Anand et al., 2007
3	20.9	1-hepten-3-one,5-hydroxy-1,7-bis(3,4-dihydroxy phenyl)-	$C_{19}H_{20}O_6$	344.1	10183	Diarylheptanoid	107;134;135;159;161;162;177;178	Jiang et al., 2006
4	22.1	4-(*p*-hydroxy phenyl)-3-buten-2-one	$C_{10}H_{10}O_2$	162.0	21520	Aromatic	117;118	NIST CAS 3160-35-8
5	23.1	5-hydroxy-7-(4-hydroxyphenyl)-l-phenyl-(1E)-l-heptene	$C_{20}H_{24}O_4$	328.1	5208	Diarylheptanoid	107;133;134;135;136;159;161;162;177;178	Suksamrarn et al., 1994
6	23.5	1,5-bis (4-hydroxy-3-methoxyphenyl)-1,4-pentadien-3-one	$C_{19}H_{18}O_5$	326.1	6801	Diarylheptanoid	164;207;209;211;219;221;225;233;237;249;251;253;255;261;265;277;279;283;297	Nugroho et al., 2009
7	25.47	Tetrahydroxybisdemethoxycurcumin	$C_{19}H_{20}O_4$	312.1	8867	Diarylheptanoid	117;118;119;120;146;161	Jiang et al., 2006
8	25.9	Tetrahydrodemethoxy curcumin	$C_{20}H_{22}O_5$	342.1	6789	Diarylheptanoid	101;113;119	Jiang et al., 2006
9	25.94	1-(4-hydroxy-3-methoxyphenyl)-7-(4-hydroxy-3,5-dimethoxypheny)-4,6-heptadiene-3-one	$C_{22}H_{24}O_6$	384.1	8721	Diarylheptanoid	120;131;147;148;158;159;161;162;175;176;177;186;187;188;203;204;205;219;231	Jiang et al., 2006
10	26.18	1,5-bis(3,4-methylene dioxy-phenyl)-1,4-pentadien-3-one	$C_{19}H_{14}O_5$	322.1	33721	Diarylheptanoid	115;127;143;153;155;171;181;183;187;211;219;227;231;233;247;249;257;275;303	Ma and Gang , 2006
11	26.6	1-hydroxy-1-(3,4-dihydroxyphenyl)-7-(4-hydroxy-3-	$C_{20}H_{20}O_7$	372.1	95208	Diarylheptanoid	134;148;149;175;176;177;191	Jiang et al., 2006

		methoxyphenyl)-6-hepten-3,5-dione						
12	26.8	1,7-bis(4-hydroxy-3 methoxy phenyl) -1,4,6-heptatrien-3-one	$C_{21}H_{20}O_5$	352.0	7763	Diarylheptanoid	115;119;143;161;173;195;207;223;233;235;245;249;251;261;263;279;289;291;307	Jiang et al., 2006
13	26.9	1-(4-hydroxy-3-methoxy phenyl)-7-(4-hydroxy-3,5-dimethoxy phenyl)-1,4,6-heptatrien-3-one	$C_{22}H_{22}O_6$	382.1	5619	Diarylheptanoid	159;161;197;209;211;221;223;233;237;239;249;261;265;267;277;289;293;305;309	Jiang et al., 2006
14	34.46	1-heptene-3,5-dione, 1,7-bis(4-hydroxy phenyl)-	$C_{19}H_{18}O_4$	310.1	9921	Diarylheptanoid	117;119;120;143;145	Jiang et al., 2006
15	28.8	1-(4-hydroxy-3-methoxyphenyl)-5-(4-hydroxyphenyl)-1,4-pentadiene-3-one	$C_{18}H_{16}O_4$	296.1	8009	Diarylheptanoid	105;109;117;119;133;145;159;161;171;173;181;185;1207;209;223;233;239;251;279	Park and Kim, 2002
16	30.6	1,7-bis-(4-hydroxy phenyl)-1,4,6-heptatrien-3-one	$C_{19}H_{16}O_3$	292.1	76801	Diarylheptanoid	115;117;119;120;130;143;145	Li et al., 2011
IS	30.82	4-fluoro-4'- hydr oxybenzo phenone	$C_{13}H_9FO_2$	216.0	1375655	Carbonyl compound	120;121;133;159;161;169;185;187	Hiserodt et al., 1996
17	31.6	1,6-heptadiene-3,5-dione, 1-(3,4-dihydr oxyphenyl)-7-(4-hydroxyphenyl)-	$C_{19}H_{16}O_5$	324.0	249981	Diarylheptanoid	119;133;134;135;136;143	Jiang et al., 2006
18	32.4	1-(3,4-dihydroxy phenyl)-7-(4-hydroxy-3-methoxyphenyl) hepta-1,6-diene-3,5-dione	$C_{20}H_{18}O_6$	354.1	226327	Diarylheptanoid	134;135;158	Jiang et al., 2006
19	34.4	3-acetylcoumarin	$C_{11}H_8O_3$	188.0	82134	Coumarin	115;116;117;118;141;143	NIST CAS 3949-36-8
20	34.66	Bisdemthoxy curcumin	$C_{19}H_{16}O_4$	308.1	2354236	Diarylheptanoid	117;119;143;145	Jiang et al., 2006
21	34.7	Dihydroxy-4-5,7-methylcoumarin	$C_{10}H_8O$	144.0	6327	Coumarin	113;114;115;116;117;118;141	Chromadex
22	35.3	Demethoxy curcumin	$C_{20}H_{18}O_5$	338.1	698543	Diarylheptanoid	117;119;132;134;143;145;158;160;175	Jiang et al., 2006
23	35.87	Dihydrocurcumin	$C_{12}H_{22}O_6$	370.1	178100	Diarylheptanoid	134;135;149;160	Jiang et al., 2006
24	36.1	Curcumin	$C_{21}H_{20}O_6$	368.1	532433	Diarylheptanoid	132;134;149;158;160;161;175	Jiang et al., 2006
25	36.59	7-(3,4-dihydroxy phenyl~5-hydroxy-l-phenyl-(lE)-lheptene	$C_{19}H_{22}O_3$	298.1	16570	Diarylheptanoid	119;183;184	Suksamrarn et al., 1994
26	39.8	(-)-(12E,2S,3S,4R, 5R,6R, 9S,11S, 15R)-3,15-dibenzoyloxy-5,6-epox-ylathyr-12-en-14-one.	$C_{34}H_{38}O_6$	542.2	5683	Diterpenoid	119;145;183;211;212;237	Tian et al., 2011
27	43.6	1-heptene-3,5-dione, 1,7-bis(4-hydroxy-3-	$C_{20}H_{20}O_5$	340.1	23802	Diarylheptanoid	109;143;153;155;171;181;18	Jiang et al., 2006

		methoxyphenyl)-					3;187;199;211;219;227;231;233;247;249;251;259;275	
28	59.9	Oleic acid	$C_{18}H_{34}O_2$	282.2	7260	Fatty acid	120	Ma and Gang, 2006

Table 6.8. List of compounds identified from TIC (+) ESI-LC-MS/MS of the methanolic extracts of *C. longa* cv. Alleppey Supreme. S.No. of the compounds are incompliance with peak numbers given in Fig. 6.3. A.

S.No.	RT (min)	Compound	Formula	Mass	Abund	Compound type	Mass fragment ions	Ref
1	24.75	*ar*-turmerone	$C_{15}H_{20}O$	216.1	23545	Bisabolane sesquiterpene	103;104;105;106;107;108;115;116;117;118;119;120	Parthasarathy et al., 2008
2	25.36	turmeronol	$C_{15}H_{20}O_2$	232.1	87260	Bisabolane sesquiterpene	103;104;105;106;107;108;115;116;117;118;119;120	Ma and Gang 2006
3	26.02	1-(4-hydroxy-3-methoxyphenyl)-7-(4-hydroxy-3,5-dimethoxypheny)-4,6-heptadiene-3-one	$C_{22}H_{24}O_6$	384.1	90241	Diarylheptanoid	122;137;138	Jiang et al., 2006
4	26.2	1-(4-hydroxy phenyl)-7-(4-hydroxy-3-methoxyphenyl)1,4,6-heptatrien-3-one	$C_{20}H_{18}O_4$	322.0	8202	Diarylheptanoid	105;107;115;119;123;133;137;143;147;161	Jiang et al., 2006
5	26.4	1,7-bis(4-hydroxy-3 methoxy phenyl) -1,4,6-heptatrien-3-one	$C_{21}H_{20}O_5$	352.1	64172	Diarylheptanoid	107;119;121;135;143;147;153;163;171;337	Jiang et al., 2006
6	26.7	1-hydroxy-1-(3,4-dihydroxy phenyl) -7-(4-hydroxy-3-methoxyphenyl)-6-hepten-3,5-dione	$C_{20}H_{20}O_7$	372.1	45589	Diarylheptanoid	103;117;131;137;143;145;149;163;177	Jiang et al., 2006
7	26.9	1-(4-hydroxy-3-methoxy phenyl)-7-(4-hydroxy-3,5-dimethoxy phenyl)-1,4,6-heptatrien-3-one	$C_{22}H_{22}O_6$	382.1	46821	Diarylheptanoid	121;131;135;137;145;149;153;163;177;293	Jiang et al., 2006
8	27.2	Chavicol	$C_9H_{10}O$	134.0	55821	Terpenoid	102;115;116	Nagori et al., 2011
9	30.8	1,7-bis-(4-hydroxyphenyl)-1,4,6-heptatrien-3-one	$C_{19}H_{16}O_3$	292.1	72819	Diarylheptanoid	107;108;119;127;131	Li et al., 2011
IS	30.91	4-fluoro-4'-hydroxyl benzophenone	$C_{13}H_9FO_2$	216.0	141713	Carbonyl compound	120;121;133;159;161;169;185	Hiserodt et al., 1996
10	31.8	7-(4-hydroxy-3-methoxyphenyl)-1-(4-hydroxy phenyl)-4,6-heptadien-3-one	$C_{20}H_{20}O_4$	324.1	138675	Diarylheptanoid	107;117;119;120;122;123;131;135;137;145;146;147;148;163;195;223	Jiang et al., 2006
11	34.58	Bisdemthoxy curcumin	$C_{19}H_{16}O_4$	308.1	155456	Diarylheptanoid	107;119;120;131;147;148	Jiang et al., 2006

12	35.97	Dihydrocurcumin	$C_{12}H_{22}O_6$	370.1	24689	Diarylheptanoid	117;118;137;145; 146;149;177	Jiang et al., 2006
13	36.05	Demethoxy curcumin	$C_{20}H_{18}O_5$	338.1	418489	Diarylheptanoid	107;117;131;137; 145;147;149;177; 195;223	Jiang et al., 2006
14	36.08	Curcumin	$C_{21}H_{20}O_6$	368.1	1717345	Diarylheptanoid	117;118;145;146; 161;177	Jiang et al., 2006
15	36.67	Curcumenol	$C_{15}H_{22}O_2$	234.1	34556	Sesquiterpene	105;107;109;117; 123;125;133;137	Sirat and Meng, 2009
16	46.56	Curlone	$C_{15}H_{22}O$	218.1	71727	Bisabolane sesquiterpene	103;104;105;115; 117;118;119	Kiso et al., 1983
17	54.96	25-benzylpenta cyclo (22.3.1.0.) octacosa-1(27),3 (8),4,6,10(15),11, 13,17(22), 18,20, 24(28), 25-do decaen	$C_{35}H_{30}$	450.2	42646	Cyclic diarylheptanoid	105;107;119;121; 122	Ishida et al., 2002

Table 6.9. List of compounds identified from TIC (+) ESI-LC-MS/MS of the methanolic extracts of *C. longa* cv. Duggirala Red. S.No. of the compounds are incompliance with peak numbers given in Fig. 6.3. B.

S.No.	RT (min)	Compound	Formula	Mass	Abund	Compound type	Mass fragment ions	Ref
1	24.7	*ar*-turmerone	$C_{15}H_{20}O$	216.1	137130	Bisabolane sesquiterpene	103;104;105;106;107;108;115;116;117;118;119;120	Parthasarathy et al., 2008
2	25.36	turmeronol	$C_{15}H_{20}O_2$	232.1	56616	Bisabolane sesquiterpene	103;104;105;106;107;108;115;116;117;118;119;120	Ma and Gang 2006
3	25.9	1-(4-hydroxy-3-methoxyphenyl)-7-(4-hydroxy-3,5-dimethoxy pheny)-4,6-heptadiene-3-one	$C_{22}H_{24}O_6$	384.1	39234	Diarylheptanoid	120;131;147;148;158;159;161;162;175;176;177;186;187;188;203;204;205;219;231;232	Jiang et al., 2006
4	26.1	1-(4-hydroxy phenyl)-7-(4-hydroxy-3-methoxyphenyl)1,4,6-heptatrien-3-one	$C_{20}H_{18}O_4$	322.0	30567	Diarylheptanoid	105;107;115;119;123;133;137;143;147;161	Jiang et al., 2006
5	26.3	1,4,6-heptatrien-3-one, 1,7-bis(4-hydroxy-3-methoxyphenyl)-	$C_{21}H_{20}O_5$	352.0	31409	Diarylheptanoid	101;115;119;133;136;142;143;148;164;207;223;224;235;245;251;261;262;263;279	Jiang et al., 2006
6	26.8	1-(4-hydroxy-3-methoxy phenyl)-7-(4-hydroxy-3,5-dimethoxy phenyl)-1,4,6-heptatrien-3-one	$C_{22}H_{22}O_6$	382.1	46361	Diarylheptanoid	159;239;249;262;267;277;289;293;295;305	Jiang et al., 2006

IS	30.92	4-fluoro-4'-hydroxyl ben zophenone	$C_{13}H_9FO_2$	216.0	136296	Carbonyl compound	121;123; 124	Hiserodt et al., 1996
7	34.9	Bisdemthoxy curcumin	$C_{19}H_{16}O_4$	308.1	389061	Diarylheptanoid	117;119;120;143	Jiang et al., 2006
8	35.88	Demethoxy curcumin	$C_{20}H_{18}O_5$	338.1	497315	Diarylheptanoid	109;121;131;133;147;159;199;235;245;263	Jiang et al., 2006
9	36.15	Dihydro curcumin	$C_{12}H_{22}O_6$	370.1	37712	Diarylheptanoid	101;106;109;112;113;119;132;133;147;165;166;171;191	Jiang et al., 2006
10	36.44	Curcumin	$C_{21}H_{20}O_6$	368.1	1846401	Diarylheptanoid	132;133;134;158;160;161;175;176	Jiang et al., 2006
11	39.5	Curlone	$C_{15}H_{22}O$	218.1	26180	Bisabolane sesquiterpene	103;104;105;115;117;118;119	Kiso et al., 1983

Table 6.10. List of compounds identified from TIC (+) ESI-LC-MS/MS of the methanolic extracts of *C. longa* cv. PCT-13. S.No. of the compounds are incompliance with peak numbers given in Fig. 6.3. C.

S.No.	RT (min)	Compound	Formula	Mass	Abund	Compound type	Mass fragment ions	Ref
1	24.7	*ar*-turmerone	$C_{15}H_{20}O$	216.1	90754	Bisabolane sesquiterpene	103;104;105;106;107;108;115;116;117;118;119;120	Parthasarathy et al., 2008
2	24.93	turmeronol	$C_{15}H_{20}O_2$	232.1	116146	Bisabolane sesquiterpene	103;104;105;106;107;108;115;116;117;118;119;120	Ma and Gang 2006
3	26.0	1,5-bis(3,4-methylenedioxy-phenyl) -1,4-pentadien-3-one	$C_{19}H_{14}O_5$	322.0	5429	Diarylheptanoid	115;119;121;133;143;235;237;247;263;275	Jiang et al., 2006
4	26.5	1,7-bis(4-hydroxy-3 methoxy phenyl) -1,4,6-heptatrien-3-one	$C_{21}H_{20}O_5$	352.0	3891	Diarylheptanoid	115;143;207;223;235;251;261;263;279;291	Jiang et al., 2006
5	26.7	1-(4-hydroxy-3-methoxy phenyl)-7-(4-hydroxy-3,5-dimethoxy phenyl) -1,4,6-heptatrien-3-one	$C_{22}H_{22}O_6$	382.1	4487	Diarylheptanoid	159;239;249;262;267;277;289;293;295;305	Jiang et al., 2006
IS	30.92	4-fluoro-4'-hydroxyl benzophenone	$C_{13}H_9FO_2$	216.0	1275866	Carbonyl compound	121;123; 124	Hiserodt et al., 1996

6	34.85	Bisdemthoxy curcumin	$C_{19}H_{16}O_4$	308.1	122858	Diarylheptanoid	117;119;143;145	Jiang et al., 2006
7	35.7	Demethoxy curcumin	$C_{20}H_{18}O_5$	338.1	2213061	Diarylheptanoid	117;119;120;134;143;158	Jiang et al., 2006
8	35.9	Dihydro curcumin	$C_{21}H_{22}O_6$	370.1	488376	Diarylheptanoid	134;135;149;158;160	Jiang et al., 2006
9	36.3	Curcumin	$C_{21}H_{20}O_6$	368.1	1557089	Diarylheptanoid	132;133;134;158;160;161;175;176	Jiang et al., 2006
10	36.67	Curcumenol	$C_{15}H_{22}O_2$	234.1	213076	Sesquiterpene	105;107;109;117;123;125;133;137	Sirat and Meng, 2009
11	38.83	Chavicol	$C_9H_{10}O$	134.0	154274	Terpenoid	102;115;116	Nagori et al., 2011
12	46.50	Curlone	$C_{15}H_{22}O$	218.1	56995	Bisabolane sesquiterpene	103;104;105;115;117;118;119	Kiso et al., 1983

Table 6.11. List of compounds identified from TIC (+) ESI-LC-MS/MS of the methanolic extracts of *C. longa* cv. Prathibha. S.No. of the compounds are incompliance with peak numbers given in Fig. 6.3. D.

S.No.	RT (min)	Compound	Formula	Mass	Abund	Compound type	Mass fragment ions	Ref
1	24.6	*ar*-turmerone	$C_{15}H_{20}O$	216.1	182568	Bisabolane sesquiterpene	103;104;105;106;107;108;115;116;117;118;119;120	Parthasarathy et al., 2008
2	26.1	1,4,6-heptatrien-3-one, 1,7-bis(4-hydroxy-3-methoxyphenyl)-	$C_{21}H_{20}O_5$	352.0	71415	Diarylheptanoid	121;135;143;147;153;163;171	Jiang et al., 2006
3	26.6	1-(4-hydroxy-3-methoxy phenyl)-7-(4-hydroxy-3,5-dimethoxy phenyl)-1,4,6-heptatrien-3-one	$C_{18}H_{22}O_9$	382.1	34806	Diarylheptanoid	121;131;135;145;149;153;159;163;177	Jiang et al., 2006
4	26.9	1-(4-hydroxy-3-methoxyphenyl)-7-(4-hydroxy-3,5-dimethoxypheny)-4,6-heptadiene-3-one	$C_{18}H_{24}O_9$	384.1	133233	Diarylheptanoid	117;133;137;145;149;161;177	Jiang et al., 2006
IS	30.92	4-fluoro-4'- hydr oxyl benzo phenone	$C_{13}H_9FO_2$	216.0	175308	Carbonyl compound	121;123; 124	Hiserodt et al., 1996
5	32.9	1, 7-bis(4-hydr oxy-3, 5-dimeth oxy phenyl)- 1, 6-heptadiene-3, 5-dione	$C_{23}H_{24}O_8$	428.2	186331	Diarylheptanoid	109;123;137;159;191;209	Nurfina, 1997
6	34.6	Bisdemethoxy curcumin	$C_{19}H_{16}O_4$	308.1	957426	Diarylheptanoid	119;120;131;147;148	Jiang et al., 2006
7	35.29	Demethoxy	$C_{20}H_{18}O_5$	338.1	2385114	Diarylheptanoid	117;119;131;13	Jiang et al.,

		curcumin					7;145;147;149;177	2006
8	35.56	5'-methoxy curcumin	$C_{22}H_{22}O_7$	398.1	388655	Diarylheptanoid	117;119;129;137;145;149;161;175;207	Ravindran and Nirmal Babu, 2007
9	35.8	Dihydro curcumin	$C_{21}H_{22}O_6$	370.1	631797	Diarylheptanoid	117;118;122;137;145;146;149;161;177	Jiang et al., 2006
10	36.0	Curcumin	$C_{21}H_{20}O_6$	368.1	1110571	Diarylheptanoid	117;118;145;146;149;152	Jiang et al., 2006
11	38.3	1,7-bis(3,4-dimethoxy phenyl)-1,6-heptadiene-3,5-dione	$C_{23}H_{24}O_6$	396.2	335360	Diarylheptanoid	105;107;119;129;137;145;155;195	Chen et al., 2006
12	40.2	(6S)-2-methyl-6-[(1R,5S)-(4-methene-5-hydroxyl-2-cyclohexen)-2-hepten-4-one	$C_{15}H_{24}O_2$	236.1	229164	Bisabolane	105;106;107;108;109;119;120;121;133;135	Li et al., 2011
13	44.6	4-methylene-5-hydroxybisabola-2,10-diene-9-one	$C_{15}H_{22}O_2$	234.1	321246	Sesquiterpene	105;107;115;117;119;121;122;129;135	Sirat and Meng, 2009
14	46.50	Curlone	$C_{15}H_{22}O$	218.1	279391	Bisabolane sesquiterpene	103;104;105;115;117;118;119	Kiso et al., 1983

Table 6.12. List of compounds identified from TIC (+) ESI-LC-MS/MS of the methanolic extracts of *C. longa* cv. Salem. S.No. of the compounds are incompliance with peak numbers given in Fig. 6.3. E.

S.No.	RT (min)	Compound	Formula	Mass	Abund	Compound type	Mass fragment ions	Ref
1	24.6	*ar*-turmerone	$C_{15}H_{20}O$	216.1	46537	Bisabolane sesquiterpene	103;104;105;106;107;108;115;116;117;118;119;120;121;128;129;131;141;142;143	Parthasarathy et al., 2008
2	25.9	1-(4-hydroxy-3-methoxy phenyl)-7-(4-hydroxy-3,5-dimethoxypheny)-4,6-heptadiene -3-one	$C_{22}H_{24}O_6$	384.1	112635	Diarylheptanoid	133;134;147;148;150;151;158;165;175;176;186;187;188;189;203;204;232	Jiang et al., 2006
3	26.1	1-(4-hydroxy phenyl)-7-(4-hydroxy-3-meth oxyphenyl) 1,4,6-heptatrien-3-one	$C_{20}H_{18}O_4$	322.0	81463	Diarylheptanoid	105;107;109;115;119;123;124;127;133;137;143;147;148;151;161;171	Jiang et al., 2006
4	26.4	1,4,6-heptatrien-3-one, 1,7-bis(4-hydroxy-3-methoxyphenyl)-	$C_{21}H_{20}O_5$	352.0	171547	Diarylheptanoid	107;119;121;138;147;149;150;153;163;166;171;177;191;321	Jiang et al., 2006
5	26.6	Tetrahydroxy curcumin	$C_{21}H_{24}O_6$	372.1	82390	Diarylheptanoid	133;134;135;148;149;175	Jiang et al., 2006
6	26.8	1-(4-hydroxy-3-methoxy phenyl)-7-(4-hydroxy-3,5-	$C_{22}H_{22}O_6$	382.1	12383	Diarylheptanoid	149;159;173;197;209;211;221;233;237;239;	Jiang et al., 2006

		dimethoxy phenyl)-1,4,6-heptatrien-3-one					249;261;267;277;289;293;295;305;309	
7	30.8	1,7-bis-(4-hydroxyphenyl)-1,4,6-heptatriene-3-one	$C_{19}H_{16}O_3$	292.1	175817	Diarylheptanoid	107;108;119;127;131	Li et al., 2011
IS	30.92	4-fluoro-4'- hydroxyl benzophenone	$C_{13}H_9FO_2$	216.0	1127771	Carbonyl compound	121;123; 124	Hiserodt et al., 1996
8	32.5	1-(3,4-dihydroxyphenyl)-7-(4-hydroxy-3-methoxy phenyl)hepta-1,6-diene-3,5-dione	$C_{20}H_{18}O_6$	354.1	129110	Diarylheptanoid	119;135;143;150;151	Jiang et al., 2006
9	34.4	Bisdemethoxy curcumin	$C_{19}H_{16}O_4$	308.1	679233	Diarylheptanoid	115;117;118;119;120;143;145	Jiang et al., 2006
10	35.17	1-heptene-3,5-dione, 1,7-bis(4-hydroxy-3-methoxyphenyl)-	$C_{20}H_{20}O_5$	340.1	147750	Diarylheptanoid	109;143;153;155;171;181;183;187;199;211;219;227;231;233;247;249;251;259;275	Jiang et al., 2006
11	35.36	Demethoxy curcumin	$C_{20}H_{18}O_5$	338.1	2068275	Diarylheptanoid	117;119;131;145;147;148;149;177;195;223	Jiang et al., 2006
12	35.8	Dihydro curcumin	$C_{21}H_{22}O_6$	370.1	391518	Diarylheptanoid	117;118;137;145;146;149	Jiang et al., 2006
13	36.15	Curcumin	$C_{21}H_{20}O_6$	368.1	2287763	Diarylheptanoid	117;145;146;149;161;177	Jiang et al., 2006
14	36.84	Curcumenol	$C_{15}H_{22}O_2$	234.1	160898	Sesquiterpene	105;107;109;115;117;125;135;137	Sirat and Meng, 2009

Table 6.13. List of compounds identified from TIC (+) ESI-LC-MS/MS of the methanolic extracts of *C. aromatica* cv. Kasturi Araku. S.No. of the compounds are incompliance with peak numbers given in Fig. 6.3. F.

S.No.	RT (min)	Compound	Formula	Mass	Abund	Compound type	Mass fragment ions	Ref
1	24.2	*ar*-turmerone	$C_{15}H_{20}O$	216.3	176891	Bisabolane sesquiterpene	103;104;105;106;107;108;115;117;119;120;121;127;128;129;130;131;1333;135;141;142;143;145;146;155	Parthasarathy et al., 2008
2	25.1	1-(4-hydroxy-3-methoxyphenyl)-7-(4-hydroxy-3,5-dimethoxypheny)-4,6-heptadiene-3-one	$C_{22}H_{24}O_6$	384.1	266261	Diarylheptanoid	122;137;148	Jiang et al., 2006
3	25.2	1-(4-hydroxyphenyl)-7-(4-hydroxy-3-methoxyphenyl)1,4,6-heptatrien-3-one	$C_{20}H_{18}O_4$	322.1	79037	Diarylheptanoid	105;107;109;115;119;123;124;127;137;143;147;151;161;171	Jiang et al., 2006
4	25.5	1,7-bis(4-hydroxy -	$C_{21}H_{20}O_5$	352.1	100785	Diarylheptanoid	105;107;110;11	Jiang et al.,

		3 methoxy phenyl) -1,4,6-heptatrien-3-one					5;116;119;120;121;122;123;125;127;131;132;133;135;137;138;139;143;144;145	2006
5	25.85	Tetrahydroxy curcumin	$C_{21}H_{24}O_6$	372.1	261180	Diarylheptanoid	Tetrahydroxycurcumin	Jiang et al., 2006
6	26.8	1-(4-hydroxy-3-methoxy phenyl)-7-(4-hydroxy-3,5-dimethoxy phenyl)-1,4,6-heptatrien-3-one	$C_{22}H_{22}O_6$	382.1	116647	Diarylheptanoid	103;107;117;121;125;130;131;132;138;139;145;146;147;153;154;160;161;163;164;166;167	Jiang et al., 2006
7	28.71	1,5-bis (4-hydr oxy-3-methoxy phenyl)-1,4-pentadien-3-one	$C_{19}H_{18}O_5$	326.1	94655	Diarylheptanoid	106;115;117;118;122;123;134;137;143;145;146;149;160;177;188;207	Nugroho et al., 2009
8	30.79	1,6-heptadiene-3,5-dione, 1-(3,4-dihydroxyphenyl)-7-(4-hydroxy phenyl)-	$C_{19}H_{16}O_5$	324.1	10135	Diarylheptanoid	107;117;119;120;123;131;135;137;145;147;148;163;195;223	Jiang et al., 2006
IS	30.92	4-fluoro-4'- hydr oxyl benzo phenone	$C_{13}H_9FO_2$	216.0	314854	Carbonyl compound	121;123; 124	Hiserodt et al., 1996
9	33.4	Bisdemthoxy curcumin	$C_{19}H_{16}O_4$	308.1	1754997	Diarylheptanoid	107;119;120;131;147;148	Jiang et al., 2006
10	34.19	1-heptene-3,5-dione, 1,7-bis(4-hydroxy-3-methoxyphenyl)-	$C_{20}H_{20}O_5$	340.1	580794	Diarylheptanoid	107;108;117;119;122;137;145;146;147;148;149;177	Jiang et al., 2006
11	34.4	Demethoxy curcumin	$C_{20}H_{18}O_5$	338.1	1967687	Diarylheptanoid	107;117;119;120;131;137;145;146;147;148;149;177;195;223	Jiang et al., 2006
12	34.9	Dihydrocurcumin	$C_{21}H_{22}O_6$	370.1	744909	Diarylheptanoid	117;136;137;145;146;149;161;177;225	Jiang et al., 2006
13	35.2	Curcumin	$C_{21}H_{20}O_6$	368.1	1473597	Diarylheptanoid	117;136;137;145;146;149;161;177;225	Jiang et al., 2006
14	35.6	Curcumenol	$C_{15}H_{22}O_2$	234.1	98590	Sesquiterpene	105;107;109;110;117;119;122;123;125;137;138;151	Sirat and Meng, 2009
15	60.6	1, 7-bis(3,5-diethyl-4-hydroxy phenyl)- 1,6-heptadiene-3,5-dione	$C_{27}H_{32}O_4$	420.3	129145	Aromatic	106;107;119;120;121;122;123;144;145;146;147;171;172;175;187;197;201;209;211;213;223;237;239;321;323	Li et al., 2011
16	46.50	Curlone	$C_{15}H_{22}O$	218.1	378163	Bisabolane sesquiterpene	103;104;105;115;117;118;119	Kiso et al., 1983

Table 6.14. List of compounds identified from TIC (+) ESI-LC-MS/MS of the methanolic extracts of *C. aromatica* cv. Kasturi Avidi. S.No. of the compounds are incompliance with peak numbers given in Fig. 6.3. G.

S.No.	RT (min)	Compound	Formula	Mass	Abund	Compound type	Mass fragment ions	Ref
1	24.2	*ar*-turmerone	$C_{15}H_{20}O$	216.3	124838	Bisabolane sesquiterpene	103;104;105;106;107;108;115;117;119;120;121;127;128;129;130;131;1333;135;141;142;143;145;146;155	Parthasarathy et al., 2008
2	26.02	1-(4-hydroxy-3-methoxyphenyl)-7-(4-hydroxy-3,5-dimethoxypheny)-4,6-heptadiene-3-one	$C_{22}H_{24}O_6$	384.1	58526	Diarylheptanoid	122;137;138	Jiang et al., 2006
3	26.2	1-(4-hydroxy phenyl)-7-(4-hydroxy-3-methoxyphenyl)1,4,6-heptatrien-3-one	$C_{20}H_{18}O_4$	322.0	33103	Diarylheptanoid	105;107;115;119;123;133;137;143;147;161	Jiang et al., 2006
4	26.4	1,7-bis(4-hydroxy-3 methoxy phenyl) -1,4,6-heptatrien-3-one	$C_{21}H_{20}O_5$	352.1	36143	Diarylheptanoid	107;119;121;135;143;147;153;163;171;337	Jiang et al., 2006
5	26.7	1-hydroxy-1-(3,4-dihydroxyphenyl)-7-(4-hydroxy-3-methoxyphenyl)-6-hepten-3,5-dione	$C_{20}H_{20}O_7$	372.1	66681	Diarylheptanoid	103;117;131;137;143;145;149;163;177	Jiang et al., 2006
6	26.9	1-(4-hydroxy-3-methoxy phenyl)-7-(4-hydroxy-3,5-dimethoxy phenyl)-1,4,6-heptatrien-3-one	$C_{22}H_{22}O_6$	382.1	49699	Diarylheptanoid	121;131;135;137;145;149;153;163;177;293	Jiang et al., 2006
IS	30.92	4-fluoro-4'- hydroxyl benzo phenone	$C_{13}H_9FO_2$	216.0	122436	Carbonyl compound	121;123; 124	Hiserodt et al., 1996
7	31.0	1,7-bis-(4-hydroxyphenyl)-1,4,6-heptatrien-3-one	$C_{19}H_{16}O_3$	292.1	84005	Diarylheptanoid	107;108;119;127;131	Li et al., 2011
8	31.8	7-(4-hydroxy-3-methoxyphenyl)-1-(4-hydroxy phenyl)-4,6-heptadien-3-one	$C_{20}H_{20}O_4$	324.1	33495	Diarylheptanoid	107;117;119;120;122;123;131;135;137;145;146;147;148;163;195;223	Jiang et al., 2006
9	34.58	Bisdemthoxy curcumin	$C_{19}H_{16}O_4$	308.1	334078	Diarylheptanoid	107;119;120;131;147;148	Jiang et al., 2006
10	35.26	Demethoxy curcumin	$C_{20}H_{18}O_5$	338.1	457087	Diarylheptanoid	107;117;131;137;145;147;149;177;195;223	Jiang et al., 2006
11	35.97	Dihydrocurcumin	$C_{12}H_{22}O_6$	370.1	13901	Diarylheptanoid	117;118;137;145;146;149;177	Jiang et al., 2006
12	36.08	Curcumin	$C_{21}H_{20}O_6$	368.1	1683686	Diarylheptanoid	117;118;145;146;161;177	Jiang et al., 2006
13	37.2	Curcumenol	$C_{15}H_{22}O_2$	234.1	53116	Sesquiterpene	105;107;109;11	Sirat and

							7;123;125;133;137	Meng, 2009
14	46.2	Curlone	$C_{15}H_{22}O$	218.1	36642	Bisabolane sesquiterpene	103;104;105;115;117;118;119	Kiso et al., 1983

Commonly detected diarylheptanoids in all seven cultivars of *Curcuma*

In agreement with Jiang et al., (2006), our results indicated that majority of the diarylheptanoids are detected in negative ion mode. In addition to curcumin, demethoxycurcumin, bisdemethoxycurcumin, other diarylheptanoids like 1-(3,4-dihydroxy phenyl)-7-(4-hydroxy-methoxyphenyl) hepta-1,6-diene-3,5-dione; 1-(4-hydroxyphenyl)-7-(4-hydroxy-3-methoxyphenyl)1,4,6-heptatrien-3-one; 1,7-bis(4-hydroxy-3-methoxyphenyl)-1,4,6-heptatrien-3-one; 1-heptene-3,5-dione and 1,5-bis(4-hydroxy-3-methoxy phenyl)-1,4-pentadien-3-one were detected in rhizomes of all seven cultivars of *Curcuma* (Table 6.15). MS/MS fragmentation spectra and respective structures of these diarylheptanoids are shown in Figs. 6.4. A` to F` and 6.5. G` to L`.

Table 6.15. Common compounds detected by LC-ESI-MS/MS analysis from rhizomes of seven cultivars of *Curcuma*: five of *Curcuma longa* (cvs Alleppey Supreme, Duggirala Red, PCT-13, Prathibha, Salem) and two of *C. aromatica* (cvs. Kasturi Araku, Kasturi Avidi). MS/MS fragmentation spectra and structures of the compounds represented in the table are shown in Figs. 6.4 and 6.5.

SL.	RT (min)	Compound	Formula	m/z $M-H^-$	Compound type	Mass fragment ions	Ref
A	23.5	1,5-bis (4-hydroxy-3-methoxy phenyl)-1,4-pentadien-3-one	$C_{19}H_{18}O_5$	325.1247	Diarylheptanoid	117;118;119;120;135;143;145;146;159;161;187	Li et al., 2011
B	25.4	Tetrahydroxybis demethoxy curcumin	$C_{19}H_{20}O_4$	311.1446	Diarylheptanoid	117;118;119;120;146;161	Jiang et al., 2006
C	25.9	Tetrahydrodemethoxycurcumin	$C_{20}H_{22}O_5$	341.1272	Diarylheptanoid	101;113;119	Ravindran and nirmal babu, 2007
D	26.1	1-(4-hydroxy phenyl)-7-(4-hydroxy-3-methoxyphenyl)1,4,6-heptatrien-3-one	$C_{20}H_{18}O_4$	321.0938	Diarylheptanoid	115;117;119;121;132;133;134;143;148;174;235;237;247;263;264;274;275; 293	Jiang et al., 2006
E	26.3	1,7-bis(4-hydroxy-3methoxy	$C_{21}H_{20}O_5$	351.1123	Diarylheptanoid	108;115;119;136;143;148;16	Jiang et al., 2006

		phenyl)-1,4,6-heptatrien-3-one				4;195;207;223;224;235;245;251;261;262;263;279;291;323	
F	26.5	Tetrahydroxy curcumin	$C_{20}H_{20}O_7$	371.1686	Diarylheptanoid	133;134;135;148;149;175;176;177	Jiang et al., 2006
G	31.5	1-(3,4-dihydroxy phenyl)-7-(4-hydroxy-3-methoxy phenyl)hepta-1,6-diene-3,5-dione	$C_{20}H_{18}O_6$	353.1212	Diarylheptanoid	134; 135; 136; 150	Jiang et al., 2006
H	34.5	Bisdemthoxy curcumin	$C_{19}H_{16}O_4$	307.1132	Diarylheptanoid	117;119;120;143;145	Jiang et al., 2006
I	35.4	Demethoxy curcumin	$C_{20}H_{18}O_5$	337.1251	Diarylheptanoid	117;119;120;132;134;143;145;158; 160;175;201	Jiang et al., 2006
J	35.8	Dihydrocurcumin	$C_{21}H_{22}O_6$	369.1533	Diarylheptanoid	132;134;135;149;158;160;175	Jiang et al., 2006
K	36.2	Curcumin	$C_{21}H_{20}O_6$	367.1374	Diarylheptanoid	132;133;134;135;149;158;160;161;175	Jiang et al., 2006
L	43.2	1-heptene-3,5-dione,1,7-bis(4-hydroxy-3-methoxyphenyl)-	$C_{20}H_{20}O_5$	339.1473	Diarylheptanoid	117;119;120;134;158	Jiang et al., 2006

1,5-bis (4-hydroxy-3-methoxyphenyl)-1,4-pentadien-3-one ($C_{19}H_{18}O_5$) in Table 6.15 and Fig. 6.4. A-A`: It was eluted at RT 23.5 min. Identification of the compound was confirmed by $[M-H]^-$, m/z 325.1247. The mass fragmentation pattern $[M]^-$ of m/z are 187, 161, 159, 146, 145, 143, 135, 120, 119, 118 and 117. This compound was earlier reported by Li et al., (2011).

Tetrahydroxybisdemethoxycurcumin ($C_{19}H_{20}O_4$) Table 6.15 and Fig. 6.4. B-B`: It was eluted at RT 25.4 min. Identification of the compound was confirmed by comparing the chromatographic and mass spectral data from the previous report of turmeric by Jiang et al., (2006). Its $[M-H]^-$, m/z 311.1446 and MS fragmentation pattern $[M]^-$ were of m/z 161, 119 and 118.

Tetrahydrodemethoxycurcumin ($C_{20}H_{22}O_5$) Table 6.15 and Fig. 6.4. C-C`: It was eluted at RT 25.9 min. Identification of the compound was confirmed by its $[M-H]^-$, m/z 341.1567. The mass spectral fragmentation pattern $[M]^-$ were m/z 161, 119 and 118 similar to both afore mentioned diarylheptanoids represented in Fig. 6.4.B and

C. Further, overall fragmentation pattern of the compound is matched with data published by Jiang et al., (2006).

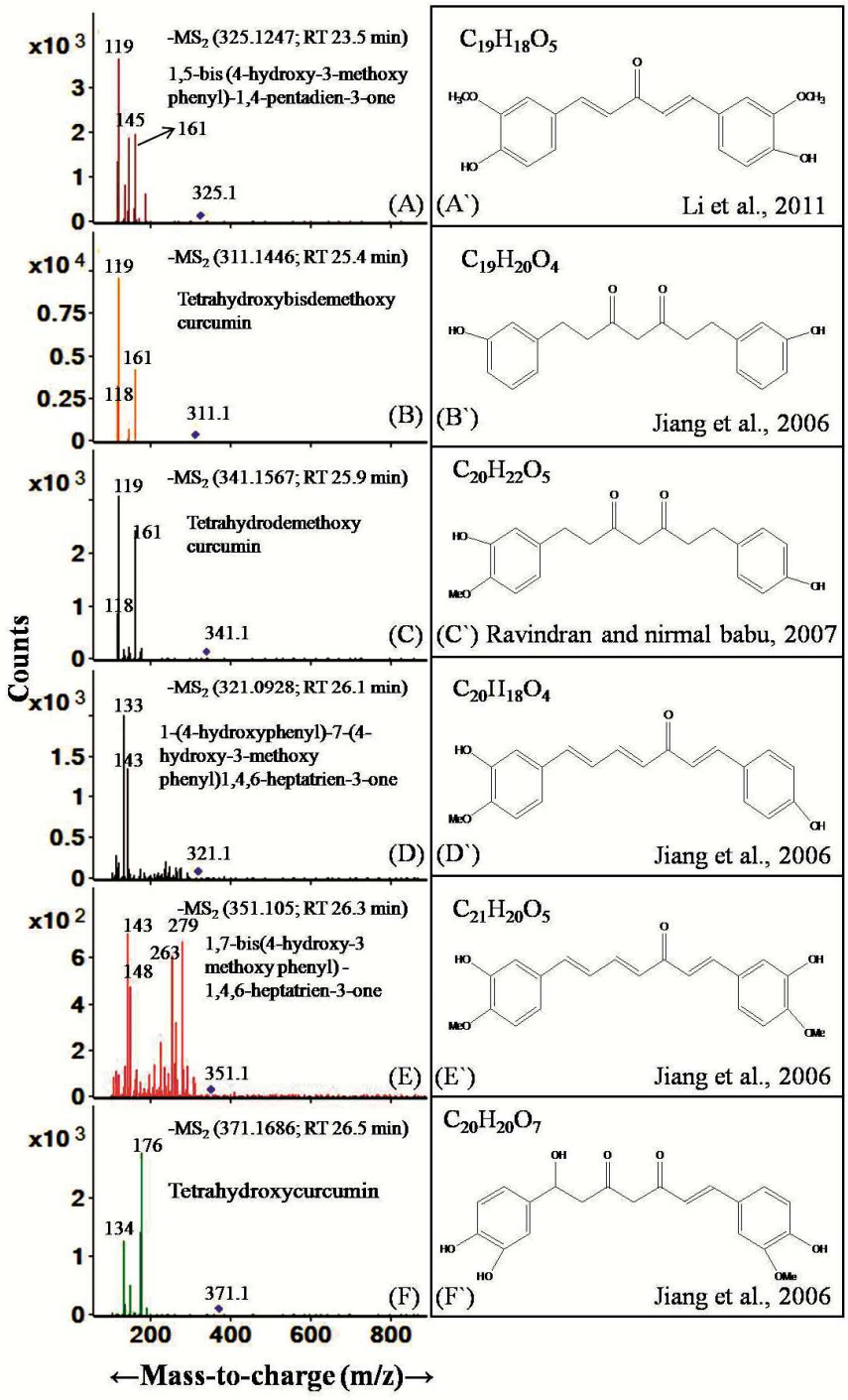

Figure. 6.4. Metabolites common in all cvs of *C. longa* and *C. aromatica* are represented in MS/MS fragmentation pattern. Details of the compounds A to F including retention time, mass, formula, abundance, fragmentation pattern and compound type are given in Table 6.15.

1-(4-hydroxyphenyl)-7-(4-hydroxy-3-methoxyphenyl)1,4,6-heptatrien-3-one ($C_{20}H_{18}O_4$) Table 6.15 and Fig. 6.4. D-D`: It was eluted at RT 26.1 min. Identification of the compound was confirmed by its $[M-H]^-$, m/z 321.0928. The mass fragmentation pattern $[M]^-$, m/z 293, 275, 274, 264, 263, 247, 237, 174, 148, 143, 132, 121, 119, 117 and 115, which are indicated in Table 6.16. The product ions m/z 143 and 133 had highest intensity; another fragment m/z 293 is also a characteristic fragment, even though its abundance is less than other peak (Fig. 6.4. D). The details of each product ion in the spectrum is similar to Jiang et al., (2006).

1,7-bis(4-hydroxy-3methoxyphenyl)-1,4,6-heptatrien-3-one ($C_{21}H_{20}O_5$) Table 6.15 and Fig. 6.4. E-E`: It was eluted at RT 26.3 min. Identification of the compound was confirmed by its $[M-H]^-$, m/z 351.1050. MS fragmentation pattern $[M]^-$ was m/z 323, 293, 291, 279, 263, 262, 261, 251, 245, 235, 224, 223, 207, 195, 164, 148, 143, 136, 119, 115 and 108. Compared to the compound in Fig 6.4. D, the mass of this compound yielded highest intensities of the fragment at m/z 323, 279, 263, 148 and 143. The details of fragmentation pattern are in agreement with Jiang et al., (2006).

Tetrahydroxycurcumin ($C_{20}H_{20}O_7$) Table 6.15 and Fig. 6.4. F-F`: It was eluted at RT 26.5 min. Identification of the compound was confirmed by its $[M-H]^-$, m/z 371.1686. The mass fragmentation pattern was [M]- of m/z 175, 149, 148, 135, 133 having the major fragments of m/z 176 and 134. The detailed information of each peak in the compound is similar to Jiang et al., (2006).

1-(3,4-dihydroxyphenyl)-7-(4-hydroxy-3-methoxyphenyl)hepta-1,6-diene-3,5-dione ($C_{20}H_{18}O_6$) Table 6.15 and Fig. 6.5. G-G`: It was eluted at RT 31.5 min. Identification of the compound was confirmed by its $[M-H]^-$, m/z 353.1207. It showed a very simple and clear fragmentation pattern with base peak m/z 150 and 143. Based on the detailed information of each peak, the compound is similar to data published by Jiang et al., (2006).

Bisdemethoxycurcumin ($C_{19}H_{16}O_4$) Table 6.15 and Fig. 6.5. H-H`: It was eluted at RT 34.5 min. Identification of the compound was confirmed by its $[M-H]^-$, m/z 307.1130. The major fragment ion was m/z 119 and many other peaks obtained were m/z 145 and 117. All these mass fragments matched with the mass data of electron

spray ionization mass spectrum of Mass Bank Record Accession # TY000243 and also previous report of turmeric by Jiang et al., (2006).

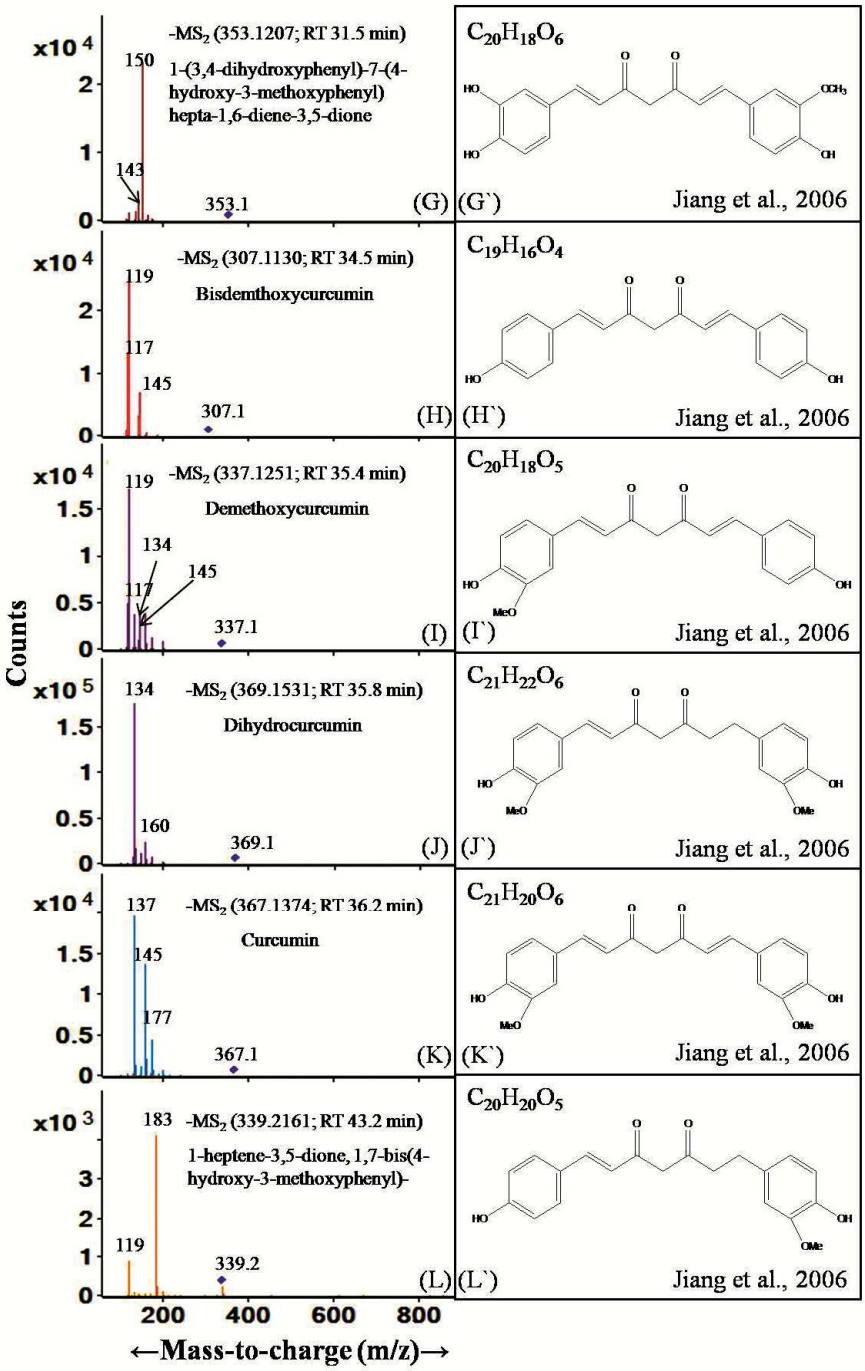

Figure. 6.5. Metabolites common in all cvs of *C. longa* and *C. aromatica* are represented in MS/MS fragmentation pattern. Details of the compounds G to L including retention time, mass, formula, abundance, fragmentation pattern and compound type are given in Table 6.15.

Demethoxycurcumin ($C_{20}H_{18}O_5$) Table 6.15 and Fig. 6.5. I-I`: It was eluted at RT 35.4 min. Identification of the compound was confirmed by its $[M-H]^-$, m/z 337.1251. MS fragmentation pattern was [M]- with m/z 145, 119 and 117 that are found to be common with m/z of bisdemthoxycurcumin but the presence of peak m/z 134 is observed only in this mass spectrum. All these mass fragments matched with the mass data of electron spray ionization mass spectrum of Mass Bank Record Accession # TY000082 and also previous report of turmeric by Jiang et al., (2006).

Dihydrocurcumin ($C_{21}H_{22}O_6$) Table 6.15 and Fig. 6.5. J-J`: it was eluted at RT 35.8 min. Identification of the compound was confirmed by its $[M-H]^-$, m/z 369.1531. The mass fragmentation pattern was $[M]^-$ of m/z 160 and 134 was observed in the spectrum of this compound. Based on the detailed information of each peak, the compound was identified (Jiang et al., 2006).

Curcumin ($C_{21}H_{20}O_6$) Table 6.15 and Fig. 6.5. K-K`: It was eluted at RT 36.2 min. Identification of the compound was confirmed by its $[M-H]^-$, m/z 367.1374. MS fragmentation pattern was $[M]^-$ of m/z 177, 145 and 137. All these mass fragments matched with the mass data of electron spray ionization mass spectrum of Mass Bank Record Accession # TY000081 and also previous report of turmeric by Jiang et al., (2006).

1-heptene-3,5-dione,1,7-bis(4-hydroxy-3-methoxyphenyl)- ($C_{20}H_{20}O_5$) Table 6.15 and Fig. 6.5. L-L`: It was eluted at RT 43.2 min. Identification of the compound was confirmed by its $[M-H]^-$, m/z 339.2161. The mass fragmentation pattern was $[M]^-$ of m/z 183 and 119 are the two major product ions produced by this compound along with the other minor fragments m/z 158, 134, 120, 119 and 117 (Table 6.16). Detailed information of each peak of the compound matched with Jiang et al., (2006).

Cultivar specific compounds in the cultivars of *Curcuma longa* and *C. aromatica*

Cultivar specific compounds detected in the methanolic extracts of *C. longa* and *C. aromatica* are given in Table 6.16. MS/MS fragmentation pattern along with structure of the metabolites are shown in Figures 6.6, 6.7 and 6.8.

Table 6.16. Representative compounds specific to each cultivar detected by LC-ESI-MS/MS in methanolic extracts from rhizomes of *C. longa* and *C. aromatica*. MS/MS fragmentation spectra and structures of the compounds represented in the table are shown in Figs. 6.6, 6.7 and 6.8.

SL.	Compound name	Formula	Mass	Compound type	Cultivar (species)	Fragment ions	Identification Reference
A	Kaempferol -3- rhamnoside	$C_{21}H_{20}O_{10}$	432.1056	Flavonoid	Alleppey Supreme *(C. longa)*	125;142;146;150;176;184;190;293;304;308;311;316;343	Ruslay et al., 2007
B	Kaempferol -3,7-O-dimethyl ether	$C_{17}H_{14}O_6$	314.0794	Flavonoid	Alleppey Supreme *(C. longa)*	125;142;146;150;176;184;190;293;304;308;311;316	Milenanikolova. 2006
C	3-acetyl coumarin	$C_{11}H_8O_3$	188.0534	Coumarin	Alleppey Supreme *(C. longa)*	115;116;117;118;141;143	Pub Chem ID 24852845 NIST 3949-36-8
D	Luteolin-7-O-glucoside	$C_{21}H_{20}O_{11}$	448.2806	Flavonoid	Alleppey Supreme *(C. longa)*	110;185;279;280	Mass bank ACCESSION: TY000145; Rahmatullah et al. 2012
E	turmeronol	$C_{15}H_{20}O_2$	232.1436	Bisabolane sesquiterpene	Alleppey Supreme *(C. longa)*	103;104;105;107;115;117;118;119;120;121;128;129;131;141;142;143	Ma and Gang 2006
F	1, 7-bis(4-hydroxy -3, 5-di meth oxy phenyl)- 1, 6-hepta diene-3,5-dione	$C_{23}H_{24}O_8$	428.2696	Diarylhepatnoid	Prathibha *(C. longa)*	109;123;137;159;191;209	Nurfina 1997
G	5'-methoxy curcumin	$C_{22}H_{22}O_7$	398.1387	Diarylhepatnoid	Prathibha *(C. longa)*	117;119;129;137;145;149;161;175;207	Ravindran and nirmal babu, 2007
H	1,7-bis(3,4-di methoxy phe nyl)-1,6-hept adiene-3,5-dione	$C_{23}H_{24}O_6$	396.2438	Diarylhepatnoid	Prathibha *(C. longa)*	105;107;119;129;137;145;155;195	Chen et al., 2006
I	(6S)-2-methyl-6-[(1R ,5S)-(4-methene-5-hy droxyl-2-cyclo hexen)-2-hepten-4-one	$C_{15}H_{24}O_2$	236.1885	Bisabolane	Prathibha *(C. longa)*	105;106;107;108;109;119;120;121;133;135	Li et al., 2011

J	4-methyl-7-methoxy coumarin	$C_{11}H_{10}O_3$	190.1953	Coumarin	PCT-13 *(C. longa)*	115;116;117;119;120	NIST CAS register No 2555-28-4. Mass Bank ACCESSION: PR100013
K	Hydroferulic acid	$C_{10}H_{12}O_4$	196.1075	Phenolic acid	Kasturi Araku *(C. aromatica)*	109;121;122	Ma and Gang, 2006
L	1,7-bis(4-hydroxy phenyl)-3,5-heptane diol	$C_{19}H_{24}O_4$	316.1653	Phenolic diarylhepatnoid	Kasturi Araku *(C. aromatica)*	105;106;107;119;121;147;148	Ma and Gang 2006
M	1, 7-bis(3,5-di ethyl-4-hydro xyphenyl)-1,6 -heptadiene-3,5-dione	$C_{27}H_{32}O_4$	420.3459	Aromatic	Kasturi Araku *(C. aromatica)*	106;107;119;120;121;122;123;144;145;146;147;171;172;175;187;197	Li et al., 2011
N	1-(4-hydroxy-3-methoxyphenyl)-5-(4-hydroxyphenyl)-1,4-pentadiene-3-one	$C_{18}H_{16}O_4$	296.1044	Diarylhepatnoid	Kasturi Araku *(C. aromatica)*	105;109;117;119;133;145;159;161;171;173;181;185;1207;209;223;233;239;251;279	Ravindran and Nirmal babu, 2007; Park and Kim 2002
O	7-(3,4-di hydr oxyl phenyl~ 5-hydroxy-l-phenyl-(lE)-lheptene	$C_{19}H_{22}O_3$	298.1597	Phenolic diarylhepatnoid	Kasturi Avidi *(C. aromatica)*	119;183;184	Suksamrarn et al., 1994
P	(-)-(12E,2S, 3S,4R, 5R, 6R, 9S, 11S, 15R)-3,15-di benzoyl oxy -5,6-epox-ylathyr-12-en-14-one.	$C_{34}H_{38}O_6$	542.2646	Diterpenoid	Kasturi Avidi *(C. aromatica)*	119;145;183;211;212;237	Tian et al., 2011

Kaempferol-3-rhamnoside ($C_{21}H_{20}O_{10}$) Table 6.16 and Fig. 6.6. A-A`: It belongs to the flavonoid class of compound and was detected only in *C. longa* cv. Alleppey Supreme. It yielded the peak in negative ion mode showing molecular ion peak at RT 10.7 min. Identification of the compound was confirmed by its $[M-H]^-$, m/z 431.9911. Further, MS fragmentation of the parent ion (m/z 431) yielded m/z 345, 184, 148 and 125. The detailed information of the peaks matched with the data published in Ruslay et al., (2007) using the fresh rhizomes of *Curcuma xanthorrhiza* and *Zingiber zerumbet*.

Kaempferol-3,7-O-dimethyl ether ($C_{17}H_{14}O_6$) Table 6.16 and Fig. 6.6. B-B`: It belongs to the flavonoid class of compound and was detected only in *C. longa* cv.

Alleppey Supreme. The negative ion mode showed molecular ion peak at RT 12.7 min. Identification of the compound was confirmed by its $[M-H]^-$, m/z 313.0721. MS fragmentation pattern $[M]^-$ of major peaks with m/z 152, 123 and 108 is matched against the published data (Milenanikolova, 2006).

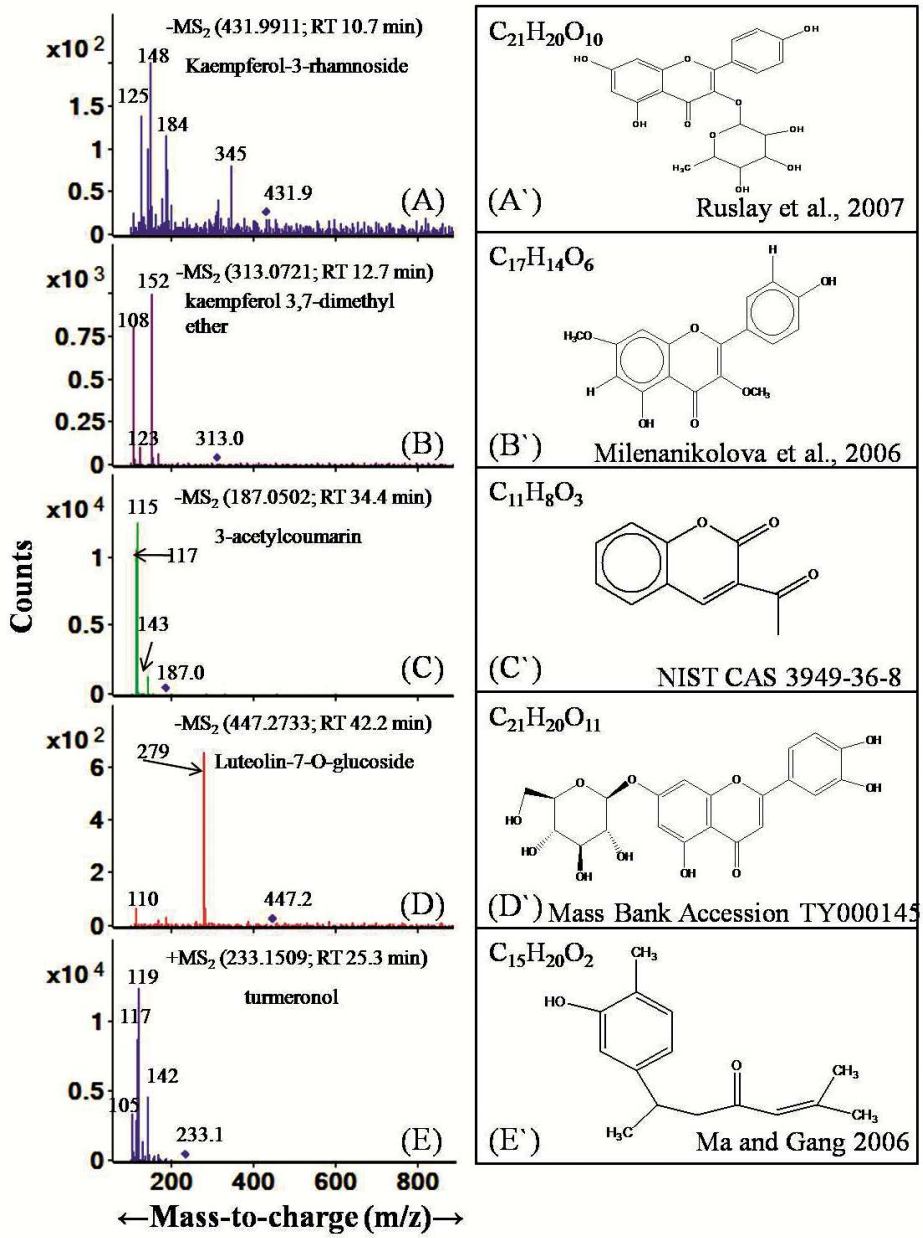

Figure. 6.6. Represents the MS/MS spectra and structure (A to E) of relative metabolites that are cultivar specific for *C. longa* cv. Alleppey Supreme. Details of the compounds A to E including retention time, mass, formula, abundance, fragmentation pattern and compound type are given in Table 6.16.

3-acetyl coumarin ($C_{11}H_8O_3$) Table 6.16 and Fig. 6.6. C-C`: It belongs to the coumarin class of compound and was detected only in *C. longa* cv. Alleppey Supreme The negative ion mode showed the molecular ion peak at RT 34.4 min. Identification of the compound was confirmed by its $[M-H]^-$, m/z 187.0502. MS fragmentation pattern $[M]^-$ was m/z 143, 117, 115 and m/z of all these mass fragments agreed with the mass data of electron spray ionization mass spectrum obtained from NIST library, CAS Registry Number 3949-36-8.

Luteolin-7-O-glucoside ($C_{21}H_{20}O_{11}$) Table 6.16 and Fig. 6.6. D-D`: It belongs to the flavonoid class of compound and was detected only in *C. longa* cv. Alleppey Supreme. The negative ion mode showed the molecular ion peak at RT 42.2 min. Identification of the compound was confirmed by its $[M-H]^-$, m/z 447.2733. The mass fragmentation pattern $[M]^-$ was m/z 279 and 110. All these mass fragments agreed with the mass data of electron spray ionization mass spectrum obtained from Mass Bank Accession # TY000145 and this compound has previously been reported from the rhizomes of *Curcuma zedoaria* (Christm.) Roscoe (Rahmatullah et al., 2012).

Turmeronol ($C_{15}H_{20}O_2$) Table 6.16 and Fig. 6.6. E-E`: It belongs to the type of bisabolane sesquiterpene and was detected only in *C. longa* cv. Alleppey Supreme. The positive ion mode showed the molecular ion peak at RT 25.3 min. Identification of the compound was confirmed by its $[M+H]^+$, m/z 233.1509. MS fragmentation pattern $[M]^+$ was m/z 142, 119, 117, 105 and this compound is previously reported from *C. longa* by Ma and Gang (2006).

1,7-bis(4-hydroxy -3, 5-di methoxy phenyl)- 1, 6-hepta diene-3,5- dione ($C_{23}H_{24}O_8$) Table 6.16 and Fig. 6.7. F-F`: It belongs to the class of diarylheptanoids and was detected only in *C. longa* cv. Prathibha. The positive ion mode showed the molecular ion peak at RT 32.9 min. Identification of the compound was confirmed by its $[M+H]^+$, m/z 429.2768. The mass fragmentation pattern of the compound $[M]^+$ with m/z 300, 191 and 137 and matched with the data presented in previously report by Nurfina et al., (1997) from the rhizomes of *Curcuma longa*.

**5`-methoxycurcumin** ($C_{22}H_{22}O_7$) Table 6.16 and Fig. 6.7. G-G`: It belongs to the class of diarylheptanoids and was detected only in *C. longa* cv. Prathibha. The

positive ion mode showed the molecular ion peak at RT 35.5 min. Identification of the compound was confirmed by its $[M+H]^+$, m/z 399.1461. The mass fragmentation pattern yielded was $[M]^+$ with m/z 175, 145 and 119. This compound was previously reported by Ravindran and nirmal babu (2007).

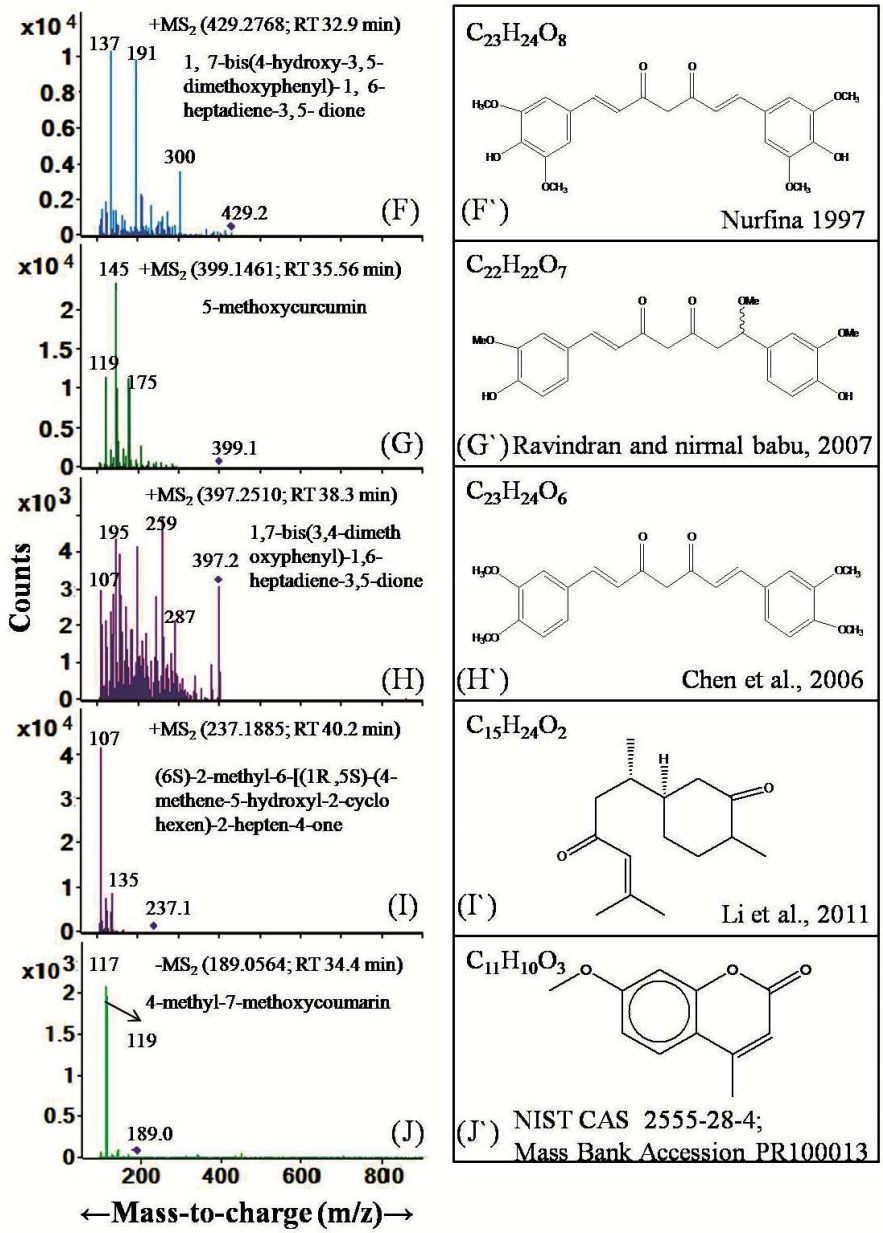

Figure. 6.7. Represents the MS/MS spectra and structures (F to I) are relative metabolites that are cultivar specific for *C. longa* cv. Prathibha and MS/MS spectra and structure (J) is cultivar specific for *C. longa* cv. PCT-13. Details of the compounds F to J including retention time, mass, formula, abundance, fragmentation pattern and compound type are given in Table 6.16.

1,7-bis(3,4-di methoxy phe nyl)-1,6-hept adiene-3,5-dione ($C_{23}H_{24}O_6$) Table 6.16 and Fig. 6.7. H-H`: It belongs to the class of diarylheptanoids and was detected only in *C. longa* cv. Prathibha. The positive ion mode showed the molecular ion peak at RT 38.3 min. Identification of the compound was confirmed by its $[M+H]^+$, m/z 397.2510. The mass fragmentation pattern yielded was $[M]^+$ with m/z 287, 259, 195 and 107. It has been previously reported from *Curcuma longa* by Chen et al., (2006).

(6S)-2-methyl-6-[(1R,5S)-(4-methene-5-hydroxyl-2-cyclohexen)-2-hepten-4one ($C_{23}H_{24}O_6$) Table 6.16 and Fig. 6.7. I-I`: It belongs to the bisabolane type of sesquiterpene compound and was detected only in *C. longa* cv. Prathibha. The positive ion mode showed the molecular ion peak at RT 40.2 min. Identification of the compound was confirmed by its $[M+H]^+$, m/z 237.1885. The mass fragmentation pattern yielded was $[M]^+$ with m/z were 135 and 107 were the major peak ions. This compound earlier reported by Li et al., (2011).

4-methyl-7-methoxycoumarin ($C_{11}H_{10}O_3$) Table 6.16 and Fig. 6.7. J-J`: It belongs to the coumarin type of compound and was detected only in *C. longa* cv. PCT-13. The negative ion mode showed the molecular ion peak at RT 34.4 min. Identification of the compound was confirmed by its $[M+H]^+$, m/z 237.1885. The mass fragmentation pattern $[M]^+$, yielded were with m/z 119 and 117, these were the major peak in the spectrum and matched with pattern of the compound CAS 2555-28-4 in NIST library.

Hydroferulic acid ($C_{10}H_{12}O_6$) Table 6.16 and Fig. 6.8. K-K`: It belongs to the class of phenolic acids and was detected only in *C. aromatica* cv. Kasturi Araku. The negative ion mode showed the molecular ion peak at RT 16.8 min. Identification of the compound was confirmed by its $[M-H]^-$, m/z 195.1075. The mass fragmentation pattern $[M]^-$ having m/z 121 as a major ion peak matched with previous report by Ma and Gang (2006).

1,7-bis(4-hydroxyphenyl)-3,5-heptanediol ($C_{19}H_{24}O_4$) Table 6.16 and Fig. 6.8. L-L`: It is a diarylheptanoid type of compound and was detected only in *C. aromatica* cv. Kasturi Araku. The negative ion mode showed the molecular ion peak at RT 22.8 min. Identification of the compound was confirmed by $[M-H]^-$, m/z 315.1653. The

mass fragmentation pattern $[M]^-$ showed m/z 147 and 106 as the major ion peaks and matched with data presented in previous report (Ma and Gang, 2006).

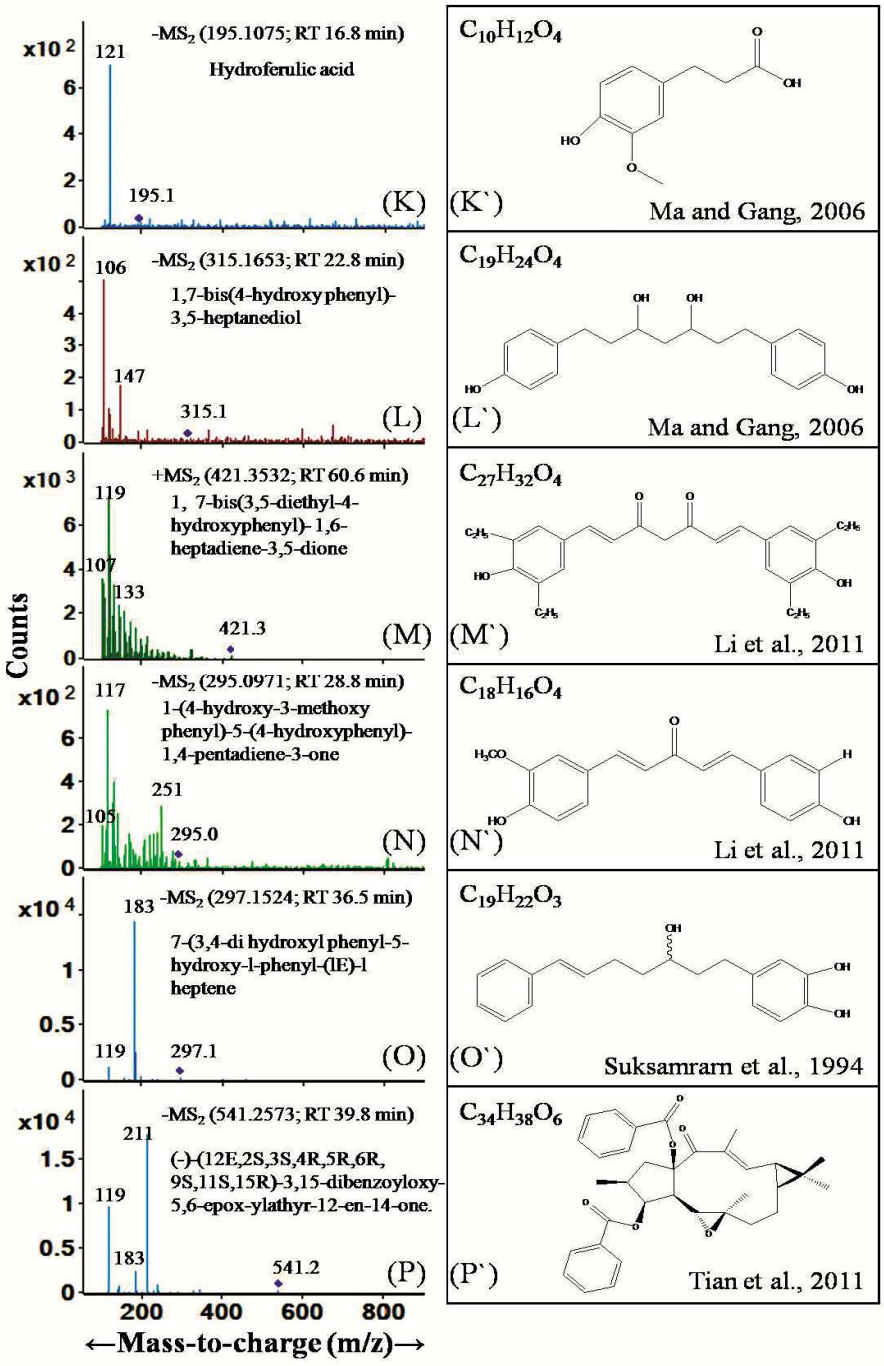

Figure. 6.8. Represents the MS/MS spectra and structures (K to M) are relative metabolites that are cultivar specific for *C. aromatica* cv. Kasturi Araku and MS/MS spectra and structure (N to P) is cultivar specific for *C. aromatica* cv. Kasturi Avidi. Details of the compounds K to P including retention time, mass, formula, abundance, fragmentation pattern and compound type are given in Table 6.16.

1, 7-bis(3,5-di ethyl-4-hydroxyphenyl)-1,6 -heptadiene-3,5-dione ($C_{27}H_{32}O_4$) Table 6.16 and Fig. 6.8. M-M`: It is an aromatic type of compound and was detected in *C. aromatica* cv. Kasturi Araku. The positive ion mode showed the molecular ion peak at RT 60.6 min. Identification of the compound was confirmed by its $[M+H]^+$, m/z 421.3532. MS fragmentation pattern $[M]^+$ showed m/z 133, 119 and 107 ions, the compound is previously reported by Li et al., (2011).

1-(4-hydroxy-3-methoxy phenyl)-5-(4-hydroxy phenyl)-1,4-pentadiene-3-one ($C_{18}H_{16}O_4$) Table 6.16 and Fig. 6.8. N-N`: It is a diarylheptanoid and was detected only in *C. aromatica* cv. Kasturi Avidi. The negative ion mode showed the molecular ion peak at RT 28.8 min. Identification of the compound was confirmed by its $[M-H]^-$, m/z 295.0791. The mass fragmentation pattern $[M]^-$ showed m/z 251, 117, 105 and the compound is previously reported by Park and Kim, 2002.

7-(3,4-dihydroxylphenyl-5-hydroxy-l-phenyl-(lE)-lheptene ($C_{19}H_{22}O_3$) Table 6.16 and Fig. 6.8. O-O`: It belongs to the class of diarylheptanoid and was detected only in *C. aromatica* cv. Kasturi Avidi and yielded the peak at RT 36.5 min. Identification of the compound was confirmed by its $[M-H]^-$, m/z 297.1524. MS fragmentation pattern $[M]^-$ yielded was with m/z 183 and 119 and the compound is previously reported by Suksamrarn et al., (1994).

(-)-(12E, 2S, 3S,4R, 5R, 6R, 9S, 11S, 15R)-3,15-dibenzoyloxy-5,6-epoxylathyr-12-en-14-one ($C_{34}H_{38}O_6$) Table 6.16 and Fig. 6.8. P-P`: It belongs to the class of diarylheptanoids and was detected only in *C. aromatica* cv. Kasturi Avidi. It yielded the peak at RT 39.8 min. Identification of the compound was confirmed by its $[M-H]^-$, m/z 297.1524. MS fragmentation pattern $[M]^-$ showed m/z 183 and 119 and matched with data presented in previous report (Tian et al., 2011).

Novel compounds identified from the rhizomes of *Curcuma*

In addition to the above information, we are for the first time reporting four novel compounds from *Curcuma,* these compounds were earlier reported from other genus as shown in Table 6.17.

Table 6.17. Compounds identified for the first time from *Curcuma* using the data generated from LC/ESI-MS/MS. MS/MS fragmentation spectra and structures of the compounds represented in the table are shown in Fig. 6.9.

SL.	Compound name	Formula	m/z	Compound Type	Cultivar (species)	Fragment ions	Plant Name /Ref
A	5,7,8-trihydroxy-2′,5′-dimethoxy-3′,4′-methylene dioxyisoflavanone	$C_{18}H_{18}O_9$	377.1059 $M\text{-}H^-$	Flavonoid	Alleppey Supreme and Duggirala Red *(C. longa)*	101;102;113;119;161;163;228;336	*Terminalia ivorensis* Family: Combretaceae **Ref** Ogundare et al., 2012
B	Kaempferol 3,7-dimethyl ether	$C_{17}H_{14}O_6$	313.0721 $M\text{-}H^-$	Flavonoid	Alleppey Supreme *(C. longa)*	108;123;152;153;167	*Lumnitzera racemosa* Family: Combretaceae *Artemisia vulgaris* L. Family: Asteraceae **Ref** Lisette et al., 2010; Milenanikolova et al., 2006
C	Chavicol	$C_9H_{20}O$	135.0794 $M+H^+$	Terpenoid	Alleppey Supreme and PCT-13 *(C. longa)*	102;115;116	*Piper betle* Family: Piperaceae **Ref** NIST CAS No: 501-92-8; Nagori et al., 2011
D	Kaempferol-3-O-rutinoside-7-O-glucoside	$C_{33}H_{40}O_{20}$	755.2655 $M\text{-}H^-$	Flavonoid	Prathibha and Salem *(C. longa)*	135;161;175;176;191;439;579;755;756	*Lycopersicon esculentum* Family: Solanaceae **Ref** Gall et al., 2003

5,7,8-trihydroxy-2′,5′-dimethoxy-3′,4′-methylene dioxyisoflavanone ($C_{34}H_{38}O_6$) Table 6.17 and Fig. 6.9. A-A`: It belongs to the class of flavonoids and was detected in cultivar species of *C. longa* cvs. Alleppey Supreme and Duggiral Red. The negative ion mode showed the molecular ion peak at RT 2.2 min. Identification of the compound was confirmed by its $[M\text{-}H]^-$, m/z 377.1059 from the MS fragmentation pattern $[M]^-$ yielded was with m/z 161, 119, 113 and 101. All these

mass fragments agreed with the mass data of electron spray ionization mass spectrum and this compound has previously been reported from the bark extracts of *Terminalia ivorensis* belongs to family of Combretaceae (Ogundare et al., 2012).

Kaempferol-3,7-O-dimethyl ether ($C_{17}H_{14}O_6$) Table 6.17 and Fig. 6.9. B-B`: It belongs to the class of flavonoids and was detected in cultivar species of *C. longa* cv. Alleppey Supreme. The negative ion mode showed for this compound, the molecular ion peak at RT 12.7 min. Identification of the compound was confirmed by its $[M-H]^-$, m/z 313.0721. MS fragmentation pattern $[M]^-$ showed m/z 152, 123 and 108. All these mass fragments agree with the mass data of electron spray ionization mass spectrum and this compound has previously reported from the mangrove species *Lumnitzera racemosa* belongs to family of Combretaceae (Lisette et al., 2010 and Milenanikolova, 2006).

Chavicol ($C_9H_{20}O$) Table 6.17 and Fig. 6.9. C-C`: It belongs to the terpenoid class of compound and was detected in cultivar species of *C. longa* cv. Alleppey Supreme and PCT-13. The positive ion mode showed molecular ion peak at RT 27.0 min. Identification of the compound was confirmed by its $[M+H]^+$, m/z 135.0794. MS fragmentation pattern $[M]^+$ yielded was with m/z 115 and 102 and all the fragments agreed and matched with pattern of the compound with the NIST CAS Registry Number 501-92-8. It was also previously reported through direct analysis in real time mass spectrometry (DART-MS) from the piper betel leaves of family Piperaceae (Nagori et al., 2011).

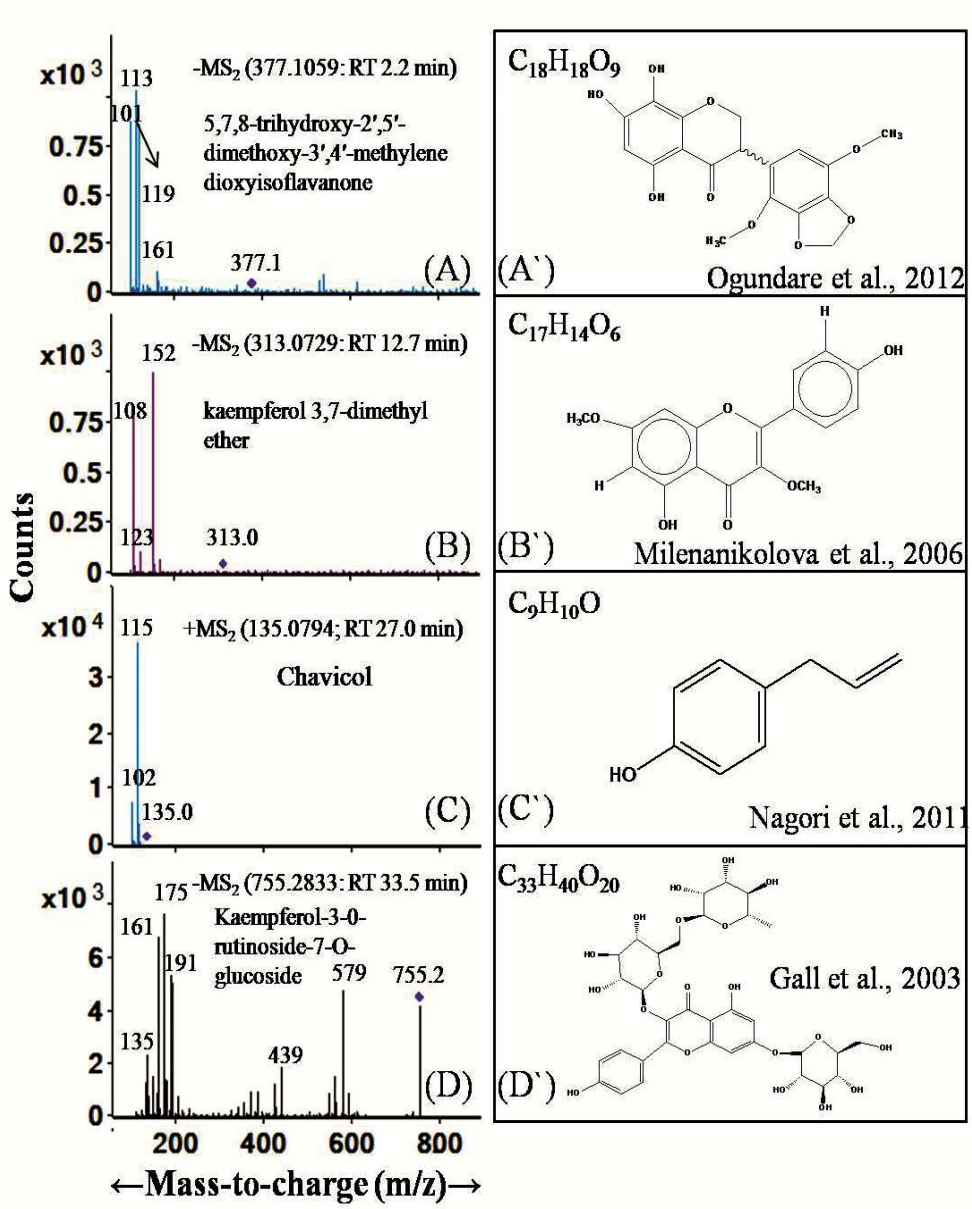

Figure. 6.9. Metabolites identified for the first time from *Curcuma* using the data generated from LC-ESI-MS/MS are shown in the MS/MS chromatogram and respective structures for the metabolite (A) 5,7,8-trihydroxy-2′,5′-dimethoxy-3′,4′-methylene dioxyisoflavanone (B) kaempferol 3,7-dimethylether (C) Chavicol and (D) Kaempferol-3-O-rutinoside-7-O-glucoside. Details of the compounds A to E including retention time, mass, formula, abundance, fragmentation pattern and compound type are given in Table 6.17.

Kaempferol-3-O-rutinoside-7-O-glucoside ($C_{33}H_{40}O_{20}$) Table 6.17 and Fig. 6.9. D-D`: It belongs to the flavonoid class of compound detected in cultivar species of *C. longa* cv. Prathibha and Salem. The negative ion mode showed molecular ion peak at

RT 33.5 min. Identification of the compound was confirmed by its $[M-H]^-$, m/z 755.2833. The mass fragmentation pattern $[M]^-$ yielded was with m/z 579, 439, 191, 175, 161 and 135. All these mass fragments agree with the mass data of electron spray ionization mass spectrum and this compound has previously reported from *Lycopersicon esculentum* of the family Solanaceae (Gall et al., 2003).

Discussion

Metabolite profiling was used to investigate the diversity of plant material within the species and between closely related species by GC-MS or LC-MS analysis (Jiang et al., 2006). LC-MS coupled to diode array detection served as a powerful tool for the complete metabolite profiling of *C. longa* derived from *in vitro* micropropagation and conventional greenhouse cultivation (Ma and Gang, 2006; Jiang et al., 2006). Fresh rhizomes of *C. domestica* were examined for total metabolite profile by LC-MS analysis (Diran et al., 2009). Present study attempted a detatiled metabolite profiling of methanolic rhizome extracts of seven cultivars of *Curcuma* (five cultivars of *C. longa* cvs. Alleppey Supreme, Duggirala Red, PCT-13, Prathibha, Salem; and two cultivars of *C. aromatica* cvs. Kasturi Araku, Kasturi Avidi) by LC-MS analysis.

Using LC-ESI-MS-MS, the data was generated for about 200 number of metabolites from each cultivar variety in both positive and negative modes of electrospray ionization (ESI) within the range of 110–1700 m/z. The differences were ascertained by comparing the chromatographic and mass spectral data from these compounds with those from Metlin Library; NIST library, Mass Bank and literature comparison. The analysis lead to the identification of several classes of phenolic compounds including diarylheptanoids, phenolic acids, flavonoids, coumarins and etc from the crude methanolic extracts of fresh turmeric rhizomes. However the data obtained is useful in building basic metabolite libraries of each cultivar can be built, which forms an important platform for further use. LC-ESI-MS-MS detected very few terpenoids which are the major compounds of essential oils. Thus our data suggests that GC-MS is an important complementary technique required for finger printing of turmeric rhizome.

High variability in Indian cultivar varieties are *C. longa* and *C. aromatica* is clearly demonstrated by the present study. A total of 51 known metabolites identified

from LCMS analysis from the selected seven cultivars of *Curcuma*. Some of the compounds are common among all the cultivars, some are unique to specific cultivar and some are shared between two or more cultivars. Out of the known compounds detected from each cultivar, only a total of eleven metabolites including three major curcuminoids were detected in all seven cultivars of *Curcuma* selected for the present study. Some of the metabolites shared between two or more cultivars. As shown in the Table 6.18, out of 37 known compounds detected from *C. longa* cv. Alleppey Supreme, 24 were in common with Duggirala Red, 20 each with PCT-13 and Prathibha, 25 each with Salem, 19 with Kasturi Araku and 25 with Kasturi Avidi.

Table 6.18. Number of known metabolites shared within the cvs of *C. longa* and *C. aromatica*

SL. No.	**Cultivars**	**Number of shared compounds within the cvs. of *C. longa* and *C. aromatica***						
		C. longa cv. Alleppey Supreme	*C. longa* cv. Duggirala Red	*C. longa* cv. PCT-13	*C. longa* cv. Prathibha	*C. longa* cv. Salem	*C. aromatica* cv. Kasturi Araku	*C. aromatica* cv. Kasturi Avidi
1	*C. longa* cv. Alleppey Supreme	37	24	20	20	25	19	25
2	*C. longa* cv. Duggirala Red	24	26	21	19	20	19	22
3	*C. longa* cv. PCT-13	20	21	25	16	18	15	19
4	*C. longa* cv. Prathibha	20	19	16	30	20	19	21
5	*C. longa* cv. Salem	25	20	18	20	32	19	25
6	*C. aromatica* cv. Kasturi Araku	19	19	15	19	19	27	18
7	*C. aromatica* cv. Kasturi Avidi	25	22	19	21	25	18	31

Note: Highlighted cells indicate the number of known metabolites detected in the specific cultivar variety.

Similarly in Duggirala Red, out of 26 known compounds (irrespective to the class of compounds) from it 21 of them found in PCT-13, 19 each in Prathibha and Kasturi

araku, 20 in Salem and 22 in Kasturi Avidi. Out of 25 compounds detected from PCT-13, 16 were found in Prathibha, 18 in Salem, 15 in Kasturi Araku and 19 in kasturi Avidi. Out of 30 known compounds detected from Prathibha, it shared 20 in common with Salem, 19 with Kasturi Araku and 21 of them Kasturi Avidi.

Out of 32 known compounds detected from Salem, it shared 25 with Alleppey Supreme, 20 in Duggirala Red, 18 in PCT-13, 20 in Prathibha, 19 and 25 metabolites in common with Kasturi Araku and Kastur Avidi respectively. Out of 27 known compounds detected from Kasturi Araku, it shared 19 each in Alleppey Supreme, Duggirala Red, Prathibha and Salem, 15 in PCT-13 and 18 in Kastur Avidi. Out of 31 known compounds detected from Kastur Avidi, it shared 25 each in Alleppey Supreme and Salem, 22 in Duggirala Red, 19 in PCT-13, 21 in Prathibha and 18 in Kasturi Araku.

Table. 6.19.Number of diarylheptanoids shared within the cvs of *C. longa* and *C. aromatica*

SL. No.	**Cultivars**	**Number of shared diarylheptanoids within cvs. of *C. longa* and *C. aromatica***						
		C. longa cv. Alleppey Supreme	*C. longa* cv. Duggirala Red	*C. longa* cv. PCT-13	*C. longa* cv. Prathibha	*C. longa* cv. Salem	*C. aromatica* cv. Kasturi Araku	*C. aromatica* cv. Kasturi Avidi
1	*C. longa* cv. Alleppey Supreme	20	18	13	16	19	15	19
2	*C. longa* cv. Duggirala Red	18	19	14	17	19	16	18
3	*C. longa* cv. PCT-13	13	14	15	14	14	12	15
4	*C. longa* cv. Prathibha	16	17	14	20	18	16	19
5	*C. longa* cv. Salem	19	19	14	18	20	16	21
6	*C. aromatica* cv. Kasturi Araku	15	16	12	16	16	19	17
7	*C. aromatica* cv. Kasturi Avidi	19	18	15	19	21	17	23

Note: Highlighted cells indicate the number of diarylheptanoids detected in that specific cultivar variety.

Majority of the compounds detected by LC-ESI-MS-MS are diarylheptanoids, most of these were detected by both negative and positive ion modes, although the negative ion mode was more effective in detecting them. Diarylheptanoids sharing

within the cultivars is shown in Table 6.19. Other phenolic compounds including coumarins, flavonoids and phenolic acids were exclusively detected by negative ion mode, and the terpenoids by positive ion mode except two terpenoids. These two are bisabolane sesquiterpenes from *C. longa* cv. Alleppey Supreme were detected by negative ion mode.

There are about eleven diarylheptanoids were detected in all seven cultivars of *Curcuma*. Some of the diarylheptanoids also can be cultivar specific; e.g. 1,7-bis(4-hydroxy-3,5-di methoxyphenyl)- 1,6-heptadiene-3,5-dione; 5'-methoxycurcumin; 1,7-bis(3,4-dimethoxyphenyl)-1,6-hept adiene-3,5-dione exclusively detected in *C. longa* cv. Prathibha, 1,7-bis(4-hydroxy phenyl)-3,5-heptanediol; 1-(4-hydroxy-3-methoxyphenyl)-5-(4-hydroxyphenyl)-1,4-penta diene-3-one detected exclusively in *C. aromatica* cv. Kasturi Araku, 7-(3,4-di hydroxylphenyl~ 5-hydroxy-l-phenyl-(lE)-lheptene exclusively detected in *C. aromatica* cv. Kasturi Avidi.

Thus the present report from LC-MS analysis suggest that seven cultivars of *Curcuma* showed high variability in their metabolite profiling. Identification of unknown compounds and also GCMS analysis with their essential oils would enable us to establish the relationship and differences between the cultivars.

Chapter 7

SUMMARY and CONCLUSIONS

The major aims of the study are (i) to evaluate antioxidant and cardioprotective property of *Boswellia serrata's* gum resin and *Terminalia arjuna's* stem bark using human blood cells and vascular endothelial cells and (ii) construct metabolite profiling of these medicinal plant extracts along with *Curcuma*. Atherosclerosis is one of the types of cardiovascular diseases, referred as chronic inflammatory blood vessel wall disease and develops as a result of interaction between oxidative stress, inflammation and thrombosis and these processes promote each other. In India traditional medicine, Ayurveda, BS-gum resin is used to treat various types of inflammatory blood disorders, and TA-stem-bark as a cardiotonic. Turmeric from *Curcuma* is also used to treat inflammatory diseases and the rhizomes of *Curcuma* are enriched with diverse array of phytochemicals. The following four objectives are framed for the present study with the selected medicinal plants based on their traditional use, scientific validation and in the light of biochemical events occur in the pathogenesis of atherosclerosis.

OBJECTIVES OF THE PRESENT STUDY

1. Phytochemical analysis of hydroalcoholic and water extracts of *B. serrata*- gum resin and *T. arjuna*-stem bark and evaluation of their antioxidant activity in human monocytic (THP-1) cells.
2. Evaluation of antiinflammatory activity of boswellic acid mixed-fraction (BAM) isolated fraction of *B. serrata* gum resin and TA-stem bark extracts on human monocytic (THP-1) and human aortic endothelial cells (HAECs).
3. Evaluation of antithrombotic property of *B. serrata*-gum resin and BAM using human platelets and coagulation factors.
4. LC-MS based metabolite profiling of cultivars of *Curcuma longa and C. aromatica* and the use of metabolite profile for constructing cultivar variability.

Objective 1: Phytochemical analysis of *B. serrata*-gum resin and *T. arjuna*-stem bark extracts and evaluation of their antioxidant activity in THP-1 cells.

Phytochemical analysis

Total phenolics, flavonoids and triterpenoid content

Alcoholic extracts of *B. serrata* gum resin (BSAE) had higher amounts of total triterpenoids and its water extracts (BSAE) had higher amounts of total phenolic (TPC) and flavonoid content (TFC) Table 3.1. The yields obtained were 4.8 % (w/w)

and 5.2 % (w/w) for BSAE and BSWE, respectively. Alcoholic extracts (TAAE) of *T. arjuna*'s stem bark had higher amounts of TPC and TFC than water extracts (TAWE). Yields obtained were 15 % (w/w) and 5 % (w/w) for TAAE and TAWE, respectively (Table 3.2).

Quantitation of AκβBA in BS-extracts by HPLC

HPLC analyses with BSAE and BSWE showed peaks corresponding to standard AκβBA with identical retention times (min) and concluded that AκβBA content was almost similar in BSAE and BSWE comprising to 9 % (w/w) and 7.8 % (w/w) of their extracts' dwt. We used standard AκβBA at different concentrations for calibration. Least amount of detection (LOD) and quantification (LOQ) under experimental conditions were 2.69 ± 0.17 µg/mL and 9.08 ± 0.58 µg/mL respectively (Fig. 3.2).

GC-MS analysis of BSAE, BSWE and BAM

Results obtained from GCMS analysis of BSAE, BSWE and isolated boswellic acid mixed- fraction (BAM) authenticated there source. BSAE had large number of aromatic components like e.g. verbenyl ethyl ether; trans-3-acetoxy-1,8-cineole and monoterpenes, sesquiterpenes and triterpenoids- e.g. α-amyrin, 3-O-acetyl-β-boswellic acid, AκβBA and etc (Table 3.3 and Fig. 3.5). BSWE showed the presences of sesquiterpenes- e.g. farnesene, 3-O-acetyl-6-methoxy cycloartenol (Table 3.4 and Fig. 3.6) and other compounds like AκβBA. Caryophyllene oxide and alcohol-1-Heptatriacotanol and fatty acids were also found to be common in BSAE and BSWE. BAM shown to have majority of pentacyclic triterpenes e.g. 11-Hydroxy-β-boswellic acid; 3-O-acetyl-11-keto-β-boswellic acid (AκβBA); β-boswellic acid; α-boswellic acid and other tirucallic acids like 3-O-acetyl-11-hydroxy-β-boswellic acid and etc (Table 3.5 and Fig. 3.8).

LC-MS analysis of TAAE and TAWE

Phytochemical analysis of TAAE and TAWE with LC-Q-TOFMS revealed the presence of metabolites belonging to the classes of phenolics and terpenes (Tables 3.6 and 3.7). Kaempferol, epigallo catechin, terminolic acid and arjunic acid were commonly found in TAAE and TAWE. Gallic acid, catechin, ellagic acid and its derivative i.e. 3'-O-methyl-4-O-(β-D-xylopyranosyl) were identified exclusively in

TAWE. Arjungenin, arjunolic acid, glycopyranosides, steroid glycoside were detected only in TAAE.

Free radical scavenging activity

Both BSAE and BSWE showed concentration dependent activity. BSAE showed significantly much higher antioxidant activity than BSWE. BSAE scavenged, 92 % of DPPH radical with the IC_{50} being 1.65 mg dwt/mL, whereas BSWE scavenged maximum of only 40 % of the radical at 10 mg dwt/mL (Fig. 3.11. A). In case of *T. arjuna*, both extracts TAAE and TAWE almost completely scavenged (> 90 %) of DPPH radical (Fig. 3.11. C) and IC_{50} values of TAAE and TAWE were 6.4 µg dwt/mL and 5 µg dwt/mL respectively.

In case of H_2O_2 radical scavenging activity, BSAE showed maximum of 60 % activity (IC_{50} 3.2 mg dwt/mL) and BSWE showed 53 % activity (IC_{50} of 3.8 mg dwt/mL) (Fig. 3.11. B). TAAE showed maximum of 58 % scavenging activity with IC_{50} 0.35 mg dwt/mL (Fig. 3.11. D). Whereas TAWE showed only maximal scavenging capacity of 38 % where its IC_{50} could not be determined.

Ferric chloride induced lipid peroxidation activity in rat tissue homogenates

All SMPE (BSAE, BSWE, TAAE and TAWE) inhibited $FeCl_3$ induced lipid peroxidation in rat liver and heart homogenates (Figs. 3.12 and 3.13). For liver lipid peroxidation, IC_{50} values of BSWE was 34 µg dwt/mL. In case of heart homogenate, IC_{50} of BSAE and BSWE were 129 µg dwt/mL and 88 µg dwt/mL respectively. Extracts showed lower effect in inhibiting heart tissue lipid peroxidation. The results indicated that water extracts of BS-gum resin were more potential than standard compound ASC in suppressing lipid peroxidation of both rat liver and heart tissue homogenates.

TAAE and TAWE inhibited about 90 % of lipid peroxidation induced by $FeCl_3$ in both liver and heart homogenates. The IC_{50} for TAAE and TAWE were 10 and 3 µg dwt/mL for liver homogenate and 30 and 10 µg dwt/mL respectively for heart homogenates.

IC_{50} values of ascorbate in case of liver and heart tissue peroxidation were 38 µg/mL and 153 µg/mL respectively. GA showed maximum inhibition of 80 % in both types of tissue homogenates with IC_{50} 1.29 µg/mL and 10 µg/mL respectively for liver and heart homogenates (Fig. 3.12. D and 3.13. C).

Cell viability in THP-1 cells

Maximal dosage of SMPE (BSAE, BSWE, BAM, TAAE or TAWE) or standard compounds determined by MTT and trypan blue exclusion methods (Figs. 3.14. A to J). At least > 95 % cells were alive at the used concentrations of SMPE or standard compounds.

Measurement of intracellular ROS scavenging potential of extracts

We evaluated the efficacy of SMPE in attenuating H_2O_2 induced ROS generation in THP-1 cells using cell permeable ROS sensitive fluorescent marker H_2DCFDA. Pretreatment of cells SMPE significantly attenuated H_2O_2 dependent fluorescence increase. The results indicated that alcohol extract of BS-gum resin was more potential than the water extract in scavenging intracellular ROS (Figs. 3.15 and 3.17. A). Literature suggests that AκβBA is active metabolite in BS-gum resin. However, phytochemical analysis of BS-gum resin extracts by HPLC revealed the presence of equal quantity of AκβBA in both BSAE and BSWE. Therefore, in order to isolate bioactive metabolites, BS-gum resin was subjected to fractionation with alkali treatment followed by acidification. Intracellular ROS activity of boswellic acid mixed fraction (BAM) and pure compounds AκβBA and α-BA (alfa-boswellic acid) were determined. BAM (100 µg dwt/mL) and AκβBA (10 µg/mL) attenuated H_2O_2 mediated ROS by ≥ 85 % in H_2O_2 treated THP-1 cells, whereas α-BA (10 µg/mL) exhibited only ≥ 60 % inhibition (Fig. 3.17. A).

In case of *T. arjuna* stem bark extracts, both TAAE and TAWE showed remarked intracellular ROS scavenging activity in THP-1 cells. Positive drug controls used for the present study, ASC (20 µg/mL), BHT (10 µg/mL) and GA (10 µg/mL), were able to scavenge ROS completely (Fig. 3.16 and 3.17. B).

Effect of SMPE on cellular redox potential and ROS scavenging enzymes

To determine the mechanism by which SMPE assist THP-1 cells in scavenging intracellular ROS, the effect of these extracts were tested on cellular ROS scavenging enzymes and redox potential (FRAP). BSAE did not show significant effect on CAT whereas BSWE increased its activity by 2-fold (Fig. 3.18. A). Both the extracts helped the cells in sustaining the cellular reducing power to great extent (Fig. 3.18. B). BAM (100 µg dwt/mL), α-BA (10 µg/mL) and AκβBA (10 µg/mL) promoted

CAT activity but showed no significant effect on cellular redox potential ie., FRAP (Fig. 3.18. B). Our results indicate that some other compounds apart from AκβBA present in BSAE is responsible for its high efficacy.

Pretreatment of THP-1 cells with TAAE (114 µg dwt/mL) caused an increase in CAT by 10-fold, GPx by 7-fold and sustained cellular reducing power up to 60 % of control (vehicle) cells. Similarly, TAWE (375 µg dwt/mL) induced 8- and 6-fold increase in CAT and GPx activities, respectively, but did not help much with cellular redox potential (Fig. 3.19). In contrast to TAAE and TAWE, standard compounds ASC increased the activity of cellular CAT, BHT helped to sustain cellular redox potential and GA promoted GPx activity (Fig. 3.19. A to C).

HMGR and LpL enzyme assays

Effect of TAAE and TAWE was tested on lipid metabolizing enzymes (HMGR and LpL) as *T. arjuna* stem bark is reported to have hypolipidaemic activity. TAAE and TAWE inhibited HMGR enzyme by more than 75 % (Fig. 3.20). Pravastatin, positive drug control, provided in the kit, inhibited about 55 % of the activity. In case of LpL, the plant extracts did not show significant inhibition, however, the positive drug control, Orlistat showed about 30 % inhibition (Fig. 3.20).

Objective 2: Evaluation of antiinflammatory activity of BAM and TA-stem bark extracts (TAAE and TAWE) on human monocytic (THP-1) and aortic endothelial cells (HAECs).

Antiinflammtory effect of selected medicinal plants in THP-1 cells

Effect of SMPE on LPS induced TNF-α secretion by THP-1 cells by ELISA

Activated monocytes and their retention within the atherosclerotic lesion contribute to the progression of plaque development. TNF-α is a proinflammatory cytokine and is secreted by activated monocytes. ELISA was performed with cell supernatants to assess the secretion of TNF-α by human THP-1 monocyte cells after exposure to LPS (0.5 µg/mL) for 3 h. Untreated cells secreted negligible amounts (20 ± 0.5 pg/mL) of TNF-α whereas LPS treated cells showed 20-fold increase in TNF-α secretion (824 ± 50 pg/mL). Pretreatment with BSWE (400 µg dwt/mL) suppressed TNF-α release down to 210 ± 33 pg/mL (10.5-fold) and BSAE (16 µg dwt/mL) inhibited to 450 ± 37 pg/mL (22.5-fold) (Fig. 4.1. B). Significant effect observed similarly in both BAM (100 µg/mL) and α-BA (10 µg/mL or 20 µM) treated cells.

AκβBA (10 µg/mL or 20 µM) showed much greater effect, TNF-α secretion was suppressed to 175 ± 32 pg/mL (8.7-fold) (Fig. 4.1. C).

Pretreatment of THP-1 cells with TAAE (120 µg dwt/mL) almost completely inhibited the LPS induced TNF-α secretion to 39 pg/mL, whereas for TAWE (250 µg dwt/mL) reduced to 220 pg/mL (Fig. 4.1. D). Thus TA-stem bark extracts also showed marked effect on TNF-α secretion by LPS induced THP-1 cells. Standard compound BHT showed significant effect but GA did not show much effect.

Effect of SMPE on LPS induced transcripts of inflammatory markers in THP-1 cells

THP-1 monocytic cells produce MCP-1 and IL-8 upon endotoxin induction. In the present study, real-time quantitative PCR showed that LPS enhanced the expression of MCP-1 and IL-8 in THP-1 cells by several folds. Pretreatment with BAM (100 µg/mL) did not show much effect on MCP-1 but markedly inhibited the expression of IL-8. Whereas pure compounds α-BA (10 µg/mL or 20 µM) and AκβBA (10 µg/mL or 20 µM) significantly reduced the transcript levels of MCP-1 but not IL-8 (Fig. 4.2. A and B).

TAAE (120 µg dwt/mL) attenuated both MCP-1 and IL-8 gene expression, whereas TAWE (250 µg dwt/mL) reduced only IL-8 expression. GA restricted MCP-1 marginally and failed to attenuate IL-8 expression (Fig. 4.2. C and D).

Antiinflammtory effect of selected medicinal plants on HAECs

Effect of SMPE on TNF-α induced mRNA transcripts of inflammatory markers in HAECs

Activated HAECs express cell adhesion molecules e.g. VCAM-1, ICAM-1, E-selectin and other proinflammatory markers, which play a major role in pathogenesis of atherosclerosis. Inhibition of VCAM-1 has pharmacological importance in treating atherosclerosis (Chen et al., 2002). In the present study, HAECs upon treatment with TNF-α (10 ng/mL) caused significant upregulation of mRNA transcript levels of VCAM-1, ICAM-1, E-selectin, MCP-1 and IL-8. Pretreatment of cells with BAM (40 µg dwt/mL) or α-BA (5 µg/mL or 10 µM) or AκβBA (6 µg/mL or 12 µM) significantly attenuated all five types of mRNA transcripts although the effect varied to some extent (Fig. 4.6. A to E). Pretreatment with alcoholic extract of TA-stem bark (TAAE) also attenuated all the tested markers significantly. In case of TAWE, HAECs showed significant response in attenuating E-selectin, MCP-1 and IL-8, but

not VCAM-1 and ICAM-1. Reference compound GA attenuated all the markers except ICAM-1 (Fig. 4.6. F to J).

Effect of SMPE on attenuating cell surface adhesion molecule expression of VCAM-1 and E-selectin in TNF-α induced HAECs by flow-cytometry

HAECs were analysed by FACScan (BD LSR Fortessa ^{TM}) to study the expression of cell surface adhesion molecules VCAM-1 (CD 106-FITC) and E-selectin (CD62E-PE). Treatment with TNF-α stimulated the cells that were positive for both VCAM-1 and E-selectin (Fig.4.7. A). Pretreatments with BAM (40 µg dwt/mL) and AκβBA (6 µg/mL or 12 µM) significantly decreased both VCAM-1 and E-selectin stained cells, whereas α-BA (5 µg/mL or 10 µM) moderately attenuated VCAM-1 and had no effect on E-selectin (Fig. 4.7. C).

Similarly pretreatment of HAECs with TAAE (20 µg dwt/mL) significantly attenuated the VCAM-1 and E-selectin positively stained cells, whereas TAWE (25 µg dwt/mL) and GA (10 µg dwt/mL) reduced VCAM-1 positive cells and did not have much effect on E-selectin marker (Fig. 4.7. D).

Effect of SMPE on attenuating the translocation of NF-κB (p65) from cytoplasm to nucleus in THP-1 cells and HAECs by confocal microscopy

In mammalian cells, expression of several proinflammatory markers including cytokines and chemokines is regulated by NF-κB transcription factor. Therefore, further to elucidate on mechanism of anti-inflammatory activity of SMPE, effect of the extracts on LPS/TNF-α induced translocation of p65 subunit of NF-κB was studied in THP-1 cells/HAECs by confocal microscopy. Cells were probed with antibody of NF-κB subunit p65 and stained using secondary antibody conjugated to Alexa Fluor 594. Nuclei were stained with DAPI. THP-1 cells induced with LPS showed translocation of p65 from cytoplasm to nucleus and such translocation was inhibited by SMPE (Figs. 4.3 and 4.4). Similarly, in HAECs, SMPE inhibited TNF-α induced translocation of p65 from cytoplasm to nucleus. Reference compound, GA also showed significant response in inhibiting p65 translocation from cytoplasm to nucleus (Fig. 4.8).

Objective 3: Evaluation of antithrombotic property of *B. serrata*-gum resin and BAM using human platelet and coagulation factors.

ADP induced platelet aggregation activity of BSAE, BSWE and BAM

20 µM ADP used in the study to induce platelet aggregation in human platelet rich plasma (PRP) sample. Platelet aggregation was monitored by decrease in the O.D. units at λ_{600nm}. BSAE and BSWE attenuated such ADP dependent platelet aggregation and were comparable to heparin. BAM (250 µg/mL), α-BA (~ 300 µg dwt/mL or 600 µM), AκβBA (~ 50 µg dwt/mL or 100 µM) also significantly inhibited platelet aggregation (Figs. 5.1 to 5.4).

Effect of BSWE, BSAE and BAM on plasma clotting times and coagulation factors

APTT and PT used to evaluate intrinsic and extrinsic clotting indices of plasma respectively were performed on a coagulometer. BAM and pure boswellic acids (3-O-acetyl-α-boswellic acid; 3-O-acetyl-β-boswellic acid; 11-keto-β-boswellic acid; 3-O-acetyl-11-keto-β-boswellic acid; α-boswellic acid; β-boswellic acid) showed moderate to significant effect on prolongation of APTT and PT clotting time periods. Hep 10 U/mL (20 µg/mL) prolonged both PT and APTT time periods (Fig. 5.5).

The effect of BAM and pure boswellic acid standards on blood coagulation factors, VIIa (extrinsic pathway), Xa (common pathway), IXa, XIa, XIIa (intrinsic pathway) was studied. Heparin was used as drug control. Factors VIIa, Xa and XIIa were significantly inhibited by BAM and pure boswellic acids, however they had no effect on factor IXa and XIa. Heparin inhibited FVIIa (extrinsic pathway) and FXa (Common pathway) and did not show effect on factors of intrinsic pathway like FIXa, FXIa, but exhibited moderate affect on FXIIa (Fig. 5.8).

Objective 4: LC-MS based metabolite profiling of cultivars of *Curcuma longa and C. aromatica* and the use of metabolite profile for constructing cultivar variability.

Methanolic rhizome extracts of *Curcuma longa* (cvs. Alleppey Supreme, Duggirala Red, PCT-13, Prathibha, Salem) and *C. aromatica* (cvs. Kasturi Araku and Avidi) were subjected to LCMS/MS analysis to detect the common and cultivar specific metabolites. Through the mass spectral analysis, combined metabolic profiles, data generated for about 200 number of metabolites for each variety in both positive and negative modes of electrospray ionization (ESI) within the range of 110–1700 m/z.

Diarylheptanoids including three major curcuminoids were detected in rhizomes of all seven cultivars of *Curcuma.* In *C. longa* cv. Alleppey Supreme, a total of 80 metabolites were obtained through raw data from which 37 metabolites were identified (known compounds) within which 11 metabolites detected commonly in both positive and negative modes and these are mostly diarlyheptanoids (e.g. 1-(4-Hydroxy phenyl)-7-(4-hydroxy-3-methoxy phenyl)1,4,6-heptatrien-3-one; 1,7-bis(4-hydroxy-3 methoxy phenyl) -1,4,6-heptatrien-3-one; Bisdemthoxycurcumin; Demethoxycurcumin; Curcumin and etc (Tables 6.1 and 6.8). Likewise analysis done with all five selected cultivars of *C. longa* and two of *C. aromatica*, were compared (Tables 6.2 to 6.14 and Figs. 6.2 and 6.3). The following are some of the cultivar specific compounds identified: Kaempferol 3,7-O-dimethyl ether and Turmeronol are specifically found in *C. longa* cv. Alleppey Supreme (Table 6.16 and Fig. 6.6). 5,7,8-Trihydroxy-2′,5′-dimethoxy-3′,4′-methylene dioxyisoflavanone detected from *C. longa* cvs. Alleppey Supreme and Duggirala Red; whereas chavicol from *C. longa* cvs. Alleppey Supreme and PCT-13; Kaempferol-3-O-rutinoside-7-O-glucoside from *C. longa* cvs. Prathibha and Salem.

Salient features of the study

1. Medicinal plant extracts selected for the present study were authenticated by phytochemical analysis through GC-MS or LC-MS analysis.
2. Alcohol and water extracts of BS-gum resin (BSAE, BSWE) and TA-stem bark (TAAE, TAWE) significantly scavenged H_2O_2 induced intracellular ROS in THP-1 monocytic cells by promoting ROS scavenging enzymes and / or sustaining cellular redox potential. LPS induced inflammatory markers in THP-1 cells and TNF-α induced marker's in HAECs were shown to attenuate by SMPE.
3. BAM, TAAE and TAWE significantly attenuated monocytic and endothelial cell activation by inhibiting LPS/TNF-α induced NF-κB subunit p65 translocation from cytoplasm to nucleus.
4. BSAE, BSWE and BAM showed dose dependent inhibition of ADP induced platelet aggregation.
5. BSAE, BSWE and BAM prolonged both PT and APTT plasma coagulation times.
6. BAM and pure boswellic acids (3-O-acetyl-α-BA; 3-O-acetyl-β-BA; β-BA; 11-

keto-β-BA; α-BA; AκβBA) showed significant inhibition on factors XIIa (intrinsic pathway); FXa (common pathway) and FVIIa (extrinsic pathway).

7. LC-MS analysis suggested that rhizomes of seven cultivars of *Curcuma* showed for the presence of phenolic acids, flavonoids, coumarins and etc in addition to curcuminoids (Curcumin (CU); Demethoxycurcumin (DMC); Bisdemethoxycurcumin (BDMC)) in common. Detailed metabolite analysis also suggested their high variability.

Concluding remarks

Gum resin of *B. serrata* and stem-bark of *T. arjuna* showed antioxidant and anti-inflammatory activity in THP-1 human monocytic cells and aortic endothelial cells. Further, BS-gum resin showed antithrombotic properties. Phytochemical analysis showed their enrichment with several bioactive compounds. Thus the study supported traditional use of these plants in treating blood related disorders especially cardiovascular diseases. Metabolite profiling of seven cultivars of *Curcuma* revealed their commonality as well as variability.

Chapter 8
Literature Cited

Adams J. L., Czuprynski C. J. 1990. Bacterial lipopolysaccharide induces release of tumor necrosis factor-α from bovine peripheral blood monocytes and alveolar macrophages *in vitro*. Journal of Leukocyte Biology 48: 549-556

Aggarwal B. B., Sung B. 2008. Pharmacological basis for the role of curcumin in chronic diseases: an age-old spice with modern targets. Trends in Pharmaceutical Sciences 2: 85-94

Ahmad I., Beg A. Z. 2001. Antimicrobial and phytochemical studies on 45 Indian medicinal plants against multi-drug resistant human pathogens. Journal of Ethnopharmacology 74: 113-123

Akram M. S., Ahmed A., Usmanghani K., Hannan. A., Mohiuddin E., Asif M. 2010. *Curcuma longa* and curcumin: A review article. Romanian Journal of Biology-Plant Biology 55: 65-70

Alam M., Khan H., Samiullah L., Siddique K. M. 2012. A review on phytochemical and pharmacological studies of kundur (*Boswellia serrata* Roxb ex Colebr.) - A Unani drug. Journal of Applied Pharmaceutical Science 02: 148-156

Ali A., Ali. M., Alam M. S. 2006. Two new oleanane triterpene glycosides from the bark of *Terminalia arjuna.* Zeitschrift Naturforsch 61b: 1282-1286

Ali Sha B., Nabi Q. G., Taneja S. C. 2009. Boswellic acids: a group of medicinally important compounds. Natural Product Reports 26: 72-89

Alon R., Kassner P. D., Carr M. W., Finger E. B., Hemler M. E., Springer T. A. 1995. The integrin VLA-4 supports tethering and rolling in flow on VCAM-1. The Journal of Cell Biology 128: 1243-1253

Ammayappan R. S., Dhanabal P., Bavadia P., Vishnuvarthan V. J., Satish kumar M. N. 2012. Antioxidant and antidiabetic activity of *Curcuma aromatica*. International Journal of Research in Ayurveda and Pharmacy 3: 401-405

Ambrose J. A., Barua R. S. 2004. The pathophysiology of cigarette smoking and cardiovascular disease an update Journal of the American College of Cardiology 43: 1731-1737

Ammon H. P. T., Safayhi H., Mack T., Sabieraj J. 1993. Mechanism of anti-

inflammatory actions of curcumine and boswellic acids. Journal of Ethnopharmacology 38: 105-112

Ammon H. P. T. 2006. Boswellic acids in chronic inflammatory diseases. Planta Medica 1-17

Anand P., Kunnumakkara A. B., Newman R. A., Aggarwal B. B. 2007. Bioavailability of curcumin: problems and promises. Molecular Pharmaceutics 4: 807-818

Angelov A. 1975. Thromboembolic complications in rheumatism, atherosclerosis and hypertension. Vutr Boles 14: 36-42

Arthur J. R. 2000. The glutathione peroxidises. CMLS, Cellular and Molecular Life Sciences 57: 1825 – 1835

Arya V., Gupta V. K. 2011. Chemistry and pharmacology of plant cardioprotectives: a review. International Journal of Pharmaceutical Sciences and Research 2: 1156-1167

Asad N. R., Asad L. M. B. O., Almedia C. E. B. de., Felzenszwalb I., Cabral N. J. B., Leitao A. C. 2004. Several pathways of hydrogen peroxide action that damages the *e. coli* genome. Genetics and Molecular Biology 27: 291-303

Asha S., Taju G. 2012. Cardioprotective effect of *Terminalia arjuna* on caffeine induced coronary heart disease. International Journal of Pharmaceutical Sciences 3: 150-153

Assimopoulou A. N., Zlatanos S. N., Papageorgiou V. P. 2005. Antioxidant activity of natural resins and bioactive triterpenes in oil substrates. Food Chemistry 92: 721–727

Avery S. V. 2011. Molecular targets of oxidative stress. Biochemistry Journal 434: 201–210

Bailey J. M., Butler J. 1973. Antiinflammatory drugs in experimental atherosclerosis part 1. relative potencies for inhibiting plaque formation. Atherosclerosis 17: 515-522.

Baqui A. A., Meiller T. F., Turng B. F., Kelley J. I., Falkler W. A. Jr. 1998. Functional changes in THP-1 human monocytic cells after stimulation with lipopolysaccharide of oral microorganisms and granulocyte macrophage

colony stimulating factor. Immunopharmacology Immunotoxicology 20: 493-518

Bass D. A., Parce W., Dechatelet L. R., Szejda P. Seeds M. C., Thomas M. 1983. Flow cytometry studies of oxidative product formulation by neutrophils: a graded response to membrane stimulation. The Journal of Immunology 130: 1910-1917

Baud O., Greene A. E., Li. J., Wang H., Volpe J. J., Rosenberg P. A. 2004. Glutathione peroxidase–catalase cooperativity is required for resistance to hydrogen peroxide by mature rat oligodendrocytes. The Journal of Neuroscience 24: 1531–1540

Beate P. F., Desousky El, S. K., Haubner R., Erben G., Owen R. W., 2010. Polyphenolic compounds in the fruits of Egyptian medicinal plants (*Terminalia bellerica*, *Terminalia chebula* and *Terminalia horrida*): Characterization, quantitation and determination of antioxidant capacities. Phytochemistry 71, 1132-1148

Beckman J. A., Creager M. A., Libby P. 2002. Diabetes and atherosclerosis-epidemiology, pathophysiology, and management. Journal of American Medical Association 287: 2570-2581

Beinke S., Ley S. C. 2004. Functions of NF-κB1 and NF-κB2 in immune cell biology. Biochemistry Journal 382: 393-409

Bele A. A., Jadhav V. M., Kadam V. J. 2010. Potential of tannins: A review. Asian Journal of Plant Sciences 4: 209-214

Belsner K., Buchele B., Werz U., Syrovets T., Simme T. 2003. Structural analysis of pentacyclic triterpenes from the gum resin of *Boswellia serrata* by NMR spectroscopy. Magnetic Resonance in Chemistry 41: 115-122

Benhusein G. M., Mutch E., Aburawi S., Williams F. M. 2010. Genotoxic effect induced by hydrogen peroxide in human heptoma cells using comet assay. Libyan Journal of Medicine 5: 1-6

Benzie I. F. F., Strain J. J. 1996. The ferric reducing ability of plasma (FRAP) as a measure of ‘‘antioxidant power’’: The FRAP assay. Analytical Biochemistry 239: 70-76

Bharani A., Ganguly A., Bhargava K. D. 1995. Salutary effect of *Terminalia arjuna*

in patients with severe refractory heart failure. International Journal of Cardiology 49: 191-19

Bharani A., Ganguly A., Mathur L. K., Jamra Y., Raman P. G. 2002. Efficacy of *Terminalia arjuna* in chronic stable angina: A double blind, placebo-controlled, crossover study comparing *Terminalia arjuna* with isosorbide mononitrate. Indian Heart Journal 54: 170-175

Bharani A., Ahirwar L. K., Jain N. 2004. *Terminalia arjuna* reverses impaired endothelial function in chronic smokers. Indian Heart Journal 56: 123-128

Bizuneh A. 2012. Phytochemistry of turmeric: an overview. chemistry: Bulgarian Journal of Science Education 21: 888-897

Blankenberg S., Rupprecht H. J., Bickel C., Torzewski M., Hafner G., Tiret L., Smieja. M., Cambien F., Meyer J., Lackner K. J. 2003. Glutathione peroxidase 1 activity and cardiovascular events in patients with coronary artery disease. New England Journal of Medicine 349: 1605-1613

Boos C. J., Lip G. Y. 2006. Blood clotting inflammation, and thrombosis in cardiovascular events: perspectives. Frontiers in Bioscience 11: 328-336

Brand K., Page S., Rogler G., Bartsch A., Brandl A., Knuechel R., Page M., Kaltschmidt C., Baeuerle P. A., Neumeier D. 1996. Activated transcription factor nuclear factor-kappa B is present in the atherosclerotic lesion. The American Society for Clinical Investigation 97: 1715–1722

Braunersreuther V., Mach F., Steffens S. 2007. The specific role of chemokines in atherosclerosis. Journal of Thrombosis and Haemostasis 97: 714-721

Brown M., Wittwer C. 2000. Flow cytometry: principles and clinical applications in hematology. Clinical Chemistry 46: 1221–1229

Broze G. J., Hickman Jr. S., Miletich J. P. 1985. Monoclonal anti-human factor VII antibodies. Detection in plasma of a second protein antigenically and genetically related to factor VII. Journal of Clinical Investigation 76: 937-946

Buchanan M. S., Carroll A. R., Wessling D., Jobling M., Avery V. M., Davis R. A., Feng Y., Xue Y., Oster L., Fex T., Deinum J., Hooper J. N. A., Quinn R. J. 2008. Clavatadine A, a natural product with selective recognition and irreversible inhibition of factor XIa. Journal of Medicinal Chemistry 51: 3583–3587

Carter W. O., Narayanan P. K., Robinson J. P. 1994. Intracellular hydrogen peroxide and superoxide anion detection in endothelial cells. Journal of Leukocyte Biology 55: 253-258

Cattaneo M., Gache C. 2001. The platelet ADP receptors. Haematologica 86: 346-348

Chatterjee S. 2000. Effect of *Terminalia arjuna* on abnormal platelet reactivity in hypercholesterolaemic rabbits. Indian Drugs 37: 135-138

Chatterjee S., Srivastava S., Khalid A., Singh N., Singh R., Sangwan., Sidhu O. P., Roy R., Khetrapal C. L., Tuli R. 2010. Comprehensive metabolite fingerprinting of *Withania somnifera* leaf and root extracts. Phytochemistry 10: 1085-1094

Chattopadhyay I., Biswas K., Bandyopadhyay U., Banerjee R. K. 2004. Turmeric and curcumin: Biological actions and medicinal applications 87: 44-53

Chen Y. H., Lin S. J., Chen J. W., Ku. H. H., Chen Y. L. 2002. Magnolol attenuates VCAM-1 expression *in vitro* in TNF-α treated human aortic endothelial cells and *in vivo* in the aorta of cholesterol-fed rabbits. British Journal of Pharmacology 135: 37-47

Chen J. W., Chen Y. H., Lin F. Y., Chen Y. L., Lin S. J. 2003.Ginkgo biloba extract inhibits tumor necrosis factor-α induced reactive oxygen species generation, transcription factor activation, and cell adhesion molecule expression in human aortic endothelial cells. Atherosclerosis Thrombosis Vascular Biology 23: 1559-1566

Chen W. F., Deng S. L., Zhou B., Yang L., Liu Z. L. 2006. Curcumin and its analogues as potent inhibitors of low density lipoprotein oxidation: H-atom abstraction from the phenolic groups and possible involvement of the 4-hydroxy-3-methoxyphenyl groups. Free Radical Biology and Medicine 40: 526 – 535

Chen-Chen Z., Li G., Zhong-xiang Z., Chao-zhan L. 2012. Triterpenes from *Callicarpa integerrima* champ. Acta Pharmaceutica Sinica 47: 77-83

Clarisse C. P., Billiet L., Bauge E., Copin C., Scott-Algara D., Genze F., Buchele B., Syrovets T., Simmet T., Rouis M. 2008. Antiinflammatory and antiatherogenic effects of the NF-κB inhibitor acetyl-11-keto-β-boswellic acid in LPS challenged Apo E-/- mice. Atherosclerosis Thrombosis Vascular Biology 28: 272-277

Cohen G., Hochste P. 1963. Glutathione peroxidase: The primary agent for the elimination of hydrogen peroxide in erythrocytes. Biochemistry 2: 1420-1428

Cohn C. A., Simon S. R., Schoonen M. A. A. 2008. Comparison of fluorescence-based techniques for the quantification of particle-induced hydroxyl radicals. Particle and Fibre Toxicology 5: 1-9

Commisso M., Strazzer P., Toffali K., Stocchero M., Guzzo F. 2013. Untargeted metabolomics: an emerging approach to determine the composition of herbal products. Computational and Structural Biotechnology Journal 4: 1-22

Cooke M. S., Evans M. D., Dizdaroglu M., Lunec J. 2003. Oxidative DNA damage: mechanism, mutation, and disease. The Journal of the Federation of American Societies for Experimental Biology 17: 1195-1214

Copeland S., Warren S. H., Lowry S. F., Calvo S. E., Remick D. 2005. Acute inflammatory response to endotoxin in mice and humans. Clinical and Diagnostic Laboratory Immunology 12: 60-67

Couffinhal T., Duplaa C., Moreau C., Lamaziere J. M., Bonnet J. 1994. Regulation of vascular cell adhesion molecule-1 and intercellular adhesion molecule-1 in human vascular smooth muscle cells. Circulation Research 74: 225-234

Daniel J. L., Dangelmaier C., Jin J., Ashby B., Simth J. B., Kunapuli S. P. 1998. Molecular basis for ADP-induced platelet activation: evidence for three distinct ADP receptors on human platelets. Journal Biological Chemistry 273: 2024-2029

Davis C., Fischer J., Ley K., Sarembock I. J. 2003. The role of inflammation in vascular injury and repair. Journal of Thrombosis and Haemostasis 1: 1699-1709

Dinges M. M., Schlievert P. M. 2001. Comparative analysis of lipopolysaccharide-induced tumor necrosis factor alpha activity in serum and lethality in mice and rabbits pretreated with the staphylococcal superantigen toxic shock syndrome toxin 1. Infection and Immunity 69: 7169-7172

Diran H., Choi J. H., El-Aty A. M. Abd., Shim J. H., Spiteller. M. 2009. Metabolite analysis in *Curcuma domestica* using various GC-MS and LC-MS separation and detection techniques. Biomedical Chromatography 23: 951-965

Dixon Z. R., Shie F. S., Warden B. A., Burri B. J., Neidlinger T. R. 1998. The effect

of a low carotenoid diet on malondialdehyde-thiobarbituric acid (MDA-TBA) concentrations in women: a placebo-controlled double-blind study. Journal of the American College of Nutrition 17: 54 –58

Dong Z. M., Chapman S. M., Brown A. A., Frenette P. S., Hynes R. O., Denisa I., Wagner D. 1998. The combined role of P- and E-selectins in atherosclerosis. The Journal of Clinical Investigation 102: 145-152

Durackova Z. 2010. Some current insights into oxidative stress. Physiological Research 59: 459-469

Dwivedi S., Jauhari R. 1997. Beneficial effects of *Terminalia arjuna* in coronary artery disease. Indian Heart Journal 49: 507-510

Dwivedi S., Aggarwal A., Agarwal M. P., Rajpal S. 2005. Role of *Terminalia arjuna* in ischaemic mitral regurgitation. International Journal of Cardiology 100: 507–508

Dwivedi S. 2007. *Terminalia arjuna* Wight and Arn- a useful drug for cardiovascular disorders. Journal of Ethnopharmacology 114: 114-129

Dwivedi A. H., Pillai S. G., Patni N. 2011. Mass spectrometry: an important tool in clinical research. Institute of Technology 1-3

Eriksson A. C., Whiss P. A. 2005. Measurement of adhesion of human platelets in plasma to protein surfaces in microplates. Journal of Pharmacological and Toxicological Methods 52: 356-365

Esper R. J., Nordaby R. A., Vilarino J. O., Paragano A., Cacharron J. L., Machado R. A. 2006. Endothelial dysfunction: a comprehensive appraisal. Cardiovascular Diabetology 5: 1-18

Evgeniy E., Sergei K. 2010. Identification of ROS using oxidized DCFDA and flow-cytometry. Advanced protocols in oxidative stress II, Methods in Molecular Biology 594

Evans C. H., Robbins P. D. 2000. Gene therapy in inflammatory diseases. Indian Academy of Sciences 1

Fahy E., Subramaniam S., Brown H. A., Glass C. K., Merrill, Jr A. H., Murphy R. C., Raetz C. R. H., Russell D. W., Seyama Y., Shaw W., Shimizu T., Spener F., Meer G. V., VanNieuwenhze M. S., White S. H., Witztum J. L., Dennis E.

A. 2005. A comprehensive classification system for lipids. Journal of Lipid Research 46: 839-862

Fang-Yun S., Sun C., Wang J. H., Qin H. L., Yang S. R., D. G. H. 2008. Arjunic acid, a strong free radical scavenger from *Terminalia arjuna*. The American Journal of Chinese Medicine 36: 197

Feldman A. M., Combes A., Wagner D., Kadakomi T., Kubota T., Li. Y. Y., McTiernan C. 2000. The role of tumor necrosis factor in the pathophysiology of heart failure. Journal of American College of Cardiology 35: 537-544

Fritts M., Crawford C. C., Quibell D., Gupta A., Jonas W. B., Coulter I., Andrade S. A. 2008. Traditional Indian medicine and homeopathy for HIV/AIDS: a review of the literature. AIDS Research and Therapy 5: 1-9

Gaetani G. F., Galiano S., Canepa L., Ferraris A. M., Kirkman H. N. 1989. Catalase and glutathione peroxidase are equally active in detoxification of hydrogen peroxide in human erythrocytes. Blood 73: 334-339

Gago-Dominguez M., Jiang X., Castelao J. E. 2007. Lipid peroxidation, oxidative stress genes and dietary factors in breast cancer protection: a hypothesis. Breast Cancer Research 9: 1-11

Gall G., Susan D. M., Mellon F. A., Davis A. L., Collins G.F., Verhoeyen M. E., Colquhoun. I. J. 2003. Characterization and content of flavonoid glycosides in genetically modified tomato (*Lycopersicon esculentum*) fruits. Journal of Agricultural Food Chemistry 51, 2438-2446

Garratt L. C., Linforth R., Taylor A. J., Lowe K. C., Power B., Davey M. R. 2005. Metabolite fingerprinting in transgenic lettuce. Plant Biotechnology Journal 3: 165-174

Gaurav V. Harlalka., Chandragauda R. Patil., Mahesh R. P. 2007. Protective effect of *Kalanchoe pinnata* pers. (Crassulaceae) on gentamicin-induced nephrotoxicity in rats. Indian Journal of Pharmacology 39: 201-205

Gauthaman K., Devaraj N. S. 2003. *Terminalia arjuna* barks protects rat heart with induction of the 72 kDa heat shock protein (Hsp 72). Biomedicine 23: 26-30

Gauthaman K., Banerjee S. K., Dinda A. K., Ghosh C. C., Maulik S. K. 2005. *Terminalia arjuna* (Roxb.) protects rabbit heart against ischemic-reperfusion injury: role of antioxidant enzymes and heat shock protein. Journal of Ethnopharmacology 96: 403–409

Gerszten R. E., Lim Y. C., Ding H. T., Snapp K., Kansas G., Dichek D. A., Cabanas C., Sanchez-Madrid F., Gimbrone M. A., Rosenzweig A., Luscinskas F. W. 1998. Adhesion of monocytes to vascular cell adhesion molecule-1–transduced human endothelial cells implications for atherogenesis. Circulation 82: 871-878

Ghosh S., Karin M. 2002. Missing piecies in the NF-κB puzzle. Cell 109: 81-96

Glish G. L., Vachet R. W. 2003. The basis of mass spectrometry in the twenty-first century. Nature 2: 140-150

Gomez-Espina J., Blanco G. E., Montes-Bay M., Sanz M. A. 2012. Elemental mass spectrometry for Se-dependent glutathione peroxidase determination in red blood cells as oxidative stress biomarker. Journal of Analytical Atomic Spectrometry 27: 1949-1954

Gosling J., Slaymaker S., Gu L., Tseng S., Zlot C. H., Young S. G., Rollins B. J., Charo I. F. 1999. MCP-1 deficiency reduces susceptibility to atherosclerosis in mice that overexpress human apolipoprotein B. The Journal of Clinical Investigation 103: 773-778

Grattendick K. J., Nakashima J. M., Feng L., Giri S. N., Margolin S. B. 2008. Effects of three anti-TNF-α drugs: etanercept, infliximab and pirfenidone on release of TNF-α in medium and TNF-α associated with the cell *in vitro*. International Immunopharmacology 8: 679-687

Grebe S. T. F., Singh R. J. 2011. LC-MS/MS in the Clinical laboratory – where to From here. The Clinical Biochemistry Reviews 32: 5-31

Griffiths J. 2008. A brief history of mass spectrometry. Analytical Chemistry 80: 5678-5683

Gupta R., Singhal S., Goyle A., Sharma V. N. 1999. Antioxidant and hypocholesterolaemic effects of *Terminalia arjuna* tree-bark powder: A randomised placebo-controlled trial. Journal of Association of Physicians of India 47: 231-235

Gupta S. K., Amit L., Vinay J., Siddhartha G., Jyoti. A. K. 2010. Phytochemistry of *Curcuma longa*-an overview. Journal of Pharmaceutical and Biomedical Sciences 4: 1-9

Hadi H. AR., Carr C. S., Suwaidi J. A. 2005. Endothelial dysfunction: cardiovascular

risk factors, therapy and outcome. Vascular Health and Risk Management 1: 183-198

Halket J. M., Waterman D., Przyborowska A. M., Patel R. K. P., Fraser P. D., Bramley P. M. 2005. Chemical derivatization and mass spectral libraries in metabolite profiling by GC/MS and LC/MS/MS. Journal of Experimental Botany 56: 219-243

Haq A. M. M., Huque M. Md., Rahman C. S. A., Nurul H. M. 2012. Cardiotonic effects of *Terminalia arjuna* extracts on guinea pig heart *in vitro*. Bangladesh Journal Pharmacology 7: 164-168

Haung D., Ou B., Prior R. L. 2005. The chemistry behind antioxidant capacity assays. Journal of Agricultural Food Chemistry 53: 1841-1856

Haven H. L., Rullkotter J. 1989. Oleanene, ursene, and other terrigenous triterpenoid, biological-marker hydrocarbons in Baffin Bay sediments. Proceedings of the Ocean Drilling Program, Scientific Results 105: 237-242

Higgins L.J., Rutledge J,C., 2009. Inflammation associated with the postprandial lipolysis of triglyceride-rich lipoproteins by lipoprotein lipase. Current Atherosclerosis Reports 11,199–205

Hiserodt R., Hartman T. G., Ho C-T., Rosen R. T. 1996. Characterization of powdered turmeric by liquid chromatography-mass spectrometry and gas chromatography-mass spectrometry. Journal of Chromatography A 740: 51-63

Hirschfield G. M., Pepys M. B. 2003. C-reactive protein and cardiovascular disease: new insights from an old molecule. An International Journal of Medicine 96: 793-807

Ho C. S., Lam C. W. K., Chan M. H. M., Cheung R. C. K., Law L. K., Lit L. C. W., Ng K. F., Suen M. W. M., Tai H. L. 2003. Electrospray Ionisation mass spectrometry: principles and clinical applications. Clinical Biochemistry 24: 3-12

Hoareau L., DaSilva E. J. 1999. Medicinal plants: a reemerging health aid. Electronic Journal of Biotechnology 2: 56-70.

Hoareau L., Bencharif K., Rondeau P., Murumalla R., Ravanan P., Tallet F., Delarue

P., Cesari M., Roche R., Festy F. 2010. Signalling pathways involved in LPS induced TNF alpha production in human adipocytes. Journal of Inflammation 7: 1-12

Hollander W. 1976. Role of hypertension in atherosclerosis and cardiovascular disease. The American Journal of Cardiology 38: 786-800

Hu C., Kitts D. D. 2001. Evaluation of antioxidant activity of epigallocatechin gallate in biphasic model systems *in vitro*. Molecular and Cellular Biochemistry 218: 147-155

Huang D., Ou B., Prior R. L. 2005. The chemistry behind antioxidant capacity assays.Journal of Agricultural and Food chemistry 53: 1841-1856

Huo Y., Ley K. F. 2004. Role of platelets in the development of atherosclerosis. Trends cardiovascular Medicine 14: 18-22

Iiyama K., Hajra L., Iiyama M., Li H., DiChiara M., Medoff B. D., Cybulsky M. I. 1999. Patterns of vascular cell adhesion molecule-1 and intercellular adhesion molecule-1 expression in rabbit and mouse atherosclerotic lesions and at sites predisposed to lesion formation. Circulation Research 85: 199-207

Imaizumi T., Itaya H., Fujita K., Kudoh D., Kudoh S., Mori K., Fujimoto K., Matsumiya T., Yoshida H., Satoh K. 2000. Expression of tumor necrosis factor-α in cultured human endothelial cells stimulated with lipopolysaccharide or interleukin-1 α. Atherosclerosis Thrombosis Vascular Biology 20: 410-415

Ishii Y., Partridge C. A., Vecchio P. J. D., Malik A. B. 1992. Tumor necrosis factor alfa mediated decrease in glutathione increases the sensitivity of pulmonary vascular endothelial cells to H_2O_2. The Journal of Clinical Investigation 89: 794-802

Ishida J., Kozuka M., Tokuda H., Nishino H., Nagumo S., Lee K. H., Nagai M. 2002. Chemopreventive potential of cyclic diarylheptanoids. Bioorganic and Medicinal Chemistry 10: 3361-3365

Jain S., Yadav P.P., Gill V., Vasudeva N., Singla. N. 2009. *Terminalia arjuna* a sacred medicinal plant: phytochemical and pharmacological profile. Phytochemical Reviews 8: 491-502

Jayaprakasha K. G., Mohan R. L. J., Sakariah K. K. 2002. Improved HPLC method

for the determination of curcumin, demethoxycurcumin and bisdemethoxycurcumin. Journal of Agricultural Food Chemistry 50: 3668-3672

Jawla S., Gupta A. K., Singla R., Gupta V. 2009. General awareness and relative popularity of allopathic, ayurvedic and homeopathic systems. Journal of Chemical and Pharmaceutical Research 1: 105-112

Jennings L. K. 2009. Mechanism of platelet activation: need for new stratergies to protect against platelet mediated atherothrombosis. Thrombosis Haemostasis 102: 248-257

Jiang. D. Q., Pu. Q. L., Huang. P., Huang. X. M., He.Y. Z., He. C. H., Zheng. Q. T., Yao. X. X. B. 1989. Studies on the chemical constituents of *Curcuma Kwangsiensis*. Acta Pharmaceutica Sinica 24: 357-359

Jiang H., Xie Z., Koo H. J., McLaughlin S. P., Timmermann B. N., Gang D. R. 2006. Metabolite profiling and phylogenetic analysis of medicinal *Zingiber* species: Tools for authentication of ginger (*Zingiber officinale* Rosc). Phytochemistry 15: 1673-1685

Jiang. H., Timmermann B. N., Gang D. R. 2006 a. Use of liquid chromatography–electrospray ionization tandem mass spectrometry to identify diarylheptanoids in turmeric (*Curcuma longa* L.) rhizome. Journal of Chromatography A, 1111, 21–31

Jie-Ping Fan., Chao-Hong He. 2006. Simulatneous quantification of three major bioactive triterpene acids in the leaves of *Diospyros Kaki* by high-performance liquid chromatography method. Journal of Pharmaceutical and Biomedical Analysis 41: 950-956

Jung Y., Lee J., Kim H. K., Moon B. C., Ji Y., Ryu D. H., Hwang G. S. 2012. Metabolite profiling of Curcuma species grown in different regions using 1h NMR spectroscopy and multivariate analysis. Analyst 137: 5597-5606

Kamath S., Blann A. D., Lip G. Y. H. 2001. Platelet activation: assessment and quantification. European Heart Journal 22: 1561-1571

Karthikeyan K., Sarala B. B. R., Gauthaman K., Sathish K. S., Niranjali D. S. 2003. Cardioprotective effect of the alcoholic extract of *Terminalia arjuna* bark in an *in vivo* model of myocardial ischemic reperfusion injury. Life Sciences 73: 2727–2739

Kaskoos R. A., Ali M., Naquvi K. J. 2012. New oleanene triterpenoids from the stem bark of *Terminalia arjuna*. Journal of Pharmacy Research 5: 2368-2372

Kenneth B. S. 2004. Fuctional metabolism. Regulation and adaptation. John Wiley and Sons

Khanna A. K., Chander R., Kapoor N. K. 1996. *Terminalia arjuna:* an ayurvedic cardiotonic, regulates lipid metabolism in hyperlipaemic rats. Phytotherapy Research 10: 663-665

Khuda B. A. R., Banerjee A., Biswas R., Pathak S., Boujedaini N., Belon P. 2008. Crude extract of turmeric reduces hepta-toxicity and oxidative stress in rats chronically fed carcinogens. Journal of Complementary and Integrative Medicine 5: 12-16

Kim C. S., Park H. S., Kawada T., Kim J. H., Lim D., Hubbard N. E., Kwon B. S., Erickson K. L., Yu R. 2006. Circulating levels of MCP-1 and IL-8 are elevated in human obese subjects and associated with obesity-related parameters. International Journal of Obesity 30: 1347–1355

Kim J. K., Park S. Y., Yeo Y., Cho H. S., Kim Y. B., Bae H., Park C. H., Lee J. H., Park S. U. 2013. Metabolite profiling of millet (*Panicum miliaceum*) using gas chromatography-time-of-flight mass spectrometry (GC-TOFMS) for quality assessment. Plant Omics Journal 1: 73-78

Kiso Y., Suzuki Y., Oshima Y., Hikino H. 1983. Sterostructure of curlone, a sesquiterpenoid of *Curcuma longa* rhizomes. Phytochemistry 22: 596-597

Kitagawa K., Matsumoto M., Sasaki T., Hashimoto H., Kuwabara K., Ohtsuki T., Hori M. 2002. Involvement of ICAM-1 in the progression of atherosclerosis in apoE-knockout mice. Atherosclerosis 160: 305-310

Kleinschnitz C., Stoll G., Bendszus M., Schuh K., Pauer H. U., Burfeind P., Renne C., Gailani D., Nieswandt B., Renne T. 2006. Targeting coagulation factor XII provides protection from pathological thrombosis in cerebral ischemia without interfering with hemostasis. The Journal of Experimental Medicine 203: 513-518

Koopman J., Maas A., Rezaee F., Havekes L., Verheijen J., Gijbels M., Haverkate F. 1997. Fibrinogen and atherosclerosis: a study in transgenic mice. Fibrinolysis and Proteolysis 11: 19-21

Korte W., Clarke S., Lefkowitz J. B. 2000. Short activated partial thromboplastin

times are related to increased thrombin generation and an increased risk for thromboembolism. American Journal of Clinical Pathology 113: 123-127

Koichi I., Nomura C., Ito S., Nagatsu A., Hino T., Oka H. 2008. Purification of curcumin, demethoxycurcumin and bisdemthoxycurcumin by high speed countercurrent chromatography. Journal of Agricultureal Food Chemistry 56: 9328-9336

Kubota K., Nakamura K., Kobayashi A. 1998. Acetoxy-1,8-cineoles as aroma constituents of *Alpinia galangal* Willd. America Chemical Society 1-4

Kumar S., Enjamoori R., Jaiswal A., Ray R., Seth S., Maulik S. K. 2009. Catecholamine-induced myocardial fibrosis and oxidative stress is attenuated by *Terminalia arjuna* (Roxb.). Journal of Pharmacy and Pharmacology 61: 1529-1536

Kumar R. 2013. Triterpenoid biomarkers in sediments. Chapter 5: 1-42

Kunle., Folashade O. E., Omoregie H., Ahmadu., Ochogu P. 2012. Standardization of herbal medicines - a review. International Journal of Biodiversity and Conservation 4: 101-112

Lacorte S., Fernandez-Alba A. R. 2006. Time of flight mass spectrometry applied to the liquid chromatographic analysis of pesticides in water and food. Mass Spectrometry Reviews 25: 866-880

Laschet J. K., Caligiuri G., Tupin E., Gaston A. T., Poirier B., Groyer E., Urbain D., Maisnier-Patin S., Sarkar R., Kaveri S. V., Lacroix D. S., Nicoletti A. 2005. Role of intrinsic coagulationpathway in atherosclerosis assessed in haemophilic apolipoprotein E knockout mice. Atheriosclerosis Thrombosis Vascular Biology 25: 1736

Lavrieux M., Jacob J., LeMilbeau C., Zocatelli R., Masuda K., Breheret J. G., Robert Disnar J. R. 2011. Occurrence of triterpenyl acetates in soil and their potential as chemo taxonomical markers of Asteraceae. Organic Geochemistry 1-35

Lee J. S., Park S. Y., Thapa D., Kim A. R., Shin H. M., Kim J. A. 2011. HMC05, Herbal formula, inhibits TNF-α induced inflammatory response in human umbilical vein endothelial cells. Evidence-Based Complementary and Alternative Medicine 1-11

Lefkowitz J. B. 2008. Coagulation pathway and physiology. American College of Pathologists. An Algorithmic Approach to Hemostasis Testing Chapter 1: 1-

12

Lentz S. R., Miller F. J., Piegors D. J., Erger R. A., Fernandez J. A., Griffin J. H., Heistad D. D. 2002. Anticoagulant response to thrombin are enhanced during regression of atherosclerosis in monkeys. Circulation 106: 842-846

Ley K., Huo Y. 2001. VCAM-1 is critical in atherosclerosis. Journal of Clinical Investigation 107: 1209-1210

Leytin V., Allen D. J., Lyubimov E., Freedman J. 2007. Higher thrombin concentrations are required to induce platelet apoptosis than to induce platelet activation. British Journal of Haematology 136: 762-764.

Li W., Feng J. T., Xiao Y. S., Wang Y. Q., Xue X. Y., Liang X. M. 2009. Three novel terpenoids from the rhizomes of *curcuma longa*. Journal of Asian Natural Products Research 6: 569-575

Li S., Yuan W., Deng G., Wang P., Yang P., Aggarwal B. B. 2011. Chemical composition and product quality control of turmeric (*Curcuma longa* L.). Pharmaceutical Crops 2: 28-54

Liang G., Shao L., Wang Y., Zhao C., Chu Y., Xiao J., Zhao Y., Li X., Yang S. 2009. Exploration and synthesis of curcumin analogues with improved structural stability both *in vitro* and *in vivo* as cytotoxic agents. Bioorganic and Medicinal Chemistry 17: 2623–2631

Libby P. 2002. Inflammation in atherosclerosis. Nature 420: 868-874

Lin T. C., Chien S. C., Chen H. F., Hsu F. L. 2000. Tannins and related compounds from Combretaceae plants (review). Chinese Pharmaceutical Journal 52: 1-26

Ling S., Nheu L., Komesaroff P. A. 2012. Cell adhesion molecules as pharmaceutical target in atherosclerosis. Mini Reviews Medicinal Chemistry 12: 175-183

Lisette D. Souza., Solimabi Wahidulla., Prabha Devi 2010. Antibacterial phenolics from the mangrove *Lumnitzera racemosa*. Indian Journal of Marine Sciences 39: 294-298

Liu S. F., Malik A. B. 2006. NF-κB activation as a pathological mechanism of septic shock and inflammation. American Journal of Physiology-Lung Cellular and Molecular Physiology 290: 622-645

Lockhart P. B., Bolger A. F., Papapanou P. N., Osinbowale O., Trevisan M., Levison

M. E., taubert K. A., Newburger J. W., Gornik H. L., Gewitz M. H., Wilson W. R., Smith S. C., Baddour L. M. 2012. Peridontal disease and atherosclerosis vascular disease: does the evidence support an independent association: a scientific statement from the american heart association. Circulation 125: 2520-2544

Lokhande P. D., Jagdale S. C., Chabukswar A. R. 2006. Natural remedies for heart diseases. Indian Journal of traditional Knowledge 5: 420-427

Lowe G. D. O. 2001. Factor IX and thrombosis. British Journal of Haematology 115: 507-513

Luisa M., Francesca C., Caterina G., Michela B., Anna M., Erika B., Eugenio R., Lisa B., Roberta S., Pietro T. 2011. A metabolite fingerprinting for the characterization of commericial botanical dietary supplements. Metabolomics 7: 437-445

Lusis A. 2000. Atherosclerosis. Nature 407: 233-241

Lusis A. J., Fogelman A. M., Fonarow G. C. 2004. Genetic basis of atherosclerosis: part I: new genes and pathways. Circulation 110: 1868-1873

Ma X. Q., Gang D. R. 2006. Metabolic profiling of turmeric (*Curcuma longa* L.) Plants derived from *in vitro* micropropagation and conventional greenhouse cultivation. Journal of Agricultural and Food Chemistry 1-11

McDonald P. P., Bald A., Cassatella M. A. 1997. Activation of the NF-κB pathway by inflammation stimuli in human neutrophils. Blood Journal 89: 3421-3433

Magesh V., Raman D., Pudupalayam K. T. 2008. Genotoxicity studies of dry extract of *Boswellia serrata*. Tropical Journal of Pharmaceutical Research 7: 1129-1135

Mahdi H. J., Ishak. A. 2010. Metabolite fingerprinting of three malaysian ginger (*Zingiber officinale* Roscoe) using gas chromatography-mass spectrometry. American Journal of Applied Sciences 1: 17-23

Malik N., Dhawan V. 2009. Inhibitory effects of *Terminalia arjuna* on platelet activation *in vitro* in healthy subjects and patients with coronary artery disease. Platelets 20: 183-90

Malinouski M., Zhou Y., Belousov V. V., Hatfield D. L., Gladyshev V. N. 2011.

Hydrogen peroxide probes directed to different cellular compartments. Public Library of Science One 6: 1-10

Manna P., Sinha M., Sil P. C. 2007. Phytomedicinal activity of *Terminalia arjuna* against carbon tetrachloride induced cardiac oxidative stress. Pathophysiology 14: 71–78

Mary K., Achuthan C.R., Babu B.H., Padikkala J., 2003. *In vitro* antioxidant and antithrombotic activity of *Hemidesmus indicus* (L) R.Br. Journal of Ethnopharmacology 87: 187–191

Mathe C., Culioli G., Archier P., Vieillescazes C. 2004. Characterization of archaeological frankincense by gas chromatography–mass spectrometry. Journal of Chromatography A, 1023: 277–285

Mathe C., Archier P., Nehme L., Vieillescazes C. 2009. The study of nabataean organic residues from mada in salih, ancient hegra, by gas chromatography-mass spectrometry. Archaeometry 51: 626-636

Mead J. R., Ramji D. P. 2002. The role of lipoprotein lipase in atherosclerosis. Cardiovascular Research 55: 261-269

Meera R., Devi P., Kameswari B., Madhumitha B., Merlin N. J. 2009. Antioxidant and hepatoprotective activities of *Ocimum basilicum* Linn. and *Trigonella foenum-graecum* Linn. against H_2O_2 and CCl_4 induced hepatotoxicity in goat liver. Indian Journal of Experimental Biology 47: 584-590

Meijers J. M., Tekelenburg W. H., Bouma B., Bertina R. 2000. High levels of coagulation factor XI as a risk factor for venous thrombosis. The New England Journal of Medicine 342: 696-701

Milenanikolova 2006. Infraspecific variability in the flavonoid composition of *Artemisia vulgaris* L. Acta Botanica Croatica 65: 13–18

Miranda-Vilela A. L., Alves P. Z., Akimoto A. K., Pereira L. S., Klautau G., Grisolia A. K. 2010. The effects of hydrogen peroxide-induced oxidative stress on leukocytes depends on age and physical training in healthy human subjects carrying the same genotypes of antioxidant enzyme's gene polymorphisms. American Journal of Human Biology 22: 807-812

Mizooku Y., Yoshikawa M., Tsuneyoshi T., Arakawa R. 2003. Analysis of oxidized epigallocatechin gallate by liquid chromatography/mass spectrometry. Rapid Communications in Mass Spectrometry 17: 1915-1918

Mohanty I., Arya D. G., Gupta S. K. 2006. Effect of *Curcuma longa* and *Oscimum sanctum* on myocardial apoptosis in experimentally induced myocardial ischemic-reperfusion injury. BMC Complementary and Alternative Medicine 6: 1-12

Moron U. M., Cortazar I. C. 2012. Protection against oxidative stress and IGF-I deficiency conditions. INTECH open Science/Open minds. Antioxidant Enzyme Chapter 1: 89-116

Morre S. A., Stooker W., Lagrand W. K., Van den Brule A. J. C., Niessen H. W. M. 2000. Microorganisms in the aetiology of atherosclerosis. Journal of Clinical Pathology 53: 647-654

Moussaieff A., Mechoulam R. 2009. Boswellia resin: from religious ceremonies to medical uses; a review of *in vitro, in vivo* and clinical trials. Journal of Pharmacy and Pharmacology 61: 1281-1293

Mrowiec Z. R., Olekowicz L., Dutcher J. P., De L. F. M., Lalezari P., Puszkin E. G. 1995. A novel technique for preparing improved buffy coat platelet concentrates. Blood Cells, Molecules, and Diseases 21: 25-33

Mullick A. E., Andrew F. P., Rama S. K., Sarada D. T., Jason P. E., John R. 2007. Apo-lipoprotein-E3 and nitric oxide-dependent modulation of endothelial cells inflammatory responses. Arteriosclerosis, Thrombosis, and Vascular Biology 27: 339-345

Nabasree D., Bratati, De. 2006. Antioxidant activity of some leafy vegetables of India: A comparative study. Food Chemistry 101, 471–474

Nagaraj M., Sunitha S., Varalakshmi P. 2000. Effect of lupeol, a pentacyclic triterpene, on the lipid peroxidation and antioxidant status in rat kidney after chronic cadmium exposure. Journal of Applied Toxicology 20: 413-417

Nagori K., Mukesh K. S., Amit A., Tekeshwar K., Dhansay D., Hemant B., Tripathi D. K. 2011. Piper betle L.: A review on its ethnobotany, phytochemistry, pharmacological profile and profiling by new hyphenated technique DART-MS (Direct Analysis in Real Time Mass Spectrometry). Journal of Pharmacy Research 4: 2991-2997

Nagpal M., Sood S. 2013. Role of curcumin in systemic and oral health: an overview. Journal of Natural Science, Biology and Medicine 4: 3-7

Nair M. P., Mahajan S., Reynolds J. L., Aalinkeel R., Nair H., Schwartz S. A., Kandaswami. C. 2006. The flavonoid quercetin inhibits proinflammatory cytokine (tumor necrosis factor alpha) gene expression in normal peripheral blood mononuclear cells via Modulation of the NF-κB system. Clinical and Vaccine Immunology 13: 319-328

Naito K., Fujikawa K. 1991. Activation of human blood coagulation factor XI independent of factor XI1. The Journal of Biological Chemistry. The American Society for Biochemistry and Molecular Biology 266: 7353-7358

Nakashima Y., Raines E. W., Plump A. S., Breslow J. L., Ross R. 1998. Upregulation of VCAM-1 and ICAM-1 at atherosclerosis-prone sites on the endothelium in the apoE-deficient mouse. Atherosclerosis Thrombosis Vascular Biology 18: 842-851

Nammi S., Gudavalli R., Ravindra B. B. S., Lodagala D. S., Boini K. M. 2003. Possible mechanisms of hypotension produced 70 % alcoholic extract of *Terminalia arjuna* (L.) in anaesthetized dogs. BMC Complementary and Alternative Medicine 3: 1-4

Norbert V. 1993. Chemical characterization of fossil resins (amber)- a critical review of methods, problems and possibilities: determination of mineral species, botanical sources and geographical attribution. Proceedings of a Symposium 147-157

Nugroho A, E., Yuniarti N., Istyastono E. P., Supardjan., Maeyama K., Hakim L. 2009. Anti-allergic effects of 1,5-bis(4'hydroxy-3-methoxyphenyl)-1,4-pentadiene-3-one on mast cell-mediated allergy model. Malaysian Journal of Pharmaceutical Sciences 7: 51-7

Nurfina A. N., Rekshohadiprodjo M. S., Timmerman H., Jenie U. A., Sugiyanto D., Vander Goot H. 1997. Synthesis of some symmetrical curcumin derivatives and their anti-inflammatory activity. European Journal of Medicinal Chemistry 32: 321-328

Oberoi L., Akiyama T., Lee K. H., Liu S. J. 2011. The aqueous extract, not organic extracts, of *Terminalia arjuna* bark exerts cardiotonic effect on adult ventricular myocytes. Phytomedicine 18: 259-265

Ogundare A. O., Olajuyigbe A. O. 2012. Bioactivity guided isolation of the antifungal components in sawdust extracts of *Piptadeniatrum africanum*, and *Terminalia ivorensis*. Malaysian Journal of Microbiology 8: 34-41

Ohkawa H., Ohushi N., Yagi. K. 1979. Assay for lipid peroxides in animal tissues by thiobarbituric acid reaction. Analytical Biochemistry 95: 351-358

Ohta H., Wada H., Niwa T., Kirii H., Iwamoto N., Fujii H., Saito K., Sekikawa K., Seishima M. 2005. Disruption of tumor necrosis factor-alfa gene diminishes the development of atherosclerosis in apoE-deficient mice. Atherosclerosis 180: 11-17

Ohtsuki K., Hayase M., Akashi K., Kopiwoda S., Strauss W. H. 2001. Detection of monocyte chemoattractant protein-1 receptor expression in experimental atherosclerotic lesions: an autoradiographic study. Circulation 104: 203-208

Okada T., Afendi F. M., Altaf-Ul-Amin M., Takahashi H., Nakamura K., Kanaya S. 2010. Metabolomics of medicinal plants: the importance of multivariate analysis of analytical chemistry data. Current Computer-Aided Drug Design 6: 179-96

Osterud B., Bjorklid E. 2003. Role of monocytes in atherogenesis. Physiological Reviews 83: 1069-1112

Ozkaya A., Celik S., Yuce A., Sahin Z., Yilmaz. O. 2010. The effects of ellagic acid on some biochemical parameters in the liver of rats against oxidative stress induced by aluminium. Kafkas University Veteiner Fakultesi Dergisi 16: 823-828

Paarakh P. M. 2010. *Terminalia arjuna* (Roxb.) Wt. and Arn. a review. International Journal of Pharmacology 6: 515-534

Pedraza-Chaverri J., Medina C. O. N., Avila L. R., Zuniga B. A. B., Orozco I. M. 2006. Reactive oxygen species scavenging capacity of different cooked garlic preparations. Life Sciences 78: 761-770

Pandey R. S., Singh B. K., Tripathi Y. B. 2005. Extract of gum resins of *Boswellia serrata* L. inhibits lipopolysaccharide induced nitric oxide production in rat macrophages along with hypolipidemic property. Indian Journal of Experimental Biology 43: 509-516

Pant P., Rastogi R. P. 1979. The triterpenoids. Phytochemistry 18: 1095-1108

Paramasivam M., Poi R., Banerjee H., Bandyopadhyay A. 2009. High performance thin layer chromatographyc method for quantitative determination of curcuminoids in *curcuma longa* germplasm. Food Chemistry 113: 640-644

Park S. Y., Kim D. S. H. L. 2002. Discovery of natural products from *Curcuma longa* that protect cells from beta-amyloid insult: a drug discovery effort against alzheimers disease. Journal of Natural Products 65: 1227-1231

Park B., Prasad S., Yadav V., Sung B., Aggarwal B. B. 2011. Boswellic acid suppresses growth and metastasis of human pancreatic tumors in an orthotopic nude mouse model through modulation of multiple targets. Public Library of Science One 6: 1-11

Parmar H. S., Panda S., Jatwa R., Kar A. 2006. Cardioprotective role of *Terminalia arjuna* bark extract is possibly mediated through alternations in thyroid hormones. Pharmazie 61: 793-795

Parthasarathy V. A., Chempakam B., Zachariah T. J. 2008. Chemistry of spices. CAB International Publishers 97-124

Parveen A., Babbar R., Agarwal S., Kotwani A., Fahim M. 2011. Mechanistic clues in the cardioprotective effect of *Terminalia arjuna* bark extract in isoproterenol-induced chronic heart failure in rats. Cardiovascular Toxicology 11: 48-57

Parthasarthy U., Johny A. K., Jayarajan K., Pathasarathy V. A. 2007. Site suitability for turmeric production in India GIS interpretation. Natural Product Radiance 6: 142-147

Pascale C. D., Graham V., Fowkes R. C., Wheeler J. C. P. D., Botham K. M. 2009. Suppression of nuclear factor-κB activity in macrophages by chylomicron remnants: modulation by the fatty acid composition of the particles. Federation of European Biochemical Societies 276: 5690-5702

Patnaik T., Dey R. K., Gouda P. 2007. Isolation of triterpenoid glycoside from bark of *Terminalia arjuna* using chromatographic technique and investigation of pharmacological behaviour upon muscle tissues. E-Journal of Chemistry 4: 474-479

Patwardhan B., Warude D., Pushpangadan P., Bhatt N. 2005. Ayurveda and traditional chinese medicine: a comparative overview. Evidence Based Complementary and Alternative Medicine 2: 465-473

Pawar R. S., Bhutani K. K. 2005. Effect of oleanane triterpenoids from *Terminalia arjuna*-a cardioprotective drug on the process of respiratory oxyburst. Phytomedicine 12: 391-393

Pitt J. J. 2009. Principles and applications of liquid chromatography-mass spectrometry in clinical biochemistry. The Clinical Biochemist Reviews 30: 19-34

Pixley R. A., Schapira M., Colman R. W. 1985. Effect of heparin on the inactivation rate of human activated factor XII by antithrombin III. Blood 66: 198-203

Pizzimenti S., Toaldo C., Pettazzoni P., Dianzani M. U., Barrera G. 2010. The "two-faced" effects of reactive oxygen species and the lipid peroxidation product 4-hydroxynonenal in the hallmarks of cancer. Cancers 2: 338-363

Poeckel D., Tausch L., Kather N., Jauch J., Werz O. 2006. Boswellic acids stimulate arachidonic acid release and 12-lipoxygenase activity in human platelets independent of ca^{2+} and differentially interact with platelet type 12-lipoxygenase. Molecular Pharmacology 70: 1071-1078

Poeckel D., Tausch L., George S., Jauch J., Werz 2006a. 3-O-acetyl-11-keto-boswellic acid decreases basal intracellular ca^{2+} levels and inhibits agonist induced ca^{2+} mobilization and mitogen activated protein kinase activation in human monocytic cells. The Journal of Pharmacology and Experimental Therapeutics 316: 224-232

Ponchel F., Toomes C., Bransfield K., Leong F. T., Douglas S. H., Field S. L., Bell S. M., Combaret V., Puisieus A., Mighell A. J., Robinson P. A., Inglehearn C. F., Isaacs J. D., Markham A. F. 2003. Real time PCR based on SYBR-green I fluorescence: an alternative to the taqman assay for a relative quantification of gene rearrangements, gene amplifications and micro gene deletions. BioMed Central Biotechnology 3: 1-13

Pradeep D., Pamila D. 2012. Research in Ayurveda: challenges and way forward. Internaltional Journal of Research in Ayurveda and Pharmacy 3: 23-26

Prasenjit M., Mahua S., Prasantha P., Parames C. S., 2007. Arjunolic acid, a triterpenoid saponin, ameliorates arsenic induced cytotoxicity in hepatocytes. Chemico-Biological Interactions 170: 187–200

Prokai L., Rivera P. N. M., Pokai T. K. 2013. Quantitative structure-activity relationships predicting the antioxidant potency of 17β-estradiol-related polycyclic phenols to inhibit lipid peroxidation. International Journal of Molecular Sciences 14: 1443-1454

Qian Y., Wang Y., Sa R., Yan H., Pan X., Yang Y., Sun Y. 2013. Metabolite

fingerprinting of *Angelica sinensis* during growth using UPLC-TOFMS and chemometrics data analysis. Chemistry Central Journal 7: 1-10

Quave C., Estevez C. M., Compadre C. M., Hobby G., Hendrickson H., Beenken K. E., Smeltzer M. S. 2012. Ellagic acid derivatives from *Rubus ulmifolius* inhibit *Staphylococcus aureus* Biofilm formation and improve response to antibiotics. Public Library of Science One 7: 1-16

Radhakrishnan R., Wadsworth R. M., Gray A. I. 1993. *Terminalia arjuna*, an Ayurvedic cardiotonic, increases contractile force of rat isolated atria. Phytotherapy 7: 266-268

Raghavan G., Subha R., Vijay k. M., Shirwaikarm A., Ajay K. Singh, R., Shanta M., Palpu P., 2003. Studies on the antioxidant activities of *Desmodium gangeticum*. Biological and Pharmaceutical Bulletin 26: 1424—1427

Ragavan B., Krishnakumari S. 2005. Effect of *Terminalia arjuna* stem bark extract on the activities of marker enzymes in alloxan induced diabetic rats. Ancient Science of Life 25: 8-15

Rahman K. Studies on free radicals, antioxidants, and co-factors. 2007. Clinical Interventions in Aging 2: 2219-236

Rahmatullah M., Md Azam N. K., Pramanik S., Sania, Rahman S., Jahan R. 2012. Antihyperglycemic activity evaluation of rhizomes of *Curcuma zedoaria* (Christm.) Roscoe and fruits of *Sonneratia caseolaris* (L.) Engl. International Journal of Pharma Tech Research 4: 125-129

Rajeswara R. B. R., Syamasundar K. V., Rajput D. K., Nagaraju G., Adinarayana G. 2012. Biodiversity, conservation and cultivation of medicinal plants. Journal of Pharmacognosy 3: 59-62

Ram A., Lauria P., Gupta R., Pradeep K., Sharma V. N. 1997. Hypocholesterolaemic effects of *Terminalia arjuna* tree bark. Journal of Ethnopharmacology 55: 165-169

Renne T., Schmaier A. H., Nickel K. F., Blomback M., Maas C. 2012. *In vivo* roles of factor XII. Blood 120: 4296-4303

Revathy S., Elumalai S., Benny M., Antony B. 2011. Isolation, purification and identification of curcuminoids from turmeric (*Curcuma longa* L.) by column chromatography. Journal of Experimental Sciences 2: 21-25

Ravishankar B., Shukla V. J. 2007. Indian systems of medicine: a brief profile. African journal of traditional, Complementary and Alternative Medicines 4: 319-337

Ravindran P.N., Nirmal B. K., Sivaraman K. 2007. Turmeric. The genus *Curcuma*. CRC Press

Ridker P. M., Rifai N., Stampfer M. J., Hennekens C. H. 2000. Plasma concentration of interleukin-6 and the risk of future myocardial infraction among apparently healthy men. Circulation 101: 1767-1772

Robert S., Baccelli C., Devel P., Dogne J. M., Leclercq J. Q. 2010. Effects of leaf extracts from *Croton zambesicus* Muell. Arg. on hemostasis. Journal of Ethnopharmacology 128: 641-648

Ross R., 1999. Atherosclerosis – an inflammatory disease. The New England Journal of Medicine 340, 115-26

Ruggeri Z. M., Mendolicchio G. L. 2007. Adhesion mechanisms in platelet function. Circulation Research 100: 1673-1685

Ruslay S., Abas F., Shaari K., Zainal Z., Maulidiani S. H., Ahmad I. D., Lajis N. H. 2007. Characterization of the components present in the active fractions of health gingers (*Curcuma xanthorrhiza* and *Zingiber zerumbet*) by HPLC–DAD–ESIMS. Food Chemistry 104: 1183–1191

Sabeti S., Exner M., Mlekusch W., Amighi J., Quehenberger P., Rumpold H., Maurer G., Minar E., Wagner O., Schillinger M. 2005. Prognostic impact of fibrinogen in carotid atherosclerosis: nonspecific indicator of inflammation or independent predictor of disease progression. Stroke 36: 1400-1404

Saha A., Pawar V. M., Jayaraman S. 2012. Characetrisation of polyphenols in *Terminalia arjuna* bark extracts. Indian Journal of Pharmaceutical Sciences 74: 339-347

Sahu N. P. 1996. Triterpenoids saponins of *Mimusops Elengi*. Phytochemistry 41: 883-886

Sano H., Tomita K., Hitsuda Y. 1997. Expression of vascular cell adhesion molecule-1 on human pulmonary artery endothelial cells and human umbilical vein endothelial cells stimulated by tumor necrosis factor-α, interleukin-1β and lipopolysaccharide. Yonago Act Medica 40: 21-30

Sarabhai S., Sharma P., Capalash N. 2013. Ellagic acid derivatives from *Terminalia Chebula* Retz. downregulates the expression of quorum sensing genes to attenuate *Pseudomonas aeruginosa* PAO1 virulence. Public Library of Science One 8: 1-11

Sasikumar B. 2005. Genetic resources of *Curcuma*: diversity, characterization and utilization. Plant Genetic Resources 2: 230-251

Sati S. C., Sati N., Sati O. P. 2011. Bioactive constituents and medicinal importance of genus Alnus. Pharmacological Reviews 5: 174-183

Saxena R., Kannan M., Choudhry V. P. 2007. Laboratory studies in coagulation disorders. Indian Journal of Pediatrics 74: 649-655

Scholz M., Gatzek S., Sterling A., Fiehn O., Selbig J. 2004. Metabolite fingerprinting: detecting biological features by independent component analysis. Bioinformatics 20: 2447-2454

Sen S., Chakraborty R., Sridhar C., Reddy Y. S. R., De B. 2010. Free radicals, antioxidants, diseases and phytomedicines: current status and future prospect. International Journal of Pharmaceutical Sciences Review and Research 3: 91-100

Sengupta K., Alluri K. V., Satish A. R., Mishra S., Golakoti T., Sarma K.V. S., Dey D., Raychaudhuri S. P. 2008. A double blind, randomized, placebo controlled study of the efficacy and safety of 5- Loxin for treatment of osteoarthritis of the jnee. Arthritis Research and Therapy 10: 1-11

Serhan C. N., Brain S. D., Buckley C. D., Gilroy D. W., Haslett C., Oneill L. A. J., Perretti M., Rossi A. G., Wallace J. L. 2007. Resolution of Inflammation: state of the art, definitions and terms. Federation of European Biochemical Societies 21: 325-332

Shah P. K. 2001. Link between infection and atherosclerosis: who are the culprits: viruses, bacteria, both or neither. Circulation 103: 5-6

Shaila H. P., Udupa A. L., Udupa S. L. 1997. Experimental and clinical studies on the effect of *Terminalia arjuna* in hyperlipidemia. Federation of European Biochemical Societies 11: 1262

Shaila H. P., Udupa S. L., Udupa A. L., 1998. Hypolipidemic activity of three indigenous drugs in experimentally induced atherosclerosis. International Journal of Cardiology

67, 119–124

Sharma M. L., Khajuria A., Kaul A., Singh S., Singh G. B., Atal. C. K. 1998. Effect of Salai guggal ex-*Boswellia serrata* on cellular and hormonal immune responses and leucocyte migration. Agents and Actions 24: 161-164

Sharma M, Kishore K., Gupta S. K., Joshi S, Arya D. S. 2001. Cardioprotective potential of *Ocimum sanctum* in isoproterenol induced myocardial infarction in rats. Molecular and Cellular Biochemistry 225: 75-83

Sharma S., Thawani V., Hingorani L., Shrivastava M., Bhate V. R., Khiyani R. 2004. Pharmacokinetic study of 11-keto-β-boswellic acid. Phytomedicine 11: 255-260

Sharma A., Mann A. S., Gajbhiye V., Kharya M. D. 2007. Phytochemical profile of *Boswellia serrata*: an overview. Pharmacognosy Reviews 1: 137-142

Sheng H., Sun H. 2011. Synthesis, biology and clinical significance of pentacyclic triterpenes: a multi target approach to prevent and treatment of metabolic and vascular diseases. Natural Products Reports 28: 543-593

Shi Q., Vandeberg J. F., Jett C., Rice K., Leland M. M., Talley L., Kushwaha R. S., Rainwater D. L., Vandeberg J. L., Wang X. Li. 2005. Arterial endothelial dysfunction in baboons fed a high-cholestrol, high-fat diet. American Journal of Clinical Nutrition 82: 751-759

Shibeko A. M., Lobanova E. S., Panteleev M. A., Ataullakhanov F. I. 2010. Blood flow controls coagulation onset via the positive feedback of factor VII activation by factor Xa. BioMed Central Systems Biology 4: 1-12

Shyur L. F., Liu C. P., Chien S. C. 2013. Metabolomics in herbal medicine research. The Hand Book of Plant Metabolomics

Siddiqui M. Z. 2011. *Boswellia serrata*, a potential anti-inflammatory agent: an overview. Indian journal of Pharmaceutical Sciences 73: 255-261

Simonini A., Moscucci M., Mullwe D. W. M., Bates E. R., Pagani F. D., Burdick M. D., Strieter R. M. 2000. IL-8 is an angiogenic factor in human coronary atherectomy tissue. Circulation 101: 1519-1526

Simopoulos A. P. 2008. The importance of the omega-6/omega-3-fatty acid ratio in cardiovascular disease and other chronic diseases. Experimental Biology and Medicine 233: 674-688

Singh G. B., Atal C. K. 1986. Pharmacology of an extract of salai guggal ex-*Boswellia serrata*, a new non-steroidal anti-inflammatory agent. Agents Actions 18: 407-412

Singh S., Sankar B., Rajesh S., Sahoo K., Subudhi E., Nayak S. 2011. Chemical composition of turmeric oil (*Curcuma longa*. L. cv. Roma) and its antimicrobial activity against eye infecting pathogens. Journal of Essential Oil Research 23: 11-18

Singh U., Tabibian J., Venugopal S. K., Devaraj S., Jialal I. 2005. Development of an *in vitro* screening assay to test the anti-inflammatory properties of dietary supplements and pharmacologic agents. Clinical Chemistry 51: 2252-2256

Singleton V. L., Orthofer R., Lamuela R. R. M. 1999. Analysis of total phenols and other oxidation susbstrates and antioxidants by means of folin-ciocalteu reagent. Methods in Enzymology 299: 152-178

Sinha M., Manna P., Sil P. C. 2008. *Terminalia arjuna* protects mouse hearts against sodium fluoride induced oxidative stress. Journal of Medicinal Food 11: 733-740

Sirat H. M., Meng L. L. 2009. Chemical components of the rhizome oil of *Curcuma Heyneana* Val. Malaysian Journal of Science 28: 323-328

Smith A. R., Johnson H. E., Hall M. 2003. Metabolite fingerprinting of salt-stressed tomatoes. Bulgarian Journal of Plant Physiology 153-163

Steffel J., Luscher T. F., Tanner F. C. 2006. Tissue factor in cardiovascular diseases: molecular mechanisms and clinical implications. Circulation 113: 722-731

Sterk V., Buchele B., Simmet T. 2004. Effect of food intake on the bioavailability of boswellic acids from a herbal preparation in the healthy volunteers. Planta Medica 12: 1155-1160

Strober W. 2001. Trypan blue exclusion test of cell viability. Current Protocol Immunology 3: 1

Subramaniam S. 2011. Anti-hyperlipidemic and antioxidant potential of different fractions of *Termianlia arjuna* Roxb. bark against PX-407 induced hyperlipidemia. Indian Journal of Experimental Biology 49: 282-288

Sultana B., Anwar F., Przybylski R. 2007. Antioxidant activity of phenolic

components present in barks of *Azadirachta indica*, *Terminalia arjuna*, *Acacia nilotica* and *Eugenia jambolana* Lam. trees. Food Chemistry 104: 1106-1114

Suksamrarn A., Eiamong S., Piyachaturawat P., Jinda C. 1994. Phenolic diarylheptanoids from *Curcuma xanthorrhiza*. Phytochemistry 36: 1505-1508

Sumner L. W., Mendes P., Dixon R. A. 2003. Plant metabolomics: large-scale phytochemistry in the functional genomics era. Phytochemistry 62: 817-836

Sundaryono A., Nourmamode A., Gardrat C., Grelier S., Bravic G., Chasseau D., Castellan A. 2003. Studies on the photochemistry of 1,7-diphenyl-1,6-heptadiene-3,5-dione, a non-phenolic curcuminoid model. Photochemical Photobiological Sciences 2: 914-20

Tabaka H. M., Peluso J., Vonesch J. L., Hentsch D., Kessler P., Reimund J. M., Dumont S., Muller C. D. 2012. Unlike for human monocytes after LPS activation, release of TNF-α by THP-1 cells is produced by a TACE catalytically different from constitutive TACE. Public Library of Science 7: 1-12

Taneja S. C., Sethi V. K., Dhar K. L., Kapil R. S. 1997. Boswellic acids composition and preparation thereof. Patent number 5,629,351

Tausch L., Henkel A., Siemoneit U., Poeckel D., Kather N., Franke L., Hofmann B., Schneider G., Angioni C., Geisslinger G., Skarke C., Holtmeier W., Beckhaus T., Karas M., Jauch J., Werz O. 2009. Identification of human cathepsin G as a functional target of boswellic acids from the anti-inflammatory remedy frankincense. Journal of Immunology 183: 3433-3442

Taylor S. J., McDowell I. J. 1992. Determination of the curcuminoid pigments in turmeric (*Curcuma domestica* Val) by reversed-phase high-performance liquid chromatography. Chromatographia 34: 73-77

Tedder T. F., Steeber D., Chen A., Engel P. 1995. The selectins: vascular adhesion molecules. Federation of American Societies for Experimental Biology 9: 866-873

Teramoto S., Tomita T., Matsui H., Ohga E., Matsus. T., Ouchi Y. 1999. Hydrogen peroxide induced apoptosis and necrosis in human lung fibroblasts: protective roles of glutathione. Japan Journal of Pharmacology 79: 33-40

Tetali S. D., Budamagunta M. S., Simion C., Den Hartigh L. J., Kalai T., Hideg K., Hatters D. M., Weisgraber K. H., Voss J. C., Rutledge J. C., 2010. VLDL lipolysis products increase VLDL fluidity and convert apolipoprotein E4 into a more expanded conformation. Journal of Lipid Research 51, 1273-83

Tian Y, Xu W, Zhu C, Lin S, Li Y, Xiong L, Wang S, Wang L, Yang Y, Guo Y, Sun H, Wang X, Shi J. 2011. Lathyrane diterpenoids from the roots of *Euphorbia micractina* and their biological activities. Journal Natural Products 27: 1221-1229

Tilak J. C., Devasagayam T. P. A., Adhikari S., Lele R. D., Kon T., Handa O., Naito Y.,Yoshikawa T. 2006. Cellular membrane protection against reactive oxygen species by *Terminalia arjuna* and its active component baicalein. Journal of Clinical Biochemistry and Nutrition 39: 75-87

Tomkin G. H., Owens D. 2012. LDL as a cause of atherosclerosis. The Open Atherosclerosis and Thrombosis Journal 5: 13-21

Tsao R. 2010. Chemistry and biochemistry of dietary polyphenols. Nutrients 2: 1231-1246

Villas-Boas S. G., Noel S., Lane G. A., Attwood G., Cookson A. 2006. Extracellular metabolomics: a metabolic footprinting approach to assess fiber degradation in complex media. Analytical Biochemistry 349: 297-305

Vivek K. G., Surendra K. S. 2006. Plants as natural antioxidants. Natural Product Radiance 5: 326-334

Wang W., Ali Z., Shen Y., Li X. C., Khan I. A. 2010. Ursane triterpenoids from the bark of *Terminalia arjuna*. Fitoterapia 81: 480-484

Wang W., Ali Z., Li X. C., Shen Y., Khan I. A. 2010a. Triterpenoids from two *Terminalia* species. Planta Medica 76: 1751-1754

Weber C. 2008. Chemokines in atherosclerosis, thrombosis, and vascular biology. Artherosclerosis Thrombosis Vascular Biology 28: 1896

Wiese G., Barthel S. R., Dimitroff C. J. 2009. Analysis of physiologic E-selectin mediated leukocyte rolling on microvascular endothelium. Journal of Visualized Experiments 1-5

Wulf D. 2002. Free radicals in the physiological control of cell function. Physiological Reviews 82: 47-95

Woulfe D., Yang J., Brass L. 2001. ADP and platelets: the end of the beginning. The Journal of Clinical Investigation 107: 1591-1598

Xian-Guo He. 2000. On-line identification of phytochemical constituents in botanical extracts by combined high-performance liquid chromatographic– diode array detection–mass spectrometric techniques. Journal of Chromatography A 880: 203-232

Xie Z., Ma X., Gang D. R. 2009. Modules of co-regulated metabolites in turmeric (*Curcuma longa*) rhizome suggest the existence of biosynthetic modules in plant specialized metabolism. Journal of Experimental Botany, Vol. 60, No. 1, pp. 87–97

Yadav D., Yadav S. K., Khar R. K., Mujeeb M., Akhtar M. 2013. Turmeric (*Curcuma longa* L.): A promising spice for phytochemical and pharmacological activites. International Journal of Green Pharmacy 7: 85-89

Yang X.X., Tang Y.M., Zhao S.Y., Shao Z.Y., 2011. A triterpenoid and phenolic compounds from *Myrica rubra* seeds. Chemistry of Natural Compounds 47, 658-659

Yagi K. 1988. Lipid peroxides as a cause of atherosclerosis. The role of oxygen radicals in cardiovascular Diseases 271-286

Yeh M., Leitinger N., Martin R., Onai N., Matsushima K., Vora D. k., Berliner J. A., Reddy S. T. 2001. Increased transcription of Il-8 in endothelial cells is differentially regulated by TNF- alfa and oxidized phospholipids. Atherosclerosis Thrombosis Vascular Biology 221: 1585-1591

Yeh C. H., Fredenburgh J. C., Weitz J. I. 2012. Oral direct factor Xa inhibitors. Circulation Research 28: 1069-1078

Yoshikawa T., Naito Y. 2002. What is oxidative stress?. The Journal of the Japan Medical Association 124: 1549-1553

Zhang L., Wang Q., Guo Q., Chang Q., Zhu Z., Liu L., Xu H. 2012. Growth, physiological characteristics and total flavonoid content of *Glechoma longituba* in response to water stress. Journal of Medicinal Plants Research 6: 1015-1024

Zhou J. Y., Tang F-d., Mao G., Bian R. 2004. Effect of alfa-pinene on nuclear translocation of NF-κB in THP-1 cells

Zhou L., Schmaier A. H. 2005. Platelet aggregation testing in platelet rich plasma. American journal of Clinical Pathology 123: 172-183

Zhou Q., Bea F., Preusch M., Wang H., Isermann B., Shahzad K., Katus H. A., Erwin B. 2011. Evaluation of plaque stability of advanced atherosclerotic lesions in apo-E deficient mice after treatment with the oral factor Xa inhibitor rivaroxaban. Mediators of Inflammation 1-9

Zhu Y. Z., Huang S. H., Tan B. K. H., Sun J., Whiteman M., Zhu Y. C. 2004. Antioxidants in chinese herbal medicines: a biochemical perspective. Natural Products Reports 21: 478-489

Zucker M. B., Nachmias V. T. 1985. Platelet activation. Atherosclerosis Thrombosis Vascular Biology 5: 2-18

Annexure I

RESEARCH PAPERS

Praveen K. Kokkiripati, Lepakshi Md. Bhakshu, Swathi Marri, K. Padmasree, Anupama T. Row, Agepati S. Raghavendra, Sarada D. Tetali. Gum resin of *Boswellia serrata* inhibited human monocytic (THP-1) cell activation and platelet aggregation. Journal of Ethnopharmacology 137 (2011) 893-901.

Praveen K. Kokkiripati, Ratnam V. Kamsala, Leena Bashyam, Nalini Manthapuram, Prasanth Bitla, Vidyadhari Peddada, Agepati S. Raghavendra, Sarada D. Tetali. Stem-bark of *Terminalia arjuna* attenuates human monocytic (THP-1) and aortic endothelial cell activation. Journal of Ethnopharmacology 146 (2013) 456-464.

ORAL PRESENTATION

Praveen Kumar. Kokkiripati., L. Md. Bakshu., Sudhansu Sekhar Choudhury., A.S. Raghvendra, Sarada D. Tetali. Free radical scavenging and in vitroanti-diabetic properties of *Terminalia arjuna*. AP AKADEMI OF SCIENCES and OSMANIA UNIVERSITY, 14th-16th November 2008, HYDERABAD

POSTERS PRESENTED

Praveen Kumar. Kokkiripati., L. Md. Bakshu., Sudhansu Sekhar Choudhury., A.S. Raghvendra, Sarada D. Tetali. Evaluation of antioxidant and anti-diabetic properties of Indian medicinal plant extracts by *in vitro* assays. BIO QUEST 24th JANUARY 2009, UNIVERSITY OF HYDERABAD, HYDERABAD

ATTENDED CONFERENCE

International Conference on Novel Updates In Reproductive Biology and Comparative Endocrinology and The 27th Annual Meeting Of The Society For Reproductive Biology And Comparative Endocrinology (SRBCE-XXVII) JANUARY19-21st, 2009. UNIVERSITY OF HYDERABAD, HYDERABAD

Journal of Ethnopharmacology 137 (2011) 893–901

Contents lists available at ScienceDirect

Journal of Ethnopharmacology

journal homepage: www.elsevier.com/locate/jethpharm

Gum resin of *Boswellia serrata* inhibited human monocytic (THP-1) cell activation and platelet aggregation

Praveen K. Kokkiripati[a], Lepakshi Md. Bhakshu[a,1], Swathi Marri[a,1], K. Padmasree[b], Anupama T. Row[c], Agepati S. Raghavendra[a], Sarada D. Tetali[a,*]

[a] *Department of Plant Sciences, University of Hyderabad, Hyderabad 500046, India*
[b] *Department of Biotechnology, University of Hyderabad, Hyderabad 500046, India*
[c] *University Health Centre, University of Hyderabad, 500046, India*

ARTICLE INFO

Article history:
Received 26 January 2011
Received in revised form 31 May 2011
Accepted 2 July 2011
Available online 8 July 2011

Keywords:
Anticoagulant
Antioxidant
Antiplatelet
Boswellia serrata gum resin
Monocytes
Śallakī

ABSTRACT

Ethnopharmacological relevance: Stem bark gum resin extract of *Boswellia serrata* is traditionally used in India for its hemostatic, antiinflammatory and cardiovascular health effects and it is named as Śallakī in Ayurvedic medicine.
Aim of the study: This study was conducted to evaluate the antioxidative and antithrombotic properties of stem bark gum resin extracts of *Boswellia serrata* (BS).
Materials and methods: The inhibitory activity of the BSWE and BSAE on $FeCl_3$ induced lipid peroxidation (*in vitro*) in rat liver and heart homogenates was measured spectrophotometrically. Their effect on H_2O_2 induced reactive oxygen species (ROS) generation in human monocytic (THP-1) cells was investigated by tracking intensity of a cell permeable fluorescent dye, H_2DCFDA and subjecting the cell samples to confocal microscopy. Further, the effect of BSAE and BSWE on ADP-induced platelet aggregation was assessed using a multimode detection plate reader, plasma coagulation times using an automated blood coagulation analyzer and on human blood clotting factors Xa and XIa using chromogenic substrate. Phytomarker analysis of the water (BSWE) and hydroalcoholic (BSAE) extracts of BS-gum resin was done through HPLC using a standard compound AKβBA.
Results: BSAE and BSWE inhibited, to varied extents, the lipid peroxidation in liver (80%) and heart (50%) tissue homogenates of male Wistar rats. Further, BSAE (30 μg dwt/mL) and BSWE (300 μg dwt/mL) attenuated ≥60% of H_2O_2 mediated ROS generation in THP-1 cells. In case of standard compounds, ascorbate (20 μg dwt/mL) and butylated hydroxytoluene (BHT) (10 μg dwt/mL) completely scavenged ROS in the cells. BSAE and BSWE at 3 mg dwt/mL completely inhibited ADP induced platelet aggregation and activities were comparable to 20 μg/mL of heparin. The extracts also showed very high activity in prolonging coagulation time periods. Both types of extracts extended prothrombin time (PT) from ~13 to >60 s and activated partial thromboplastin time (APTT) from ~32 s to >90 s. BSAE inhibited clotting factors Xa and XIa remarkably at 6 μg of dwt where as BSWE did not show much effect on FXa and showed 30% inhibition on FXIa at 120 μg. 10 μg of heparin was required to inhibit about 30% activity of the above factors. HPLC analyses suggested that BSAE and BSWE had AKβBA of 9% (w/w) and 7.8% (w/w) respectively.
Conclusion: Present study demonstrated antioxidant and antithrombotic anticoagulant activities of water and hydroalcoholic extracts of *Boswellia serrata*'s gum resin. We suggest that BS-gum resin as a good source for lead/therapeutic compounds possessing antioxidant, antiplatelet and anticoagulant activities.

Abbreviations: AKβBA, 3-acetyl-11-keto-β-boswellic acid; APTT, partial thromboplastin time; BHT, butylated hydroxytoluene; BSAE, hydroalcoholic extract of *Boswellia serrata*'s gum resin; BSWE, water extract of *Boswellia serrata*'s gum resin; H_2DCFDA, 2′,7′-dichlorofluorescin diacetate; PPP, platelet poor plasma; PRP, platelet rich plasma; PT, prothrombin time; ROS, reactive oxygen species; THP-1, human acute monocytic leukemia cell line.

* Corresponding author at: Department of Plant Sciences, School of Life Sciences, University of Hyderabad, Hyderabad 500046, India. Tel.: +91 40 2313 4512; fax: +91 40 2301 0120.
E-mail addresses: sdtsl@uohyd.ernet.in, saradakanakagiri@gmail.com (S.D. Tetali).

[1] These authors contributed equally to the work.

0378-8741/$ – see front matter © 2011 Elsevier Ireland Ltd. All rights reserved.
doi:10.1016/j.jep.2011.07.004

1. Introduction

Extracts of *Boswellia serrata*'s stem bark gum resin (Śallakī or Salai guggal or Frankincense) are traditionally used in India (Ayurvedic/ethnomedicine) to treat various types of blood disorders, inflammatory health ailments, pain and cardiac debility (Paranjpe, 2001). There are several scientific reports on pharmacological activities of BS-gum resin. Gummy exudates of *Boswellia serrata*'s stem bark or its major constituents, boswellic acids have anti-inflammatory (Ammon, 2006; Shen and Lou, 2008), anticancerous (Aman et al., 2009) and anti-ulcerous (Singh et al., 2008) activities. Molecular targets for *Boswellia* extract in the inflammation pathway are identified and these include leukotrienes (inflammatory chemical messengers), 5-lipoxygenase, human leukocyte elastase, toposiomerase I and II, as well as IκB kinases (Poeckel and Werz, 2006).Clinical trials with *Boswellia serrata*'s gum resin extracts indicated its non-toxic nature (Arieh et al., 2010). A patented polyherbal formulation BHUx, containing gum resin of *Boswellia serrata* as one of the herbal components is formulated for treating atherosclerosis (Tripathi, 2009), a cardiovascular disease (CVD). Lately, CVD is recognized to develop as a result of complexed interactions between the processes of inflammation, oxidative stress and thrombosis (Ross, 1999; Boos and Lip, 2006). The objective of the present study is to investigate, if BS-gum resin extract can interrupt these complexed interactions and thus offer cardioprotective effect. To the best of our knowledge, there are no reports on antithrombotic properties of *Boswellia serrata*'s gum resin. Inhibition of platelet function represents a promising way for the prevention of thrombosis. Drugs with anticoagulant and antithrombotic effects, e.g. heparin, are among the primary drugs of choice, for the prevention of thromboembolic disorders. However, alternative drugs for heparin are in high demand due to the long-term side effects of heparin. Therefore, the objective of the present study is to evaluate antioxidant and antithrombotic activities using *in vitro* and cell based assays and to provide scientific basis for the traditional use of *Boswellia serrata*'s gum resin.

2. Materials and methods

2.1. Chemicals

Ascorbic acid, butylated hydroxytoulene (BHT) ferric chloride, 3-(4,5-dimethylthiazol-2-yl)-2,5-diphenyltetrezolium bromide (MTT), sodium acetate trihydrate, 2,4,6-tripyridyl-s-triazine (TPTZ) were from Hi-media, India. 3-Acetyl-11-keto-β-boswellic acid (AKβBA), 2,7-dichlorofluorescin diacetate (H_2DCFDA), ursolic acid, 2-thiobarbituric acid (TBA), and trypan blue were purchased from Sigma–Aldrich (Germany). RPMI 1640 medium, L-glutamine, and fetal bovine serum (FBS) were purchased from Invitrogen. Hydrogen peroxide (H_2O_2) obtained from Merck. Heparin purchased from Samarth Life Sciences (Mumbai). Human blood clotting factors Xa, XIa purchased from American Diagnostic Inc., Stanford. All other reagents used were of analytical grade.

2.2. Plant material and animal tissues

The voucher specimen (# 428) was identified by Dr. K. Madhava Chetty and deposited at Sri. Venkateshwara University Herbarium, Tirupati. Male Wistar rats were housed in ventilated cages and fed with pellet diet and water. Liver and heart tissues were kindly provided by Prof. P. Prakash Babu, Department of Biotechnology, University of Hyderabad.

2.3. Preparation of medicinal plant extracts.

Hydroalcoholic extract (BSAE) of gum resin was prepared by soaking dried gum powder in 80% ethanol followed by continuous stirring at 40 °C for 5–6 h. Water extract (BSWE) was prepared by soaking gum powder in water for overnight at room temperature. The extracts were centrifuged at 10,000 rpm for 10 min and subjected to various studies. BSAE or BSWE, obtained from 1 g of gum resin, was subjected to complete dryness under vacuum. Dry weight of the extract was determined to calculate the yield.

2.4. Phytochemical analysis of plant extracts

Preliminary phytochemical screening of the extracts showed positive reaction for triterpenoids, polyphenols and flavonoids. Using standard compound, i.e. one of the major boswellic acids, 3-acetyl-11-keto-β-boswellic acid (AKβBA) of 95% purity (Sigma), quantity of AKβBA in BSAE and BSWE has been quantitated by subjecting the extracts to HPLC analyses. The analysis was outsourced to Pharmatrain, Kukatpally, Hyderabad, methodology in brief is as follows. The instrument used for this analysis was Waters HPLC 2487 dual λ absorbance detector and 2695 separation module. The separation was performed on C_{18} 100 Å (250 mm × 4.6 mm, make: Waters) reverse phase analytical column. Compound was eluted using a mobile phase consisted of water (A) and acetonitrile (B), used in 35A and 65B in an isocratic mode at a flow-rate of 0.6 mL/min for 9 min. Absorption spectra and retention times were recorded at 210 with a UV detector connected to the HPLC system.

2.5. Cell culture

THP-1 human monocytes were purchased from National Centre for Cell Science (NCCS Pune, India) and cultured in RPMI 1640 medium (10 mM HEPES, 1 mM sodium pyruvate, 4.5 g/L glucose, 1.5 g/L sodium bicarbonate) supplemented with 2 mM L-glutamine and 10% fetal bovine serum. Cells were maintained in 5% CO_2 and 95% air at 37 °C during growth and treatments.

Treatments with BSAE, BSWE or standard compounds were conducted at a cell density of ~0.5×10^6 cells/mL for 16–18 h. Vehicle (alcohol or water) concentration was limited to <1% of the cell culture volume. Cell viability was monitored after all the treatments using trypan blue exclusion and cell count was performed using an inverted microscope (Leica DMR) with the aid of a haemocytometer. MTT cell viability assay was performed according to manufacturer's protocol. Briefly, THP-1 cells were seeded in 24-well plates (2×10^5 cell per well). Cells were pre-treated with and without plant extracts or BHT for 24 h or with ascorbate for 1 h. After respective time periods of incubation, cells were washed twice with medium in order to remove trace amounts of extracts or standard compounds. Similarly, wells with media without cells were processed. MTT (5 mg/mL) was added to all the wells with or without cells and incubated for 3 h. The converted MTT dye was solubilised with 0.04 N HCl in isopropanol. Absorbance of the dye was measured at a wavelength of 570 nm with background subtraction at 690 nm. Media without cells with respective concentrations of extracts or standard compounds were taken as blanks.

2.6. Lipid peroxidation assay

2.6.1. Liver tissue homogenate lipid peroxidation

The peroxide formation was monitored according to the method of Gaurav et al. (2007) by measuring the colour of thiobarbituric acid reactive substances (TBARS) formed at the end of the reaction. The reaction mixture contained rat liver homogenate, 1 mM ferric chloride and various concentrations of BSAE/BSWE. Lipid peroxidation was initiated by adding 100 μl of 1 mM fer-

ric chloride and incubated for 30 min at 37 °C. The reaction was terminated by addition of 2 mL of ice cold HCl (0.25 N) containing 15% trichloroacetic acid (TCA), 0.38% TBA to the reaction mixture followed by heating at 80 °C for 60 min. The samples were then cooled and centrifuged at 5000 × *g* for 15 min, and the absorbance of supernatants was measured at 532 nm against the blank. Identical experiments were performed to determine the normal and induced lipid peroxidation. The protective effects of different extracts against lipid peroxidation were calculated as follows: % Inhibition = (control − sample/control) × 100. Ascorbic acid was used as a reference compound.

2.6.2. Heart tissue homogenate lipid peroxidation

This assay was performed according to the method reported by Meera et al. (2009). The reaction volume composed of 50 μL heart homogenate, 10 mM ferric chloride, and various concentrations of BSAE/BSWE. Buffer blank was prepared w/o ferric chloride. All the tubes were incubated at 37 °C for 1 h. After incubation, 500 μL of 70% ethanol was added to all the tubes to arrest the reaction. TBA (1%, 1 mL) was added to all the tubes followed by boiling in water bath for 20 min. After cooling to room temperature the tubes were centrifuged to clear the solution and the supernatants collected. To the supernatants, 50 μL of acetone was added. TBARS were measured at 532 nm using a spectrophotometer. An assay medium corresponding to 100% oxidation was considered by adding tissue homogenate, ferric chloride, without BSAE/BSWE. Ascorbic acid was used as a reference compound.

2.7. Measurement of ROS generated by H_2O_2 in THP-1 monocyte cell line using H_2DCFDA

Intracellular ROS were measured by using cell permeable fluorescent dye, H_2DCFDA according to Evgeniy et al. (2010). THP-1 cells were seeded in 24-well plates and pre-treated with or without different concentrations of BSAE/BSWE for overnight at 37 °C in a humidified atmosphere containing 5% CO_2. After incubation, wells were loaded with 5 μM H_2DCFDA and incubated for 30 min at 37 °C. Then the cells were washed twice with the growth medium to ensure the removal of unbound dye as well as plant extract in the medium containing the cells. After washing, cells were exposed to 10 μM H_2O_2 for 10 min. Images were obtained by subjecting the cells to confocal laser-scanning electron microscopy using excitation and emission wavelengths at 488 nm and 525 nm respectively. The quantitation of fluorescence intensities of the cell samples was done by spectrofluorimetry.

2.8. Assay of ROS scavenging potential in THP-1 cells

ROS scavenging assays were done in THP-1 cell lysates after the treatments done as detailed in Section 2.5. Cells were washed twice prior to exposure with H_2O_2 to avoid direct interaction between plant extracts and H_2O_2. After two washes, cells were exposed to H_2O_2 and then sonicated, thus obtained cell lysates were centrifuged at 10,000 rpm for 2 min. Supernatants were subjected to the following assays.

2.8.1. Catalase assay

Catalase (CAT) enzyme assay was done according to the method of Prasenjit et al. (2007). 7.5 mM H_2O_2 was added to cell-lysates and the decrease in absorbance at 240 nm was monitored at 37 °C using a multimode microplate reader for about 5 min and absorbance was recorded at an interval of 10 s. CAT activity was expressed in fold change which reduced 1 μmol of H_2O_2 per min at 25 °C.

2.8.2. Ferric reducing/antioxidant power (FRAP) assay

The FRAP assay was done according to the method of Prasenjit et al. (2007), with cell lysates by measuring the changes in absorbance at 593 nm. 1.5 mL of freshly prepared and prewarmed (37 °C) FRAP reagent (300 mM acetate buffer, pH 3.6, 10 mM TPTZ in 40 mM HCl and 20 mM $FeCl_3 \cdot 6H_2O$ in the ratio of 10:1:1) was added to THP-1 cell lysates and incubated at 37 °C for 10 min. Blue colored Fe^{II}-tripyridyltriazine compound formed from the colorless oxidized Fe^{III} form by the action of electron donating antioxidants was assayed. The absorbance of the sample was read against reagent blank (1.5 mL FRAP reagent + 50 μL distilled water) at 593 nm.

2.9. Antiplatelet aggregation assay

Platelet aggregation activity was determined according to Mary et al. (2003). 10 mL of blood was obtained from normal healthy volunteers. Platelet rich plasma (PRP) was collected after centrifugation of blood at 200 × *g* for 5 min. 1.5 mL of acid citrate dextrose (ACD) was used as anticoagulant for every 8.5 mL of blood. Platelet poor plasma (PPP) collected by centrifugation (1500 × *g* for 5 min) was kept as reference. PRP with or without different concentrations of BSAE or BSWE or heparin were added to microwell plate. Aggregation of platelets in PRP was initiated by adding ADP to a final concentration of 20 μM. Absorbance of the samples was recorded at 600 nm using multimode detection plate reader preset at 37 °C for a time period of 12 min at an interval of 2 min. Commercial heparin (20 μg/mL) was used as reference compound.

2.10. Assay plasma clotting times

Prothrombin time (PT) and activated partial thromboplastin time (APTT) assays belong to the class of diagnostic tests were done to assess the function of coagulation system. APTT measures contact activation (intrinsic) pathway and PT measures tissue factor (extrinsic) pathway and initiated by release of tissue factor. To assay the effect of BSAE/BSWE on extrinsic and intrinsic pathways of coagulation, PT and APTT time periods of normal human plasma were compared in the presence of BSAE/BSWE. These reactions were carried out using kit UNIPLASTIN obtained from Tulip Diagnostics (Goa, India) by using the instrument MC100 single channel coagulation analyzer. Samples were outsourced commercially to analyse at Regional Diagnostic Centre, Hyderabad. The protocol followed was briefly as follows: 0.9 mL of blood sample was transferred into a 0.109 M trisodium citrate (1:9, v/v) and then centrifuged at 1800 × *g* for 10 min to obtain plasma. 100 μL of the plasma were mixed with different concentrations of BSAE/BSWE and the coagulation was started by addition of $CaCl_2$, 100 μL of thromboplastin and thrombin added to the incubated plasma for PT and APTT assays individually.

2.11. Clotting factor assays

Human clotting factors were assayed according to Robert et al. (2010). Incubations were performed in 96-well plates. The final concentration of the reactants included 70 ng of factor Xa or 100 ng of factor XIa and different concentrations of test sample in 100 μL of 50 mM Tris, pH 8.3 containing 5 mM calcium chloride and 0.2 mM sodium chloride. Factor Xa/XIa was added last to initiate the reaction. After 60-s of incubation at room temperature, 0.8 mM of chromogenic peptide substrate (CH3OCO-D-CHA-Gly-Arg-pNA-AcOH) for the above factor was added, and the absorbance at 405 nm was recorded for 5 min. Heparin was used as positive drug control.

2.12. Statistical analysis

All data obtained were analyzed by one way analysis of variance (ANOVA) test using Statistical Package for the Life Sciences (SPLS version 11). All results were expressed as mean ± standard deviation of mean (S.D.). $p < 0.001$ was considered to be statistically highly significant.

3. Results

3.1. Plant extracts

Hydroalcoholic extracts yielded 4.8% (w/w) and water extracts yielded 5.2% (w/w) based on their starting material of dried gum resin. The phytochemical screening of gum resin showed positive reaction for polyphenols, flavonoids and triterpenoids. BSAE contained 0.647 ± 0.09 UAE mg/mg dwt; 22.5 ± 1.6 GAE μg/mg dwt and 2.29 ± 1.4 QE μg/mg dwt. Whereas BSWE contained 0.271 ± 0.026 UAE mg/mg dwt, 79.2 ± 2.8 GAE μg/mg dwt and 6.35 ± 3 QE μg/mg dwt. In summary hydroalcoholic extracts had higher amounts of total triterpenoids and water extracts had higher amounts of TPC and flavonoids.

3.2. Quantititation of AKβBA

Under the experimental conditions, retention time of standard compound AKβBA was 4.784 min (Fig. 1B). HPLC analyses with BSAE and BSWE showed peaks corresponding to standard AKβBA with retention times of 4.623 and 4.616 respectively (Fig. 1C). Calculations with corresponding peak areas determined that AKβBA content of BSAE to 9% (w/w) and BSWE to 7.8% (w/w) of their extracts' dwt.

To test the linearity of the compound, we used standard solutions of AKβBA in the range from 10 μg/mL to 120 μg/mL. 20 μL of these standard solutions were injected for each assay, which correspond to 200–2400 ng. Least amount of detection and quantification under the experimental conditions was 2.69 (± 0.17) μg/mL and 9.08 (± 0.58) μg/mL respectively. Each sample was measured in triplicate (Fig. 1A).

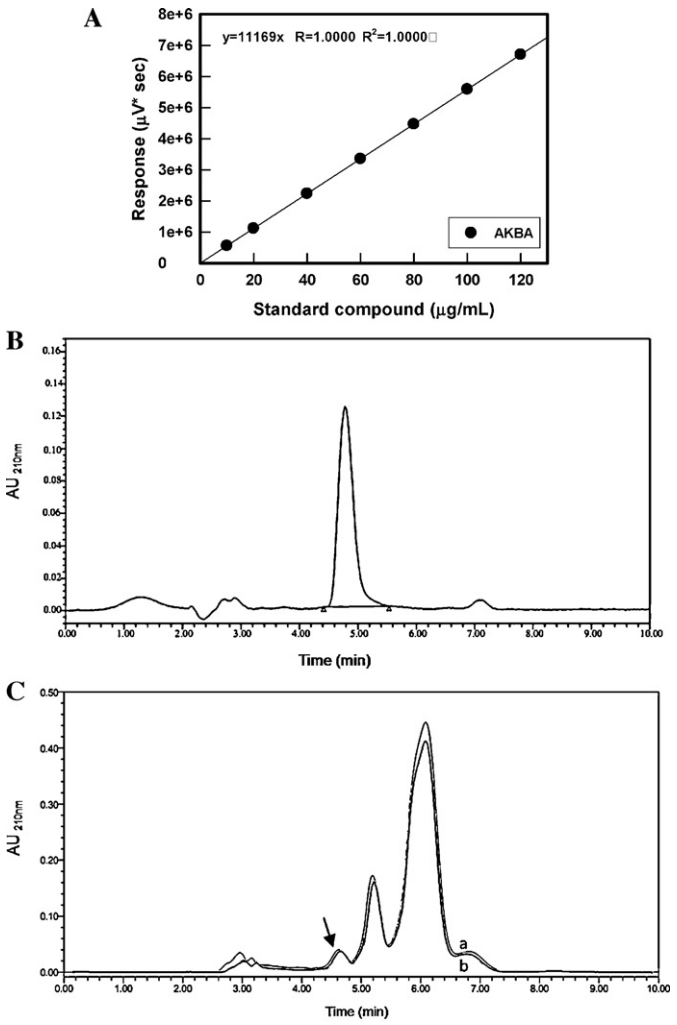

Fig. 1. HPLC analysis for quantification of AKβBA in plant extracts. (A) Regression plot with varied concentrations of AKβBA ranging from 20 to 120 μg/mL. LOD and LOQ of AKβBA are 2.69 ± 0.17 μg/mL and 9.08 ± 0.58 μg/mL. (B) An example chromatogram of standard compound AKβBA showing a peak with the retention time period of 4.784 min. (C) Example chromatograms of BSAE (a) and BSWE (b), with marked peak, corresponding to standard AKβBA with retention times of 4.623 min and 4.616 min respectively. Peak areas were used to determine the AKβBA content in the extracts.

3.3. Lipid peroxidation inhibition activity of BSAE/BSWE

BSWE inhibited $FeCl_3$ induced peroxidation in liver homogenates by 70% where as BSAE showed maximum inhibition of only 40% (Fig. 2A). In case of heart homogenate, both types of extracts inhibited maximum of 50% lipid peroxidation (Fig. 2B). The concentration of the BSWE needed for 50% inhibition in liver homogenate was 34 μg dwt/mL. In case of heart homogenate, IC_{50} of BSAE and BSWE were 129 μg dwt/mL and 88 μg dwt/mL respectively. Extracts showed lower effect in inhibiting peroxidation in heart tissue homogenates from 200 μg dwt/mL onwards. IC_{50} values for standard compound ascorbate were 38 μg/mL and 153 μg/mL for lipid peroxidation in liver and heart tissues respectively. Ascorbate showed maximum inhibition of 80% lipid peroxidation in liver tissue but only 55% inhibition with heart tissue. Thus our results indicated that water extracts of BS-gum resin were more potential than standard compound ascorbate in suppressing lipid peroxidation of both rat's liver and heart homogenates.

3.4. Cell viability

Dosage of plant extracts or standard compounds for THP-1 cell treatments were determined based on cell viability experiments (Fig. 3). At the used concentrations of plant extracts or standard compounds for the present study, no cell death was found, >95% cells were alive (Fig. 3). In case of standard compounds, there was no cell death found after treatments with ascorbate up to 50 μg/mL for 1 h time period (Fig. 3A) with BHT up to 10 μg/mL for 24 h time period (Fig. 3B). Cell death was not found after treatments with BSAE up to 40 μg dwt/mL (Fig. 3C) and up to 400 μg dwt/mL of BSWE (Fig. 3D). Therefore, we restricted our dosage of standard compounds and plant extracts to the maximum of above cited concentrations.

3.5. Attenuation of H_2O_2 induced ROS by BSAE/BSWE in THP-1 Cells

We evaluated the potential of BS-extracts in scavenging intra cellular ROS in human monocytic cell line using a cell permeable ROS sensitive fluorescent marker H_2DCFDA. THP-1 cells treated with 10 μM H_2O_2 for 10 min showed much brighter fluorescence compared to cells not treated with H_2O_2 (Fig. 4A). THP-1 cells treated with 10 μM H_2O_2 for 10 min showed 4.5 folds greater fluorescence compared to cells not treated with H_2O_2 (Fig. 4B). Pretreatment of cells with BSAE (30–40 μg dwt/mL) or BSWE (300–400 μg dwt/mL) markedly attenuated H_2O_2-dependent flu-

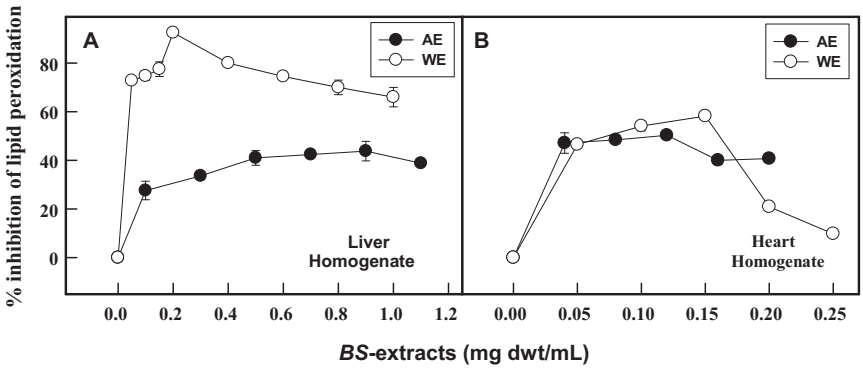

Fig. 2. Effect of BS-gum resin on ferric chloride induced lipid peroxidation on (A) liver and (B) heart tissue homogenates of rat. Data presented are mean ± S.D., $n = 6$. S.D. not seen where S.D. values are within the symbol of data point.

orescence increase with statistical significance of p value <0.001. IC_{50} of BSAE (0.011 mg dwt/mL) is much lower than IC_{50} of BSWE (0.08 mg dwt/mL), which reflects that alcoholic extract was highly potential in scavenging intra cellular ROS. Washing H_2DCFDA dyed cells twice with medium prior to the exposure of cells to H_2O_2 ensured not only the removal of excess fluorescent dye, but also removal of BS-extracts from the medium, otherwise there is a possibility of extracts scavenging H_2O_2 extracellularly in the medium. Positive drug controls, ascorbic acid at 20 μg/mL and BHT at 10 μg/mL completely scavenged intracellular ROS (Fig. 4B).

3.6. Effect of BSAE/BSWE on scavenging mechanisms of cellular ROS

To elucidate the mechanism offered by plant extracts in scavenging intracellular ROS, effect of BSAE/BSWE treatments (concentrations, from Fig. 4B, at which the extracts were effective in scavenging intracellular ROS), cells were treated similarly and subjected to cellular catalase enzyme and total reducing power assays.

On exposure of cells to H_2O_2 for a short period, catalase activity was increased by 40% (Fig. 5A) in THP-1 cells. Whereas, catalase activity was increased by two fold in the cells treated with BSWE at 300 μg dwt/mL, with a statistical significance of p value <0.001. BSAE treated cells showed an increase in the enzyme activity by only 40%. Ascorbate (20 μg/mL) increased catalase activity by two folds but BHT (10 μg/mL) inhibited the enzyme by 50% (Fig. 5A).

Total reducing power of the THP-1 cells was rapidly declined by 70% upon treatment with H_2O_2 (Fig. 5B). Plant extracts or standard compound treated cells maintained cellular reducing power even after treatment with H_2O_2 (Fig. 5B). BSAE at 30 μg dwt/mL sustained cellular reducing power by 80%, BSWE at 300 μg dwt/mL by 70%, standard compounds, ascorbate (20 μg/mL) by 60% and BHT

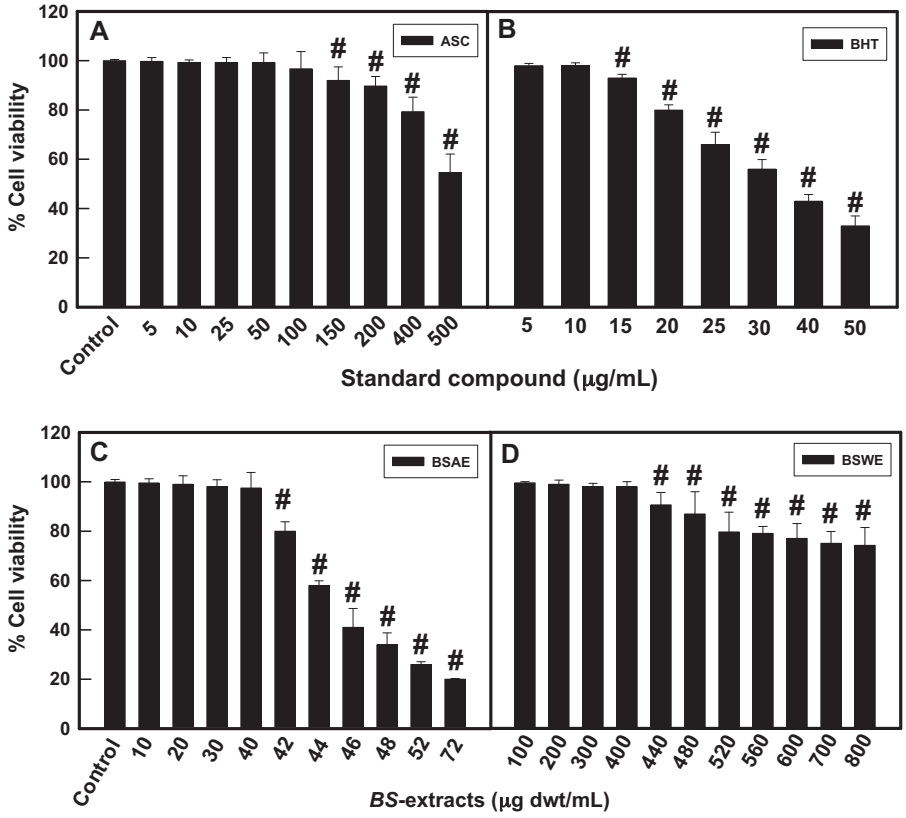

Fig. 3. Cell viability was checked by MTT assay after treatment with (A) ascorbate for 1 h, (B) BHT for 24 h, (C) BSAE for 24 h, (D) BSWE for 24 h, at 37 °C and 5% CO_2. Media without cells but with respective concentrations of standard compounds or plant extracts were used as appropriate blanks. Data presented are mean ± S.D., $n = 6$.

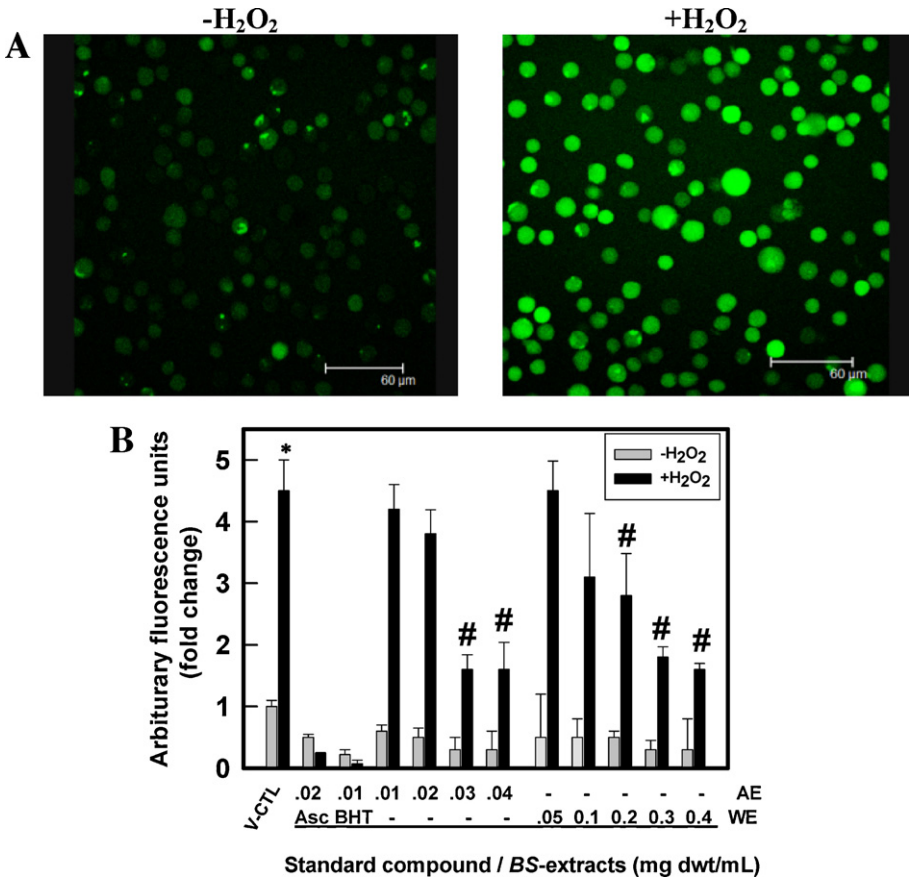

Fig. 4. Effect of BS-gum resin extracts on H_2O_2 induced ROS generation in THP-1 cells. (A) Confocal images: left panel – control cells – H_2O_2; right panel – cells + H_2O_2. ROS species were detected by cell permeable fluorescent dye, H_2DCFDA, and cells were observed with a fluorescence microscope. (B) Fluorescence intensity of H_2DCFDA taken by the cells treated as above was measured by spectrofluorimetry at excitation wavelength of 488 nm and emission wavelength of 525 nm. One-way ANOVA test was performed between the experimental groups represent mean ± S.D. ($n = 4$), *statistical significance of $p < 0.001$ within the control groups i.e. cells + H_2O_2 *vs* cells – H_2O_2, #statistical significance of $p < 0.001$ for groups of cells treated with H_2O_2 in the presence of BS-extracts *vs* in the absence of BS-extracts.

(10 μg/mL) by 100% that of H_2O_2 untreated cells. These results suggest that the selected plant extracts help the cells in maintaining their total reducing power under oxidative stress conditions and thus help in scavenging excess ROS.

3.7. Antiplatelet aggregation and anticoagulant activity of BSAE/BSWE

Addition of 20 μM ADP to human platelets caused the decrease in absorbance units indicating the aggregation of platelets (Fig. 6). In the present study heparin was used as positive drug control, which inhibited ADP-induced platelet aggregation as shown in Fig. 6. BSAE and BSWE markedly inhibited the platelet aggregation in a concentration dependent manner (Fig. 6). Both types of extracts BSAE and BSWE (3 mg dwt/mL) showed high antiplatelet aggregatory activity with p value <0.001 (Fig. 6). Activity of the extracts was comparable to heparin. Thus our results demonstrated antiplatelet aggregatory effect of BS gum resin.

Blood coagulation system, not only initiated by complex coagulation pathways but also involves the interactions between platelets and plasma factors. In this regard, APTT is used to evaluate intrinsic clotting index and PT for extrinsic index, these tests used to identify the coagulation risk factors.

The concentration-dependent effects of BSAE and BSWE on the PT and APTT clot times of human plasma are shown in Fig. 7. Both BSAE and BSWE showed very potent activity in prolongation of clot times. BSAE and BSWE prolonged APTT time period by 2.6 fold and PT time period by 4 folds. Thus our data on prolongation of both PT and APTT clotting times by both types of BS extracts clearly demonstrate anticoagulant property of BS-gum resin.

In order to know target sites of BSAE or BSWE in clotting cascade pathway, we tested the effect of extracts on human clotting factors Xa and XIa. BSAE inhibited both the factors significantly ($p < 0.001$). BSAE at 6 and 8 μg dwt/mL inhibited 70% of FXa (Fig. 8A) and 55% of FXIa (Fig. 8B). BSWE did not show inhibitory effect on FXa and showed about 25% inhibition on FXIa. Heparin showed about 35% on both the factors (Fig. 8A and B).

4. Discussion

The interest in natural plant products is on a steep rise due to their increased use of traditional medicine to treat chronic metabolic diseases (Mukherjee et al., 2010). *Boswellia serrata*'s gum resin is one such plant used in Indian Ayurvedic and folk medicine to treat blood disorders, curtail inflammatory diseases like rheumatoid arthritis and to promote cardiac health (Clarisse et al., 2008; Arieh et al., 2010). Present study is designed to investigate the mechanism by which BS-gum resin offers cardiac health. The link between the oxidative stress, inflammation and thrombosis leading to cardiovascular disease is well established (Ross, 1999; Libby, 2002; Boos and Lip, 2006). Therefore, antioxidant and antithrombotic properties of BS-gum resin have been investigated.

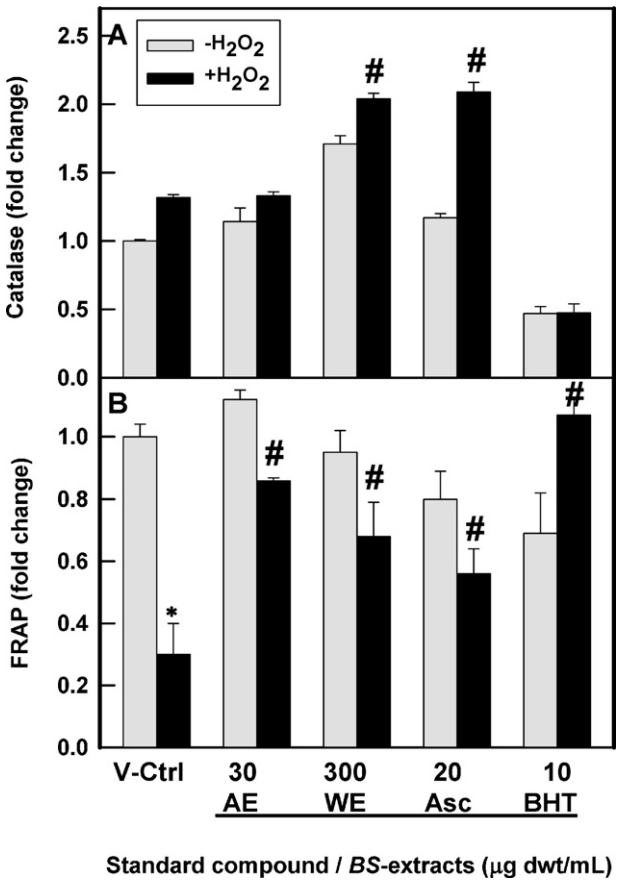

Fig. 5. (A) Effect of BS-extracts on catalase enzyme activity in THP-1 cells exposed to H_2O_2. Ascorbic acid and BHT serve as positive drug control. (B) FRAP assay performed with cells pretreated with BS-gum resin and induced with H_2O_2. Data represented mean ± S.D., $n = 4$; *statistical significance of $p < 0.001$ within the control groups i.e. cells + H_2O_2 *vs* cells − H_2O_2, #statistical significance of $p < 0.001$ for groups of cells treated with H_2O_2 in the presence of BS-extracts *vs* in the absence of BS-extracts.

4.1. Antioxidant activity of BS-gum resin

The enrichment of BS-gum resin with triterpenoids (Assimopoulou et al., 2005; Bushra et al., 2007; Magesh et al., 2008) implies their antioxidant activity based on its chemical composition but direct line of evidences for such antioxidant activity was not available. Investigating antioxidant activity of the BS-gum resin during our experiments, BSAE and BSWE showed anti-lipid peroxidation activity when checked with liver and heart

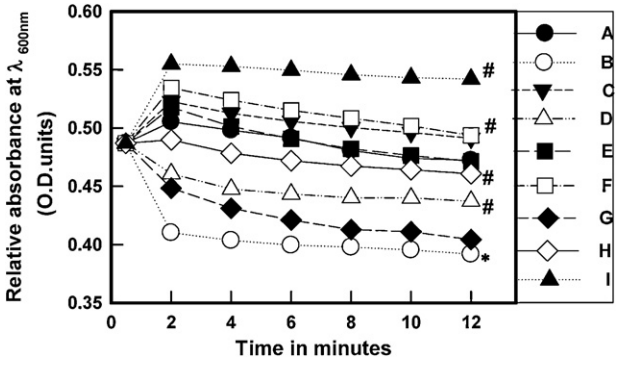

Fig. 6. Effect of BS-extracts on ADP induced aggregation of human platelets. (A) PRP; (B) PRP + ADP (20 μM); (C) PRP + Hep (20 μg/mL) + ADP; (D) PRP + BSAE (1 mg dwt/mL) + ADP; (E) PRP + BSAE (2 mg dwt/mL) + ADP; (F) PRP + BSAE (3 mg dwt/mL) + ADP; (G) PRP + BSWE (1 mg dwt/mL) + ADP; (H) PRP + BSWE (2 mg dwt/mL) + ADP; (I) PRP + BSWE (3 mg dwt/mL) + ADP. Data presented are mean ± S.D., $n = 3$. S.D. not seen where S.D. values are within the symbol of data point. #$p < 0.001$ between platelets treated with BS extracts and ADP *vs* treated with ADP alone, *$p < 0.001$ indicates comparison between PRP + ADP *vs* PRP alone.

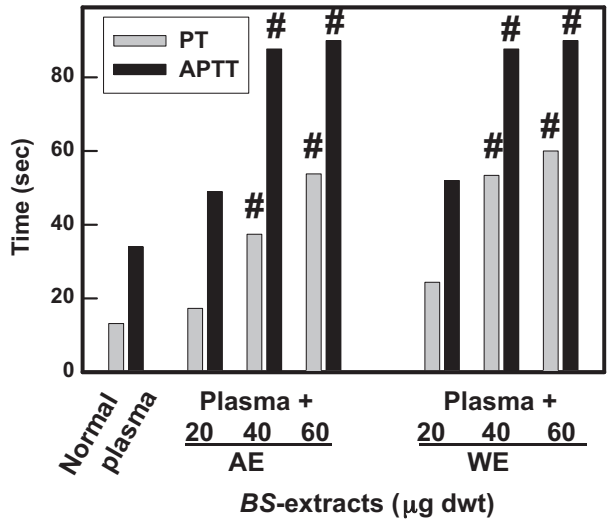

Fig. 7. Effects of BS-gum resin on clotting PT and APTT time periods. Data presented are mean ± S.D., $n = 3$. S.D not seen where S.D. values are within the symbol of data point. Statistically significant values are indicated by # with $p < 0.001$.

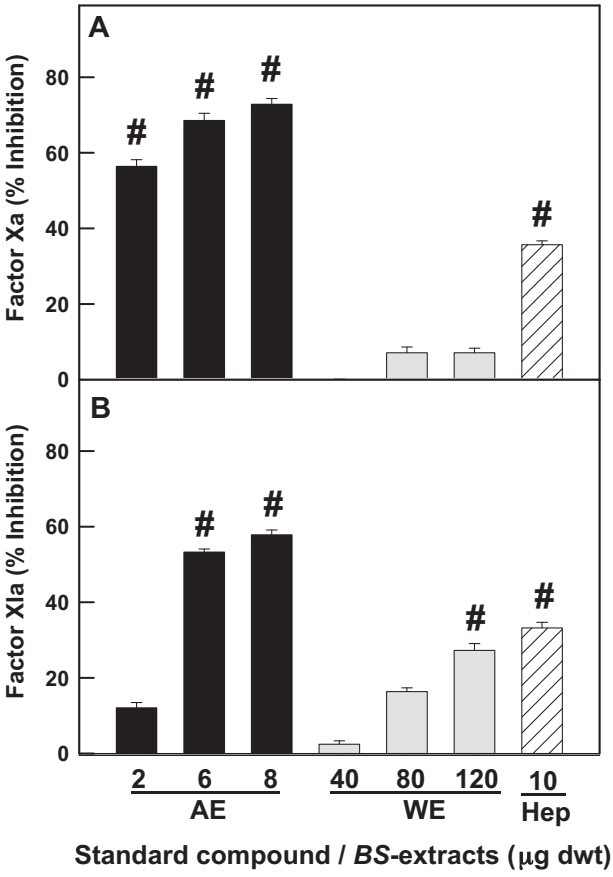

Fig. 8. % Inhibitory effect of BS-extracts or heparin on (A) factor Xa and (B) factor XIa. Clotting assays were conducted by monitoring decrease in the absorbance of chromogenic substrate using microplate reader. Values in the bar graphs represent mean ± S.D. ($n = 4$), #$p < 0.001$ highly significant compared with control.

homogenates. These extracts were also capable of scavenging ROS in human monocytic (THP-1) cells (Fig. 4B). Since activated monocytes promote inflammatory cascade of events (Ross, 1999) leading to atherosclerosis. The cellular ROS scavenging activity offered by BSAE and BSWE may help in attenuating the above outlined cascade of events.

BSAE did not show significant effect on catalase where as BSWE significantly increased cellular catalase activity in Thp-1 cells (Fig. 5A). BSAE and BSWE helped Thp-1 cells in sustaining their cellular reducing power to great extent, even on exposure to H_2O_2 (Fig. 5B). Therefore, we think that BSAE and BSWE scavenge excess ROS generated by oxidative stress by modulating either cellular reducing power or catalase enzyme activity.

The reasons for higher potential of BSAE (IC_{50}: 0.011 mg dwt/mL), that of BSWE (IC_{50}: 0.08 mg dwt/mL) in terms of ROS scavenging, cannot be explained based on the analyzed phytomarker, AKβBA. BSAE and BSWE contained AKβBA of 9% (w/w) and 7.8% (w/W) respectively. Detailed chemical composition analyses of these extracts may help in knowing other active metabolites.

4.2. Antithrombotic potential of BS-extracts

To further elucidate antiatherogenic potential of BS-gum resin, antiplatelet aggregation and anticoagulant activities of the extracts were examined. Platelets of the blood play an important role in the process of hemostasis. Platelet activation is essential to perform many of their functions, however, activated platelets also has tendency to stick to each other and form aggregates leading to thrombosis and clot formation in the vessel and thus contributes to cardiovascular disease and stroke (Ross, 1999; Boos and Lip, 2006). Inhibition of platelet aggregation and enhancing coagulation time can help to a great extent in the management of atherosclerosis (Ross, 1999). Alternative drugs to heparin are of great interest in view of its limitations and allergic problems (Henry et al., 2009). Therefore, efforts on identifying factor Xa inhibitors (Pinto Donald et al., 2010) and screening herbal resources possessing significant antithrombotic activity with minimal side effects are highly essential (Winston, 1999; Kim et al., 2010). To the best of our knowledge, there are no scientific studies reported on antithrombotic effect of BS-gum resin. In our present study, both BSAE and BSWE inhibited platelet aggregation (Fig. 6). We used ADP to induce platelet aggregation since it is an important endogenous aggregating agent involved in thrombus formation (Park et al., 2004). BSAE and BSWE at 3 mg dwt/mL showed stronger effect in inhibiting platelet aggregation and are as potential as positive drug control, heparin.

Both BSAE and BSWE also enhanced PT and APTT coagulation time periods (Fig. 7). Blood coagulation is not only the result of a complex process initiated by the intrinsic system or the extrinsic system and or/a common pathway, but also a highly regulated process involving interaction between platelets, plasma coagulation factors, and the vessel wall. Anticoagulant drugs are screened using PT and APTT tests (Arif et al., 2007). BSAE at 57 μg dwt and BSWE at 40 μg dwt exhibited maximum of 2.65 fold increase in clotting time period of APTT. The same concentrations increased clotting time periods of PT by four fold. The above concentrations of BSAE significantly inhibited FXa and FXIa and this could be the possible mechanism by which it enhanced the clotting time of both PT and APTT. Where as BSWE did not inhibit FXa but inhibited FXIa by 25%. Mechanism of enhancing PT time period by BSWE needs to be elucidated. Detailed analysis of these extracts on various factors and enzymes involved in clotting cascade may reveal the mechanism of action.

5. Concluding remarks

Conclusively, our results indicated that both water and hydroalcoholic extracts of *Boswellia serrata*'s gum resin contain high amounts of AKβBA and other boswellic acids, also contain significant levels of phenolic compounds, which may be responsible for its exhibited high antioxidant and antithrombotic activity. BSAE and BSWE showed cellular ROS scavenging, antiplatelet aggregation and anticoagulation activities. With all these shown wide spectrum of activities of phytomedicine, BS-gum resin can be considered as an effective antiatherogenic resource for preventing coronary artery diseases and may serve as a good source for isolating lead compounds of antiplatelet and anticoagulant therapeutics.

Acknowledgements

We are grateful to Prof. P. Prakash Babu, Department of Biotechnology for providing rat liver and heart tissue samples and Dr. Madhava Chetty, Department of Botany, S.V.U. Tirupathi for providing plant material. We are thankful to Ms. Nalini Manthapuram, CIL for her assistance in collecting confocal images. We are also thankful to Pharma Train, Hyderabad for their timely help on HPLC analyses. This part of the work is supported by DBT (BT/PR/10972/GBD/27/123/2008) and UGC (37/532/2010 SR) research projects of Sarada D. Tetali. Dr. D.S. Kothari F.4-2/2006(BSR)/13-252/2009(BSR) dated 15/02/2010 of Dr. L. Md. Bhakshu. We are thankful to DBT-CREBB, DBT-FIST and UGC-SAP for supporting infra structural facilities of Department of Plant Sciences and School of Life Sciences.

References

Aman, U., Balu, G., 2009. Pharmacological activities of *Boswellia serrata* Roxb—mini review. Ethnobotanical Leaflets 13, 766–774.
Ammon, H.P.T., 2006. Boswellic acid in chronic inflammatory diseases. Planta Medica 72, 1100–1166.
Arieh, M., Raphael, M., 2010. *Boswellia* resin: from religious ceremonies to medical uses: a review of *in-vitro*, *in-vivo* and clinical trials. Journal of Pharmacy and Pharmacology 61, 1281–1293.
Arif, H.K., Ayalew, T., Rajiv, K.P., 2007. How to interpret and pursue an abnormal prothrombin time activated partial thromboplastin time, and bleeding time in adults. Mayo Clinic Proceedings 82, 864–873.
Assimopoulou, A.N., Zlatanos, S.N., Papageorgiou, V.P., 2005. Antioxidant activity of natural resins and bioactive triterpenes in oil substrates. Food Chemistry 92, 721–727.
Bushra, S., Farooq, A., Roman, P., 2007. Antioxidant activity of phenolic components present in barks of *Azadirachta indica*, *Terminalia arjuna*, *Acacia nilotica*, and *Eugenia jambolana* Lam. Trees Food chemistry 104, 1106–1114.
Boos, C.J., Lip, G.Y.H., 2006. Blood clotting inflammation and thrombosis in cardiovascular events: perspectives. Frontiers in Bioscience 11, 328–336.
Clarisse, C., Ludivine, B., Eric, B., Corinne, C., Daniel, S.A., Felicitas, G., Berhold, B., Tatiana, S., Thomas, S., Mustapha, R., 2008. Antiinflammatory and antiatherogenic effects of the NF-kB inhibitor acetyl-11-keto-β-boswellic acid in LPS-challenged ApoE−/− mice. Arteriosclerosis, Thrombosis, and Vascular Biology 28, 272–277.
Evgeniy, E., Sergei, K., 2010. Identification of ROS using oxidized DCFDA and flow-cytometry. Advanced Protocols in Oxidative Stress II, Methods in Molecular Biology, 594.
Gaurav, V.H., Chandragauda, R.P., Mahesh, R.P., 2007. Protective effect of *Kalanchoe pinnata* pers (Crassulaceae) on gentamicin-induced nephrotoxicity in rats. Indian Journal of Pharmacology 39, 201–205.
Henry, B.L., Jay, N.T., Erika, J.M., Donald, F.B., Umesh, R.D., 2009. Characterization of the plasma and blood anticoagulant potential of structurally and mechanistically novel oligomers of 4-hydroxycinnamic acids. Blood Coagulation and Fibrinolysis 20, 27–34.
Kim, S.Y., Koo, Y.K., Koo, J.Y., Ngoc, T.M., Kang, S.S., Bae, K.H., Kim, Y.S., Yun-Choi, H.S., 2010. Platelet anti-aggregation activities of compounds from *Cinnamomum cassia*. Journal of Medicinal Food 13, 1069–1074.
Libby, P., 2002. Inflammation in atherosclerosis. Nature 420, 868–874.
Meera, R., Devi, P., Kameswari, B., Madhumitha, B., Merlin, N.J., 2009. Antioxidant and hepatoprotective activities of *Ocimum basilicum* Linn. and *Trigonella foenum-graecum* Linn. against H_2O_2 and CCl_4 induced hepatotoxicity in goat liver. Indian Journal of Experimental Biology 47, 584–590.
Magesh, V., Raman, D., Pudupalayam, K.T., 2008. Genotoxicity studies of dry extract of *Boswellia serrata*. Tropical Journal of Pharmaceutical Research 7, 1129–1135.

Mary, K., Achuthan, C.R., Babu, B.H., Padikkala, J., 2003. *In vitro* antioxidant and antithrombotic activity of *Hemidesmus indicus* (L) R.Br. Journal of Ethnopharmacology 87, 187–191.

Mukherjee, P.K., Venkatesh, P., Venkatesh, M., Ponnusankar, S., Khan, Y., 2010. Strategies for revitalization of traditional medicine. Chinese Herbal Medicines 2, 1–15.

Pinto Donald, J.P., Smallheer Joanne, M., Cheney Daniel, L., Knabb Robert, M., Wexler Ruth, R., 2010. Factor Xa inhibitors: next generation antithrombotic agents. Journal of Medicinal Chemistry 53, 6243–6274.

Prasenjit, M., Mahua, S., Prasantha, P., Parames, C.S., 2007. Arjunolic acid, a triterpenoid saponin, ameliorates arsenic induced cyto-toxicity in hepatocytes. Chemico-Biological Interactions 170, 187–200.

Paranjpe, P., 2001. Śallakī – *Boswellia serrata*. In: Indian Medicinal Plants – Forgotten Healers: A Guide to Ayurvedic Herbal Medicine. Chaukhamba Sanskrit Pratishthan Publishers, Delhi, pp. 233–234.

Park, W.H., Ahn, J.C., Kim, H., Lee, Y.C., Kim, C.H., 2004. Effects of Korean herbal formulation Silsosangami, consisting of seven medical herbs and its seven herbs on endotoxin induced experimental thrombosis in rats. Phytotherapy Research 18, 224–229.

Poeckel, D., Werz, O., 2006. Boswellic acids: biological actions and molecular targets. Current Medicinal Chemistry 13, 3359–3369.

Robert, S., Baccelli, C., Devel, P., Michel Donge, J., Quetin-Leclercq, J., 2010. Effects of leaf extracts from *Croton zambesicus* Muell. Arg. on hemostasis. Journal of Ethanopharmacology 128, 641–648.

Ross, R., 1999. Atheroscelerosis—an inflammatory disease. New England Journal of Medicine 340, 115–126.

Shen, T., Lou, H., 2008. Bioactive constituents of myrrh and frankincense, two simultaneously prescribed gum resins in Chinese traditional medicine. Chemistry and Biodiversity 5, 540–553.

Singh, S., Khajuria, A., Taneja, S.C., Khajuria, R.K., Singh, J., Johri, R.K., Qazi, G.N., 2008. The gastric ulcer protective effect of boswellic acids, a leukotriene inhibitor from *Boswellia serrata*, in rats. Phytomedicine 15, 408–415.

Tripathi, Y.B., 2009. BHUx: a patented polyherbal formulation to prevent hyperlipidemia and atherosclerosis. Recent patents on inflammation allergy and drug. Discovery 3, 49–57.

Winston, J.C., 1999. Health-promoting properties of common herbs. American Journal of Clinical Nutrition 70, 491S–499S.

Journal of Ethnopharmacology 146 (2013) 456–464

Contents lists available at SciVerse ScienceDirect

Journal of Ethnopharmacology

journal homepage: www.elsevier.com/locate/jep

Stem-bark of *Terminalia arjuna* attenuates human monocytic (THP-1) and aortic endothelial cell activation

Praveen K. Kokkiripati [a], Ratnam V. Kamsala [a], Leena Bashyam [b], Nalini Manthapuram [b], Prasanth Bitla [b], Vidyadhari Peddada [b], Agepati S. Raghavendra [a], Sarada D. Tetali [a,*]

[a] Department of Plant Sciences, University of Hyderabad, Hyderabad 500046, India
[b] School of Life Sciences, University of Hyderabad, Hyderabad 500046, India

ARTICLE INFO

Article history:
Received 30 August 2012
Received in revised form
6 December 2012
Accepted 29 December 2012
Available online 24 January 2013

Keywords:
Endothelial cells
LPS
Monocytes
Terminalia arjuna stem bark
TNF-α
VCAM-1

ABSTRACT

Ethnopharmacological relevance: *Terminalia arjuna* – stem bark extract is traditionally used as cardiotonic in Ayurvedic medicine.
Aim of the study: The present study was aimed to evaluate the molecular basis for cardioprotective potential of *Terminalia arjuna* (TA) stem bark, using cell cultures of human monocytic (THP-1) and human aortic endothelial cells (HAECs).
Materials and methods: Inhibitory effect of alcoholic (TAAE) and aqueous (TAWE) extracts of TA-stem bark was assessed on human 3-hydroxy-3-methylglutaryl coenzyme A (HMG-CoA) reductase, lipoprotein lipase (LpL) and lipid peroxidation in rat (wistar) liver and heart homogenates. The patterns of H_2O_2 induced reactive oxygen species (ROS) generation were observed by confocal microscopy. The activities of antioxidant enzymes and reducing power of the cells were measured in a microplate reader. Gene transcripts of proinflammatory markers in THP-1 and HAECs were assayed by real time PCR and levels of inflammatory protein markers by ELISA or flow cytometry. Phytochemical analyses of TAAE and TAWE were done using liquid chromatography, coupled to mass spectrometry (LC-MS).
Results: TAAE and TAWE inhibited the lipid peroxidation and HMG-CoA reductase but had no effect on LpL. Both the extracts attenuated H_2O_2 mediated ROS generation in THP-1 cells by promoting catalase (CAT), glutathione peroxidase (GPx) activities, and by sustaining cellular reducing power. TAAE was highly effective in attenuating proinflammatory gene transcripts in THP-1 cells and HAECs, whereas the response to TAWE depended on the type of transcript and cell type. Both extracts decreased the levels of typical inflammatory marker proteins, *viz.* LPS induced tumor necrosis factor (TNF)-α secreted by THP-1 cells and TNF-α induced cell surface adhesion molecules on HAECs, namely vascular cell adhesion molecule-1 (VCAM-1) and E-selectin. Phytochemical analyses indicated the richness in phenolic compounds and terpenes of TAAE and TAWE, while revealing variability in their metabolite profile.
Conclusion: Our study scientifically validates the antioxidative and antiinflammatory properties of *Terminalia arjuna* stem bark. The marked effects on cultured human monocytic and aortic endothelial cells (HAEC) provide the biochemical and molecular basis for therapeutic potential of TA-stem bark against cardiovascular diseases (CVD).

1. Introduction

Terminalia arjuna's (Combretaceae family) stem bark is traditionally used as a cardiac tonic and is a key constituent of several polyherbal formulations (Tripathi et al., 2004; Koti et al., 2009; Murkute et al., 2011). Clinical studies demonstrated TA-stem bark's nontoxic nature and efficacy in treating cardiovascular disorders (Dwivedi and Jauhari, 1997; Dwivedi et al., 2005; Choudhari et al., 2011). Efforts have earlier been made to understand the scientific basis of heart health benefits due to TA-stem bark (Dwivedi, 2007; Choudhari et al., 2011). Animal studies indicated the protective effect of TA-stem bark during high

Abbreviations: AE, alcohol extract; Butylated hydroxytoluene, (BHT); H2DCFDA, 2,7-dichlorofluorescin diacetate; HAECs, Human aortic endothelial cells; 3-hydroxy-3-methylglutaryl coenzyme A, HMG-CoA reductase; ICAM-1, Intercellular adhesion molecule-1; IL-8, Interleukin-8; LpL, Lipoprotein lipase; MCP-1, Monocyte chemotactic protein-1; ROS, reactive oxygen species; TA, *Terminalia arjuna*; THP-1, human acute monocytic leukemia cell line; VCAM-1, vascular cell adhesion molecule 1; WE, water extract

* Corresponding author. Tel.: +91 40 2313 4512; fax: +91 40 2301 0120.
E-mail addresses: sdtsl@uohyd.ernet.in, saradakanakagiri@gmail.com (S.D. Tetali).

0378-8741/$ - see front matter © 2013 Elsevier Ireland Ltd. All rights reserved.
http://dx.doi.org/10.1016/j.jep.2012.12.050

fat-mediated aortic architectural changes and atherosclerotic lesion formation (Subramaniam et al., 2011), and also against other chronic heart disorders (Gauthaman et al., 2001; Karthikeyan et al., 2003; Arya and Gupta, 2011; Parveen et al., 2011a; Asha and Taju, 2012). In addition, animal studies suggested TA-stem bark's effect in reducing hyperglycemia and hyperlipidemia (Shaila et al., 1998; Ragavan and Krishnakumari, 2005; Parveen et al., 2011b; Subramaniam et al., 2011). However, the exact mechanism at cellular and molecular level by which TA-stem bark extract offers the atheroprotection in humans is not clear.

TA-stem bark extracts are known to be enriched with phytochemicals, such as terpenes, phenolics and flavonoids (Dwivedi, 2007). Flavonoids can be antiatherogenic by attenuating endothelial cell activation (Carluccio et al., 2003) and platelet aggregation (Ruff, 2003). In fact, TA-stem bark was shown to inhibit platelet activation (Malik et al., 2009), but its inhibitory effects on activation of endothelial cells and monocytes is not known. Drug candidates or their resources targeting activation of vascular cells and blood monocytes are good choices in controlling pathophysiology of cardiovascular diseases (CVD). The present study is therefore designed to investigate the antiinflammatory and antioxidant effects of alcoholic and aqueous extracts of TA-stem bark in monocytes and endothelial cells.

2. Materials and methods

2.1. Chemicals

Butylated hydroxytoluene (BHT), 2,7-dichlorofluorescin diacetate (H_2DCFDA), glutathione, human tumor necrosis factor (TNF-α), HMG-CoA reductase kit, nicotinamide adenine dinucleotide phosphate (NADPH), lipoprotein lipase (LpL; bovine milk), lipopolysaccharide-*Escherichia coli* (LPS), orlistat, p-nitrophenyl butyrate, 2-thiobarbituric acid (TBA), trypan blue, gallic acid (GA) were purchased from Sigma Aldrich (Germany). M200 medium, RPMI 1640 medium, L-glutamine, fetal bovine serum (FBS), low serum growth supplement (LSGS), penicillin, streptomycin, trypsin neutralizer, trypsin EDTA were purchased from Invitrogen (Germany), human tumor necrosis factor (TNF-α) kit and CD106-FITC and CD62E-PE antibodies from BD Bioscience (USA). All other reagents used were of analytical grade.

2.2. Plant material and animal tissues

The voucher specimen (# 528) of *Terminalia arjuna's* stem bark was authenticated by Dr. K. Madhava Chetty and deposited at Sri Venkateshwara University Herbarium, Tirupati. Male Wistar rats were housed in ventilated cages (in animal house) and fed with pellet diet and water. Liver and heart tissues of these rats were kindly provided by Prof. P. Prakash Babu, Department of Biotechnology, University of Hyderabad.

Preparation of plant extracts: Plant extraction procedures were designed, based on the protocols mentioned for hydroalcoholic extract (Sharma et al., 2001) and water extract (Tilak et al., 2004). Further details of these modified extraction protocols were described in Kokkiripati et al. (2011). In brief, hydroalcoholic extract of TA-stem bark (TAAE) was prepared by soaking 1 g of dried stem bark powder in 20 mL of 80% (v/v) alcohol followed by heating at 40 °C by continuous stirring for 5–6 h. Water extract (TAWE) was prepared by soaking 1 g stem bark powder in 4 mL of distilled water overnight at room temperature. Both the extracts were cleared by centrifugation at 10,000 rpm for 10 min and the supernatants were used for various bioassays. Yields of TAAE and TAWE were calculated by taking the weight of the extracts subjected to complete dryness under vaccum and concentration of the extracts in the assays were represented based on their respective dry weights. The yields obtained were 15% (w/w) and 5% (w/w) for TAAE and TAWE, respectively.

2.3. ESI–LC-MS/MS analysis

LC-ESI-MS/MS analysis of TAAE and TAWE was performed on 6520 Accurate Q-TOF (Agilent Santa Clara, CA) mass spectrometer coupled to HPLC equipped with UV–VIS detector. The column was Zorbax Eclipse XDB-C 18, 4.6×50 mm, 1.8 μ; other conditions: (A) acetic acid (0.1% v/v) and (B) acetonitrile; Gradient (in solvent B): (i) 20-55%, from 0 to 15 min, (ii) 55–90%, from 15–20 min (iii) isocratic 90%, from 20 to 23 min (iv) 90–20%, from 23 to 26 min (v) isocratic 20%, from 26 to 35 min; Flow rate: 0.2 mL/min; Injection volume 2 μL; ESI parameters: Both negative and positive ion mode; Mass range 100–1700 m/z; Spray voltage 4 KV; Gas temperature 325 °C; gas flow 8 L/min; Nebulizer 35 psi.

2.4. Cell culture

2.4.1. Human acute monocytic leukemia cells (THP-1)

The cell line (THP-1) purchased from (NCCS, Pune) was cultured, as described in Kokkiripati et al. (2011). The conditions, briefly, were: RPMI 1640 medium (10 mM HEPES, 1 mM sodium pyruvate, 4.5 g/L glucose, 1.5 g/L sodium bicarbonate) supplemented with 2 mM L-glutamine and 10% fetal bovine serum. Cells were maintained in 5% CO_2 and 95% air at 37 °C during growth and treatments. Treatments were done at a cell density of 5×10^5 /mL. Vehicle control (alcohol or water) did not exceed 1% of culture volume.

2.4.2. Human aortic endothelial cells (HAECs)

HAECs were purchased from Invitrogen (USA), and grown to confluence in Medium 200, supplemented with 10% (v/v) heat-inactivated fetal bovine serum, penicillin (100 U/mL) and streptomycin (100 U/mL). All experiments were performed with cells of fifth passage. An acute inflammatory stimulus was produced by coincubating with human recombinant TNF-α. Prior to TNF-α treatment, cells were incubated with TAAE, TAWE or GA for 16–18 h.

To exclude the possibility of toxicity, cell viability at different concentrations (of TAAE or TAWE) was tested by trypan blue exclusion method. The amounts of plant extracts for the treatments for THP-1 cells or human aortic endothelial cells (HAECs) were chosen for further assays, ensuring the cell viability of $>$ 90%. Further, cell viability with various concentrations of plant extracts was assayed also by using MTT reagent, as per manufacturer's protocol and described by Kokkiripati et al. (2011).

2.5. Lipid peroxidation assay with liver/heart tissue homogenate

The lipid peroxidation was assayed in the liver and heart tissue according to Gaurav et al. (2007) and Meera et al. (2009) respectively. The extent of lipid peroxidation was monitored by thiobarbituric acid reactive substances (TBARS) reagent, as per the details described earlier (Kokkiripati et al., 2011). The liver or heart tissue of male wistar rats, homogenized in ice-cold KCl (0.15 M), was exposed to 10 mM ferric chloride, in the presence or absence of TAAE, TAWE or GA.

2.6. Measurement of 3-hydroxy-3-methylglutaryl-CoA (HMG-CoA) reductase and lipoprotein lipase (LpL)

Effect of TAAE and TAWE on HMG-CoA reductase was assayed using a kit, as per manufacturer's instructions (Sigma-Aldrich).

The assay was done using an Infinity M200 microplate reader (Tecan, Germany) by measuring the decrease in absorbance at 340 nm (represents the oxidation of NADPH) in the presence of the substrate HMG-CoA. Pravastatin (0.5 μM) included in the kit was used as standard inhibitor.

The LpL activity was assayed with the help of a kit that monitors the release of *p*-nitrophenol and as per manufacturer's protocol (Sigma-Aldrich), using a microplate reader. Enzyme activity was determined from increase in absorbance at 410 nm against substrate blank (without substrate). Orlistat was used as the standard inhibitor.

2.7. Measurement of intracellular ROS in THP-1 cells

Measurement of ROS in cultured THP-1 cells was performed using the ROS sensitive 2', 7',-dichlorofluorescein-diacetate (H_2DCFDA) and described earlier by Kokkiripati et al. (2011). Cells (5×10^5 cell per well) were pre-incubated with or without different concentrations of TAAE and TAWE for overnight at 37 °C in a humidified atmosphere containing 5% CO_2. After preincubation, 5 μM H_2DCFDA was added. After 30 min incubation at 37 °C, the cells were washed twice with RPMI medium. Cells were treated with 10 μM H_2O_2 to induce intracellular ROS. Images were obtained using confocal laser-scanning electron microscope (Leica DMR). Spectrofluorimetry analysis was done to quantitate intracellular ROS using excitation and emission wavelengths at 488 and 525 nm respectively.

2.8. Measurement of antioxidant enzymes and/ reducing power of the THP-1 cells

Activities of catalase (CAT), glutathione peroxidase (GPx) and ferric reducing/ antioxidant power (FRAP) in THP-1 cell lysates were measured according to Prasenjit et al. (2007). Prior to lysing the cells by sonication, cells were exposed to 10 μM H_2O_2 for 5 min.

CAT was assayed by adding 7.5 mM H_2O_2 to cell lysate and consumption of H_2O_2 is recorded at time scan of every 10 s for about 5 min at 240 nm in micro plate reader. CAT activity was expressed in fold change which reduced 1 μmol of H_2O_2 per min at 25 °C.

GPx assay was done with cell lysates by mixing with 550 μL of 0.1 M KH_2PO_4 buffer containing 1 mM EDTA (pH 7.5), 50 μL of 2 mM NaN_3, 100 μL of GR (2.4 U/mL) and 100 μL of 10 mM GSH. After 10 min of incubation at 37 °C, 100 μL of 1.5 mM NADPH in water was added to the above mixture. The reaction was initiated by adding 100 μL of pre-warmed (37 °C) 1.5 mM H_2O_2 and the decrease in absorbance at 340 nm were monitored for 5 min in microplate reader.

FRAP was determined in a reaction mixture containing freshly prepared and prewarmed (37 °C) FRAP reagent (300 mM acetate buffer, pH 3.6, 10 mM TPTZ in 40 mM HCl and 20 mM $FeCl_3 \cdot 6\,H_2O$ in the ratio of 10:1:1) and cell lysate incubated at 37 °C for 10 min. Colorless oxidized Fe^{III} is converted to blue

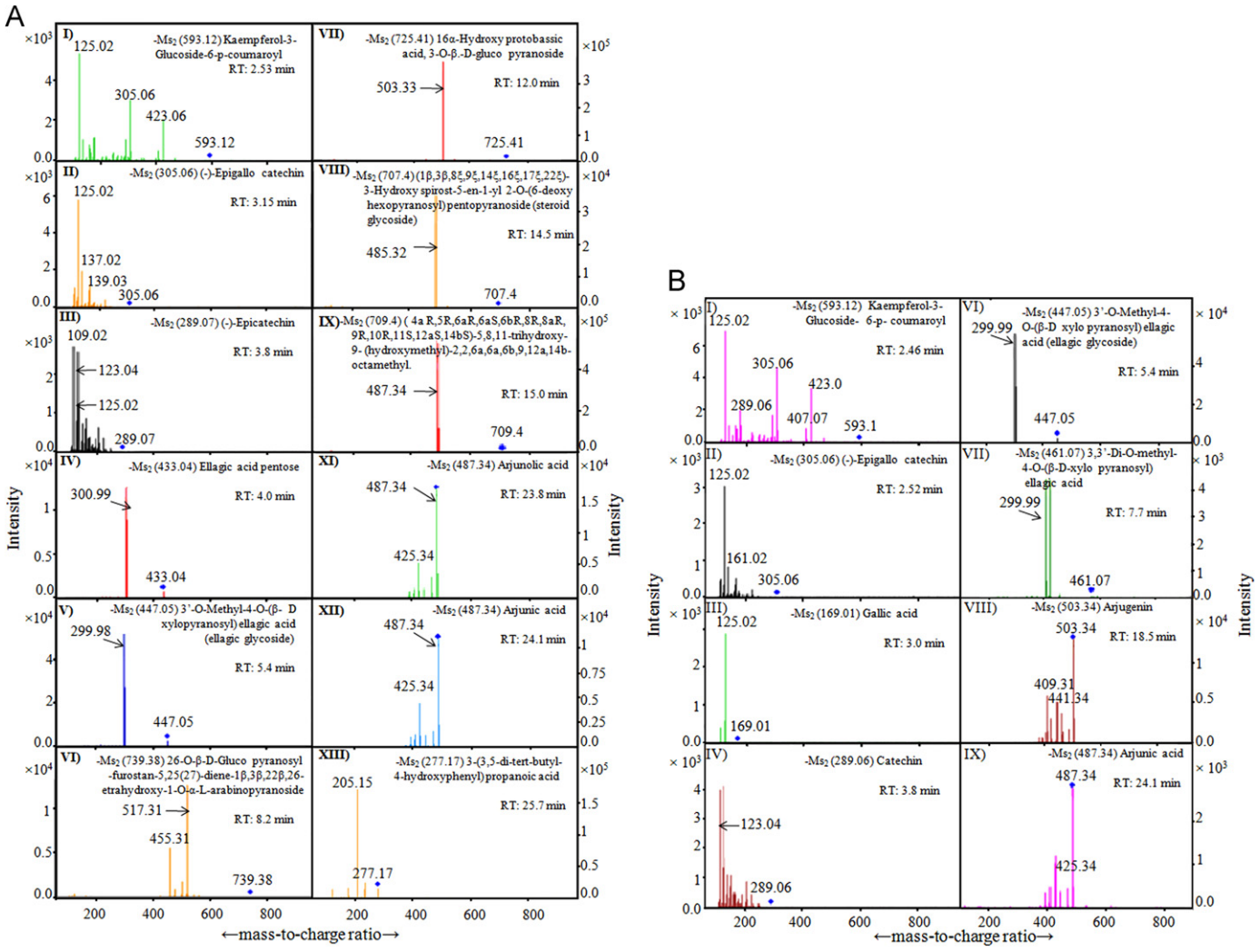

Fig. 1. Negative ion (–) ESI/MS/MS of: (A) alcoholic (TAAE) and (B) water extracts (TAWE) of TA-stem bark. Product ion labels correspond to fragments.

colored Fe^{II}-tripyridyltriazine compound formed was assayed as antioxidant power of extracts by reading absorbance at 593 nm.

2.9. RNA isolation

After respective treatments, the total RNA was isolated from THP-1 cells/ HAECs using TRIZOL reagent as per manufacturers protocol (Invitrogen). RNA was estimated using nanodrop method. Total RNA (1 μg) was used to synthesize cDNA (BioRad kit) for subsequent assays.

2.10. Real-time quantitative PCR

Two microlitres of cDNA was used for real-time quantitative PCR assay with 1 × FG, power SYBR green PCR master mix (Applied bio systems, Carlsbad, CA, USA). The specificity of the SYBR green fluorescence was tested by plotting fluorescence as a function of temperature to generate the melting curve of the amplicon. The melting peaks of the amplicon were as expected (not shown). We used primer sets (Supplementary Table 1), whose specificities were confirmed by manufacturer (Eurofins genomics, Bangalore India). The transcript levels of marker genes were normalized with GAPDH mRNA.

2.11. LPS induced TNF-α release by THP-1 cells

The THP-1 cells were pretreated with or without TA-extracts, for 16 h in 5% CO_2 at 37 °C. After treatment with LPS (0.5 μg/mL for 3 h), cells were centrifuged (10,000 rpm, 5 min, 4 °C), and the supernatants were stored at −80 °C, until assayed. Supernatants were subjected to TNF-α assay according to BD OptEIA™ Set Human TNF-α kit method (BD Bioscience).

2.12. Measurement of cell surface adhesion molecules (VCAM-1 and E-selectin) by flow cytometry

Expression of VCAM-1 and E-selectin on HAECs was assayed with a BD LSR Fortessa™ FACScan. For each sample, 5000–10,000 events were collected, with triplicate samples. Staining of HAECs for flow cytometry was performed according to manufacturer's instructions (BD Bioscience) and further details were given in Mullick et al. (2007). Trypsinized cells were incubated for 30 min in dark at 4 °C with CD106–FITC (VCAM-1) and CD62E-PE (E-selectin) antibodies (BD Biosciences). At the end of incubation, cells were washed twice and fixed with Cytofix/Cytoperm (BD Biosciences) and subjected to FACS analysis. Data analysis was done with FACS Diva software. Positive and negative controls for each fluorophore were performed to determine optimal levels of PMV gain and sensitivity and set correct parameters for compensation.

2.13. Statistical analysis

All the data were subjected to one way analysis of variance (ANOVA) test using Statistical Package for the Life Sciences (SPLS version 11). The values were expressed as mean ± standard deviation (S.D.). Variance at $p < 0.001$ was considered to be highly significant.

3. Results

3.1. Phytochemical analysis

Phytochemical analysis of TAAE and TAWE with LC-Q-TOFMS was done to obtain the metabolite profiles in the extracts and to examine their differences, if any. The MS-MS spectra of the compounds are shown in Fig. 1A and B. The identity of compounds was confirmed by mass fragmentation analysis. Negative ion mode detected a total of 13 metabolites from TAAE (Supplementary Table 2A) and 9 from TAWE (Supplementary Table 2B). These metabolites were either phenolics (e.g. catechin, ellagic acid pentose, epicatechin, epigallo catechin) or terpenes (e.g. terminolic acid, arjunolic acid, arjunic acid). Positive ion mode did not yield any known compounds. Compounds which were common in both TAAE and TAWE were: kaempferol, epigallo catechin, ellagic acid pentose, ellagic glycoside, terminolic acid and arjunic acid. In contrast, only TAAE contained glycopyranosides, steroid glycoside, (-)-epicatechin and arjunolic acid, whereas TAWE contained gallic acid, catechin and a derivative of ellagic acid i.e. 3'-O-methyl-4-O-(β-D-xylopyranosyl) ellagic acid.

3.2. Inhibition of lipid peroxidation by TA-stem bark extracts

The bark extracts of TA-stem were evaluated for their ability to inhibit lipid peroxidation, as such peroxidation, particularly, of unsaturated fatty acids in membranes can trigger pathophysiological changes. The presence of TAAE or TAWE inhibited the lipid peroxidation induced by $FeCl_3$ in liver or heart homogenates by about 90%. The IC_{50} values for such inhibition of TAAE and TAWE were 10 and 3 μg dwt/mL for liver homogenate and 30 and 10 μg dwt/mL for heart homogenate, respectively. The standard compound (GA) caused an inhibition of 80% in both tissue homogenates; with IC_{50} values of 1.29 μg/mL and 10 μg/mL for liver and heart homogenates, respectively (Fig. 2A and B).

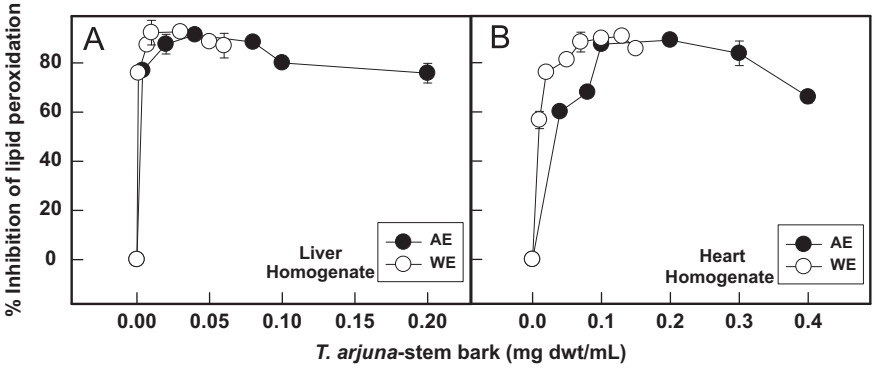

Fig. 2. Ferric chloride induced lipid peroxidation activity of TA-stem bark on (A) liver (B) heart tissue homogenate of rat. Data shown mean value of 6 independent experiments. If not seen, S.D. values were within the symbol of data point. All values are statistically significant $^{\#}p < 0.001$ vs. control.

3.3. Effect of TA-stem bark extracts on HMG-CoA reductase and LpL enzymes

The addition of TAWE inhibited HMG-CoA reductase enzyme activity (in vitro) by about 90% at 125 μg dwt/mL, and TAAE inhibited by 80% at 75 μg dwt/mL. Pravastatin (0.5 μM), a drug-control (included in Sigma kit), inhibited by about 55% (at the concentration recommended in the manufacturer's protocol). Under our experimental conditions, TAAE and TAWE did not inhibit LpL, whereas the drug control, Orlistat (4 mM), caused about 30% inhibition over control (Fig. 3).

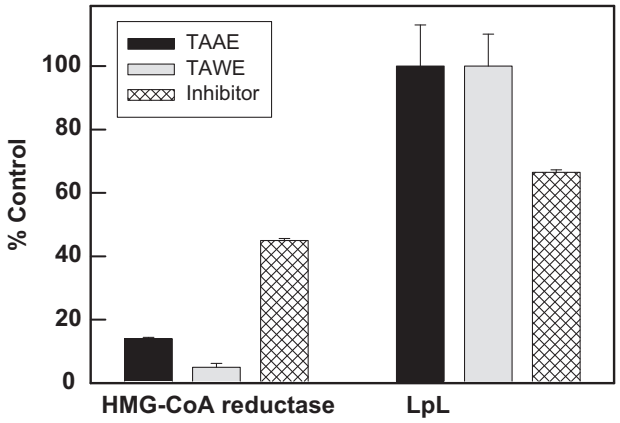

Fig. 3. Effect of TA-stem bark on activities of HMG-CoA reductase and lipoprotein lipase enzyme. Data shown mean value of 3 independent experiments. If not seen, S.D. values are within the symbol of data point.

3.4. Attenuation of H_2O_2 induced ROS by TA-stem bark extracts in THP-1 cells

H_2O_2, one of the main reactive oxygen species (ROS), can rapidly cross the cell membranes and generate different types of ROS e.g. hydroxyl radicals, which are highly harmful. In spite of scavenging systems in cells, excess ROS can lead to oxidative stress mediated pathophysiology. Therefore, we evaluated the efficacy of TAAE and TAWE in attenuating H_2O_2 induced ROS generation in a monocytic (THP-1) cell line. Exposure to H_2O_2 markedly increased intracellular ROS levels in THP-1 cells (Fig. 4B), compared to the unexposed cells (Fig. 4A). Pretreatment of cells with TAAE or TAWE markedly attenuated the H_2O_2 induced ROS production, in a dose-dependent manner (Fig. 4C). The related IC_{50} values for TAAE and TAWE were 16 and 75 μg dwt/mL, respectively. Thus, our results demonstrate that both TAAE and TAWE possess significant ROS scavenging activity, similar to standard compounds (BHT and GA). At the concentrations used, TAAE, TAWE, BHT or GA did not affect the cell viability. No cell death was observed up to 150 μg dwt/mL for TAAE and 500 μg dwt/mL for TAWE (Supplementary Fig. 1A and B). In case of standard

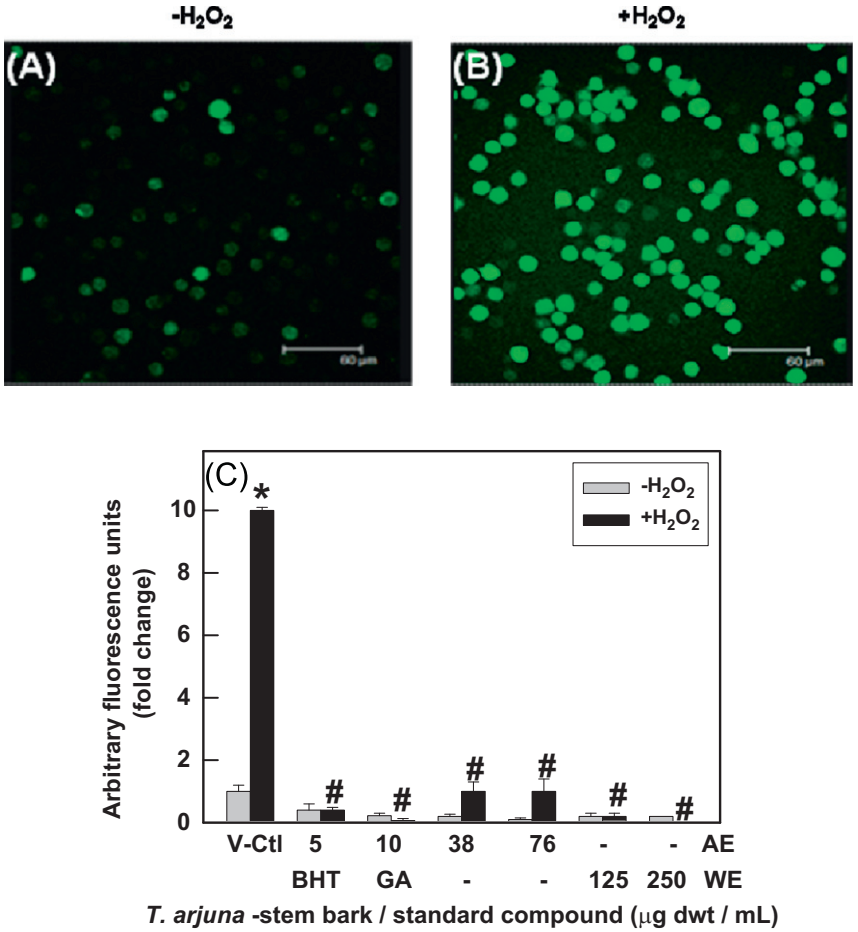

Fig. 4. Effect of TA-stem bark on H_2O_2 induced ROS generation in THP-1 cells. Confocal images: (A) control cells – no H_2O_2 (B) cells + 10 μM H_2O_2. ROS generation was detected by H_2DCFDA dye, and cells were observed with a fluorescence microscope. (C) Fluorescence intensity of H_2DCFDA taken up by the treated cells was measured by spectrofluorimetry (Ex 488 nm, Em 525 nm). One-way ANOVA test was performed between the experimental groups. Data shown mean value of 4 independent experiments ± S.D. $^{\#}p < 0.001$ vs. Control groups, $^{*}p < 0.001$, for comparison between treated and untreated groups with the control.

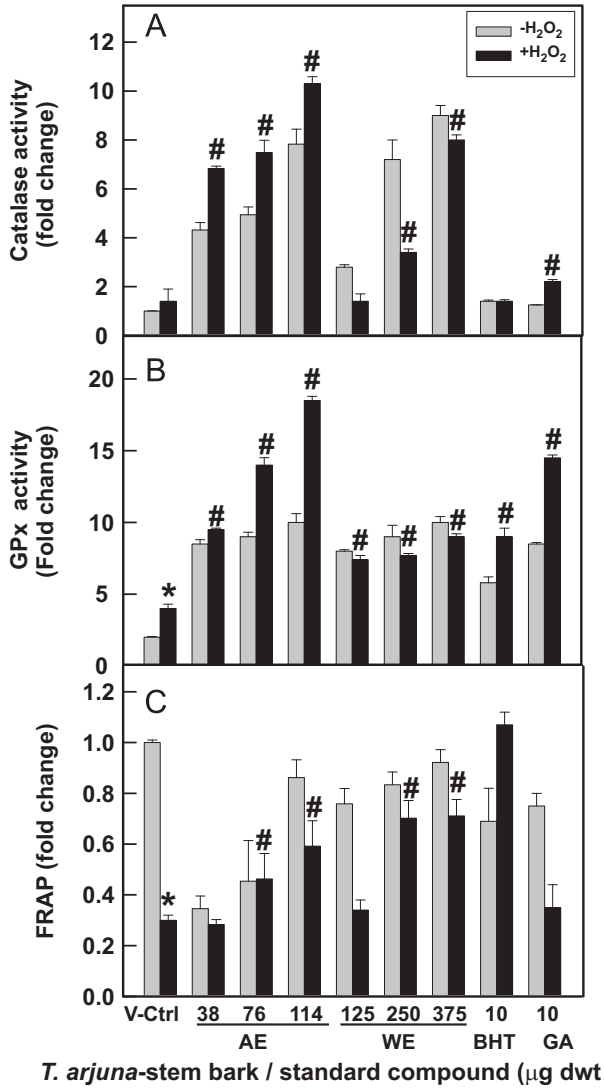

Fig. 5. The activities of CAT (A), GPx (B) and levels of FRAP (C) in either normal or H_2O_2 exposed THP-1 cells. GA served as positive drug control. Data shown mean value of 4 independent experiments ± S.D. $^{\#}p < 0.001$ compared between treated and untreated with controls, $^{*}p < 0.001$ between the control groups.

compounds, there was no cell death up to 150 μg/mL of GA (Supplementary Fig. 1C) and 10 μg/mL BHT (Kokkiripati et al., 2011).

3.5. Effect of TA-stem bark extracts on scavenging enzymes and FRAP

To determine the mechanism by which TAAE and TAWE can scavenge intracellular ROS in THP-1 cells, their effects on CAT, GPx and cellular reducing power were assayed. Pretreatment with TAAE (114 μg dwt/mL) caused an increase in CAT by 10-fold and GPx by 7-fold, compared to control (vehicle) cells. Similarly, TAWE (375 μg dwt/mL) induced 8- and 6-fold increase in CAT and GPx activities, respectively. In contrast to TAAE and TAWE, GA (10 μg/mL) stimulated activity of CAT and GPx activity by only 2 and 4.5-fold, respectively. The changes induced in CAT and GPx activities were all significant. The reducing power of THP-1 cells declined to 30% upon treatment with H_2O_2 (Fig. 5C) compared to control (vehicle) cells. TAAE at 114 μg dwt/mL sustained reducing power to be kept at 60%, and TAWE at 375 μg dwt/mL at 70%. GA (10 μg/mL) did not help much (being as low as only 30%), but BHT (10 μg/mL) completely restored cellular reducing power (Fig. 5C).

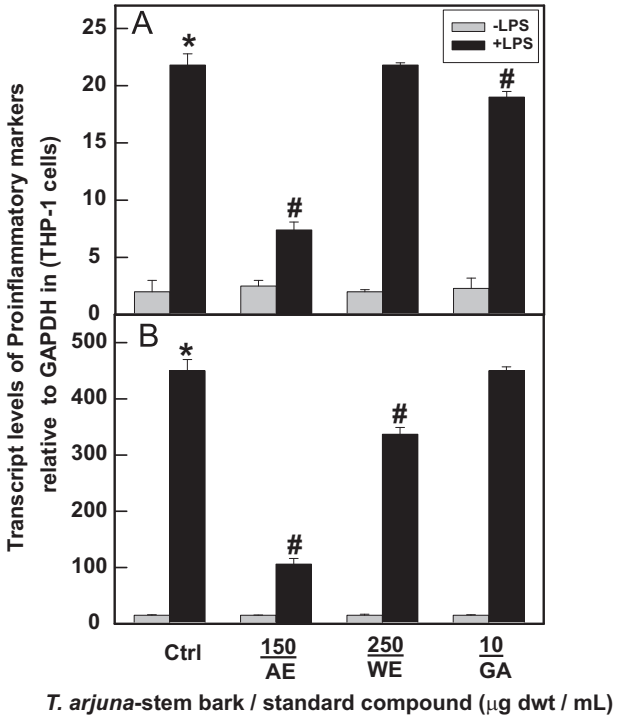

Fig. 6. TA-stem bark extracts decrease mRNA expression of (A) MCP-1 (B) IL-8 in LPS induced THP-1 monocytic cells. Data shown mean value of 3 independent experiments ± S.D. # $p < 0.001$ and * $p < 0.001$ between the control groups.

3.6. Effect of TAAE/TAWE on LPS induced inflammatory markers in THP-1 cells

Real-time quantitative PCR showed that LPS enhanced the expression, of monocyte chemotactic protein-1 (MCP-1) (22-fold increase) and interleukin-8 (IL-8) (450-fold increase) in THP-1 cells (Fig. 6). Such stimulation in proinflammatory gene expression with LPS was markedly restricted by TAAE and TAWE. At 150 μg dwt/mL, TAAE restricted MCP-1 expression to 7-fold and IL-8 to 106-fold. Similarly, TAWE at 250 μg dwt/mL did not restrict MCP-1 expression, while reducing the expression of IL-8 to 330-fold. GA (10 μg/mL) restricted marginally MCP-1 to 19-fold and failed to attenuate IL-8. (Fig. 6A and B).

The next set of experiments looked at LPS induced TNF-α secretion by THP-1 cells. Control cell secreted negligible amounts of TNF-α, whereas LPS stimulated cells (5×10^5 cells/mL) secreted 824 pg/mL of TNF-α (Fig. 7). Pre-treatment with TA-stem bark extracts attenuated such stimulation. The secretion of TNF-α was reduced to 39 pg/mL due to TAAE extracts, and to 220 pg/mL, with TAWE. Thus, TAAE was more potent than TAWE, in inhibiting the activation of THP-1 cells.

3.7. Effect of TAAE/TAWE on TNF-α induced inflammatory markers in HAECs

In unstimulated HAECs, the transcripts of VCAM-1, E-selectin, MCP-1, IL-8 and intercellular adhesion molecule-1 (ICAM-1) markers were at very low level and are considered as one. Upon stimulation with TNF-α (10 ng/mL) for 4 h, HAEC's the expression of inflammatory markers increased: VCAM-1 (~2-fold), E-selectin (86-fold), MCP-1 (210-fold), IL-8 (95-fold) and ICAM-1 (347-fold). Pretreatment of HAECs with TAAE/TAWE inhibited such stimulation in gene expression. The reductions in mRNA levels by treatment with TAAE (18.75 μg dwt/mL) of all the markers were significant compared to TNF- α treated cells. The reduction by

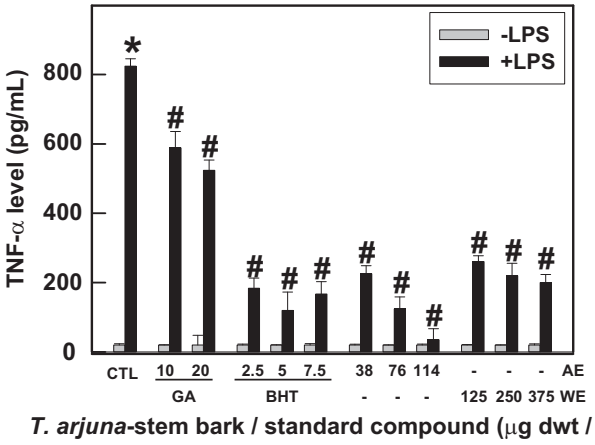

Fig. 7. The effect of TA-stem bark extracts mediated attenuation of LPS-induced TNF-α secretion. THP-1 cells (5×10^5 cells/mL) were pretreated with extracts and were then further treated with LPS for 3 h. Secretory levels of TNF-α (pg/mL) from the supernatants of cells were measured by ELISA. Data shown mean value of 3 independent experiments ± S.D. ($\#p < 0.001$), $^*p < 0.001$ between the control groups.

treatment with TAWE (25 μg dwt/mL) was significant only in E-selectin, MCP-1 and IL-8 mRNA transcripts but not in VCAM-1 and ICAM-1 (Fig. 8A–E).

3.8. TAAE/TAWE attenuates surface adhesion molecule expression

Treatments of HAECs with TNF-α (10 ng/mL) for 4 h resulted in increased VCAM-1 and E-selectin protein expression (Fig. 8A and C). Less than 1% of control cells expressed VCAM-1 and E-selectin markers, whereas TNF-α administration increased VCAM-1 and/or E-selectin positive population to 41% and 82%, respectively (Fig. 8C). Cells pretreated with TAAE/TAWE had significantly decreased proportion of VCAM-1 and E-selectin positive cells. Such reduction in inflammatory adhesion molecule expression was similar to that of cells coincubated with GA. The expression of VCAM-1 was completely attenuated by the extracts as well as GA. About 90% of HAECs cells were live at the concentration of TAAE up to 40 μg dwt/mL and TAWE, up to 25 μg dwt/mL (Supplementary Fig. 2A) and 25 μg/mL in case of GA (Supplementary Fig. 2B).

4. Discussion

Traditionally, TA-stem bark has been used as a cardiotonic in Ayurvedic medicine. Clinical and animal studies suggested the efficacy of TA-stem bark in treating various types of cardiovascular diseases (Dwivedi, 2007), but its mechanism of action was not clear. To the best of our knowledge, this is the first report that provides the cellular and molecular basis of cardio-protective activity of TA-stem bark extracts.

4.1. Hypolipidaemic and antioxidant activity of TA-stem bark

Hypolipidaemic and antioxidant nature of TA-stem bark has been reported in animal models (Tiwari et al., 1990, Shaila et al., 1998; Gauthaman et al., 2001; Gupta et al., 2001; Verma and Vinaya, 2009). In the present study, both the extracts of TA-stem (TAAE and TAWE) were found to inhibit the activity of HMG-CoA reductase (Fig. 3), a key enzyme in sterol biosynthesis and often targeted for developing cholesterol lowering drugs (Daniel et al., 1999). In view of proinflammatory nature of lypolysis products generated from very low density lipoproteins (Higgins and Rutledge, 2009; Tetali et al., 2010), the inhibition of LpL is desirable. However, the TAAE and TAWE did not inhibit LpL activity (Fig. 3).

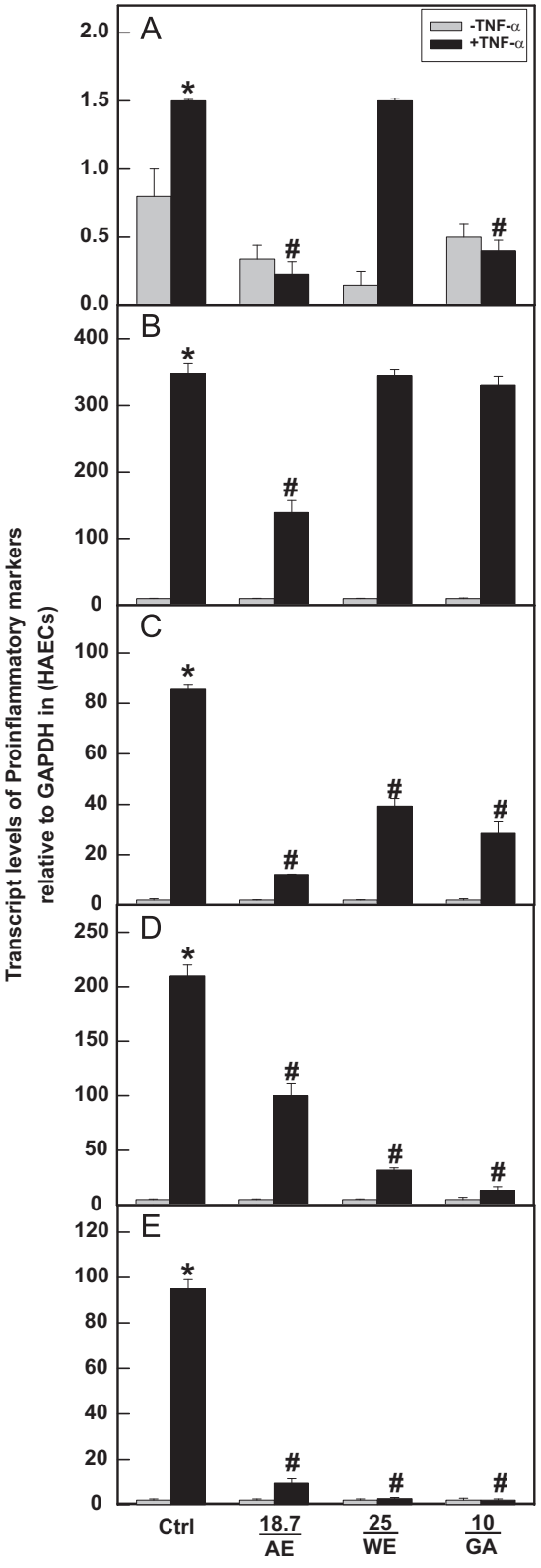

Fig. 8. TA-stem bark extracts decreases mRNA expression of (A) VCAM-1 (B) ICAM-1 (C) E-selectin (D) MCP-1 (E) IL-8 in TNF-α-induced HAECs. Data shown mean value of 3 independent experiments ± S.D. # $p < 0.001$ and $^*p < 0.001$ between the control groups.

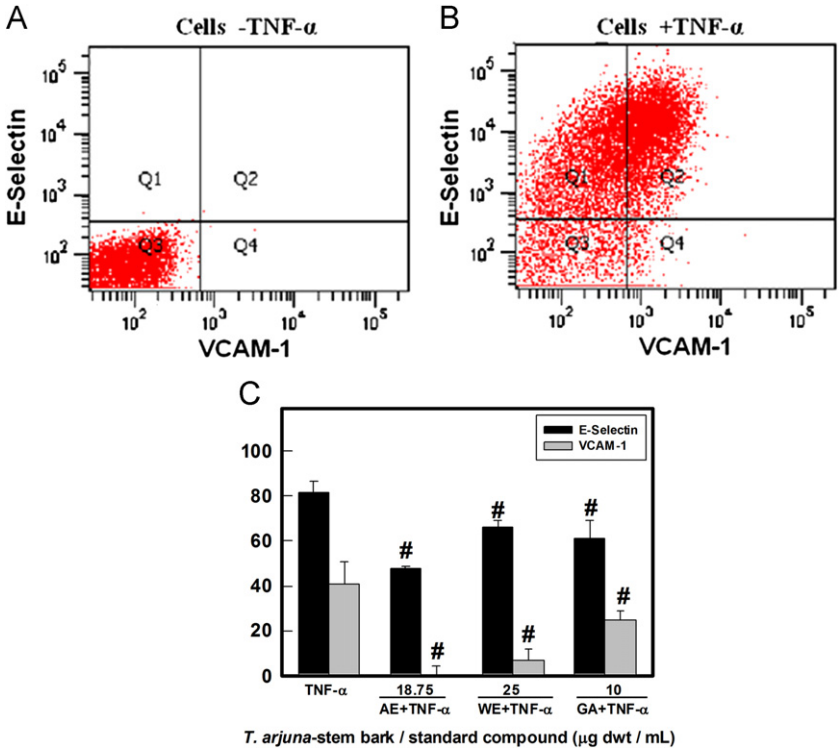

Fig. 9. HAECs untreated (A) and treated with TNF-α (B) TAAE/TAWE attenuated TNF-α induced protein expression of VCAM-1 and E-selectin. HAECs were stimulated with TNF-α (10 ng/mL) for 4 h and cells were analyzed by flow cytometry for surface expression of VCAM-1 and E-selectin using flow cytometry. Cells analyzed for antibody staining. HAECs exposed to only TNF-α. Cells coincubated with TNF-α and AE (18.75 μg dwt/mL); WE (25 μg dwt/mL) and GA (10 μg/mL). A reduction in both VCAM-1 and E-selectin expression was seen in cells with AE/WE coincubation. Data shown mean value of 3 independent experiments ± S.D. # $p < 0.05$ Fig. (C).

Resources for antioxidant compounds, which can alleviate oxidative stress, are popular candidates for therapeutics (Tiwari, 2004). Besides hypolipidaemic property, TAAE and TAWE showed potential antioxidant activity. The extracts markedly inhibited lipid peroxidation in liver and heart tissues (in vitro) and exhibited ROS scavenging activity in human monocytic (THP-1) cells (Fig. 4). In H_2O_2 treated monocytes, cellular reducing power decreased substantially compared to control cells. The small increase in CAT and GPx enzyme activity in cells due to H_2O_2 treatment would not be sufficient enough to scavenge the intracellular ROS generated. Pretreatments with TA-stem bark extracts enhanced markedly the overall antioxidant potential of cells by enhancing antioxidant enzyme activities as wells as reducing power (Fig. 5). Such antioxidant activity of extracts can be attributed to the presence of several phenolics and terpenes in TAAE and TAWE (Fig. 1A and B; Supplementary Tables 2A and 2B).

4.2. Antiinflammatory activity of TA-stem bark

Atherosclerosis can be caused by acute or chronic inflammation in the blood vessel wall (Ross, 1999; Libby, 2002). Several conditions including oxidative stress, hypercholesterolemia, hyperglycemia and postprandial lipolysis, activate monocytes and platelets in the peripheral blood, there-by cause endothelial cell dysfunction and vessel wall permeability (Esper et al., 2006). Breaking such inflammatory dialog between these cell types would help in controlling the development/advancement of atherosclerosis. Although several anti-inflammatory drugs have been evaluated for their possible antiatherosclerotic effects, only a few such compounds were helpful in treating atherosclerosis, e.g. Aspirin (Moubayed et al., 2007). Therefore, herbal extracts having ability to target inflammatory cascade in the blood vessel wall would be of great interest. Such studies with traditional medicinal plant extracts are highly limited (Chen et al., 2003). The TA-stem bark was shown to have anti-platelet aggregatory activity by attenuating Ca^{2+} release and CD62P expression Malik et al. (2009). We observed that both TAAE and TAWE markedly inhibited secretion of proinflammatory cytokine TNF-α by in THP-1 cells induced with LPS, which causes inflammation during infection (Fig. 7).

Since the literature suggested that low expression of VCAM-1 was associated with significant reduction in atherosclerotic lesions in the aorta (Cybulsky et al., 2001), immunomodulatory effect of the extracts on cell surface adhesion molecules in HAECs was investigated. Imaging VCAM-1 has been suggested for early CVD risk assessment in individual patients (Nahrendorf et al., 2009). Pretreatments of human aortic endothelial cells (HAECs) with TAAE attenuated TNF-α induced gene transcripts of cell surface adhesion molecules (VCAM-1, ICAM-1, E-selectin) and chemokines (MCP-1 and IL-8). The effect of TAWE on the levels of proinflammatory gene transcripts varied, depending on the cell type and nature of the marker. The inability of TAWE in inhibiting MCP-1 and IL-8 transcripts in THP-1 cells and VCAM-1 and ICAM-1 in HAECs could be due to difference in its metabolite profile from TAAE. Present study showed that pretreatments of HAECs with TAAE or TAWE significantly attenuated TNF-α dependent induction in VCAM-1 and E-selectin (Fig. 9), confirming their roles as potent immunomodulator.

5. Concluding Remarks

The present manuscript presents a critical evaluation of TA-stem bark's cardioprotective effect using human cell culture models, allowing a focussed evaluation of the cellular and molecular basis of these effects. The results demonstrate for the first time, that the TA-stem bark extracts are enriched with phenolics and terpenes and possess significant antiatherosclerotic activity. These extracts restricted at least three components: (i) oxidative stress induced ROS generation in human monocytic

cells (ii) LPS induced TNF-α secretion by THP-1 cells, and (iii) TNF-α induced cell surface adhesion molecules, VCAM-1 and E-selectin on HAECs. Thus, our study is a scientific validation and molecular elucidation of therapeutic potential use of TA-stem bark for cardiac protection. It would be necessary to test TA-stem bark's vascular protective effects, e.g. on endothelial dysfunction, atherosclerosis formation etc. in animal models of diabetic mice/rats or apolipoprotein E–deficient (apoE−/−) mouse. These experiments would be taken up in our next phase of work.

Acknowledgments

Authors are grateful to Dr. Madhava Chetty, Department of Botany, S.V.U. Tirupathi for providing the authenticated plant material and Prof. P. Prakash Babu, Department of Biotechnology for providing rat liver and heart tissue samples. This part of the work is supported by the UGC (37/532/2010 SR) research project (to SDT) and J.C. Bose National Fellowship (No. SR/S2/JCB-06/2006) of DST, New Delhi (to ASR). Ratnam V. Kamsala thankful to DBT-CREBB for a PDF. Authors are thankful to Department of Animal Sciences (for flow cytometry facility), DST-FIST (Dept of Plant Sciences), DBT-CREBB and UGC-SAP (School of Life Sciences) for infra-structural facilities.

Appendix A. Supporting information

Supplementary data associated with this article can be found in the online version at http://dx.doi.org/10.1016/j.jep.2012.12.050.

References

Asha, S., Taju, G., 2012. Cardioprotective effect of *Terminalia arjuna* on caffeine induced coronary heart disease. International Journal of Pharmaceutical Sciences and Research 3, 150–153.

Arya, V., Gupta, V.K., 2011. Chemistry and pharmacology of plant cardioprotectives: a Review. International Journal of Pharmaceutical Sciences and Research 2, 1156–1167.

Carluccio, M.A., Sicuella, L., Ancora, M.A., 2003. Olive oil and red wine antioxidant polyphenols inhibit endothelial activation: atherogenic properties of mediterranean diet phytochemicals. Arterosclerosis Thrombosis and Vascular Biology 23, 622–629.

Chen, J.W., Chen, Y.H., Lin, F.Y., Chen, Y.L., Lin, S.J., 2003. *Ginkgo biloba* extracts inhibits tumor necrosis factor-α induced reactive oxygen species generation, transcription factor activation, and cell adhesion molecule expression in human aortic endothelial cells. Atheroscelerosis Thrombosis Vascular Biology 23, 1559–1566.

Choudhari, A.B., Nazim, S., Gomase, P.V., Khairnar, A.S., Shaikh, A., Choudhari, P., 2011. Phytopharmacological review of *arjuna* bark. Journal of Pharmacy Research 4, 580–581.

Cybulsky, M.I., Iiyama, K., Hongmei, Li., Zhu, S., Chen, M., Iiyama, M., Davis, V., Gutierrez-Ramos, J.C., Connelly, P.W., Milstone, D.S., 2001. A major role for VCAM-1, but not ICAM-1, in early atherosclerosis. Journal of Clinical Investigation 107, 1255–1262.

Daniel, E.H., Jeffrey, O.P., Syed, M.M., Ryschon, L., Pedersen, A., 1999. A population-based treat-to-target pharmacoeconomic analysis of HMG-CoA reductase inhibitors in hypercholesterolemia. Clinical Therapeutics 3, 536–562.

Dwivedi, S., Jauhari, R., 1997. Beneficial effects of *Terminalia arjuna* in coronary artery disease. Indian Heart Journal 49, 507–510.

Dwivedi, S., Aggarwal, A., Agarwal, M.P., Rajpal, S., 2005. Role of *Terminalia arjuna* in ischaemic mitral regurgitation. International Journal of Cardiology 100, 507–508.

Dwivedi, S., 2007. *Terminalia arjuna* Wight & Arn.—a useful drug for cardiovascular disorders. Journal of Ethnopharmacology 114, 114–129.

Esper, R.J., Nordaby, R.A., Vilarino, J.O., Paragano, A., Cacharron, J.L., Machado, R.A., 2006. Endothelial dysfunction: a comprehensive appraisal. Cardiovascular Diabetology 4, 1–18.

Gauthaman, K., Maulik, M., Kumari, R., Manchanda, S.C., Dinda, A.K., Maulik, S.K., 2001. Effect of chronic treatment with bark of *Terminalia arjuna*: a study on the isolated ischemic-reperfused rat heart. Journal of Ethnopharmacology 75, 197–201.

Gupta, R., Singhal, S., Goyle, A., Sharma, V.N., 2001. Antioxidant and hypocholesterolaemic effects of *Terminalia arjuna* tree-bark: a randomized placebo-controlled trial. Journal Associations of Physicians of India 49, 231–235.

Gaurav, V.H., Chandragauda, R.Patil, Mahesh, R.Patil, 2007. Protective effect of *Kalanchoe pinnata* Pers. (Crassulaceae) on gentamicin-induced nephrotoxicity in rats. Indian Journal of Pharmacology 39, 201–205.

Higgins, L.J., Rutledge, J.C., 2009. Inflammation associated with the postprandial lipolysis of triglyceride-rich lipoproteins by lipoprotein lipase. Current Atherosclerosis Reports 11, 199–205.

Karthikeyan, K., Sarala Bai, B.R., Gauthaman, K., Sathish, K.S., Niranjali, D.S., 2003. Cardioprotective effect of the alcoholic extract of *Terminalia arjuna* bark in an in vivo model of myocardial ischemic referfusion injury. Life Sciences 73, 2727–2739.

Kokkiripati, P.K., Lepakshi, B., Marri, S., Padmasree, K., Row, A.T., Raghavendra, A.S., Tetali, S.D., 2011. Gum resin of *Boswellia serrata* inhibited human monocytic (THP-1) cell activation and platelet aggregation. Journal of Ethnopharmacology 137, 893–901.

Koti, B.C., Vishwanathswamy, A.H.M., Jyoti, W., Thippeswamy, A.H.M., 2009. Cardioprotective effect of lipistat against doxorubicin induced myocardial toxicity in albino rats. Indian Journal of Experimental Biology 47, 41–46.

Libby, P., 2002. Inflammation in atherosclerosis. Nature 420, 868–874.

Meera, R., Devi, P., Kameswari, B., Madhumitha, B., Merlin, N.J., 2009. Antioxidant and hepatoprotective activites of *Ocimum basilicum* Linn. and *Trigonella foenum-graecum* Linn. against H_2O_2 and CCl_4 induced hepatotoxicity in goat liver. Indian Journal of Experimental Biology 47, 584–590.

Malik, N., Dhawan, V., Bahl, A., Kaul, D., 2009. Inhibitory effects of *Terminalia arjuna* on platelet activation in vitro in healthy subjects and patients with coronary artery disease. Platelets 20, 183–190.

Moubayed, S.P., Heinonen, T.M., Tradif, J.C., 2007. Antiinflammatory drugs and atherosclerosis. Current Openion in Lipidology 18, 638–644.

Murkute, V.K., Vyawahare, N.S., Narkhede, S.G., Sarode, S.P., Pund, K.V., Kahane, M.A., Zope, B.R., Talele, S.G., 2011. Review on polyherbals in management of cardiovascular disease:—an Ethnopharmacological Approach. Inventi Rapid: Ethnopharmacology 3, 1–5.

Mullick, A.E., Andrew, F.P., Rama, S.K., Sarada, D.T., Jason, P.E., Rutledge, J.C., 2007. Apolipoprotein E3- and nitric oxide-dependent modulation of endothelial cell inflammatory Responses. Arteriosclerosis Thrombosis and Vascular Biology 27, 339–345.

Nahrendorf, M., Keliher, E., Panizzi, P., Zhang, H., Hembrador, S., Figueiredo, J.L., Aikawa, E., Kelly, K., Libby, P., Weissleder, R., 2009. 18F-4V for PET-CT imaging of VCAM-1 expression in atherosclerosis. JACC Cardiovascular Imaging 2, 1213–1222.

Parveen, A., Rashmi, B., Sarita, A., Anita, K., Mohammad, F., 2011a. *Terminalia arjuna* enhances baroreflex sensitivity and myocardial function in isoproterenol-induced chronic heart failure rats. Cardiovascular Toxicology 11, 48–57.

Parveen, K., Khan, R., Siddiqui, W.A., 2011b. Antidiabetic effects afforded by *Terminalia arjuna* in high fat-fed and streptozotocin-induced type 2 diabetic rats. International Journal of Diabetes and Metabolism 19, 23–33.

Prasenjit, M., Sinha, M., Pal, P., Sil, P.C., 2007. Arjunolic acid, a triterpenoid saponin, ameliorates arsenic induced cytotoxicity in hepatocytes. Chemico–Biological Interactions 170, 187–200.

Ragavan, B., Krishnakumari, S., 2005. Effect of *Terminalia arjuna* stem bark extract on the activites of marker enzymes in alloxan induced diabetic rats. Ancient Science of Life 25, 8–15.

Ross, R., 1999. Atherosclerosis—an inflammatory disease. The New England Journal of Medicine 340, 115–126.

Ruff, J.C., 2003. Wine and polyphenols related to platelet aggregation and atherothrombosis. Drugs under Experimental and Clinical Research 25, 125–131.

Shaila, H.P., Udupa, S.L., Udupa, A.L., 1998. Hypolipidemic activity of three indigenous drugs in experimentally induced atherosclerosis. International Journal of Cardiology 67, 119–124.

Sharma, M., Kishore, K., Gupta, S.K., Joshi, S., Arya, D.S., 2001. Cardioprotective potential of *Ocimun sanctum* in isoproterenol induced myocardial infraction in rats. Molecular and Cellular Biochemistry 225, 75–83.

Subramaniam, S., Subramaniam, R., Subasini, U., Gnanamanickam, V.R., Dubey, G.P., 2011. Anti-atherogenic activity of ethanolic fraction of *Terminalia arjuna* Bark on hypercholesterolemic rabbits. Evidence-Based Complementary and Alternative Medicine, 1–8.

Tetali, S.D., Budamagunta, M.S., Simion, C., den Hartigh, L.J., Kalai, T., Hideg, K., Hatters, D.M., Weisgraber, K.H., Voss, J.C., Rutledge, J.C., 2010. VLDL lipolysis products increase VLDL fluidity and convert apolipoprotein E4 into a more expanded conformation. Journal of Lipid Research 51, 1273–1283.

Tripathi, Y.B., Reddy, M.M., Pandey, R.S., Subhashini, J., Tiwari, O.P., Singh, B.K., Reddanna, P., 2004. Anti-inflammatory properties of BHUx, a polyherbal formulation to prevent atherosclerosis. Inflammopharmacology 12, 131–152.

Tilak, J.C., Adhikari, S., Devasagayam, T.P., 2004. Antioxidant properties of *Plumbago zeylanica*, an Indian medicinal plant and its active ingredient, plumbagin. Redox Report 9, 219–227.

Tiwari, A.K., Gode, J.D., Dubey, G.P., 1990. Effect of *Terminalia arjuna* on lipid profiles of rabbit fed hypercholesterolemic diet. International Journal of Crude Drug Research 28, 43–47.

Tiwari, A.K., 2004. Antioxidants: New-generation therapeutic base for treatment of polygenic disorders. Current Science 8, 1092–1102.

Verma, N., Vinaya, K.M., 2009. Effect of *Terminalia arjuna* on antioxidant defence system in cancer. Molecular Biology Reports 36, 159–164.